Characterisation of embryonic ventral mesencephalon grafts in a rat model of Parkinson's disease

This dissertation is submitted for the degree of Doctor of Philosophy at the University of Cardiff

Marija Fjodorova

Supervisors:

Professor S. B. Dunnett

Dr E. M. Torres

September 2013

Dedication

I dedicate this thesis to my parents,

Olga and Andrejs Fjodorovs,

who have raised me to be the person I am today.

Thank you for your words of encouragement and push for tenacity.

Most of all, thank you for believing in me.

Summary

The work discussed in this thesis adds further knowledge regarding the survival of embryonic dopaminergic grafts, derived from the rat ventral mesencephalon, in the rat model of Parkinson's disease, in terms of the populations of cells involved, their distribution within the grafts, and how these are affected by the donor age and the host environment in to which they are implanted.

The current data further reinforce the notion that harvesting ventral mesencephalic tissue at embryonic day 12 (E12) before the peak of dopamine neurogenesis yields more dopamine cells in the grafts and, more importantly, also yields more nigral A9 type dopamine neurons, which are an important determinant for functional recovery.

Following on from this, commitment of dopamine neural precursor cells to the two dopamine neuron phenotypes, and how this is affected by the host environment was investigated, by grafting rat E12 and E14 ventral mesencephalon tissue into different cerebral targets. Brain regions were chosen that receive either the nigral A9 type dopamine, ventral tegmental A10 type dopamine or noradrenaline innervation. The yield of A9 type dopamine neurons was found to be influenced both by the environment within the graft and by the host environment in the transplantation site to a higher extent than the yield of A10 type dopamine neurons.

Dopaminergic progenitors procured from rat embryos at E12 were shown to have a greater potential to proliferate post-grafting and differentiate into mature dopamine neurons as compared to embryos at E14. In vivo proliferation of younger precursor cells significantly contributed to the higher yields of the A9 type dopamine neurons in the grafts. If this improved yield of the A9 type dopamine neurons could be reproduced in human trials, fewer human donors might suffice to produce functional grafts in Parkinson's disease patients.

Declaration

This work has not previously been accepted in substance for any degree and is not concurrently submitted in candidature for any degree.

Signed ……(candidate) Date …….

STATEMENT 1

This thesis is being submitted in partial fulfillment of the requirements for the degree of PhD.

Signed ……..…..(candidate) Date …….

STATEMENT 2

This thesis is the result of my own independent work/investigation, except where otherwise stated.

Other sources are acknowledged by explicit references.

Signed ……(candidate) Date …….

STATEMENT 3: PREVIOUSLY APPROVED BAR ON ACCESS

I hereby give consent for my thesis, if accepted, to be available for photocopying and for inter-library loans **after expiry of a bar on access previously approved by the Graduate Development Committee.**

Signed ……...(candidate) Date ……..…

Acknowledgements

First and foremost I would like to thank my supervisors, Prof Stephen Dunnett and Dr Eduardo Torres for giving me an opportunity to work in the Brain Repair Group and for providing me with support and guidance which helped me complete the project on time. When I was a project student, Dr Torres inspired me greatly to work in cell transplantation research. I am grateful to both my supervisors for giving me so many opportunities in the last three years to become a critical, independent and much better researcher.

I would also like to thank the Wellcome Trust for funding my project, for the moral support and all the encouraging feedback over the years.

This research would not have been possible without the support of the members of the Brain Repair Group, past and present, namely Jane Heath, Ngoc Nga Vinh, Ludivine Breger, Rike Zieltow, Zübeyde Bayram-Weston, Claris Diaz, Amy Evans, and last but not least Victoria Roberton, who have provided support, advice and inspiration when it was required. I owe my gratitude to Kate Shires and Mariah Lelos for their invaluable assistance with statistical analyses, without you I would have never been on speaking terms with SPSS. I would like to thank Anne-Marie McGorrian for the help and support she has given me over the years. Thank you all for creating a friendly, exciting and inspirational atmosphere in which to work.

Finally, yet importantly, I would like to express my heartfelt thanks to my beloved parents for their blessings, my partner and my friends for their help and wishes for the successful completion of this project.

List of abbreviations

µl: microlitres

µm: micrometres

^{18}F-dopa: ^{18}fluorodopa

3-NT : 3-nitrotyrosine

5-HT: serotonin

6-OHDA: 6-hydroxydopamine

ANOVA: analysis of variance

AP: stereotaxic coordinates on the anterior-posterior axis from bregma

bLHL: basic helix-loop-helix

BrdU: 5-Bromodeoxyuridine

CA: catecholamine

cm: centimetres

CRL: crown-rump length

CV: Cresyl Violet

DA: dopamine

DAB: diaminobenzidine tetrahydrochloride hydrate

DAT: dopamine transporter

DBS: deep brain stimulation

DMEM: Dulbecco's minimum Eagle Medium F-12

DNA: deoxyribonucleic acid

DNAse: deoxyribonuclease I from bovine pancreas

DPX: di-styrene plasticizer and xylene mounting medium

DV: stereotaxic coordinates deep from dura

E: embryonic day

EIF4G1: eukaryotic translation initiation factor 4 gamma 1

FoxA2: forkhead/winged helix A2

FP: floor plate

g: grams

GABA: γ-amino butyric acid

GID: graft induced dyskinesia

Girk2: G-protein-activated inward-rectifier potassium channel 2

GLM: general linear model

GPe: globus pallidus external

GPi: globus pallidus internal

HBSS: Hanks' balanced salt solution

HCl: hydrochloric acid

hESCs: human embryonic stem cells

HNPCs: human neural progenitor cells

hPSCs: human pluripotent stem cells

i.p.: intra-peritoneal

IHC: immunohistochemistry

iPSCs: induced pluripotent stem cells

-ir: immunoreactive

kg: kilograms

LB: Lewy body

LC: locus coeruleus

L-DOPA: L-3,4-dihydroxyphenylalanine

LID: L-DOPA-induced dyskinesia

Lmx1a: LIM homeobox transcription factor 1

LRRK2: leucine-rich repeat kinase 2

MAO-B: B monoamine oxidase

MFB: medial forebrain bundle

mg: milligrams

min: minutes

ml: millilitres

ML: stereotaxic coordinates lateral from the midline

mm: millimetres

mM: millimolar

MPTP: 1-methyl-4-Phenyl-1,2,3,6-Tetrahydropyridine

mRNA: messenger ribonucleic acid

MTOP: medical terminations of pregnancies

N.Acc: Nucleus Accumbens

NA: noradrenaline

NeuN: Neuronal Nuclei

Ngn2: Neurogenin-2

NMDA: N-Methyl-D-aspartic acid

Nurr1: Nuclear receptor related-1

PARK2: parkin

PBS: phosphate buffered saline

PD: Parkinson’s disease

PET: positron emission tomography

PFA: paraformaldehyde

PFC: prefrontal cortex

PINK1: phosphatase and tensine homolog (P-TEN)-induced putative kinase 1

Pitx3: pituitary homeobox 3

rpm: rotations per minute

RRF: retrorubral field

s.c.: subcutaneously

SD: Sprague Dawley

SEM: standard error of mean

Shh: sonic hedgehog

SNpc: substantia nigra pars compacta

SNpr: substantia nigra pars reticulata

STN: subthalamic nucleus

TBS: TRIS buffered saline

TGF-*β:* transforming growth factor

TH: tyrosine hydroxylase

TNS: TRIS non-saline buffer

TXTBS: 0.2% Triton-X-100 TBS

VEGF: vascular endothelial growth factor

VIM: thalamic ventralis intermedius nucleus

VM: ventral mesencephalon

VPS35: vacuolar protein sorting 35

VTA: ventral tegmental area

Table of Contents

Chapter 1. General Introduction

1.1 Mesencephalic dopamine neuron system in the brain

1.1.1 Anatomy of the ventral mesencephalon

The study of dopamine (DA) neurons and their axonal projections in the brain goes back to the early 1960s and it is now one of the best known neurotransmitter systems. Catecholamine (CA) DA neurons together with noradrenaline (NA) neurons were first identified in discrete neuronal systems in the brain using formaldehyde histofluorescence method (Carlsson et al., 1962, Falck et al., 1962). Immunohistochemistry (IHC) for tyrosine hydroxylase (TH), a rate-limiting DA-synthesizing enzyme, was introduced in the 1970s and allowed mapping of CA systems more accurately and distinction of different CA neuron types. Whilst the use of TH IHC has confirmed the original anatomical organisation and projection patterns of DA systems, it has also revealed large numbers of cells labelled with TH that were negative for DA or NA in striatal and cortical areas in primates and humans (Kohler et al., 1983, Gaspar et al., 1985, Gaspar et al., 1987). Even though TH expression is not exclusive to DA neurons throughout the whole brain, TH IHC accurately identifies DA neurons in the ventral mesencephalon (VM) and because there are no NA neurons in this structure all TH-immunoreactive (TH-ir) cells in the VM can be safely considered to be DA-producing neurons.

In the rat VM, between 21,000 – 25,000 DA neurons (bilaterally) are located in the substantia nigra pars compacta (SNpc), around the same number of DA neurons make up the ventral tegmental area (VTA) and approximately 2,600 – 6,100 DA neurons reside in the retrorubral field [RRF; (German and Manaye, 1993, Nair-Roberts et al., 2008)]. Each DA neuron of the SNpc makes thousands of synaptic connections with striatal neurons. The proportions of DA cell populations in the VM differ between species, e.g. the total number of DA neurons in the VM is between 160,000 – 320,000 in rhesus monkeys and 400,000 – 600,000 in humans, with >70% of the neurons making up the SNpc (Emborg et al., 1998, Chu et al., 2002). This phylogenetic increase in the total number of DA neurons and the proportion of SNpc DA neurons follows the expansion of the DA innervated neocortex, which receives many more ascending DA projections in humans than rodents.

Out of nine DA neuron cell groups in the brain three are present in the mammalian VM, namely the A8 type DA neuron population in the RRF, the A9 type in the SNpc and the A10 type in the VTA (Dahlstrom and Fuxe, 1964). In a very

simplified model, the A9 type DA neurons in the SNpc and their ascending axonal projections to the dorsolateral striatum comprise the nigrostriatal pathway while the A10 type DA neurons in the VTA extend their axons to the limbic and cortical areas along the mesolimbic and mesocortical pathways, respectively. However, a number of studies have shown that different populations of DA neurons are intermixed within the VM regions but their ascending axonal projections rarely (1-5% of cases) deviate from their primary pathway (Fallon and Loughlin, 1982, Loughlin and Fallon, 1984). Cells located in the ventral tier of the SNpc as well as the ventrolateral region of the VTA and the A8 cell group innervate the dorsolateral striatum (Gerfen et al., 1987, Prensa and Parent, 2001). These DA neurons are angular in shape, most express G-protein-activated inward-rectifier potassium channel 2 (Girk2) and high levels of DA transporter (DAT) and comprise the nigrostriatal pathway (Hurd et al., 1994, Thompson et al., 2005, Reyes et al., 2012). The VTA and the dorsal tier of the SNpc contain DA neurons which together with A8 type DA neurons project to the more central and ventral striatum and prefrontal cortex (PFC) as well as to the matrix compartment of the dorsal striatum (Gerfen et al., 1987, Lyndbalta and Haber, 1994, Williams and Goldman-Rakic, 1998). These cells are relatively round in shape, mostly expressing calcium binding protein, calbindin, and low levels of DAT (Hurd et al., 1994, Thompson et al., 2005, Reyes et al., 2012) and are the key players in the mesolimbic and mesocortical pathways that are implicated in reward and reinforcement behaviours, and cognitive behaviours (reviewed in Schultz, 2007). However, recent studies suggest that strong levels of Girk2 protein are also detected in DA neurons in the dorsal tier of the SNpc in mice and humans (Reyes et al., 2012). Interestingly, although the A9 type and A10 type DA neurons are very different both functionally and morphologically, they share up to 97% of their genetic profile (Grimm et al., 2004, Chung et al., 2005, Greene et al., 2005).

1.1.2 Regulation of movement via nigrostriatal dopamine neurotransmission

The basal ganglia and the frontal cortex operate together to orchestrate and execute planned, motivated behaviours involving motor, cognitive and limbic circuits. The subcortical nuclei of the basal ganglia include the caudate nucleus and the putamen (together they form striatum in primates), the external and internal (entopeduncular nucleus in rodents) segments of the globus pallidus (GPe and GPi, respectively), and three closely related structures, the subthalamic nucleus (STN), VTA, and the SN [both SNpc and SN pars reticulata (SNpr)]. The A9 type DA neurons in the SNpc project and release DA in the caudate nucleus and the putamen regulating the coordination of

movement via modulation of the cortical and thalamic inputs (Carlsson and Carlsson, 1989, Brotchie et al., 1991).

The most authenticated working model of the basal ganglia is the direct and indirect pathway model first described in the 80s (Ilinsky et al., 1982, Deniau and Chevalier, 1985). According to this model, the striatum is the main input structure to the basal ganglia. It receives all glutamatergic cortical signals and relays them to the output nuclei of the basal ganglia, GPi and SNpr, via two distinct pathways, enroute to the thalamus which provides glutamatergic input back to the cortex. The monosynaptic connection of the striatum to the GPi is called the "direct pathway" while the polysynaptic connection of the striatum to the GPi/SNpr via the GPe and then STN is referred to as the "indirect pathway". In the direct pathway, the DA input from the SNpc to the putamen activates a population of striatal γ-amino butyric acid (GABA)-ergic medium spiny neurons, that express dynorphin and substance P, via DA binding to the D_1-family receptors (Gerfen et al., 1990). These GABA-ergic neurons in the putamen provide an inhibitory input to the GPi, which in turn projects GABA-ergic fibres to the thalamus. Thus, activation of the direct pathway results in the reduced inhibition of the thalamus. In the indirect pathway, release of DA in the striatum inhibits a population of GABA-ergic neurons, that express enkephalin, via DA binding to the D_2-family receptors (Gerfen et al., 1990). This leads to a reduced inhibition of the GPe and increases a GABA-ergic output from the GPe to the STN, which provides an excitatory input to the GPi and SNpr. Reduced activity of the STN causes lower excitation of the GPi/SNpr and, in turn, leads to the reduced GABA-ergic input to the thalamus. Thus, normal basal ganglia functions are achieved when coordinated balance in the cortical and thalamic excitation from the direct and indirect pathway is modulated via DA neurotransmission. This oversimplified basal ganglia model has been updated with the inclusion of reciprocal connections between functionally related regions and non-reciprocal pathways between functionally different regions of the basal ganglia, and reviewed in details elsewhere (Haber, 2003).

Hypokinetic (e.g. Parkinson's disease) and hyperkinetic (e.g. Huntington's disease) movement disorders of basal ganglia origin are thought to result from the imbalance in the activity of the two pathways (Reiner et al., 1988, Waters et al., 1988, Albin et al., 1989). Failure of the nigrostriatal DA neurotransmission in Parkinson's disease and its restoration are discussed in-depth in the following sections.

1.2 Parkinson's disease

Parkinson's disease (PD) is the most common neurodegenerative movement disorder that presents in the second half of the 6th decade of life in majority of patients. The incidence of the disease rises steeply with age, from 1% of the population at 65 years of age suffering from PD to up to 9% of people being affected by the age of 80, with a lifetime risk of developing the disease of 1-5% (deRijk et al., 1995, Lang and Lozano, 1998, Bower et al., 1999). However, one in five affected persons develops the disease before they are 50 years old, a case of "early-onset PD". The mean lifespan of PD patients is 15-20 years from the time of diagnosis, depending on the age at onset, with a mortality rate 1.5 times higher than in unaffected individuals of the same age (Katzenschlager et al., 2008, Fahn, 2009). The cause of death is usually a concurrent unrelated illness or a condition, which develops due to the effects of decreased mobility, increased falling with subsequent trauma or respiratory disturbances. For instance, pneumonia has been identified as independent predictor of mortality among PD patients in nursing homes (Fernandez and Lapane, 2002). A number of studies have identified gender as a risk factor with men being 1.5 times more likely to develop PD than women, however these findings appear to be restricted to western populations over the age of 70 (Twelves et al., 2003, Wooten et al., 2004).

In 1817, the first formal complete description of what later became known as PD was published by the English physician James Parkinson in a slim monograph entitled "An Essay on the Shaking Palsy", in which he described 6 patients presenting with "*Involuntary tremulous motion with lessened muscular power, in parts not in action and even when supported: with a propensity to bend the trunk forwards and to pass from a walking to a running pace: the senses and intellect being uninjured*" (reprinted: Parkinson, 2002). In recognition of his clear description of the unrecognized disorder, the syndrome was named after James Parkinson in 1877 by Jean Martin Charcot, the "father of neurology", who referred to the condition as "maladie de Parkinson" (Parkinson's disease). Although physicians have found fragmentary descriptions of PD in Sanskrit texts, Egyptian hieroglyphics, the Ayurvedic and biblical texts (Stern, 1989), none were as complete and satisfying as that provided by Parkinson. Numerous accounts of PD incidents made by different civilisations over the centuries make it highly unlikely for race, creed or historic events, such as industrial revolution, to be related to the causes of the disease (Lees et al., 2009). Indeed, although important

genetic and environmental clues have been identified, the exact causes of PD remain unknown.

1.2.1 Symptoms and diagnosis

Currently, the diagnosis of PD relies on clinical criteria; no definitive test for PD has yet been developed. An accurate diagnosis in early stages of the disease remains an extremely challenging task because a number of other neurological disorders such as multiple system atrophy, diffuse Lewy body disease, vascular parkinsonism and progressive supranuclear palsy, collectively called Parkinsonian syndromes, may present with similar symptoms (Wenning et al., 1995, Zijlmans et al., 2004, Williams and Lees, 2005). Therefore, initial diagnosis of PD is based on the assessment of the cardinal motor symptoms that were described by James Parkinson, associated and exclusionary symptoms, and is later confirmed by a substantial (70-100%) clinical response to levodopa therapy (Gelb et al., 1999, Lees et al., 2009). Although PD affects both sides of the body, it always presents with an asymmetrical onset of symptoms and this criterion is one of the associated symptoms used to confirm the diagnosis. However, only post-mortem histopathological examination of the brain can provide definitive proof of the disease.

PD is diagnosed when a combination of at least two cardinal motor deficits is present: unequivocal bradykinesia with either tremor at rest, muscle rigidity or loss of postural reflexes. Bradykinesia is the most characteristic clinical feature of PD and refers to slowness of spontaneous movements and gesturing (Berardelli et al., 2001), reduced reaction times (Cooper et al., 1994), loss of facial expression, decreased blinking, impaired swallowing (Bagheri et al., 1999), and reduced arm swing while walking. PD is also characterised by a slow 4-6 Hz tremor of the hands during rest that disappears when the hand is engaged in a task or during sleep (Jankovic, 2008). Lower limbs are often affected by the resting tremor in early-onset PD patients while older patients might develop facial tremors of the jaw, chin, lips and tongue (Lees et al., 2009). Previous findings suggest that resting tremor presents in 69% of patients at disease onset (Hughes et al., 1993) and post-mortem clinical analysis of 65 patients revealed that all confirmed PD patients had tremor at some point (Rajput et al., 1991). One of the earliest manifestations of PD is muscle rigidity, which causes increased resistance to flexion, extension or rotation of a limb about a joint. However, it often presents 0-2 years before the onset of other cardinal PD motor symptoms and might easily be misdiagnosed as arthritis (Riley et al., 1989). Loss of postural reflexes occurs

in the late stages of the disease after manifestation of other clinical features. Freezing of gait is also very common in PD and presents in 50% of cases, affecting women less than men and manifesting less frequently in patients whose main symptom is tremor (Macht et al., 2007). Together with postural instability they are the main cause of falls in PD patients and, hence, the most disabling symptoms of the disease (Giladi et al., 2001, Williams et al., 2006). PD patients also develop a number of secondary motor abnormalities, including re-emergence of the primitive glabellar and palmomental reflexes (Brodsky et al., 2004), micrographia (Rao et al., 2003) and mirror movements of the limbs (Li et al., 2007). However, these symptoms are not specific for PD; they also manifest in other Parkinsonian syndromes and therefore are not used in the diagnosis of PD.

Although traditionally PD has been primarily regarded as a motor disorder, clinical observations and scientific research have uncovered a wide range of cognitive and psychiatric symptoms in PD patients in the last 8-10 years and have shifted this view towards a more widespread disruption of multiple brain systems caused by the disease. PD patients develop the following non-motor symptoms: cognitive impairments in different aspects of executive function (Hely et al., 2005), autonomic sexual and sweating dysfunctions (Pursiainen et al., 2007, Kotkova and Weiss, 2013), sleep disorders (Schenck et al., 2013), hyposmia (Wenning et al., 1995, Ponsen et al., 2004), depression (Aarsland et al., 2007), visual hallucinations (Williams and Lees, 2005, Aarsland et al., 2007). However, a detailed discussion of these symptoms is beyond the scope of this thesis and the reader is referred to some recent reviews of this topic (Chaudhuri and Schapira, 2009, Chaudhuri et al., 2011, Lima et al., 2012). Early onset hyposmia (Wenning et al., 1995) and late onset of visual hallucinations (Williams and Lees, 2005) might aid the initial diagnosis of PD and help rule out alternative Parkinsonian syndromes, respectively. Also, hyposmia (Ponsen et al., 2004) and rapid eye movement sleep behaviour disorder (Borek et al., 2007, Schenck et al., 2013) have been reported to manifest before the first motor symptoms of the disease appear and might serve as predictors for PD. However, none of the predictive tests have yet been developed into a clinical tool more effective than motor-based assessment.

1.2.2 Neurobiology of Parkinson's disease

PD is a progressive disorder characterised by a substantial loss of the melanised A9 type DA neurons in SNpc and subsequent failure to supply DA to the dorsal striatum (Kish et al., 1988). The putamen is severely affected by the loss of midbrain DA

neurons in the initial stages of the disease. Before any symptoms appear, compensatory upregulation of dopamine receptors occurs in the depleted striatum as revealed by animal studies and post-mortem studies of PD patients. The postsynaptic GABA-ergic neurons become hypersensitive and increase the number of DA receptors (Ungerstedt, 1971b, Heikkila et al., 1981). Simultaneously, the number of TH-positive neurons in the striatum increases several-fold as observed in parkinsonian monkeys (Betarbet et al., 1997, Palfi et al., 2002) and PD patients (Porritt et al., 2000, Porritt et al., 2006). This increase in TH-positive neurons is not due to neurogenesis of DA neurons in the striatum but is likely due to an upregulation of TH in GABA-ergic interneurons that are already present (Mao et al., 2001, Tande et al., 2006). This compensatory mechanism has only a transient beneficial effect and eventually chronic DA depletion causes degeneration of the spines of striatal projection neurons involved in the indirect pathway of the basal ganglia (Day et al., 2006). At the same time, the reduced nigral output to the striatum affects both the direct and indirect pathways resulting in the hyperactivity of the GPi and SNpr nuclei and causing strong inhibition of the thalamus and severely decreased excitatory output to the cortex and an overall decrease in motor behaviour (Gerfen et al., 1990). Thus, by the time patients present with clinically assessable motor symptoms, SNpc is already severely degenerated with up to 60% DA neuronal loss and 80% reduction in DA release in the striatum (Kish et al., 1988, Waters et al., 1988).

Neurodegeneration also occurs in other regions of the VM. The loss of the A8 type DA neurons in the RRF has been observed in PD patients with prominent tremor while this area was intact in patients without tremor (Rajput et al., 1991, Hughes et al., 1993). Degeneration of acetylcholine projections from the pedunculopontine nuclei has been observed in patients with gait and posture problems (Hirsch et al., 1987). NA neurons in the locus coeruleus (LC) degenerate in the later stages of the disease leading to a decreased NA levels in the hypothalamus, hippocampus and the cortex (Mann and Yates, 1983, Braak et al., 2003). Also, reductions in capacity for function have been reported in dorsal motor vagus nucleus, raphe nuclei and the nucleus basalis of Meynert and together with cell loss in LC have been associated with mental impairment in PD patients (Mann and Yates, 1983). Due to lesions in raphe nuclei, serotonergic (5-HT) input to the caudate putamen, frontal cortex and the hypothalamus is greatly reduced. Although neuron loss mainly occurs in the SNpc, widespread neurodegeneration of multiple cell populations in different regions of the brain and their association with manifestation of different symptoms in patients highlight the important fact that PD is a

heterogeneous disease. This has significant implications for the treatment of disorder which will be discussed further in this chapter.

1.2.3 Lewy bodies

Intracellular Lewy body (LB) formation has been associated with a number of neurodegenerative diseases including PD, Parkinsonian syndromes, depression and Alzheimer's disease (Spillantini et al., 1997, Arima et al., 1998, Baba et al., 1998, Masliah et al., 2001, Braak et al., 2003). However, the composition of LBs differs between the diseases. Post-mortem studies of patients with PD revealed that intracellular inclusions in the tissue contained aggregates of phosphorylated filamentous proteins mainly consisting of α-synuclein protein, and to a lesser extent of ubiquitin protein (Lowe et al., 1988, Gibb and Lees, 1989, Spillantini et al., 1997, Baba et al., 1998, Braak et al., 2003, Kuusisto et al., 2003). The diagnosis of PD is confirmed post-mortem if, in addition to extensive DA neuron loss in the SNpc, there are LBs present in the brain. Intracellular inclusions are found in all major regions of the brain affected with PD including the SNpc, LC and the cortex. The exact role of LB in aetiology of PD, however, remains unknown because they are also sparsely distributed throughout a normal aged brain (Parkkinen et al., 2001, Bloch et al., 2006). LB formation has been observed in the autonomic nuclei of the spinal cord, peripheral autonomic nervous system and the olfactory nerves in neurologically unimpaired elderly subjects (Bloch et al., 2006). Autonomic failure has been reported as a pre-motor symptom of PD which suggests that neurodegeneration might first occur outside the central nervous system in autonomic postganglionic neurons (Kaufman et al., 1983). Also, the appearance of LBs seems to follow the onset of symptoms with the first intracellular inclusions appearing in the dorsal efferent motor nucleus of the vagus nerve and in the anterior olfactory nucleus (Braak et al., 2003). Thus, early LB formation in these areas might contribute to the initial non-motor symptoms of the PD including loss of smell, constipation and other autonomic dysfunctions. LBs then spread through the brainstem and the basal forebrain in the ascending pattern [raphe nuclei – LC – amygdala – SNpc (which corroborates the manifestation of motor symptoms)] before propagating to the anteromedial temporal mesocortex, the higher order sensory association neocortex, the PFC and eventually reaching the primary sensory and motor cortical areas (Braak et al., 2003). While the propagation of LBs seems to generally correspond to the onset of symptoms as PD progresses, LB density does not appear to correlate with the neuronal loss, the severity of clinical symptoms or the disease duration (Galvin et al., 2006,

Libow et al., 2009, Greffard et al., 2010). A recent study revealed that most of the α-synuclein aggregates, much smaller than LBs, were located at the presynapses of neurons and, while the presynapses were relatively preserved, dendritic spines were retracted suggesting a neurotransmitter deprivation (Kramer and Schulz-Schaeffer, 2007). This raises an alternative hypothesis that smaller aggregates of proteins, not LBs, play a role in neurodegeneration via modulation of neurotransmitter release (Lundblad et al., 2012).

1.2.4 Aetiology of Parkinson's disease

Although several environmental and genetic risk factors have been identified, the cause of PD is still as elusive now as it was in 1817 when the condition was first described. The majority of PD cases are sporadic (idiopathic) and only 15 to 20% of PD patients have an affected first-degree relative (Samii et al., 2004, McDonnell et al., 2006). Therefore, most PD patients are believed to have a complex aetiology due to an interaction of genetic and environmental factors.

1.2.4.1 Genetic risk factors

To date, molecular genetic analyses of familial cases of PD have improved understanding of the disease mechanisms underlying PD pathology and identified mutations in seven disease associated genes: α-synuclein (Polymeropoulos et al., 1997), leucine-rich repeat kinase 2 [LRRK2, (Funayama et al., 2002, Zimprich et al., 2004)], parkin [PARK2, (Kitada et al., 1998)], phosphatase and tensine homolog (P-TEN)-induced putative kinase 1 [PINK1, (Valente et al., 2004)], DJ-1 (Bonifati et al., 2003), eukaryotic translation initiation factor 4 gamma 1 [EIF4G1, (Chartier-Harlin et al., 2011)], and vacuolar protein sorting 35 [VPS35, (Vilarino-Gueell et al., 2011, Zimprich et al., 2011)]. Mutations in the α-synuclein, LRRK2, EIF4G1 and VPS35 genes are implicated in the autosomal dominant late-onset forms of PD while mutations in the PARK2, PINK1 and DJ-1 genes are associated with the autosomal recessive early-onset PD. Familial cases of PD follow a Mendelian distribution. Mutations in several genes have been implicated in sporadic forms of PD such as α-synuclein muations (Michell et al., 2005, Kay et al., 2008), LRRK2 mutations (Puschmann et al., 2012), and PINK1 mutations (Valente et al., 2004). Also, LRRK2 mutations are the most common genetic risk factors for PD due to their location within a common haplotype (Di Fonzo et al., 2005, Lesage et al., 2006).

Overexpressed α-synuclein is misfolded and aggregated to form LBs predominantly in neurons and to some extent in glial cells, as revealed by post-mortem studies of PD patients (Spillantini et al., 1997, Braak et al., 2003). Additionally, pathological studies from autopsies report LBs in carriers of PINK1 mutation and one variant of LRRK2 mutation (G2019S) but not in carriers of PARK2 mutations or other LRRK2 mutations (Samaranch et al., 2010, Poulopoulos et al., 2012). PARK2 and PINK1 mutations lead to cell loss restricted to the VM. Heterozygous PARK2 carries have been associated with LB pathology (Pramstaller et al., 2005). Patients with mutations in the α-synuclein develop more severe autonomic dysfunction and cognitive decline than normal PD patients (Zarranz et al., 2004, Somme et al., 2011). Mutations in LRRK2, PARK2 and PINK1 genes have been associated with the impairment of autophagy-lysosomal pathways which, in turn, might result in the increased accumulation of α-synuclein protein and induce neurotoxicity in nigral DA neurons (Narendra et al., 2008, Narendra et al., 2010, Dehay et al., 2013). PINK1 and DJ-1 have been implicated in mitochondrial functions and mutations in the genes might disrupt the normal activity of the mitochondria leading to abnormal oxidative stress in cells and eventually cell death (Martinat et al., 2004, Narendra et al., 2010). However, the exact link between mutations in these genes and DA neuron loss in the SNpc and non-motor symptoms of PD remains unknown.

1.2.4.2 Environmental risk factors

The majority of sporadic PD cases occur without a known definite cause. Thus, it is more likely that a combination of genetic and environmental factors is implicated in the onset of idiopathic PD. Epidemiological studies revealed age (Bennett et al., 1996, Morens et al., 1996) and 1-methyl-4-Phenyl-1,2,3,6-Tetrahydropyridine [MPTP, (Davis et al., 1979, Langston et al., 1983)] as two environmental risk factors for PD. The A9 type DA neurons are more vulnerable to MPTP toxicity and repeated exposure to MPTP results in severe DA cell loss in the SNpc (Langston et al., 1984, Chung et al., 2005). Further studies failed to produce strong evidence for other environmental factors (Elbaz and Moisan, 2008). However, Paraquat, a widely used herbicide, has been shown to exert neurotoxic effects on DA neurons in the SNpc and therefore has been associated with an increased risk of PD incident; however, its penetration to the brain is highly limited by the blood-brain barrier (Naylor et al., 1995, McCormack et al., 2002). Also, insecticide rotenone (Betarbet et al., 2000) and fungicide Maneb (Hertzman et al., 1990, Thiruchelvam et al., 2000) have been proposed as potential risk factors of PD, however,

the evidence in literature is inconsistent and has been challenging to replicate in animal models of PD.

Oxidative stress (Martinat et al., 2004), mitochondrial dysfunction (Narendra et al., 2008), environmental toxins (Elbaz and Moisan, 2008), cerebral ischemia, and excitotoxicity (Lotharius and Brundin, 2002) have all been proposed as possible mechanisms implicated in PD onset. Mitochondrial dysfunction caused by either environmental toxins or genetic mutations, or the interaction between the two, may induce excitotoxicity and oxidative stress in neurons leading to protein isoforms accumulating within cells and eventually the onset of neurodegeneration (Betarbet et al., 2002). Even though three different populations of DA neurons form a continuous sheet throughout the midbrain, they exhibit different degrees of vulnerability to oxidative stress induced by the administration of neurotoxins, and results are consistent between animal models and patients with PD (Burns et al., 1983, Schneider et al., 1987, Gibb and Lees, 1991, German et al., 1996, Hung and Lee, 1998, Grant and Clarke, 2002, McCormack et al., 2006). The A9 type DA neurons in the ventral SNpc are the most vulnerable population, most likely due to the huge metabolic load they experience in order to sustain signalling with hundreds of thousands of target neurons (Lotharius and Brundin, 2002, Smits et al., 2006). The concept of free radical involvement in selective neurodegeneration is supported by increased basal lipid peroxidation in SNpc in PD patients (Dexter et al., 1989). Interestingly, the same cellular mechanisms have been proposed to cause neuronal loss in normal ageing and PD and a combination of genetic and environmental factors in PD might just accelerate an already ongoing process in the ageing brain (Collier et al., 2011).

1.3 Animal models of Parkinson's disease

Animal models are research tools of paramount importance to study the pathogenesis and progression of human diseases as well as for the testing of novel therapeutics. Like many other human diseases, PD does not naturally occur in animals and, therefore, has to be artificially initiated. PD is a complicated multi-symptom disease with unclear molecular mechanisms for the observed pathology, which makes it hard to model. To date, no single animal model exists that would fully capture PD but there are a number of models available that incorporate particular aspects of the disease pathology and the choice of a suitable model always depends on the planned study, i.e.

the research question. Methods to induce DA neuron loss range from neurotoxins to overexpression and down-regulation of disease-related genes.

1.3.1 6-hydroxydopamine model

First demonstration of neurotoxic effects of 6-hydroxydopamine (6-OHDA) and the development of a 6-OHDA rat model of PD took place in the 1970s (Ungerstedt, 1968, Ungerstedt and Arbuthnott, 1970). The neurotoxin 6-OHDA was demonstrated to be effective to the same extent in other species as well, e.g. mice, monkeys, cats, and dogs (Bezard et al., 1998). Only CA neurons are affected by the toxin while other cell types are spared because the neurotoxin 6-OHDA has a similar structure to DA and NA and is reuptaken by CA neurons through transporters in the membrane (Breese and Traylor, 1971). The toxin has an inhibitory effect on the mitochondrial compounds I and IV and two components that it produces inside the cells, hydrogen peroxide and paraquinone, are highly toxic (Glinka et al., 1997). Such high selectivity makes the 6-OHDA toxin a perfect tool to target DA and/or NA pathways in the brain (Ungerstedt and Arbuthnott, 1970, Lotharius and Brundin, 2002, Blandini et al., 2008, Terzioglu and Galter, 2008). The neurotoxin cannot cross the blood-brain barrier and therefore is directly injected in to the brain regions of interest. Bilateral 6-OHDA lesions induce severe motor impairment, inability to swallow, absence of thirst, and may lead to death of animals (Ungerstedt, 1971a, Smith and Young, 1974). In contrast, unilateral lesions of SNpc, medial forebrain bundle (MFB) or the striatum are well tolerated by the animal, resulting in asymmetrical behavioural deficits with the benefit of the intact side of the brain providing an internal control (Ungerstedt et al., 1973). Administration of DA agonists, such as methamphetamine, is routinely used in the assessment of 6-OHDA lesions, by quantification of net circling behaviour towards the lesioned side. This occurs when the intact striatum is flooded with DA and drives ipsilateral rotations (Ungerstedt, 1971c). The magnitude of such behaviour depends on the degree of the lesion (Ungerstedt and Arbuthnott, 1970, Ungerstedt, 1971c, Torres et al., 2011). Similarly, other motor tests and sensory tests (e.g. stepping test, cylinder test, nose-poking tests, etc.) assess the extent of DA depletion by comparing behavioural impairments on the two sides of the body (Dowd and Dunnett, 2005a, Dowd and Dunnett, 2005b). This model has been widely used to assess the efficacy of new drugs, cell transplantation and gene therapies in reducing DA imbalance (Jiang et al., 1993, Collier and Sortwell, 1999, Bjorklund et al., 2002, Kirik et al., 2002, Dowd and Dunnett, 2004, Torres et al., 2007, Torres et al., 2008a, Grealish et al., 2010, Back et al.,

2013). Apart from selective DA neuron loss in SNpc, 6-OHDA lesion model does not mimic any other features of PD pathogenesis. Nevertheless, it remains a relatively cheap and very useful model to understand DA function, assess replacement of lost DA neurons and restoration of DA supply to the striatum. Thus, this model was chosen for the research presented here.

1.3.2 MPTP model

The administration of another neurotoxin MPTP in mice, rats, monkeys, and guinea pigs, induces parkinsonian motor symptoms and mitochondrial dysfunction (Chiueh et al., 1984, Langston et al., 1984, Doudet et al., 1985, Gerlach et al., 1991, Heikkila and Sonsalla, 1992, Gerlach et al., 1996, Yazdani et al., 2006). MPTP can also induce such hallmarks of PD as motor impairments, oxidative stress, energy failure and inflammation in humans (Langston et al., 1983). MPTP crosses the blood-brain barrier and is metabolized by astrocytes into the toxic MPP^+, which then enters neurons via DAT where it inhibits complex 1 of the mitochondria causing oxidative stress and degeneration of the cell (Javitch et al., 1985). Both acute and chronic models of PD using different doses of MPTP have been developed over the years (Bezard et al., 1997, Iravani et al., 2005, Blesa et al., 2010). Susceptibility to MPTP, however, is highly variable between different mouse strains (Terzioglu and Galter, 2008) and was found to be lower in rats than in mice (Chiueh et al., 1984). Moreover, MPTP models lack inclusions and LB formation in the brain (Forno et al., 1993, Halliday et al., 2009). However, chronic administration of MPTP is probably the best model of PD in non-human primates, as characterised by cardinal motor dysfunctions and responsiveness to levodopa therapy. Electrophysiological studies using this model identified the STN as a target for deep brain stimulation to alleviate motor symptoms and led to the emergence of this therapy in PD patients (Bergman et al., 1990, Limousin et al., 1995). The MPTP model has been used in genetically modified mice to study molecular mechanisms of PD (Vila et al., 2001, Dauer et al., 2002, Thomas et al., 2011) whereas MPTP models in monkeys are used to evaluate behavioural and non-motor symptoms of PD (Vezoli et al., 2011).

1.3.3 Other neurotoxin models

Striatal DA deficiency can be induced by pharmacological agents and environmental toxins to model symptoms of PD. Reserpine was the first such agent to

be used in rabbits. The mechanism behind reserpine induced akinesia is disruption of monoamine storage in synaptic vesicles (Carlsson et al., 1957). The same effect was later demonstrated in monkeys (Windle and Cammermeyer, 1958). Restoration of this deficit could be achieved by levodopa therapy (Carlsson et al., 1957, Gossel et al., 1995). This provided evidence that DA depletion of the striatum causes motor symptoms of PD and eventually led to the development of the first neurotransmitter replacement therapy for the treatment of PD. However, reserpine provided only transient DA depletion of the striatum and did not cause any morphological changes in the DA neurons in SNpc.

As mentioned earlier, evidence from PD patients and animal models suggests that oxidative stress and free radicals are involved in neurodegeneration (Dexter et al., 1989, Yoritaka et al., 1996, Cassarino et al., 1997). Protein nitration is affected when neurons are subject to oxidative stress as seen from animal models and PD patients (Good et al., 1998, Giasson et al., 2000, Yu et al., 2010). Free 3-nitrotyrosine (3-NT) induced oxidative stress in the striatum of mice caused loss of DA neuronal terminals, degeneration of DA neurons in SNpc and the development of motor deficits (Mihm et al., 2001). However, this model fails to mimic the progressive nature of PD, no protein aggregations and cellular inclusions were found in DA neurons. Similarly to the reserpine model, the free 3-NT model is very limited but could be used for antioxidant therapy screening.

Evidence from pesticide and herbicide models of PD is rather ambiguous with some studies showing a loss of DA neurons in SNpc after administration of paraquat (Brooks et al., 1999, McCormack et al., 2002) and other studies failing to replicate this (Thiffault et al., 2000, Thiruchelvam et al., 2000). Rotenone has also been used to model PD in mice (Inden et al., 2007, Inden et al., 2011) and rats (Betarbet et al., 2000, Alam et al., 2004). Although intravenous administration of rotenone has been shown to induce damage to DA neurons, α-synuclein aggregations and LB-like formation as well as oxidative stress and gastrointestinal problems in rats (Sherer et al., 2003, Cannon et al., 2009), again this has been difficult to reproduce in mice and monkeys (Ferrante et al., 1997, Thiffault et al., 2000, Kordower et al., 2006) and evidence of DA neuron loss in SNpc is slim (Wu and Johnson, 2011). It is not clear whether this model has any advantages over 6-OHDA or MPTP models. Furthermore, there is no strong evidence for rotenone-induced PD in humans (Blesa et al., 2012).

1.3.4 Genetic models

Discovery of rare genetic mutations in familial cases of PD led to the development of transgenic animal models of PD (Dawson et al., 2010). Two mutations (A53T, A30P) in the α-synuclein gene have been linked to PD (Kruger et al., 1998). Mice expressing A53T human α-synuclein show severe motor phenotype and eventually paralysis as well as having LB-like inclusions but show no DA neuron loss in SNpc (Masliah et al., 2000, Giasson et al., 2002). This phenotype, however, is not found in A30P transgenic mice. Knockout models of α-synuclein showed that the loss of this protein has no effect on neurodegeneration (Blesa et al., 2012). A Drosophila knockin model of PD results in motor deficits, DA neuron loss, reduced TH expression in SNpc and intracellular inclusions (Feany and Bender, 2000). However, the exact function of α-synuclein is still elusive, let alone its involvement in PD. Similar to α-synuclein, knocking out LRRK2 has no effect on neuronal death and overexpression of LRRK2 in mice produces a only a minimal level of neurodegeneration (Li et al., 2009). Transgenic PARK1, DJ-1, and PINK1 animal models do not demonstrate any of the cardinal features of PD, only in PINK1 knockout mice is DA release in the striatum reduced (Moore and Dawson, 2008). Transgenic models are good tools for discovery of gene functions and modelling developmental diseases but generally fail to model disease of ageing. Recently, conditional transgenic models have become available, which allow genes to be switched on and off at adult age and it has been demonstrated that shutting down PARK1 expression in adult mice causes DA neuron loss in SNpc (Shin et al., 2011). However, these types of models require high levels of mouse breeding expertise and are very laborious to generate and maintain. Another problem with transgenic mouse models of PD is that mouse life span might not be long enough to allow accurate modelling of PD. In other words, the role of age in aetiology of PD has to be borne in mind when working and translating any findings from rodent transgenic models.

1.4 Conventional treatments for Parkinson's disease

There is no therapy available to cure PD, current treatments only alleviate the symptoms and substantially improve quality of life but do not stop the progression of the disease. Deep brain stimulation (DBS) is the major surgical approach, with levodopa therapy still remaining the most effective pharmacological treatment available but due to its long-term severe side effects every effort is made to postpone its usage.

1.4.1 Early pharmacological treatments

Early medical interventions are aimed at stabilising levels of endogenous DA in the striatum by blocking its metabolisation. The selective type B monoamine oxidase (MAO-B) inhibitors, selegiline and rasagiline, when used as a mono-therapy, offer mildly effective symptomatic benefit as long as there is a sufficient number of DA terminals left in the putamen (Schapira, 2011, Pagonabarraga and Cruz Rodriguez-Oroz, 2013). Rasagiline has been implicated in the delayed disease progression and might act as a disease modifying agent (Akao et al., 2002, Maruyama et al., 2002). MAO-B inhibitors are also used in later stages of PD in combination with levodopa therapy to prolong the effect of the latter (Minguez-Minguez et al., 2013, Pagonabarraga and Cruz Rodriguez-Oroz, 2013).

Dopamine agonists are also used as a mono-therapy in the early stages of the disease to directly stimulate postsynaptic D_1 and D_2 receptors in the putamen (Perachon et al., 1999, Foley et al., 2004). They are slowly metabolised in the brain and provide a physiological and more continuous stimulation of the receptors than levodopa (Bonuccelli et al., 2009). They are a preferred first-line treatment in patients under the age of 55 but additional medical interventions are usually necessary within 3 years of diagnosis. DA agonists may also cause a wide range of side effects such as gastrointestinal problems, sleepiness and impulse control disorders but do not provoke dyskinesia (Lader, 2008, Lim et al., 2008, Micallef et al., 2009). The DA agonist Apomorphine is used as an adjunctive therapy to levodopa to help reduce motor fluctuations.

1.4.2 L-DOPA therapy

As the disease progresses and DA depletion of the putamen worsens, motor symptoms no longer respond to MAO-B and DA agonist mono-therapies. Therefore, all PD patients eventually require levodopa therapy. As mentioned in 1.3.3, administration of DA precursor L-3,4-dihydroxyphenylalanine (L-DOPA) to restore DA supply to the putamen was introduced nearly 60 years ago and has been the ‘gold-standard’ therapy in PD ever since (Carlsson et al., 1957, Birkmayer and Hornykiewicz, 1961, Worth, 2013). Peripherally administered L-DOPA is transferred across the blood-brain barrier through large amino acid transporters, and is converted into DA by remaining functional DA neurons and by 5-HT neurons and is stored in vesicles within neurons before being released in the synapse (Wade and Katzman, 1975, Carta et al., 2007). Uncontrolled

release of DA by 5-HT neurons, due to lack of feedback mechanisms, overstimulates DA receptors and the long-term effects of this can lead to severe and disabling motor complications (Cotzias et al., 1969, Rajput et al., 2002). Patients start to experience motor fluctuations between few hours of drug-induced "on" phase with therapeutic benefit and disease-induced "off" phase with behavioural decline and in severe cases immobility (Quinn, 1998, Obeso and Lang, 2006). The "off" phase is believed to occur due to impaired DA retention in the striatum caused by long-term administration of L-DOPA (Murata and Kanazawa, 1993). The "on-off" phenomenon reflects fluctuations in absorption, transport and plasma concentrations of the drug and continuous administration of L-DOPA produces a stable clinical state (Nutt et al., 1984, Pincus and Barry, 1987, Eriksson et al., 1988).

Hyperkinetic and dystonic involuntary movements, called L-DOPA-induced dyskinesias (LIDs), appear after long-term treatment and are the most disabling side effect of the levodopa therapy. LIDs are uncontrollable abnormal, sometimes painful, movements and postures affecting facial muscles, head, neck and in severe cases limbs (Thanvi et al., 2007, Goetz et al., 2008). Uncontrolled DA overstimulation of hypersensitive putamen by 5-HT neurons has been implicated in LIDs (Carlsson et al., 2007, Carta et al., 2007, Munoz et al., 2008). Dyskinesias, in large, are a more severe manifestation of "on-off" motor fluctuations with "on-phase" LIDs, in response to high concentrations of L-DOPA in the brain and plasma, being the most common. However, manifestation of dyskinesias varies between patients and LIDs may also occur during "off" phases or in between "on" and "off" phases. As the disease progresses, higher doses of L-DOPA, required to alleviate motor symptoms, inevitably contribute to the increased risk of developing dyskinesias and their severity once they appear as demonstrated by a dose-dependent onset and worsening of LIDs in healthy and MPTP-lesioned primates (Di Monte et al., 2000, Pearce et al., 2001) .

Motor symptoms respond to L-DOPA treatment for 10-15 years but, as the disease progresses, symptomatic relief starts to wane after about 5-10 years and 40% of patients develop LIDs after 4-6 years of treatment (Marsden, 1994, Ahlskog and Muenter, 2001, Obeso and Lang, 2006). The risk of developing dynkinesias increases with every additional year on medication. Current anti-dyskinetic amantadine therapy, a weak glutamate N-Methyl-D-aspartic acid (NMDA) antagonist, is efficient only for a few years in a subset of patients (Elahi et al., 2012). Continuous infusion of L-DOPA results in a stable clinical state with markedly reduced "on-off" motor fluctuations and LIDs in mild and severe PD patients (Nutt et al., 1984, Antonini et al., 2007). However,

this novel therapy is very expensive and requires an invasive surgery to implant L-DOPA intestinal-delivery system (Duodopa) and then subsequent constant maintenance of the portable Duodopa device. Also, cases of symptomatic peripheral neuropathy, sometimes severe, have been reported in patients receiving this treatment (Antonini et al., 2007, Manca et al., 2009, Muller et al., 2013).

Due to heterogeneous manifestation of the PD in patients, effects of drug treatments considerably vary from patient to patient. Thus, clinicians are faced with a challenging task of developing pharmacological therapies, via different combinations of drugs and dosages, almost on a patient to patient basis. Moreover, none of the current pharmacological treatments stop progression of the disease, restore the functional circuitry in the brain or provide DA delivery to the putamen in the physiological fashion. All these factors together with inevitability of the severe side-effects such as LIDs require the development of alternative therapies.

1.4.3 Surgical treatments

In the 1940s and 50s before the introduction of L-DOPA as a treatment for PD, surgical lesions to the thalamus, globus pallidus, caudate nucleus and STN were used to alleviate motor symptoms such as tremor, muscle rigidity, bradykinesia and dyskinesia (Meyers, 1942, Meyers, 1951, Krayenbuhl and Yasargil, 1960, Svennilson et al., 1960, Krayenbuhl et al., 1961). However, the damage induced by bilateral electrolytic or thermolesions was severe and irreversible and the lesions were not well tolerated. DBS of the same structures replaced surgical lesions in the late 1980s. DBS involves the bilateral placement of several electrodes most commonly in the STN, GPi and thalamic ventralis intermedius nucleus (VIM) that stimulate the areas concerned and block the abnormal signalling in those nuclei. An external controller allows the patient to switch the device on and off (Benabid et al., 1987, Siegfried and Lippitz, 1994, Limousin et al., 1995, Krack et al., 1998, Benabid et al., 1999, Caparros-Lefebvre et al., 1999). The optimal firing frequency, typically around 130 Hz, can be adjusted for each patient. All motor symptoms respond well to the stimulation of the STN, while stimulation of the VIM alleviates tremor and GPi stimulation most effectively treats LIDs and motor fluctuations (Benabid et al., 1999, Caparros-Lefebvre et al., 1999). In parallel to the DBS treatment, medication regimes are continued at lower doses which results in a further reduction in dyskinesias (Limousin et al., 1999, Mentzel et al., 2012). It is believed that DBS modifies irregular neuronal firing as demonstrated by animal studies (Lee et al., 2004, Chang et al., 2007), however, despite its widespread application, the

exact mechanisms underlying the effects of this therapy remain unclear. Similar to pharmacological treatments, DBS therapy only addresses the symptoms and does not have any effect on the progression of the disease. Neural transplantation is a more ambitious alternative approach to restore function, based on the idea that grafted foetal or stem cells can replace the lost DA neurons and their connections.

1.5 Cell transplantation therapy for Parkinson's disease

In the early 20th century, organ and tissue transplantation emerged as an exciting approach in medicine and research to replace and repair non-functional organs or parts of organs (Hamilton, 2012). Using cell transplantation to replace lost neurons, reverse the damage caused by neurodegeneration and restore normal function in the brain circuitry was an ambitious idea and attracted a lot of interest in the scientific community. One of the main early findings was that survival of the transplanted neural tissue in the host brain could be improved by using immature donor brain tissue from postnatal animals rather than adult brain tissue (Dunn, 1917). It was concluded that damage induced by severing axonal projections during tissue excision process was more detrimental in mature brains due to a highly complicated neuronal arborisation and the donor age was established as a very important factor influencing the efficacy of cell therapy. Precise targeting of specific brain regions for neural tissue transplantation in humans was not possible until the invention of the stereotaxic apparatus by two American neurosurgeons, Ernest A. Spiegel and Henry T. Wycis, in 1947 (reviewed in: Lasak and Gorecki, 2009). Also, the development of the strong immunosuppressive drug cyclosporine in the 1970s (Borel et al., 1976) allowed the progress of xenograft transplantation research and the start of clinical trials for transplantation in PD. Initally, patient's own adrenal medullar cells, which produce CA, were successfully used for transplantation into the putamen in two studies (Backlund et al., 1985, Madrazo et al., 1987) but the beneficial outcome of this approach was somewhat debatable because other studies found moderate improvement only in 19% of patients and associated this therapy with a high level of morbidity and mortality (Quinn, 1990, Goetz et al., 1991). Therefore, the focus of cell therapy research transferred to the use of foetal VM containing developing DA neurons obtained from surgical terminations of pregnancy.

1.5.1 Foetal cell transplantation in animal models

Considering that there is a substantial DA neuron loss in the SNpc by the time PD patients present with diagnosable motor symptoms, cell replacement therapy has been widely investigated as an alternative to pharmacological and DBS treatments since the late 1970s (Bjorklund and Stenevi, 1979, Perlow et al., 1979, Bjorklund et al., 1980a). During embryogenesis, DA neurons are born in the VM and extend axonal projections to the putamen guided by chemical signals forming the nigrostriatal pathway of the basal ganglia (Altman and Bayer, 1981, Specht et al., 1981, Bayer et al., 1995, Gates et al., 2004). Reconstruction of this pathway in the adult PD-affected brain presents a major challenge due to the large distance between the two cerebral targets that axons would have to cover and the absence of developmental chemoattractive and chemorepulsive cues. Adult myelinated pathways were shown to contain inhibitory factors that impede axonal growth and neural regeneration (Schnell and Schwab, 1990, Schwab, 1990). Indeed, animal studies confirmed that DA neurons transplanted into the SNpc alone did not achieve behavioural recovery in unilaterally 6-OHDA lesioned rats while single and multiple implants in the striatum reversed behavioural asymmetries (Dunnett et al., 1983). Similar studies in MPTP-lesioned monkeys showed no extensive axonal outgrowth rostrally along the MFB and modest but detectable behavioural improvement (Collier et al., 2002). Substantial restoration of efferent nigrostriatal connections and a lack of afferent striatonigral connections were demonstrated by ectopic transplantation of VM grafts into the rat striatum (Freund et al., 1985, Clarke et al., 1988, Doucet et al., 1989, Mendez et al., 1991). Transplantation of human foetal VM tissue into the cortex or ventricle adjacent to the DA-depleted striatum revealed target specific TH-ir fibre outgrowth in immunosuppressed rats (Stromberg et al., 1992). Also, the degree of graft-derived DA innervation of the putamen in primates was found to influence behavioural recovery (Redmond et al., 2008). Grafted DA neurons synthesised and released DA at rates characteristic of the intact nigrostriatal system (Schmidt et al., 1982) and exhibited normal electrophysiological profile (Wuerthele et al., 1981). While these studies provided proof that nigral grafts in the putamen were able to supply DA continuously in a physiological manner, they also revealed a lack of graft regulation by the host. Simultaneous intrastriatal and itranigral DA neuron transplantation or multiple graft placements along the MFB restored the pathway in the adult 6-OHDA lesioned rat brain and achieved a greater behavioural recovery (Dunnett et al., 1989, Mendez et al., 1996). Also, foetal VM grafts transplanted into the SNpc and

the STN promoted the sensorimotor behavioural recovery obtained by intrastriatal grafts (Mukhida et al., 2001). Similarly, combined transplantation of multiple foetal VM grafts into the stratum and foetal striatal grafts, rich in GABA-ergic neurons, into the the SNpc induced additive effects of behavioural recovery observed in the forelimb akinesia test (Winkler et al., 1999). Later studies associated focal graft placement, not widespread multiple grafting, in the striatum with the development of hyperkinetic forelimb and facial movements (Maries et al., 2006). These findings suggest that transplantation into the putamen alone is not sufficient to restore the basal ganglia circuit and complete functional recovery of complex motor behaviours in 6-OHDA models with selective loss of DA neurons let alone PD. Therefore, the main strategy in clinical cell transplantation has been to place multiple foetal VM grafts ectopically primarily into the putamen and in some cases also into the caudate nucleus.

Grafts transplanted as dissociated cell suspensions produced similar numbers of DA neurons as solid tissue grafts but induced a smaller host immune response (Bjorklund et al., 1980b, Bjorklund et al., 1983a, Bjorklund et al., 1983b, Freeman et al., 1995b, Redmond et al., 2008). Dissociation of the tissue into a cell suspension eliminates immunogenic vascular elements which might aid in the reduction of the immune response in the host brain. Animal studies in rodents and monkeys demonstrated that embryonic VM neurons must be collected for transplantation during the peak stage of DA neurogenesis when the neurons are already committed to the DA phenotype but before substantial outgrowth of axonal fibres occurs (Brundin et al., 1985a, Simonds and Freed, 1990, Annett et al., 1997). Transplantation of human foetal DA neurons into 6-OHDA lesioned immunosuppressed rats revealed that the best survival rates were achieved when the VM was derived from embryos aged 6 – 9 weeks after conception, Carnegie stage 15 – 23 (Freeman et al., 1995b). However, more recent studies in rodents, using rat embryonic VM, showed that transplantation of younger immature DA precursor cells improved the yield of TH-ir neurons in the graft and achieved a similar level of behavioural recovery (Torres et al., 2007, Torres et al., 2008a, Bye et al., 2012). These results further highlighted the donor age as an important parameter and drew a lot of interest in the scientific community towards the use of younger donor age tissue for cell transplantation therapy.

Detectable behavioural recovery was observed with only approximately 125 TH-ir neurons in the nigral grafts derived from rat embryos and transplanted into the striatum of 6-OHDA lesioned rats (Brundin et al., 1985a). A number of animal studies in mice and rats demonstrated that grafts containing at least 200 – 1000 DA neurons

ameliorated a range of lesion-induced deficits in drug-induced rotational behaviour, spontaneous locomotor activity, lateralised choice reaction time task, rotarod test and corridor test (Bjorklund et al., 1980a, Dowd and Dunnett, 2004, Chaturvedi et al., 2006, Kuan et al., 2007, Heuer et al., 2013b, Heuer et al., 2013a). Similarly, embryonic DA neurons transplanted into the striatum of 6-OHDA lesioned marmosets significantly reduced amphetamine-induced rotations (Annett et al., 1997). Recent studies showed that mouse VM grafts contained both the A9 and the A10 type DA neurons and transplants derived from younger embryos were both enriched for Girk2-ir DA neurons and contained reduced numbers of 5-HT neurons (Thompson et al., 2005, Jonsson et al., 2009, Grealish et al., 2010, Bye et al., 2012). The majority of DA neurons that co-labelled with Girk2 were found in the periphery of the graft while DA neurons in the centre of the graft predominantly coexpressed calbindin (Thompson et al., 2005, Bye et al., 2012). Mouse grafts enriched for the A9 type DA neurons and transplanted into 6-OHDA lesioned rats improved performance of animals on amphetamine-induced rotation test and cylinder test, while animals transplanted with the VM tissue selectively lacking in the A9 type DA neurons remained impaired (Grealish et al., 2010). The number of the A9 type DA neurons in the grafts was found to be an important determinant of the degree of rotational recovery, the recovery of sensorimotor function in paw-reaching test, and the level of LID recovery (Kuan et al., 2007). Yields of the TH-ir cells and the A9 type DA neurons were lower, although the differences were statistically insignificant, in animals that were treated with L-DOPA prior to transplantation as compared to animals that received graft treatment only. Another study demonstrated that pre-exposure to chronic L-DOPA treatment significantly reduces behavioural and neurochemical efficacy of foetal DA neuron grafts (Steece-Collier et al., 2009) These findings suggest that the A9 type DA neuron-enriched grafts can be derived from younger embryos and may be the key to an effective PD cell replacement therapy but that long-term L-DOPA treatment prior to transplantation might hamper the positive outcome.

1.5.2 Foetal cell transplantation in patients

Human foetal DA neurons used in transplantation research were derived from embryos collected from surgical terminations of pregnancies which raised important ethical questions that still remain subject to active debate (Boer, 1994). Nevertheless, based on the evidence obtained from animal studies the first open clinical trial of human foetal VM transplants started in 1989 in Sweden where 2 patients with MPTP-induced

parkinsonism received grafts into the putamen (Lindvall et al., 1989, Lindvall et al., 1990). The patients showed significant clinical improvement and positron emission tomography (PET) detected increased ^{18}fluorodopa (^{18}F-dopa) binding in the putamen 6 months after the surgery, marking the first milestone in the history of cell transplantation. A series of open labelled (Freed et al., 1992, Lindvall et al., 1992, Spencer et al., 1992, Molina et al., 1994, Peschanski et al., 1994, Freeman et al., 1995a, Levivier et al., 1997, Wenning et al., 1997, Kordower et al., 1998, Hagell et al., 1999, Brundin et al., 2000b, Mendez et al., 2002, Mendez et al., 2005) and two double-blind (Freed et al., 2001, Olanow et al., 2003) clinical studies have been conducted in several centres worldwide over the next 13 years, with more than 200 patients receiving foetal tissue transplants. These studies have provided proof of principle that (i) the grafted DA neurons can survive and reinnervate the surrounding tissue; (ii) the graft can integrate with the host brain and restore regulated DA release in a physiological manner; (iii) transplantation therapy can achieve measurable clinical improvement in a subset of patients. The next clinical trial has already been initiated with the transplantation surgeries scheduled to take place in 2014 (TransEUro).

Behavioural improvements such as increased length of the "on" phase were detectable quite early, between 3 to 6 months after transplantation (Lindvall et al., 1989, Levivier et al., 1997). In most cases PET scans detected increased ^{18}F-dopa uptake in the putamen and/or the caudate nucleus correlated with significant clinical improvements and in several cases patients were able to stop L-DOPA treatment (Lindvall et al., 1994). The preference for the postcomissural putamen and caudate nucleus as transplantation targets stems from the connectivity of these two brain regions with the motor and associative cortices, respectively. The putamen was the primary transplantation target both in open label and double-blind clinical trials and in some cases patients also received transplants into either the caudate nucleus or the SNpc in open label studies. American double-blind studies showed significant behavioural improvement among younger patients (60 years old or younger) but not in older patients and 15% of patients developed graft induced dyskinesias (GIDs) even after discontinuation of L-DOPA treatment (Freed et al., 2001). The second double-blind study, demonstrated clinical improvement in a subset of patients with milder PD and detected GIDs in 54% of grafted patients (Olanow et al., 2003). Exclusion of the caudate nucleus as the transplantation target might have contributed to the lower clinical improvement observed in these two studies because transplants in caudate nucleus alone were shown to be capable of inducing behavioural recovery in PD patients several

months after transplantation and maintaining it for 5 years (Lopez-Lozano et al., 1997). Some patients developed too severe dyskinesias and had to undergo DBS treatment of the GPi which resolved the side effects (Graff-Radford et al., 2006, Herzog et al., 2008). In both these studies, grafts were transplanted as solid tissue pieces, a transplantation method associated with significantly increased hyperkinetic movements in 6-OHDA lesioned rats (Steece-Collier et al., 2003). Mild GIDs were observed 3 years after transplantation in a subset of patients grafted in Swedish trials (Hagell et al., 2002). GIDs were an unexpected finding which halted clinical transplantation research for over 10 years and forced scientists to go back to the bench and re-evaluate the methods.

Post-mortem studies in two patients, grafted as part of double-blind trials, who continued to decline after transplantation surgery demonstrated reduced levels of TH and DAT immunoreactivity in the transplants and the presence of immune markers in the grafts despite good neuron viability (Kordower et al., 2008a, Kordower et al., 2008b). Also, termination of immunosuppressive cyclosporine treatment reduced efficacy of some foetal transplants (Olanow et al., 2003). Solid tissue grafting approach used in these studies was implicated in the host immune response in animal studies (Redmond et al., 2008). This suggests that slow ongoing immune response is facilitated by solid tissue transplantation method and might detrimentally influence grafted foetal neuron function contributing to the disappointingly low clinical improvement in PD patients.

Nevertheless, data from grafted patients continues to emerge. Despite an ongoing disease progression, [11C]-raclopride PET scans of the synaptic DA release by grafted neurons demonstrated maintenance of restored levels of D_2 receptor binding in a patient 10 years after transplantation surgery (Piccini et al., 1999). Patients, who already showed modest clinical improvements within the first year after transplantation surgery, continued to improve further for the next 2 years and some showed an additional increase in the ^{18}F-dopa uptake in the putamen since the first PET scan (Lindvall et al., 1994, Piccini et al., 2000). These findings suggest that clinical recovery in PD patients depends on DA delivery to the putamen as well as the functional integration of the graft within the host brain. Robust, albeit quite low, survival of transplanted DA neurons, typically only 5 – 10%, was observed in post-mortem studies of grafted patients from different research centres (Kordower et al., 1996, Kordower et al., 1997b, Mendez et al., 2005, Kordower et al., 2008a, Kordower et al., 2008b, Li et al., 2008, Mendez et al., 2008).

Post-mortem analysis of the brain tissue from two patients demonstrated that, although numerous TH-ir cells were present in the implants, PD-induced LB pathology transferred from the host tissue into grafted nigral neurons in 14-year-old transplants from double-blind clinical trials (Kordower et al., 2008a, Kordower et al., 2008b). A Swedish study showed the presence of α-synuclein-ir LBs in some grafted neurons while the majority of DA neurons remained unimpaired in two patients 11 – 16 years after surgery (Li et al., 2008). These observations provided the first evidence that PD was an ongoing process, which could propagate from the host to graft tissue and affect both in a similar manner while leaving the grafts functional until death. In contrast, another post-mortem analysis of 5 PD patients 9 – 14 years after transplantation revealed no LB pathology in the implanted neurons and excellent survival of DA neurons with very little inflammation in the grafts (Mendez et al., 2008). These findings are important for the understanding of the aetiology of pathogenesis in VM DA neurons and future use of cell transplantation therapy.

Both A9 and A10 type DA neurons were found in the grafts transplanted into the post-commissural putamen and the SNpc (Mendez et al., 2005). A higher proportion of TH-ir neurons coexpressed Girk2 (68 – 71%) than calbindin (26 – 48%) in grafts in the putamen and fewer TH-labelled neurons coexpressed Girk2 in grafts in the SNpc. Girk2-ir neurons were predominately found in the periphery of the graft while in the centre of the graft DA neurons were more often calbindin-ir or did not co-label with either Girk2 or calbindin. DA neuron survival was 15 – 30% in grafts in the putamen in contrast with 4 – 8% survival in transplants in the SNpc suggesting that differences may exist in survival depending on region specific factors and conditions. Another study from the same centre demonstrated similar Girk2 and calbindin expression patterns in VM DA neurons grafted into the putamen (Mendez et al., 2008). Although grafts also contained 5-HT neurons, no GIDs were observed in any subjects. Uncontrolled release of DA by 5-HT neurons in the grafts was shown to exacerbate LIDs in animals and to influence apomorphine-induced dyskinesias in animal models of GIDs (Carlsson et al., 2007, Carta et al., 2007). Also, in PD patients, who showed functional improvements after receiving a cell transplant, post-mortem analysis revealed astrocytes around and inside the VM grafts, potentially graft-derived astrocytes (Mendez et al., 2005). Astrocytes play a crucial role in the development of DA VM neurons and animal studies demonstrated that immortalized human foetal VM astrocytes potentiated *in vitro* differentiation of human embryonic stem cells (hESCs) into engraftable A9 type DA

neurons (Roy et al., 2006). However, it is still unclear whether graft-derived astrocytes are crucial for the efficacy of cell transplantation therapy.

Foetal DA VM transplantation has achieved the most clinical improvement in younger patients as demonstrated by several studies discussed above and still presents a promising treatment for PD. However, a very limited supply of foetal tissue, a requirement for six to eight donors per unilateral transplantation, a lack of full quality control, logistic challenges, a high variability in functional outcomes, and significant ethical concerns, all have prevented the use of human embryonic tissues for transplantation from being developed into a therapy. Hence, we see a widespread search for alternative sources of effective transplantable tissues that circumvent or avoid these constraints.

1.5.3 Alternative cell sources for transplantation therapy

Human neural progenitor cells (HNPCs) represent an alternative source of transplantable neurons for cell therapy in PD. HNPCs derived from the embryonic forebrain can be easily expanded in large numbers and maintained long-term *in vitro* (Svendsen et al., 1998, Carpenter et al., 1999, Caldwell et al., 2001). When transplanted into the adult rat brain, they were shown to exhibit high survival rates (Fricker et al., 1999, Englund et al., 2002). However, HNPCs survived poorly when transplanted into the DA-depleted striatum of 6-OHDA lesioned rats and did not achieve significant behavioural recovery (Svendsen et al., 1997). Also, transplants in the SNpc of 6-OHDA lesioned rats did not improve behavioural recovery in animals despite good cell survival rates and significant degree of cell migration towards the striatum along the nigrostriatal pathway (Burnstein et al., 2004). Survival rates of HNPCs were greatly improved when the tissue was grafted into the STN of 6-OHDA lesioned rats and correlated with a significant recovery of the amphetamine-induced rotational behaviour (Anderson and Caldwell, 2007). Once again, it has been demonstrated that the STN plays a key role in the recovery of the normal basal ganglia function. Grafted cells produced vascular endothelial growth factor (VEGF), showed extensive migration and were observed throughout the grafted hemisphere including the striatum. HNPCs are believed to support the host environment and promote neuroprotection by remaining in the immature state and releasing trophic factors (Ourednik and Ourednik, 2004, Pluchino et al., 2005). This therapy merely plays a supportive role in the recovery process and, on its own, is not sufficient to address PD-induced neurodegeneration and associated behavioural deficits.

Stem cell transplantation is a promising therapy for PD but research in this field is still in its infancy. hESCs can potentially provide an unlimited supply of DA neurons for transplantation generated in standardised and quality-controlled conditions, but they are not yet as efficient as human foetal VM tissue in yielding high DA neuron survival rates after transplantation. One reason for this might be that stem cell grafts do not contain the range of cell types found in the developing midbrain, many or all of which might be involved in the differentiation and survival of dopamine neurons.

We already know that human pluripotent stem cells (hPSCs) can be differentiated into midbrain DA neurons (Perrier et al., 2004), but when transplanted into the striatum stem cell-derived DA neurons generally show poorer *in vivo* performance than foetal transplants (Roy et al., 2006, Cho et al., 2008). Recent studies demonstrated successful induction of DA neurons from VM floor plate (FP) precursor cells derived from either hESCs or induced pluripotent stem cells [iPSCs from a sporadic PD patient; (Kriks et al., 2011)]. *In vivo* survival and function of these FP-derived human DA neurons was demonstrated in PD models using three host species and, while the yield of DA neurons in the grafts was improved and amphetamine-induced rotational behaviour was fully restored, behavioural deficits in stepping and cylinder tests were only partially restored. Both A9 and A10 type DA neurons were present in the grafts. Another study demonstrated that co-grafts of rat foetal VM and pituitary homeobox 3 (Pitx3) overexpressing neural stem cells were enriched for the A9 type DA neurons and achieved improved behavioural recovery in 6-OHDA lesioned rats (O'Keeffe et al., 2008). These results highlight the importance of the A9 type DA neurons in mediating the functional benefits of cell transplants in PD. The enhancement of the survival and function as well as safety of stem cell-derived DA grafts still remains a major challenge faced by the scientific community before this therapy can be brought into the clinic.

1.6 Development of mesencephalic dopamine neurons

An understanding of the normal development of DA neurons in the VM is thought to be the key to determining the cell population most suitable for DA neuron transplantation therapy in PD. Neurogenesis of VM DA neurons and the formation of the nigrostriatal pathway are directed by a combination of spatially and temporally restricted chemical cues. Hence, the optimal cell type for transplantation may be found in different VM regions at different developmental stages and therefore may express

distinct markers. Also, distinct factors may be required to correctly specify and differentiate DA neural progenitor cells, extracted at different time points during embryogenesis, into mature DA neurons to obtain appropriate innervation of the host brain region after transplantation.

Neural tube pattering into four domains along the anterior-posterior and dorso-ventral axes is the first necessary step in DA neuron development (Verney et al., 2001). One of these domains is the floor plate, a glia-rich structure, which in the VM gives rise to DA neurons (Bonilla et al., 2008). Early studies of the ontogeny of the rat VM demonstrated that developing DA neurons aligned along radial glial cells, which originated in the aqueduct region and extended to the pial surface (Shults et al., 1990). Recent studies in mice confirmed that floor plate cells that give rise to DA neurons express transcription factor Gli1 a day before they start to express glycoprotein sonic hedgehog (Shh) and the expression of Gli1, initially confined to the VM midline at embryonic day (E)7.5, expands laterally and then is downregulated in the VM midline (Blaess et al., 2011). Gli1, a zinc finger transcription factor in the Shh signalling pathway, is transcribed in cells that receive high levels of Shh signalling and are close to the Shh source (Bai et al., 2002). Thus, secretion of Shh directs expression of Gli1 in a medio-lateral direction and then expression of Shh expands in the same direction further directing floor plate cell specification. Being downstream of Shh signalling, Gli1 signalling is of vital importance for normal DA neuron development (Cayuso et al., 2006). Another similar study showed that Gli1 lineage, following lateral expansion, exclusively contributed to the lateral domain of the VM while Shh lineage expanded more broadly across the VM (Hayes et al., 2011). Also, early Gli1 and Shh lineages were demonstrated to specify DA neurons of the SNpc while late Gli1 and Shh lineages maintained their progenitor state for a longer period of time in the posterior VM to extend the production of DA neurons in the VTA. This step in the neurogenesis of DA neurons is often referred to as regionalisation.

Further floor plate cell specification is directed by a complex combination of intrinsic and extracellular signals, including Wnt signalling and continued Shh signalling (Joksimovic et al., 2009, Hayes et al., 2011). Expression of LIM homeobox transcription factor 1 (Lmx1a) by floor plate cells and expression of proneural (basic helix-loop-helix) bLHL transcription factors Mash1 and Neurogenin-2 (Ngn2) in the ventricular zone within and lateral to the floor plate are essential for regulating neurogenesis in the developing VM (Thompson et al., 2006, Kim et al., 2007, Nelander et al., 2009). Loss-of-function studies demonstrated that Ngn2 is required for normal

VM DA neuron development and correct fate specification (Andersson et al., 2006, Kele et al., 2006). The forkhead/winged helix A2 (FoxA2) transcription factor is another key factor involved in VM DA neuron generation and its expression in the human floor plate extends laterally beyond the Lmx1a domain and Mash1/Ngn2 domain (Nelander et al., 2009). Finally, as DA neural precursor cells exit the mitotic progenitor stage they begin to express the orphan Nuclear receptor related-1 gene (Nurr1), Pitx3 and TH, thereby finalising VM identity (Andersson et al., 2006, Smits et al., 2006, Nelander et al., 2009). Newly born VM DA neurons send axonal projections towards appropriate cerebral targets under the guidance of chemoattractive and chemorepulsive cues (Gates et al., 2004). Axonal outgrowth is initially attracted to the MFB and directed away from the midbrain followed by chemoattraction to the striatum. By E19, TH-ir fibres extend rostrally into the developing striatum in rats. In human embryos, first TH-ir cells in the VM are detectable 5 – 6 weeks post-conception and a large increase in DA neurons is observed between 6 – 8 weeks followed by a cessation of DA neurogenesis at 10 – 11 weeks (Freeman et al., 1991, Almqvist et al., 1996, Nelander et al., 2009).

1.7 Aims of this thesis

Although animal studies have provided a substantial amount of evidence that DA neuron transplantation is a promising treatment for PD, clinical trials have failed to report consistent clinical efficacy of this therapy in patients. Furthermore, pre-clinical studies showing improved yield of both global DA neurons and of functionally important A9 type DA neurons in grafts derived from immature VM tissue have raised questions about the currently accepted human embryonic donor age for this therapy. We are now able to distinguish A9 and A10 DA neuronal subtypes within the graft using co-labelling with Girk2 and calbindin, respectively. The main aim of the current thesis was to investigate the populations of A9 and A10 type DA neurons in the rat PD model, looking at how these cells are distributed within the grafts, how the DA neuron yields are affected by the donor age of the tissue implanted, and whether or not survival and differentiation of the implanted cells are influenced by the host environment.

This thesis focuses on the rat foetal VM transplantation in the 6-OHDA, unilaterally lesioned rat model and characterises in depth the A9 and A10 type DA neuron subpopulations in the VM grafts. Since grafts derived from younger donor embryos significantly improve DA neuron yield, this work first measures the impact of

the donor age on the neuronal composition of intrastriatal rat VM grafts and the distribution of A9 type and A10 type DA neurons within the graft. Following on from this, commitment of DA neural precursor cells to the two DA neuron phenotypes, and how this is affected by the host environment was investigated, by grafting rat E12 and E14 VM tissue into different cerebral targets. Brain regions were chosen that receive either the A9 type DA, A10 type DA or NA innervation and the influence of these different transplantation sites on the neuronal composition of VM grafts was analysed. Finally, the ability of immature VM DA neuronal cell precursors to proliferate in the host and give rise to the two DA neuron subpopulations was determined by birth dating cells within intrastriatal rat E12 and E14 VM grafts after transplantation.

The main aims of this PhD work were:

1. To assess the impact of the donor age on the A9 type and A10 type DA neuron populations in intrastriatal VM grafts (Chapter 3)
2. To investigate the influence of the transplantation site on the DA neuron phenotypes in the grafts (Chapter 4)
3. To determine whether DA cell birth after transplantation gave rise to a specific DA neuron subpopulation in the grafts (Chapter 5)

Chapter 2. General Methods

2.1 Experimental animals

All experiments were conducted under UK Home Office personal and project licences in accordance with the requirements of the UK Animal (Scientific Procedures) Act 1986. Every effort was made to minimise the number of animals used and their suffering. Sprague Dawley (SD) rats, weighing 200 – 250 g, were supplied by Charles River UK and housed under standard conditions with *ad libitum* access to food (14% protein, Harlan) and water under 14h:8h light-dark cycle. Female (4 per cage) and male (1 per cage) rats were housed in standard cages (length: 54 cm, width: 37 cm, depth: 21 cm) lined with hygienic animal bedding (Lignocel). Animals were provided with a cardboard tube and wood stick for environmental enrichment.

2.2 Procurement of donor embryos

2.2.1 In-house breeding protocol

Pregnant SD dams were bred in-house following a previously established protocol (Weyrauch et al., 2009). On the morning of breeding day, females in oestrus were established by the vaginal lavage method. The rat was slightly restrained in one hand, with her back to the palm, to obtain a vaginal smear. A fire-polished glass pipette with a rubber bulb was used to flush 200 µl of sterile saline (0.9% Sodium chloride, Baxter) into the vagina which was then sucked back in to the pipette. The collected sample was then smeared onto a glass slide and analysed under a Leica light microscope with the condenser diaphragm closed to provide differential contrast. The rat was designated as being oestrus cycle if the sample contained predominantly cornified epithelial cells with few uncornified epithelial cells and no inflammatory cells (Figure 2.1). Eligible females were paired with a male at 1:1 ratio in the male's home cage for a maximum of three hours, typically between 10:30 a.m. and 1:30 p.m. Females then returned to their home cages and the day of mating was recorded as E0 (Weyrauch, 2009).

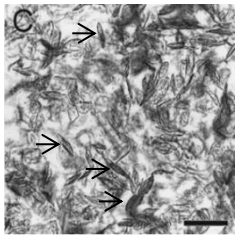

Figure 2.1 Photomicrograph of the vaginal smear illustrating oestrus stage. Scale bar: 100 µm [modified from Weyrauch *et al* (2009)].

2.2.2 Confirmation of pregnancy

At 10 a.m. on the morning of E12, rats were lightly anaesthetised in an induction chamber with 2-3% Isoflurane (AbbVie Ltd) in oxygen and the pregnancy was confirmed if palpation of the abdomen revealed several swellings in the uterine horns. Embryos were harvested straight away if the desired embryonic age was E12, alternatively pregnant dams returned to their home cages until E14.

2.2.3 Procurement of embryos

Pregnant dams were terminally anaesthetised with an intra-peritoneal (i.p.) injection of 400 mg/kg pentobarbital sodium (200 mg/ml Euthatal, Merial Animal Health Ltd) and subsequently killed by cervical dislocation. The embryos were excised from the uterine horns and transferred to the laboratory in Hanks' balanced salt solution (HBSS, Gibco). The embryos were placed on their side in HBSS in a petri dish and their crown-rump length (CRL; Figure 2.2) was measured under a Leica binocular microscope using a ruler placed under the petri dish. The short mating-period protocol used here produced embryos with a mean CRL of 6.1 ± 0.36 mm at E12 and 11.21 ± 0.44 mm at E14 (CRL reported as mean ± standard deviation), even though E14 embryos were slightly bigger than expected, results were comparable to a recently updated staging scale (Torres et al., 2008b).

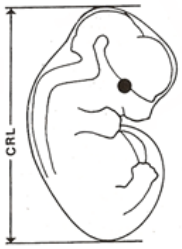

Figure 2.2 Schematic representation of the CRL measurement in an embryo (adapted from Dunnett and Bjorklund, 1992).

2.3 Surgery

Animals were first anaesthetised in the induction chamber with 3-4% Isoflurane in oxygen prior to being transferred to a Kopf stereotaxic frame where anaesthesia was maintained at 2-3% Isoflurane in a 2:1 mixture of oxygen and nitrous oxide. Blunt ear bars were used to restrain the animal in the frame with the nose bar set at -4.5 mm below the intra-aural line. Animals received post-operative analgesia during each surgical session. Once in the frame rats were injected subcutaneously (s.c.) with 30 µl of Metacam (Boehringer Ingelheim) using an insulin syringe. Also, 5 ml of 0.18% sodium

chloride, 4% glucose (Aquapharm) were injected s.c. for hydration. Upon completion of the surgery, the wound was cleaned and sutured with Vicryl 4-0 sutures [coated VICRYL® (polyglactin 910) Sutures, ETHICON, VWR] and the animal was placed in a recovery chamber at 30˚ C until fully awake and mobile. Health and weight of the animals were monitored daily for first 3 days following the surgery and then weekly.

2.3.1 Medial forebrain bundle lesions

For the unilateral nigro-striatal lesion, the animals received an intra-cerebral injection of 6-OHDA into the right MFB (Figure 2.3) following a recently refined protocol (Torres et al., 2011). The neurotoxin 6-OHDA was supplied as 5 mg of hydrobromide salt powder, of which 0.2 mg (4%) was ascorbic acid, added for stabilisation (Sigma-Aldrich). The toxin was dissolved in 0.8 ml of sterile saline, divided into 100 µl aliquots and frozen quickly for future use. The resulting solution contained 25 mM 6-OHDA (equivalent to 5.14 mg/ml free-base weight of 6-OHDA) and 0.025% ascorbic acid. Each animal received a single injection of 3 µl of the 6-OHDA toxin at the following stereotaxic coordinates: -4.0 mm caudal from bregma (AP); -1.3 mm lateral from the midline (ML); -7.0 mm deep from dura (DV). The toxin was delivered at a rate of 1 µl/min using a 30 gauge stainless steel cannula connected by polyethylene tubing to a 10 µl Hamilton syringe mounted on a Harvard micro-drive infusion pump. The toxin was allowed to diffuse for 2 minutes after the injection before the cannula was carefully withdrawn.

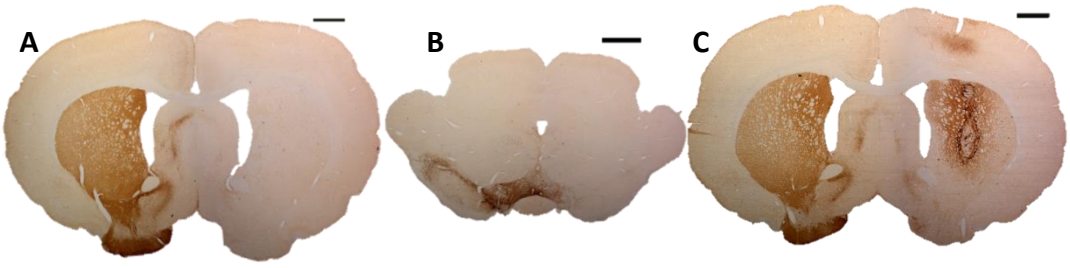

Figure 2.3 Photomicrographs of TH-immunoreactivity in coronal sections through the adult rat brain. Administration of the 6-OHDA neurotoxin into ascending DA fibres in the right MFB resulted in ipsilateral **(A)** DA depletion in the striatum and **(B)** retrograde DA neuron death in the substantia nigra **(C)** Grafted embryonic VM tissue partially reinstated lost DA supply and innervation of the striatum (E12 VM graft is shown here). Scale bar: 1 mm.

2.3.2. Ventral mesencephalon transplantation

The VM tissue was derived from either E12 or E14 rat embryos and DA cell-rich grafts were prepared as a cell suspension according to a standard protocol (Dunnett and Bjorklund, 1992, 1997). After the CRL measurements had been obtained, embryos were decapitated and the brains were collected in HBSS. Using scissors and fine point forceps, each VM was dissected as shown in Figure 2.4. Note that the ventral meningeal layer of tissue was removed from the E14 VM pieces but was included in E12 VM dissections because it was too friable to be removed.

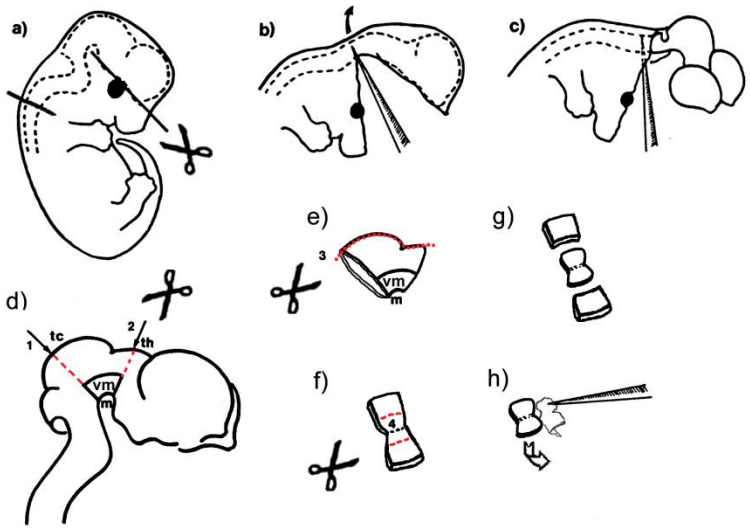

Figure 2.4 Dissection of the VM tissue from an embryo (modified from Dunnett and Bjorklund 1992). **(A)** Using scissors, the embryo was decapitated and a cut was made between the forebrain and the eye. **(B)** The skin and skull were pulled out with the forceps and **(C)** the brain was removed. **(D-G)** The VM was dissected from the mesencephalic flexure (m) using tectum (tc) and thalamus (th) as landmarks. **(H)** The ventral meningeal layer of tissue was carefully removed from the E14 VM pieces.

Pooled VMs from all donors in each litter were washed in HBSS and then incubated in 500 µl of pre-heated (37˚ C) 0.1% trypsin (Trypsine EDTQ 0.05%, Gibco) with 0.05% DNAse (Deoxyribonuclease I from bovine pancreas, Sigma-Aldrich) in Dulbecco's minimum Eagle Medium F-12 (DMEM, Gibco) for 20 minutes at 37˚ C. The trypsin was then removed and the tissue incubated in 500 µl of DNAse (0.05% in DMEM medium) for 5 minutes at 37˚ C. After removal of the supernatant, the tissue was suspended in 200 µl of DNAse and gently triturated with 1000 µl and 200 µl Gilson pipettes to create a homogenous single cell suspension. Cell viability was assessed from 2 x 2 µl samples of the cell suspension each diluted with 8 µl of 0.4% Trypan blue

solution (Sigma) and counting cells using a haemocytometer slide. The cell suspension was then centrifuged at 2,000 rpm for 2 minutes, after which all the supernatant was removed, and the pellet of cells was re-suspended in a sufficient volume of DMEM/DNAse to obtain the required concentration of either one full VM (Chapters 3 and 5) or one half of a VM (Chapter 4) per 2 µl. The final cell suspension was stored at room temperature during surgery. As expected, Figure 2.5 shows that E12 rat embryos contained fewer cells per VM than E14 rat embryos (Mann Whitney test, $p<0.001$). Note that the numbers of cells per VM in each experiment were consistently lower than those previously reported for SD rat embryos of the same age (Torres et al., 2007). This highlights the importance of user-to-user variability in embryonic dissections in cell transplantation therapy research.

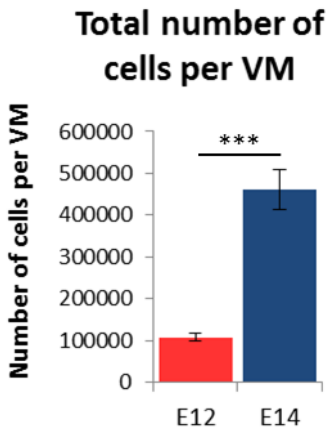

Figure 2.5 Average numbers of cells per VM dissected from E12 and E14 rat embryos. Data presented as group mean ± standard error of mean (SEM), significance level: *** $p<0.001$.

Each animal was transplanted with the number of cells equivalent to the same proportion of the VM in 2 µl of the cell suspension to allow a valid comparison to be made between grafts of different donor ages. Depending on the experiment, grafts were implanted into either the DA depleted striatum alone or, in combination with grafts into the nucleus accumbens (N.Acc.), PFC and hippocampus. Each chapter specifies the stereotaxic co-ordinates used, as determined from the stereotaxic rat brain atlas (Paxinos and Watson, 2003). Cells were transplanted as a single deposit at 2 depths 0.5 mm apart. The cell suspension was injected into the brain at a rate of 1 µl/min over 2 minutes using the same set up as for the 6-OHDA lesion surgery. After the first minute, the cannula was raised 0.5 mm and the second half of cells was injected at the new depth. The cannula was left in place for 3 minutes after the injection before being withdrawn to

prevent drawback of the cells up the needle track. As shown in Figure 2.3C, this method achieved a good distribution of the cells within the host striatum.

2.4 Amphetamine-induced rotations

The extent of DA depletion in the striatum was evaluated 2 and 4 weeks post-lesion based on the drug-induced rotational behaviour. Amphetamine (Methamphetamine hydrochloride, Sigma) was dissolved is sterile saline at 2.5mg/ml and administered via i.p. injection at a dose of 1ml/kg, immediately prior to testing. The animals were placed in 30 cm round bottomed bowls housed in 50 cm high perspex cylinders and harnessed to an automated rotometer system (Rotomax System, AccuScan Instruments Inc.) following a previously established protocol (Ungerstedt and Arbuthnott, 1970). The collected data is reported as the net number of rotations (ipsilateral minus contralateral) over the full 90 min session. Rats with net rotation scores of $\geq$ 540 turns in the second session were deemed sufficiently depleted of DA and were included in the experiments. This threshold has been reported as a reliable indicator of animals with stable lesions and more than 95% DA neuron loss in the ipsilateral SNpc (Dowd and Dunnett, 2005a, Torres et al., 2011). Grafted rats were tested 4 and 6 weeks post-implantation using the same method. Drug-induced rotation tests were performed blind to the treatment of the animals.

2.5 Perfusion

Upon completion of the experiment, the animals were terminally anaesthetised with the i.p. injection of 400 mg/kg Euthatal. When the rat no longer responded to both tail pinch and foot pinch the thorax of the animal was opened up to expose the heart. A small haemostat clamp was used to clamp the descending aorta and prevent flow of solutions to the lower body. The perfusion needle was then inserted in to the left ventricle via a small incision, and the right atrium was cut to allow egress of the perfusion solutions. Solutions were then delivered using a peristaltic pump at a flow rate of 50 ml/min. The upper body vasculature was first flushed with 100 ml of 0.1M phosphate buffered saline [PBS; 90 g of *Di*-Sodium hydrogen orthophosphate (VWR Chemicals) and 45 g of Sodium chloride (Fisher Scientific) in a final volume of 5 L of distilled water adjusted to pH 7.3 with orthophosphoric acid (Fisher Scientific)]. Flushing of the vasculature with PBS was followed by perfusion with 250 ml of 1.5% paraformaldehyde (PFA, Fisher Scientific) made in the same 0.1M PBS delivered over

a 5 min period. After perfusion the brains were removed from the skull and post-fixed in the same fixative solution overnight before being transferred into a solution of 25% sucrose in PBS. After equilibration in the sucrose solution, 40 µm thick coronal sections through the brain were cut on a Leica freezing stage sledge microtome, collected into 0.05% sodium azide (Fisher) in 0.1M TRIS buffered saline [TBS; 48 g TRIS base (Sigma), 36 g Sodium chloride in a final volume of 4 L of distilled water adjusted to pH 7.4 with concentrated hydrochloric acid (HCl; Fisher Scientific)], and stored at +4˚ C prior to staining (Chapters 2 and 3). In the experiment described in Chapter 5, brain sections were stored at -20˚ C in a cryoprotective solution [4.36 g *Di*-Sodium hydrogen orthophosphate and 1.256 g of Sodium dihydrogen phosphate (Fisher Scientific) in a final volume of 800 ml of 30% Glycol (Sigma-Aldrich), 30% Glycerol (Sigma-Aldrich) in distilled water].

2.6 Histological Methods

2.6.1 Immunohistochemistry

All IHC was performed on free floating sections on an automated shaker. Each chapter contains detailed information on the number of sections used (i.e. either a 1:6 or a 1:12 series of sections) and the antibodies used. In each experiment, free floating sections were collected in 15 ml Perspex containers (Greiner) capped using a fine nylon mesh that allowed the pots to be filled and emptied of solutions, whilst retaining the sections. Series of sections in the same experiment were batch processed simultaneously using the same solutions of antibodies to ensure that incubation times and washes were identical for all brains.

Sections were first washed in TBS (3 x 10 min), then transferred into a solution of distilled water with 10% Methanol (Fisher) and 10% hydrogen peroxide (30% hydrogen peroxide solution, VWR) for 5 minutes to quench endogenous peroxidases that might interfere with the final horseradish peroxidase colour reaction. After another three washes the sections were incubated for 1 hour in a blocking solution of 3% normal horse serum (NHS, Gibco) in TXTBS [0.2% Triton X-100 (Sigma) in TBS, pH 7.4] to prevent non-specific binding of antibodies to the section. Subsequently, the sections were bathed in 1% NHS in TXTBS solution containing the primary antibody for 60 hours at +4˚C with agitation. After thorough washing in TBS (3 x 10 min), tissue sections were immersed in the secondary biotinylated antibody solution containing 1% NHS in TBS overnight at room temperature. On the next morning, three washes of TBS

followed before the Vectastain Elite ABC solution (Vector) with 1% NHS in TBS was applied for 3 hours. Brain sections were rinsed in TBS (3 x 10 min) and then in 0.05M TRIS non-saline buffer [2 x 5 min; (TNS, pH 7.4)] prior to being incubated in a 0.8% solution of 3.3' – Diaminobenzidine tetrahydrochloride hydrate (DAB, Sigma) in TNS with 0.03% hydrogen peroxide for 5 – 10 minutes until the strong brown specific staining was complete. The sections were given a final 3 x 10 min washes in TBS, before being mounted on gelatine coated microscope slides and allowed to dry overnight at room temperature. The next day, slides were dehydrated by immersion in an ascending series of alcohols [75%, 90%, and 100% ethanol (Sigma) in distilled water], for 10 minutes each, then immersed in xylene (Fisher Scientific) 10 minutes to clear the tissue and cover-slipped using di-styrene plasticizer and xylene mounting medium (DPX, VWR).

Fluorescent IHC staining was performed as described above with the difference that there was no quenching step at the beginning of the staining process. Also, following the application of the tertiary antibody sections were washed in TBS (3 x 10 min) and mounted on microscope slides in TNS to avoid formation of salt crystals within the tissue that would fluoresce under the microscope. In double and triple staining, primary antibodies where applied together, for all antibody concentrations and pairings see Table 2.1.

Primary		Secondary		Tertiary	
Name, Concentration	Supplier	Name, 1:200 Concentration	Supplier	Name, 1:200 Concentration	Supplier
Immunoperoxidase Staining (Chapters 3, 4 and 5)					
Rabbit anti-TH, 1:2000	Millipore	Biotynilated anti-Rb	Vector	Streptavidin-biotin-horseradish peroxidase	Vector
Mouse anti-NeuN, 1:1000		Biotynilated anti-Ms			
Sheep anti-BrdU, 1:1000	Abcam	Biotynilated anti-Sh			
Double TH / Girk2 fluorescence labelling (Chapters 3 and 4)					
Mouse anti-TH, 1:1000	Millipore	Anti-Ms Alexa 594 or 488	Molecular Probes		
Rabbit anti-Girk2, 1:250	Alomone	Biotynilated anti-Rb	Vector	Steptavidin Cy2 or Cy3	Jackson
Double TH / Calbindin fluorescence labelling (Chapters 3 and 4)					
Rabbit anti-TH, 1:2000	Millipore	Anti-Rb Alexa 488	Molecular Probes		
Mouse anti-Calbindin, 1:10 000	Sigma	Biotynilated anti-Ms	Vector	Steptavidin Cy3	Jackson
Double Girk2 / Calbindin fluorescence labelling (Chapter 3)					
Rabbit anti-Girk2, 1:250	Alomone	Anti-Rb Alexa 488	Molecular Probes		
Mouse anti-Calbindin, 1:10 000	Sigma	Biotynilated anti-Ms	Vector	Steptavidin Cy3	Jackson
Triple BrdU / Girk2 / TH (Chapter 5)					
Sheep anti-BrdU, 1:1000	Abcam	Anti-Gt Alexa 488	Molecular Probes		
Rabbit anti-Girk2, 1:250	Alomone	Anti-Rb Alexa 594			
Mouse anti-TH, 1:1000	Millipore	Biotynilated anti-Ms	Vector	Streptavidin Alexa 350	Molecular Probes
Triple BrdU / calbindin / TH (Chapter 5)					
Sheep anti-BrdU, 1:1000	Abcam	Anti-Gt Alexa 488	Molecular Probes		
Mouse anti-Calbindin, 1:10 000	Sigma	Anti-Ms Alexa 594			
Rabbit anti-TH, 1:2000	Millipore	Biotynilated anti-Rb	Vector	Streptavidin Alexa 350	Molecular Probes

Table 2.1 A summary of antibodies used for immunohistochemistry

2.6.2 Cresyl Violet Staining

Cresyl Violet (Nissl) stain was used for anatomical analysis of sections and labelling of all grafted neurons where Neuronal Nuclei (NeuN) staining could not be performed. The brain sections were mounted on gelatine coated microscope slides, dried overnight, dehydrated in an ascending series of alcohols (75%, 95% and 100% ethanol; 10 minutes each) before delipidisation in 50% chloroform (Sigma) solution in ethanol for 20 minutes. The tissue was then re-hydrated in a descending series of 95% ethanol, 75% ethanol and distilled water (10 minutes each) prior to being stained in 0.7% cresyl fast violet (CV, Sigma) solution in distilled water with 0.5% sodium acetate (Sigma) at 3.5 pH. The sections were saturated with the dye, then washed in distilled water and the excess dye was differentially removed during dehydration in the ascending series of alcohols, for a minimum of five minutes in each alcohol solution, adjusted to obtain the optimal degree of staining. Slides were then cleared in xylene before cover-slipping in DPX.

2.6.3 Haemotoxylin Stain

Following 5-Bromodeoxyuridine (BrdU, Sigma-Aldrich) DAB IHC, the brain sections were mounted onto gelatine coated glass slides and allowed to dry overnight before exposure to a solution of Mayers Haemalum (Raymond A Lamb Ltd) for 1 minute. The slides were then washed in distilled water for 5 minutes and the stain fixed by placing the slides in a container with running tap water for 20 minutes. The sections were then dehydrated in the ascending concentrations of alcohols, and slides cover-slipped as described above.

2.7 BrdU Methods

2.7.1 BrdU incorporation

BrdU was added to sterile saline with 10% ethanol at a concentration of 60 mg/ml, sonicated for 15 minutes and then heated in a water bath at 55º C for 1.5-2 hours until fully dissolved. Immediately after that, BrdU was administered via i.p. injection (120 mg/kg) into grafted animals.

2.7.2 BrdU immunohistochemistry

To detect BrdU post-mortem, free-floating sections were washed in TBS and incubated in 1M HCl for 1 hour in a 37ºC water bath. This unfolds double stranded deoxyribonucleic acid (DNA) and allows the primary antibody to attach to the BrdU. The brain sections were then washed in TBS to remove residual HCl before proceeding with the standard IHC protocol.

2.8 Quantification and microscopy

All quantifications of cell populations in the grafts were performed blind to the experimental condition.

2.8.1 Light microscopy

TH-ir neurons were counted from all sections containing the graft on a Leica DMRB light microscope at x10 magnification and BrdU-ir nuclei in grafted cells were quantified at x20 magnification using a 10x10 eyepiece graticule. Total numbers of DA neurons and BrdU-ir cells in the grafts were estimated using the Abercrombie correction formula (Abercrombie, 1946):

$$N = \sum n \times F \times \frac{T}{T + d}$$

where n = number of counted cells, F = 1/frequency of sections (1/6 or 1/12), T = thickness of the section (40 µm), d = mean diameter of cells.

Volumes of grafts were calculated from cross-sectional areas of grafts measured on a 1:6 or 1:12 series of TH-stained sections through the entire graft as follows:

$$V = \sum A \times T \times F$$

where A = area of the graft, T = thickness of the section (40 µm), F = 1/section frequency.

Neuron quantification in the grafts from CV and NeuN stained sections was carried out on an automated stereology microscope (Olympus BX50) at x100 magnification using image analysis C.A.S.T. – grid software version 1.6 (Olympus). The area of the graft was outlined by the user and the software set up randomised statistical sampling within the defined area so that at least 150-200 cells per animal were counted from at least 200 sampling fields. Sampling parameters, i.e. area of the sampling frame (285 μm^2) and step size between the samples, were held constant for all

animals in each experiment. In the case of very small grafts, the step size was proportionally reduced, e.g. by 25%. The total number of neurons in the grafts was estimated using the following formula:

$$N = \sum \left\{ \frac{n \times A}{a} \right\} \times F \times \frac{T}{T + d}$$

where n = number of counted cells, A = area of the graft, a = total sampling area, F = 1/section frequency (12), T = thickness of the section (40 µm), d = mean diameter of cells.

2.8.2 Fluorescent microscopy

To quantify cells labelled with fluorochromes, pictures of all sections containing the graft were taken on a Zeiss Image Z2 microscope at x10 magnification (Figure 2.6A) and single-, double- and triple-labelled cells were counted in Adobe Photoshop CS5 software (Adobe Systems, Inc). The total number of cells was estimated using the Abercrombie method as described in 2.8.1. Using a grid generated in Photoshop as a reference, a 230 µm high strip (2.5 grid divisions) was selected from the widest area of the graft (Figure 2.6B) and the distribution of Girk2-ir/TH-ir and Calbindin-ir/TH-ir neurons within the graft was analysed by counting cells in the fields sampled from either the periphery (25% of width of the graft from each side) or the centre (50%) of the graft and grouping them accordingly for statistical analysis.

2.9 Statistical Analysis

Statistical analyses were performed in SPSS Statistics 20 (IBM Corporation). Details of statistical methods used to analyse data are specified in each chapter. In short, general linear model (GLM) Univariate function was used to perform two-factor and higher analyses of variance (two-way and higher ANOVAs) to analyse data from IHC staining. GLM with repeated measures was used to analyse DA neuron subpopulations and their distribution in the grafts as well as drug-induced rotational behaviour. Bonferroni correction for multiple comparisons was used to reveal significant differences between individual groups. One-way ANOVAs were performed where appropriate. Results were considered to be significant if $p<0.05$ (*), however higher significance levels (** $p<0.01$, *** $p<0.001$) are also reported in the text.

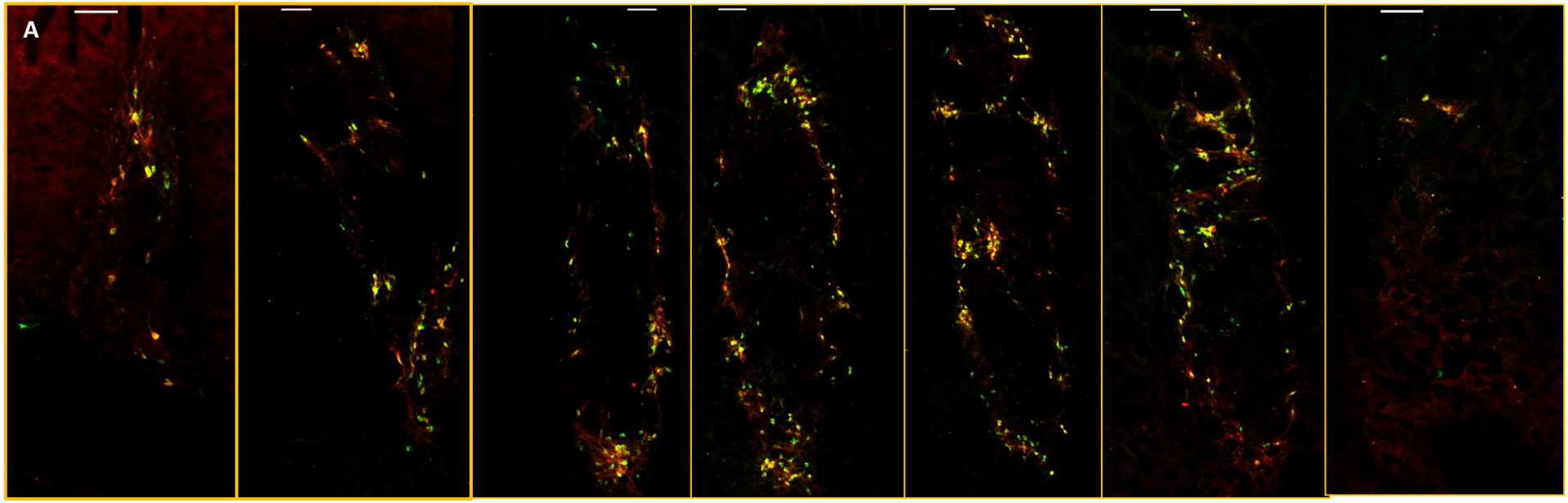

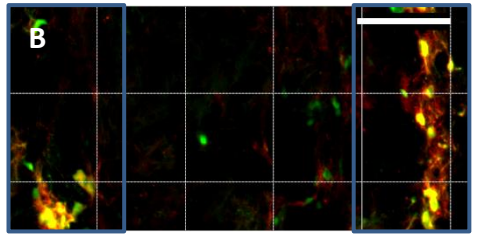

Figure 2.6 (A) Photomicrographs of all coronal sections through the striatum that contain the graft illustrating Girk2 (red) and TH (green) staining in the graft derived from E12 VM. TH-ir and Girk2-ir/TH-ir neurons were counted in Photoshop software. **(B)** Representation of sampled fields in the periphery (blue rectangles) and the centre of the graft. Scale bar: 100 µm.

Chapter 3. Analysis of Dopamine Neuron Subtypes in Ventral Mesencephalic Grafts

Summary

The aims of this chapter were to determine the survival and distribution of the A9 type and A10 type DA neurons within the implants derived from rat E12 and E14 VM tissue. To that end, 6-OHDA unilaterally lesioned rats received grafts into the striatum. Younger donor grafts produced significantly more DA neurons, and more importantly, significantly more A9 type DA neurons, which induce functional recovery in lesioned animals. E14 grafts displayed a typical morphology with the majority of the DA neurons located in the periphery of the graft rather than in the centre while a more homogeneous distribution of TH-ir neurons was observed in grafts in the E12 group. The majority of DA neurons in the periphery of all grafts were of A9 type while in the centre of the graft similar proportions of DA neurons were of either subtype. This suggests that the striatal environment may influence differentiation of DA neural precursor cells and may attract A9 type DA neuron migration towards the periphery of the graft.

3.1 Introduction

The longstanding problem of relatively poor survival of transplanted DA neurons has greatly hampered the use foetal VM tissue for the treatment of PD. In the last 30 years, researchers have refined the methods for the dissection of the VM, preparation of the cell suspensions, and the implantation of DA neurons leading to improved reproducibility of the results and increased graft survival. However, typically only 5 – 10% of untreated transplanted DA neurons survive in grafts both in animal models (Brundin et al., 2000a) and human patients (Kordower et al., 1996, Kordower et al., 1997a, Kordower et al., 2008a, Kordower et al., 2008b). The low DA neuron yield in transplants is considered to be a major reason for the poor clinical outcome of the transplantation therapy seen in many trials.

In an attempt to improve the survival of transplanted DA neurons, the optimal embryonic donor age for DA grafts was recently readdressed. The yield of TH-ir neurons was greatly improved in grafts derived from the rat E12 VM tissue, which is 2 days younger than E14-derived grafts that have been broadly used for transplantation studies in animal models over the years (Torres et al., 2007). The same study also reported that the similar extent of striatal reinnervation was achieved by single placement grafts derived from E12 and E14 VM tissue, and the survival of DA neurons was boosted up to a survival rate of 35% of the expected complement of TH-ir neurons in the adult VM by using grafts derived from younger embryos. A similar impact of the donor age was observed in mouse VM grafts where DA neuron yield was 2.6-fold higher in grafts derived from the E10 VM tissue as compared to the E12 VM tissue (Bye et al., 2012). In another study, multiple rat E12 VM-derived intrastriatal grafts produced even higher yields of DA neurons (75% survival rate) and reinnervated a greater volume of the striatum but did not offer behavioural recovery beyond levels that were achieved by E14 VM-derived transplants (Torres et al., 2008a). This suggests that either a more extensive reinnervation of the stratum is required to further improve the behavioural recovery or that there is a limit to the behavioural recovery that can be achieved by DA supply to the striatum. Nevertheless, the VM tissue derived from younger embryos is believed to be a better source of transplantable DA neurons due to higher graft survival rates it is able of achieving.

DA neural precursor cells contained in the developing VM comprise two major populations: A9 type DA neurons of the SNpc that give rise to the nigrostriatal pathway

and A10 type DA neurons of the VTA that give rise to the mesolimbic and mesocortical pathways (Dahlstrom and Fuxe, 1964). In the adult human and mouse VM, TH-ir neurons located in the SNpc are large and angular in shape and coexpress Girk2, whilst TH-ir neurons located in the VTA and dorsal tier of the SNpc are smaller and round in shape and coexpress calbindin (Thompson et al., 2005, Reyes et al., 2012). Several studies have demonstrated that these distinctive features of the two DA neuron populations seem to be retained after transplantation of embryonic VM and can be used to distinguish DA neurons of the SNpc- and VTA-phenotypes in the graft (Mendez et al., 2005, Thompson et al., 2005, Grealish et al., 2010, Bye et al., 2012). By retrograde axonal tracing, Thompson and colleagues showed that innervation of the DA-depleted striatum was derived almost exclusively from the A9 type DA neurons located in the periphery of the graft while the A10 type DA neurons, densely distributed within the centre and scattered throughout the periphery of the graft, innervated the PFC and probably other targets in the forebrain. Grealish and colleagues demonstrated the importance of the A9 type DA neurons in mediating functional recovery by showing that mouse grafts with a typical A9/A10 composition restored 6-OHDA lesion-induced deficits in rats while animals transplanted with the VM tissue which was selectively lacking A9 type DA neurons remained impaired. This raises the possibility that improved graft survival without enhanced behaviour achieved by rat E12 VM transplants as compared to E14 VM transplants (Torres et al., 2008a) might be linked to distinct patterns of preferential differentiation and/or survival of one population of DA neurons over another in grafts derived from different donor age embryos, an issue which has not yet been addressed experimentally.

3.1.1 Aims of the chapter

The present experiment was undertaken to determine whether donor age had an impact on the two DA neuron populations in transplants derived from rat E12 and E14 VM tissue. The aims of this experiment were:

1. To determine the A9 type and A10 type DA neuron yields in E12 and E14 VM grafts
2. To investigate the distribution of the two DA neuron phenotypes within the grafts

3.2 Experimental Procedure

All of the methods used in this study are described in Chapter 2. In this experiment, female SD rats (n = 18) received a unilateral lesion to the right MFB via the injection of 6-OHDA (Chapter 2.3.1) and the lesions were confirmed with drug-induced rotation tests (Chapter 2.4). The animals were allocated into 2 homogeneous groups based on the number of amphetamine-induced ipsilateral rotations (mean ± SEM; **E12:** 1154.1 ± 119.5; **E14:** 1152.1 ± 116) and no statistical differences between the groups were confirmed with a one-way ANOVA (Group, $F_{(1,16)} = 0.00$; n.s.).

Six weeks post-lesion, two VM cell suspensions from one E12 and one E14 litters were prepared for grafting as described in Chapter 2.3.2 (**E12:** 128,500 cells/VM, viability – 94.27%; **E14:** 294,600 cells/VM, viability – 92.61%). Every animal received a graft containing cell numbers equivalent to 1 VM in 2 µl of the cell suspension via the injection into the striatum at stereotaxic co-ordinates AP: +0.6 mm, ML: -3.0 mm, DV: -5.0 mm (Paxinos and Watson, 2003). Efficacy of grafts was assessed with drug-induced rotation tests 4 and 6 weeks post-graft. All animals were transcardially perfused 7 weeks after transplantation and coronal brain sections were collected for IHC processing (Chapter 2.5).

A one-in-twelve series of sections was stained for CV (Chapter 2.6.2). A second series was stained for DAB TH; three series were processed for TH and Girk2, TH and calbindin, and Girk2 and calbindin, respectively, using fluorescent double labelling IHC (Chapter 2.6.1). Stained cells were counted blind to the experimental condition abiding by the stereological principles (Chapter 2.8). Double labelled cells in the centre and the periphery of the graft were counted as described in Chapter 2.8.2.

Statistical analyses were performed in SPSS as described in Chapter 2.9. Behavioural data from drug-induced rotation tests was analysed using a two-way ANOVA with repeated measures. One-way ANOVAs were performed to analyse cell counts obtained from CV staining, DAB TH staining, graft volumes, DA neuron density in the grafts, as well as to compare percentages of double labelled cells from Girk2/calbindin staining. DA neuron subpopulations and their distribution within the graft were analysed using two- and three-way ANOVAs with repeated measures, respectively. A two-way ANOVA with repeated measures was used to analyse the A9 type and the A10 type DA cell diameters. Bonferroni correction for multiple comparisons was used to reveal significant differences between individual groups and results were considered to be significant if $p<0.05$ (*).

3.3 Results

3.3.1 Functionality of the grafts

The ability of the graft to release DA and ameliorate lesion-induced rotational asymmetry in response to amphetamine was assessed by recording the net number of drug-induced rotations (ipsilateral minus contralateral) towards the lesioned side, performed over 90 minutes at 4 weeks and 6 weeks post-transplantation (Figure 3.1). Post-lesion, all animals rotated ispilaterally in response to the dopaminergic drug, the classic motor deficit induced by the unilateral 6-OHDA lesion to the MFB. Six weeks after transplantation two animals in the E14 group did not show any improvement and were excluded from subsequent analysis. Later, TH IHC confirmed virtually no surviving DA neurons in the striatum of these rats. In other animals, graft-derived DA release in the striatum significantly ameliorated the lesion-induced rotational behaviour 4 weeks and 6 weeks after transplantation (within subject factor – Transplantation, $F_{(2, 28)} = 43.18$, $p<0.001$). There were no significant differences in the net number of rotations between the two donor age groups (Donor Age, $F_{(1,14)} = 0.51$, n.s.; Donor Age x Transplantation, $F_{(2, 28)} = 2.19$, n.s.). Animals in the E12 group already showed a significant behavioural recovery in the first 4 weeks after transplantation ($p<0.01$) while animals in the E14 group remained partially impaired 4 weeks post-grafting but significantly improved during the following 2 weeks ($p<0.01$).

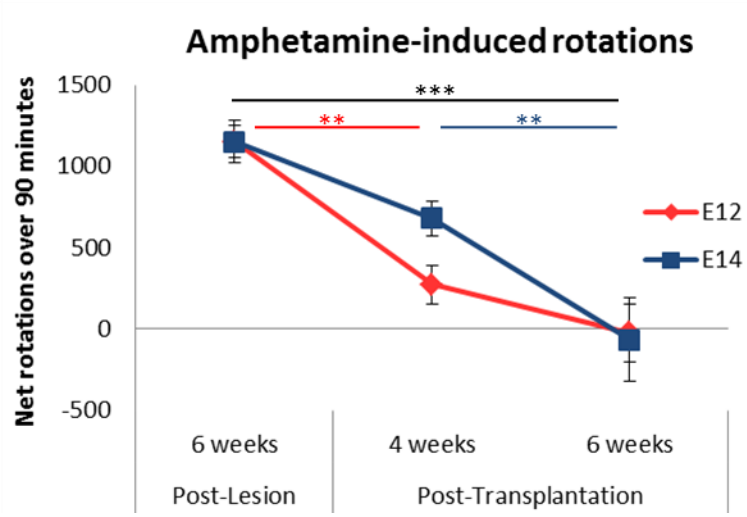

Figure 3.1 Amphetamine-induced rotational behaviour in lesioned and grafted rats in the E12 (red) and the E14 (blue) groups. Both donor age graft groups produced a significant recovery of the lesion-induced behavioural deficit. There was a (***) change from ipsilateral rotation observed post-lesion to a net contralateral rotation post-grafting, the classic over-compensatory response ($F_{(2,28)}$ = 43.18, $p<0.001$). Data are presented as a mean number of net rotations (ipsilateral minus contralateral) over 90 minutes; error bars indicate SEM; significance levels: ** $p<0.01$, *** $p<0.001$.

3.3.2 Total cell yield in the grafts

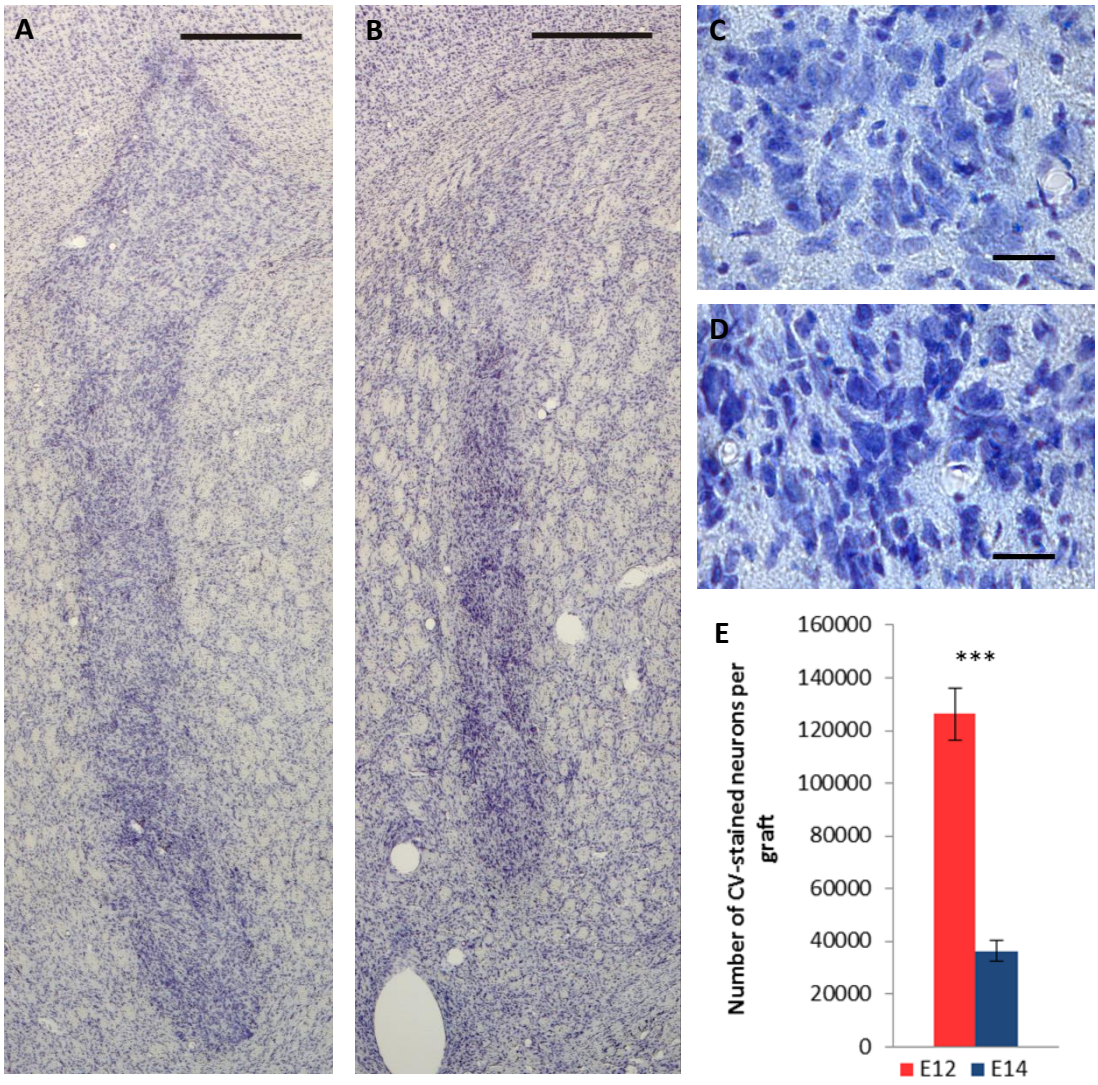

Figure 3.2 Photomicrographs of CV staining in the intrastriatal grafts in the E12 **(A)** and the E14 **(B)** groups 7 weeks post-transplantation. Mixed populations of neuronal and non-neuronal cells were homogeneously distributed within the grafts. Higher magnification of grafts showing cell morphology and distribution in grafts in the E12 **(C)** and in the E14 groups **(D)**. Scale bars: 500 µm (A, B); 25 µm (C, D). **(E)** Total number of CV-stained neurons in grafts in each donor age group. Transplants derived from the E12 VM tissue yielded 3-fold more neurons than E14 VM-derived grafts ($F_{(1,14)}$ = 56.38, $p<0.001$). Columns depict group means; error bars illustrate SEM; significance level: *** $p<0.001$.

Examination of CV stained sections revealed well positioned grafts in the striatum of all 9 animals in the E12 group and 7 animals in the E14 group. Grafts contained homogeneously distributed mixed populations of neuronal and non-neuronal cells without any evidence of inflammatory reaction within the graft or in the surrounding striatum (Figure 3.2). To estimate the total number of neurons in the grafts CV stained cells were counted using the Nissl body distribution within the cell body as

criterion to identify neurons. Cells were considered neuronal if Nissl bodies stained by CV clearly demonstrated the soma. We recognise that CV staining methos is an imperfect way to estimate neuronal number but for technical reasons it was unavoidable in this experiment. Despite the fact that implanted E14 VM tissue contained twice as many cells as E12 VM tissue, grafts in the E12 group yielded 3-fold more neurons than grafts in the E14 group at 7 weeks after transplantation. This suggests that cells derived from younger embryonic tissue might survive transplantation, differentiate and mature in the host significantly better than cells derived from more mature tissue. Also, there might be greater numbers of neural precursors in the E12 VM tissue than in the E14 VM tissue that continue to proliferate after transplantation, thus contributing to higher yields of cells. As shown in Figure 3.2E, stereological analysis of CV stained sections revealed that E12 grafts contained significantly more neurons than E14 grafts ($F_{(1,14)}$ = 56.38, $p<0.001$).

3.3.3 DA neuron yield in the grafts

Examination of TH-stained sections showed large numbers of TH-ir cells in the grafts with extensive transplant-derived reinnervation of the surrounding striatum (Figure 3.3). In the E12 group, grafts displayed a homogeneous distribution of TH-ir neurons throughout the graft together with areas of dense DA innervation within the graft. The majority of TH-ir neurons in the periphery of the graft had an angular and elongated shape while the cells within the centre of the graft typically had a round, symmetrical morphology. Fewer DA neurons were observed in transplants in the E14 group with most TH-ir neurons located in the periphery of the graft and only a few seen in the centre of the graft. As shown in Figure 3.3E, 5.23-fold more DA neurons were found in transplants in the E12 group than E14 group indicating that younger E12 DA neural precursor cells survived the transplantation, differentiated into mature DA neurons and integrated in the host striatum better than more mature DA neurons in the E14 VM tissue ($F_{(1,14)}$ = 30.66, $p<0.001$). When compared with 40,000 DA neurons in a healthy adult rat VM (German and Manaye, 1993), TH-ir cell yield in grafts in the E14 group represents 4% of the expected complement of DA neuron population in the adult VM. A significantly higher DA neuron yield was seen in grafts in the E12 group and corresponded to 19% of the expected adult complement. Based on an adjacent series of sections that was stained for CV, the percentage of TH-ir neurons was calculated and shown to differ significantly between the two donor age groups ($F_{(1,14)}$ = 12.18, $p<0.01$; Figure 3.3F). Thus, although significantly more neurons were found in grafts derived

from the E12 VM tissue as compared to the E14 VM tissue, the increase in DA neuron population outweighed the general gain in neuron yield.

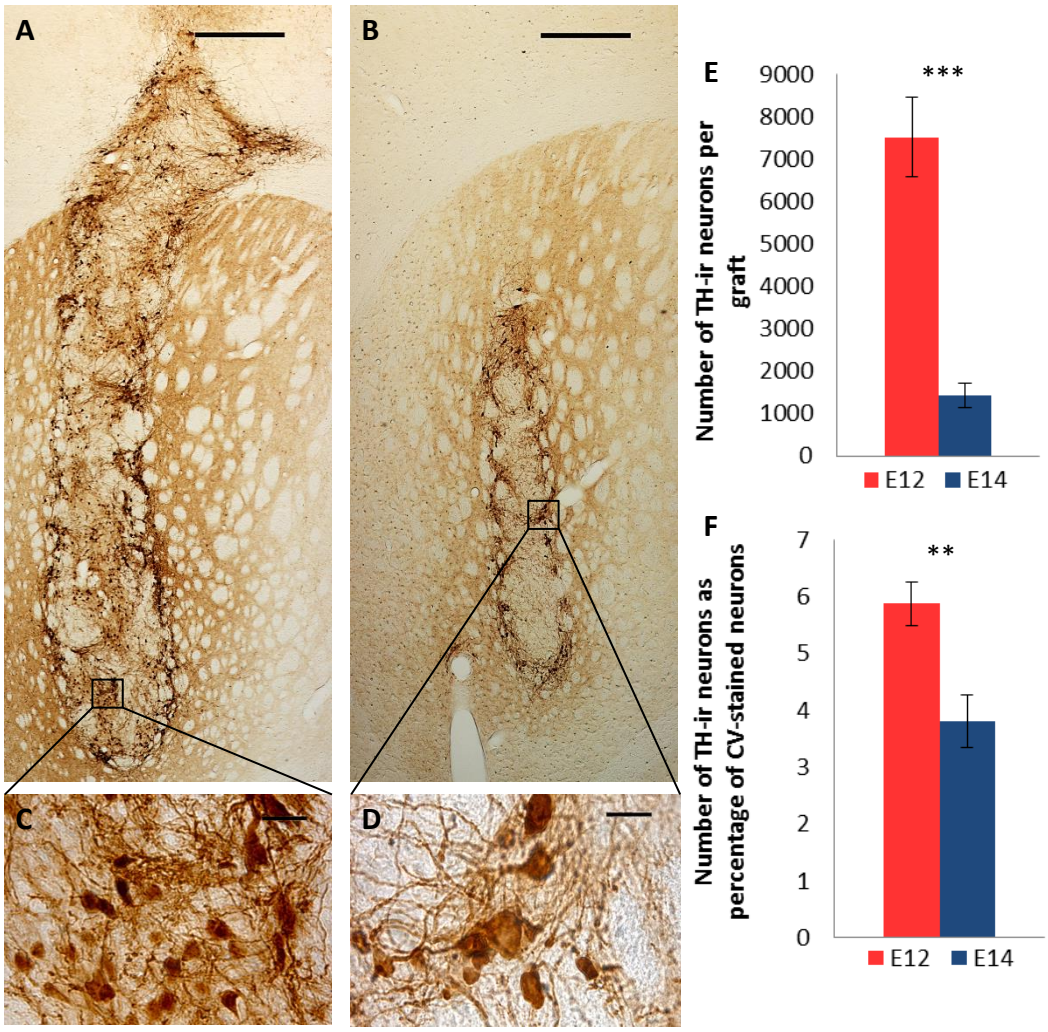

Figure 3.3 Photomicrographs of DA grafts derived from E12 and E14 donor embryos (TH stained sections). **(A)** A low power image of the representative graft in the E12 group containing many TH-ir cells in the periphery of the graft and clusters of DA cells in the centre of the graft, and dense innervation of the striatum. **(B)** A low power image of the graft in the E14 group containing less TH-ir neurons, which are mostly located in the periphery of the graft, and innervating a smaller volume of the striatum. Higher magnification of implanted TH-ir neurons showing cell morphology in grafts in the E12 **(C)** and in the E14 groups **(D)**. Scale bars: 500 µm (A, B); 25 µm (C, D). **(E)** Total numbers of DA neurons in the grafts. Grafts in the E12 group contained significantly more TH-ir neurons than grafts in the E14 group ($F_{(1,14)}$ = 30.66, $p<0.001$). **(F)** Effect of the donor age on the percentage of TH-ir/CV-stained neurons in the grafts. A significantly higher percentage of neurons were of DA phenotype in grafts in the E12 group than E14 group ($F_{(1,14)}$ = 12.18, $p<0.01$). Data are presented as group means; error bars illustrate SEM; significance levels: ** $p<0.01$, *** $p<0.001$.

As seen in Figure 3.3, grafts derived from the E12 VM tissue were notably larger than grafts in the E14 group and occupied a large part of the striatal volume. In addition, transplants in the E12 group were unusually large in a rostro-caudal direction, in some cases extending more than 2 mm. Not only did the DA grafts derived from younger embryos occupy a 3.76-fold larger volume of the striatum (Figure 3.4A; $F_{(1,14)} = 40.09$, $p < 0.001$), they were also more densely populated with TH-ir neurons (Figure 3.4B; $F_{(1,14)} = 8.52$, $p < 0.05$).

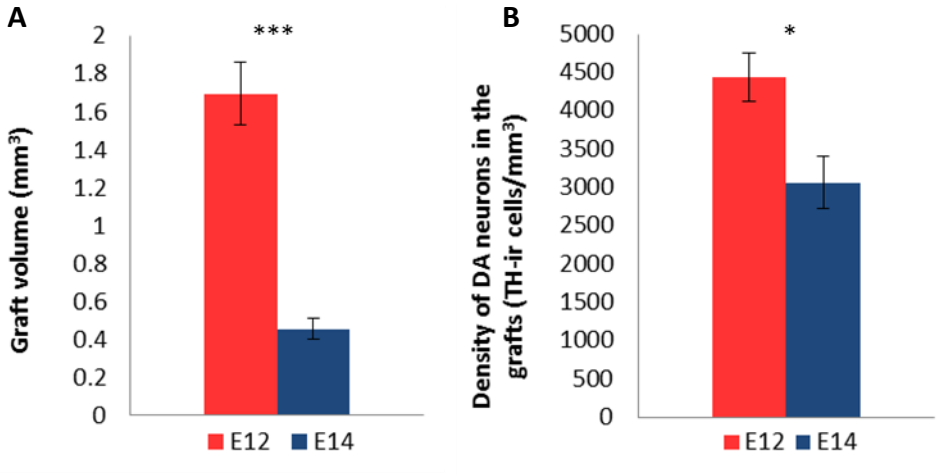

Figure 3.4 (A) A summary of graft volumes in each donor age group. Grafts derived from the E12 VM tissue were significantly bigger than grafts obtained from the 14 VM tissue ($F_{(1,14)} = 40.09$, $p<0.001$). **(B)** DA neuron density in grafts in each donor age group. TH-ir cells displayed a homogeneous and more denser distribution in grafts in the E12 group as compared to E14 group ($F_{(1,14)} = 8.52$, $p<0.05$). Columns depict group means; error bars illustrate SEM; significance levels: * $p<0.05$; *** $p<0.001$.

3.3.4 The A9 and A10 type DA neurons in the grafts

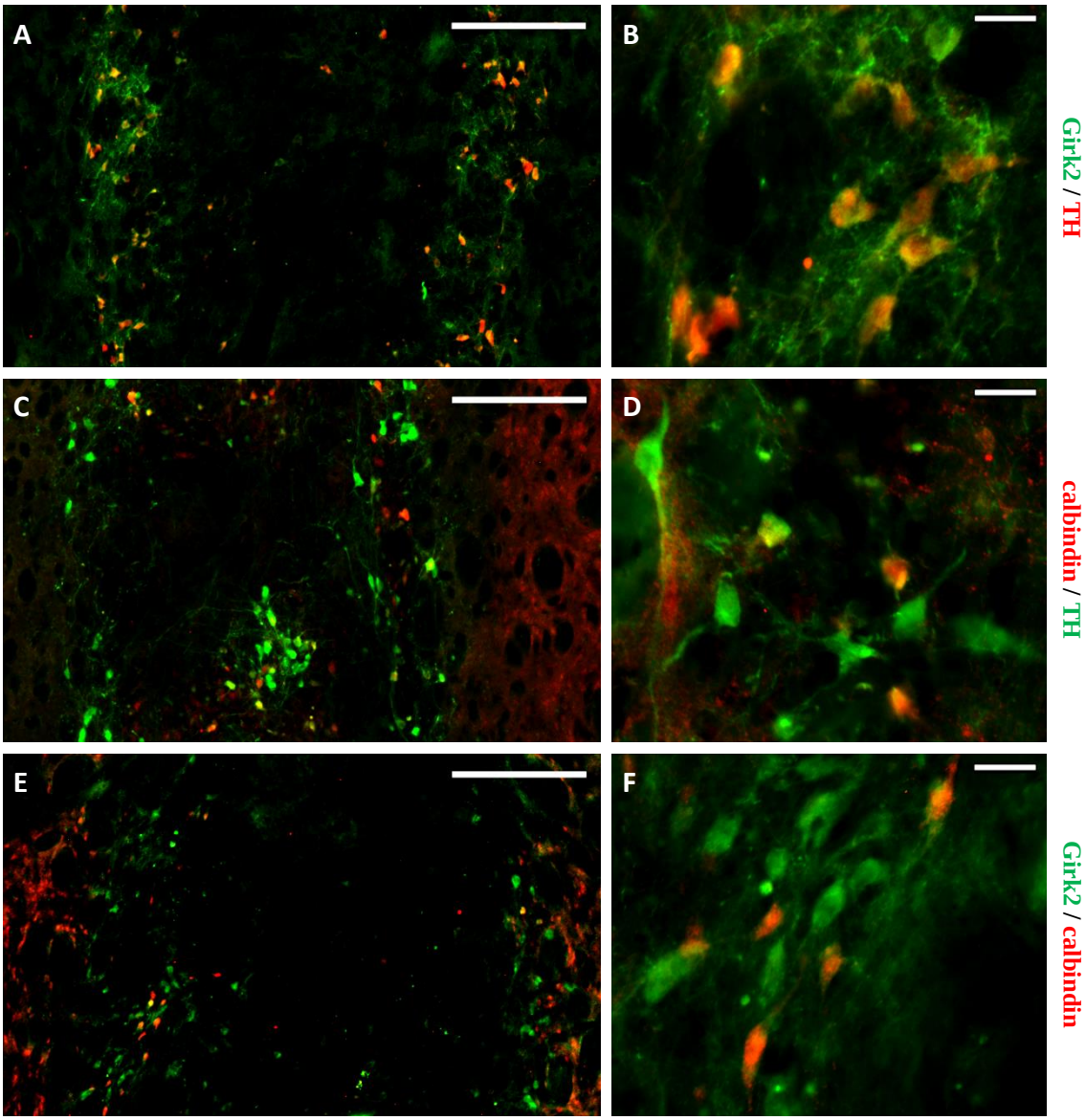

Figure 3.5 Coronal sections through the grafts in the E12 group illustrating double fluorescent labelling for **(A, B)** Girk2(green)/TH(red), **(C, D)** calbindin(red)/TH(green), and **(E, F)** Girk2(green)/calbindin(red). Scale bars: 200 µm (A, C, E); 20 µm (B, D, F).

Two subpopulations of TH-ir neurons were identified in the grafts based on the coexpression of Girk2 and calbindin proteins, respectively. The majority of TH-ir cells co-labelled with Girk2 in all grafts and a smaller subpopulation of TH-ir neurons coexpressed calbindin. A few Girk2-ir and calbindin-ir neurons that were negative for TH were observed in the grafts in the two series double labelled for Girk2/TH and calbindin/TH, respectively. In the sections stained for Girk2/calbindin, a small number of calbindin-ir neurons in the grafts also coexpressed Girk2; however, it was not clear whether they were TH-ir because triple labelling was not performed in the current

experiment. Previous studies have suggested that 5 – 25% of calbindin-ir/TH-ir cells co-label with Girk2 in the adult mouse and human VM (Thompson et al., 2005, Reyes et al., 2012). In the present experiment, 17.49 ± 1.93% and 11.62 ± 2.23% of calbindin-ir cells co-labelled with Girk2 in the E12 and E14 groups, respectively, but the difference between the two donor age groups was not significant ($F_{(1,14)} = 3.97$, n.s.).

Cell counts revealed that grafts derived from E12 VM tissue yielded significantly higher numbers of both the A9 type and A10 type DA neurons than transplants in the E14 group (Figure 3.6; Donor Age, $F_{(1,14)} = 38.86$, $p<0.001$). A highly significant difference between the two subpopulations of DA neurons in the grafts was found (within-subject factor – Staining, $F_{(1,14)} = 66.77$, $p<0.001$; Staining x Donor Age, $F_{(1,14)} = 32.31$, $p<0.001$). Implants in the E12 group contained significantly more A9 type than A10 type DA neurons ($p<0.001$) and, although grafts in the E14 group also yielded higher numbers of Girk2-ir/TH-ir cells than calbindin-ir/TH-ir cells, the difference was not significant. Grafts in the E12 group were significantly more enriched for the A9 type DA neurons than transplants in the E14 group (within subject factor – Cell count %, $F_{(1,14)} = 2021.19$, $p<0.001$; Donor Age, $F_{(1,14)} = 77.12$, $p<0.001$) as indicated by a higher percentage of TH-ir neurons double labelled with Girk2 (80% and 68%, respectively; $p<0.001$). Also, a higher percentage of DA neurons were of the A10 phenotype in implants derived from the E12 VM tissue than E14 VM tissue (27% and 24%, repsectively; $p<0.05$). Note that the percentages of TH-ir neurons double labelled with Girk2 and calbindin added up to more than 100% in grafts in the E12 group, at least 8% of DA neurons did not coexpress either the Girk2 or calbindin comarkers in transplants in the E14 group. A higher proportion of TH-ir neurons that do not belong to either DA phenotype observed in grafts in the E14 group might be a result of inability of implanted post-mitotic DA neurons committed to the A10 phenotype to assume the A9 phenotype under the influence of the striatal environment. There is a possibility that without access to A10 functional targets in the striatum these neurons silence their A10 phenotype.

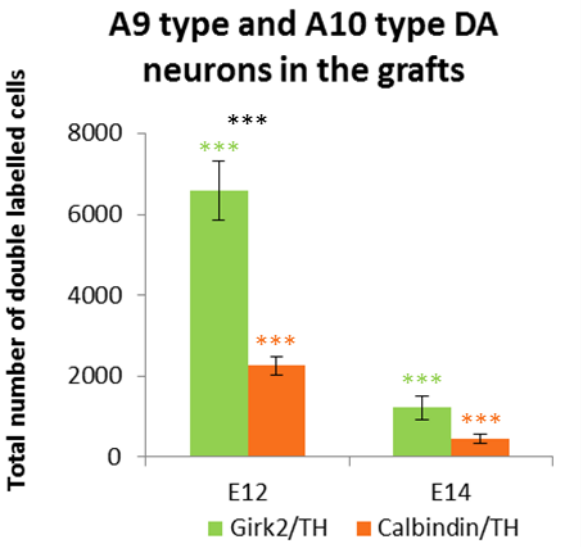

Figure 3.6 Total numbers of Girk2-ir/TH-ir (green) and calbindin-ir/TH-ir (orange) neurons in the grafts. Grafts in the E12 group produced higher numbers of both DA neuron subtypes than in the E14 group. Also, Girk2-ir/TH-ir neurons were more abundant than calbindin-ir/TH-ir neurons in grafts in the E12 group. Significant differences between individual groups are depicted on the graph. Columns depict group means; error bars illustrate SEM; significance level: *** $p<0.001$.

Graft morphology was looked at to determine the distribution of DA neurons in the graft, with particular reference to their position either in the periphery or in the central core of the graft. Analysis showed that the majority of TH-ir neurons in the periphery were of the A9 phenotype in all grafts while, similar proportions of the TH-ir neurons coexpressed either Girk2 or calbindin in the centre of the grafts (Figure 3.7). The composition of the periphery of the graft was confirmed to be significantly different than the composition of the centre of the graft (within-subject factor – Location, $F_{(1,14)} = 6.63$, $p<0.05$). In the periphery of the transplant, significantly more TH-ir neurons coexpressed Girk2 than calbindin both in the E12 group ($p<0.001$) and E14 group ($p<0.01$). In the centre of the graft, no significant differences were found between the percentages of DA neurons that co-labelled with either Girk2 or calbindin. Also, the distribution of A9 type DA neurons within the graft was significantly different from the distribution of the A10 type DA neurons (within-subject factor – Staining, $F_{(1,14)} = 12.56$, $p<0.01$). In the E12 group, a higher percentage of TH-ir neurons coexpressed Girk2 in the periphery than in the centre of the graft ($p<0.01$). Conversely, a higher percentage of TH-ir neurons co-labelled with caldindin in the centre of the graft than in the periphery of the graft ($p<0.05$). This suggests that younger DA neural precursor cells in the periphery of the graft might be directed towards the nigral phenotype by the environmental cues present in the surrounding striatum while, in the centre of the graft,

similar proportions of DA neural precursor cells survive and/or differentiate into either DA neuron phenotype. Although, the majority of A9 type DA neurons were also found in the periphery of transplants in the E14 group, no significant differences in the proportion of A9 and A10 phenotypes between the periphery and the centre were detected. The donor age influenced only the percentage of TH-ir neurons that coexpressed calbindin in the periphery of grafts with a higher proportion of DA neurons in the periphery of grafts being of the A10 phenotype in transplants derived from older VM tissue ($p<0.01$). This suggests that post-mitotic DA neurons contained in the E14 VM tissue might be more committed to the VTA-phenotype and are less likely to assume SNpc identity under the influence of the striatal environment. Interestingly, proportions of TH-ir cells that co-labelled with either Girk2 or calbindin in the periphery of the graft added up to almost 100% in both donor age groups. Whereas there were ~30% of TH-ir neurons in the centre of the grafts in both groups that did not co-express neither Girk2 nor calbindin. This suggests that differentiation of DA neural precursor cells might be influenced by the environment in the centre of the graft. Also, the total yield of TH-ir neurons in the periphery of the graft was higher than in the centre of the graft, 3-fold in the E12 group ($p<0.001$) and 5-fold in the E14 group ($p<0.01$). This indicates that either the survival of DA neurons might be significantly influenced by the local environment within the graft or that transplanted DA neurons migrate towards the periphery of the graft towards their functional targets.

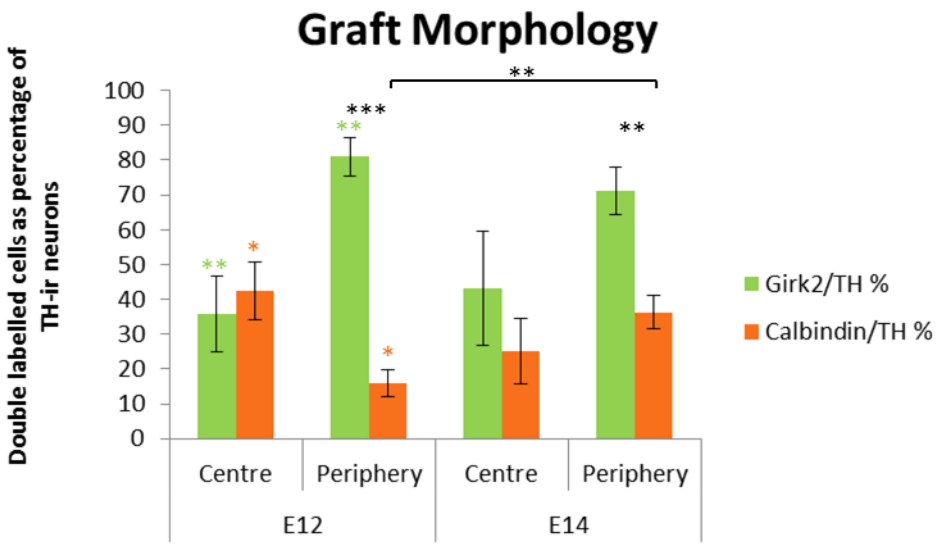

Figure 3.7 A summary of the distribution of the A9 type and A10 type DA neurons within the grafts. The majority of DA neurons coexpressed Girk2 in the periphery of the grafts while similar proportions of TH-ir neurons co-labelled with either Girk2 or calbindin in the centre of the grafts in both donor age groups. The A9 type DA neurons were predominantly found in the periphery of grafts; however this was significant only in the E12 group. The A10 type DA neurons were predominantly found in the centre of grafts in the E12 group while they displayed a more homogeneous distribution in grafts in the E14 group. Significant differences between individual groups are depicted on the graph. Columns depict group means; error bars illustrate SEM; significance levels: * $p<0.05$, ** $p<0.01$, *** $p<0.001$.

Girk2-ir/TH-ir cells displayed predominantly angular and elongated morphology while calbindin-ir/TH-ir were smaller and round in shape, and as demonstrated in Figure 3.8, a significant difference in cell diameters was found in both donor age groups ($F_{(1,14)} = 14.93$, $p<0.01$).

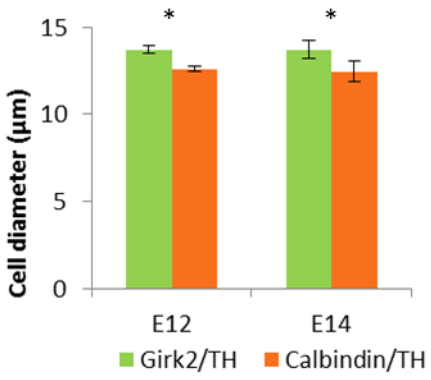

Figure 3.8 A summary of cell diameters in grafts in the E12 and E14 groups. The A9 type DA neurons were significantly bigger than the A10 type DA neurons in both donor age groups. Individual differences between the groups are depicted on the graph. Data are presented as group means ± SEM, significance level: * $p<0.05$.

3.4 Discussion

This study has confirmed previously published results demonstrating that grafts derived from the rat E12 VM tissue yield significantly higher DA neuron numbers than E14 VM-derived grafts (Torres et al., 2007, Torres et al., 2008a). When compared with 40,000 DA neurons in the healthy adult rat VM (German and Manaye, 1993), the present DA neuron yield in grafts in the E12 group represents 19% of the expected adult complement, a much better result than conventional E14 grafts, which were able to achieve only 4%. The two principal TH-ir cell types in adult VM are: (1) large, angular Girk2-ir cells predominantly found in the SNpc and (2) smaller, round calbindin-ir cells mainly restricted to VTA regions (Thompson et al., 2005, Reyes et al., 2012). It has been hypothesised that E12 and E14 grafts might be different in terms of the A9 and A10 DA neuron subtypes they contain.

In PD, neurodegeneration in the SNpc occurs in a distinct pattern with A9 type DA neurons in the ventral tier of the SNpc rapidly disappearing and A10 DA neurons in the dorsal tier of the SNpc remaining intact until late stages of the disease (Braak et al., 2003). The differential distribution of Girk2 channels, ion channels modulating neuronal excitability (Lacey et al., 1987), in DA neurons has been suggested to contribute to this early selective cell loss of the ventral tier. This has prompted the use of Girk2 as a marker of A9 type DA neurons. Previous studies in rodents have demonstrated widespread Girk2 messenger ribonucleic acid (mRNA) expression in both the SNpc and the lateral VTA DA neurons with higher levels of mRNA expression found in the SNpc than the VTA (Schein et al., 1998, Chung et al., 2005, Eulitz et al., 2007). Localisation of the Girk2 protein initially was reported to be restricted to neurons in the ventral tier of the SNpc in mice, rats and humans (Mendez et al., 2005, Thompson et al., 2005) but later studies have demonstrated that the entire SNpc and lateral but not midline regions of the VTA contain Girk2-ir DA neurons in mice and humans (Lammel et al., 2008, Reyes et al., 2012). Also, a highly variable overlap between Girk2 and calbindin coexpression in TH-ir neurons was observed in the aforementioned studies, with 5 – 25% of calbindin-ir/TH-ir also being positive for Girk2. Differences in the reported results on Girk2 protein localisation may have been influenced by a number of factors, which include species differences, changes with age and post-mortem delay, different fixation procedures, the use of different antibodies.

Thompson and colleagues (2005) have shown that cell morphology and Girk2/calbindin expression in DA neurons were retained after transplantation and could be used to distinguish between the A9 type and A10 type DA cells in the grafts. The present results suggest that TH-ir cells in embryonic rat grafts can be distinguished as two major subtypes of DA neurons based on their cell morphology and coexpression of either Girk2 or calbindin. In both donor age groups, grafts contained large populations of Girk2-ir/TH-ir and calbindin-ir/TH-ir cells. However, there was an overlap between the two cell populations as indicated by the sum of proportions of TH-ir neurons that coexpressed either Girk2 or calbindin in grafts in the E12 group being higher than 100%. At least a 7% overlap existed in grafts derived from younger embryos, a figure that is within a previously reported range of 5 – 25% overlap in Girk2 and calbindin expression in DA neurons (Thompson et al., 2005, Reyes et al., 2012). TH-ir neurons that co-labelled with Girk2 were larger in size and displayed an angular cell morphology as compared to smaller and round in shape calbindin-ir/TH-ir cells in both donor age groups.

Grafts derived from younger VM tissue produced neuron yields of 126229 ± 10023, which were almost equal to the number of cells transplanted (128,500 cells/graft). As the implanted cell suspensions contained a mixture of neuronal and non-neuronal cells, the high yield of CV-stained neurons in the grafts suggests that neural precursor cells in the E12 VM tissue continued to proliferate after transplantation significantly contributing to neuron-rich grafts. Indeed, previous research in our lab has demonstrated that cells grafted at E12 continued to proliferate in the host for at least 2 days post-transplantation significantly contributing to high DA neuron yields (Weyrauch, 2009). Transplants in the E12 group yielded higher numbers of both the A9 type and A10 type DA neurons and were more enriched for the functionally important DA neurons of the nigral phenotype than grafts derived from E14 VM tissue. Previous studies have demonstrated that the A9 type DA neurons are an important determinant for behavioural recovery. Reinnervation of the DA-depleted striatum has been shown to be derived predominantly from the A9 type DA neurons in the grafts (Thompson et al., 2005). Another study has shown that transplants selectively lacking in the A9 type DA neurons produced only a partial recovery of drug-induced rotational behaviour in 6-OHDA lesioned rats (Grealish et al., 2010). Previous studies using grafts derived from E12 rat embryos have demonstrated a 5-fold increase in DA neuron yield but that behavioural recovery of lesion-induced deficits was no better than that observed with E14 VM-derived grafts (Torres et al., 2008a). The present results show that transplants

derived from younger embryos produce 5-fold more A9 type DA neurons than grafts obtained from E14 VM tissue which suggests that similar behavioural recovery in animals in the E12 and E14 groups cannot be associated with different preferential yields of one DA phenotype over another in grafts derived from different donor age embryos.

Results from this study allow to make a direct comparison of the distribution of the A9 type and A10 type DA neurons within rat E14 VM-derived grafts and mouse E12.5 VM-derived grafts, as these two ages are considered to correspond to similar developmental stages of the embryogenesis in the two rodent species (Thompson et al., 2005). In the E12.5 mouse grafts, large A9 type DA neurons, which expressed Girk2, were mostly found at the periphery of the graft whilst smaller A10 type DA neurons, which expressed calbindin, were abundant in the centre of the graft. Similarly, in the present study, the periphery of the rat E14 VM-derived grafts was predominantly composed of the A9 type DA neurons. However, the proportions of the two populations of DA neurons in the centre of grafts were highly variable between the subjects, with most DA neurons being of the A9 phenotype, but this difference was not significant. Such great variance of the present results may be due to a significantly lower yield of TH-ir neurons in the centre than in the periphery of the grafts. Using an unbiased method of visual field sampling in the centre and in the periphery of the graft (Chapter 2.8.2), on average 3 TH-ir neurons were captured in the centre of E14 VM-derived grafts. Nevertheless, a 4-fold higher proportion of TH-ir neurons coexpressed Grik2 in the centre of rat E14 VM-derived grafts as compared to mouse E12.5 VM-derived grafts suggesting that, in rats, DA neurons may not need to be located at the periphery of the graft to survive and project to the surrounding striatum to differentiate into the A9 type DA neurons (though, the majority are).

The distribution of the A9 type and A10 type DA neurons in grafts derived from the E12 VM tissue was similar to the E14 VM-derived grafts. However, the A10 type DA neurons were more represented in the centre rather than in the periphery of the graft in the E12 group. Also, the proportion of the A10 type DA neurons in the periphery of the graft was two-fold smaller in the E12 group than E14 group but the associated increase in the proportion of the A9 type DA neurons in the periphery of the graft in the E12 group was not significant. Moreover, while there was a 7% overlap in the percentages of TH-ir neurons that coexpressed either Girk2 (71%) or calbindin (36%) in the periphery of the graft in the E14 group, at least 5% of TH-ir neurons in the periphery of the graft in the E12 group failed to co-label with either Girk2 or calbindin. This

might indicate that DA neural precursor cells derived from younger donor tissue are able to use environmental cues in the striatum to direct their differentiation away from the A10 phenotype and towards the A9 phenotype with some of the DA neuron progenitor cells succeeding in that endeavour and some failing to become either type of DA neurons. Also, the yield of TH-ir neurons was higher in the periphery of the graft than in the centre in both donor age groups. It is unlikely that the survival of DA neurons is affected by the environment within the graft as CV-stained grafts display a homogeneous neuron distribution within the graft; however this was not quantified in the present study. Implanted cells have been shown to be able to migrate up to several hundred microns away from the needle tract further into the target area (Schmidt et al., 1981, Sotelo and Alvaradomallart, 1987). Thus, another possibility is that DA neurons, attracted by the environmental cues in the striatum, might be migrating towards the periphery of the graft post-transplantation.

A significant 5-fold increase in the number of A9 type DA neurons in the grafts derived from younger embryos reported here has important implications for cell transplantation therapy for PD. At present, post-mitotic DA neurons are derived from human embryos aged 6 – 9 weeks post-conception, and due to major cell loss post-transplantation (90-95% of grafted DA cells die in the host), 6 – 8 human donor embryos are required per unilateral transplant in PD patients. The difficulty of sourcing this number of embryos of the correct age within a time window of 3 – 4 days has been one of the major limitations of translation of this therapy into widespread use. An improved yield of DA neurons provided by both rat and mouse grafts derived from younger VM tissue suggests that it ought to be possible to achieve a similar improvement of human foetal transplantation therapy by using younger DA neural precursor cells (Torres et al., 2007, Torres et al., 2008a, Bye et al., 2012). Post-mortem studies of PD patients that received DA transplants have demonstrated that 68 – 71% of TH-ir neurons in the graft coexpressed Girk2 and 26 – 48% co-labelled with calbindin indicating that human foetal DA neurons retain Girk2/calbindin expression after transplantation (Mendez et al., 2005). Moreover, grafts derived from younger rat embryos here and younger mouse embryos in the previous study reported in the literature (Bye et al., 2012) contained a higher proportion of TH-ir neurons that coexpressed Girk2 suggesting that, in addition to the improved yield of the A9 type DA neurons, an improved enriched composition of the grafts can be achieved by using younger embryonic VM tissue. The goal is to use one human embryo per patient for PD transplantation, and the results from grafts derived from younger donors in animal

models indicate that the required number of surviving DA neurons and the proportion of the nigral type DA neurons could be achieved by using younger human donors.

3.5 Conclusion

The present experiment has further underlined the significant impact of the donor age on grafted DA neuron yield. Harvesting rat foetal VM tissue before the peak of DA neurogenesis has significantly improved yields of DA neurons and, more importantly, also yields of A9 type DA neurons, which are an important determinant for functional recovery. The A9 type DA neurons were found to be influenced by the environment within the graft with the majority of DA neurons of nigral phenotype located in the periphery of the graft while the distribution of the A10 type DA neurons was more homogeneous. Also, the current data suggest that DA neural precursor cells derived from younger donor tissue might be able to use environmental cues in the striatum to direct their differentiation away from the A10 phenotype and towards the A9 phenotype. A future experiment will investigate the influence of the environment in the transplantation site on the two DA neuron subpopulations in grafts derived from the E12 VM and E14 VM tissue.

Chapter 4 The Influence of Environment on the Dopaminergic Grafts

Summary

The aims of this chapter were to investigate the influence of the transplantation site on (i) the A9 type and A10 type DA neuron yield in the graft and (ii) distribution of the two DA cell subpopulations within the graft. To that end, 6-OHDA unilaterally lesioned rats received E12 VM- and E14 VM-derived implants into either the striatum, N.Acc, PFC or the hippocampus. The transplantation site was shown to have little impact on both the total number of neurons and the DA neuron yield in the grafts. A higher yield of TH-ir cells was observed in the E12 grafts than equivalent E14 grafts in all four transplantation sites. This is comparable to previously observed properties of the rat E12 VM tissue to yield a several-fold greater number of DA neurons than equivalent E14-derived grafts (Chapter 3 and Torres et al., 2007). A9 type DA neurons were found to be influenced both by the environment within the graft and by the host environment in the transplantation site to a higher extent than the A10 type DA neurons. The highest yield of A9 type DA neurons was found in grafts implanted into the striatum, which receives the A9 type DA innervation from the midbrain, followed by a progressive decrease in the number of A9 type DA neurons in grafts in the N.Acc, PFC and the hippocampus in the absence of the A9 type DA innervation. Also, A9 phenotype was more influenced by the transplantation site in younger DA precursor cells in E12 grafts than in post-mitotic DA neurons in the E14 grafts. The evidence suggests that differentiation of DA neural precursor cells rather than their survival might be affected by the afferent DA innervation of the transplantation site. Also, the A9 type DA neurons failed to reach the normal cell body size in E12 grafts in the PFC and hippocampus, most likely due to being less metabolically active in the absence of target innervation.

4.1 Introduction

Donor age effect in DA neuron grafts has been the subject of interest for some time now (Torres et al., 2007, Torres et al., 2008a, Jonsson et al., 2009). VM tissue derived from E12 rat embryos provided a 5-fold greater yield of DA neurons than E14 VM-derived grafts but achieved similar levels of recovery in lesioned rats (Torres et al., 2008a). This suggests that a threshold number of DA neurons in the graft are required to provide sufficient DA supply and reinnervation of the lesioned striatum to restore behavioural deficits but a further increase in DA neuron yield does not improve the recovery. Previous studies have demonstrated that further recovery of finer motor skills requires a more global restoration of the basal ganglia circuitry which can be achieved by simultaneous grafts in the striatum, the SNpc and the STN (Mukhida et al., 2001, Mukhida et al., 2008). The subtypes of dopamine neurons within embryonic VM grafts have been the focus of many studies (Mendez et al., 2005, Thompson et al., 2005, Grealish et al., 2010). It has been proposed that the restoration of function by DA grafts is mainly due to the presence of the A9 type DA neurons of SNpc within the graft which re-innervate the surrounding striatum (Kuan et al., 2007, Grealish et al., 2010). Whereas the A10 type DA neurons of the VTA appear to innervate extra-striatal targets and are considered less important in restoring behavioural deficits (Thompson et al., 2005, Kuan et al., 2007, Grealish et al., 2010).

The A9 and A10 DA neuron subtypes were identified in mice VM grafts based on the coexpression of Girk2 and calbindin in DA neurons, respectively, and cell morphology (Thompson et al., 2005). DA neuron subtypes in grafts derived from rat E12 and E14 VM tissue have been characterised in the previous experiment (Chapter 3). Implants in the E12 group were significantly more enriched for the A9 type DA neurons than transplants in the E14 group as indicated by a higher percentage of TH-ir cells double labelled with Girk2 (80% and 68%, respectively). The periphery of the grafts contained predominantly A9 type DA neurons in both donor age groups with a two-fold reduction in the A10 type DA neurons in the periphery of grafts in the E12 group as compared to the E14 group. The centre of grafts in the E12 group contained the same levels of two different DA neuron subtypes. More A9 type than A10 type DA neurons were observed in the centre of grafts in the E14 group but the difference was not significant. A third of neurons positive for TH in the centre of grafts in both donor age groups failed to co-label with either Girk2 or calbindin. However, there was a 15%

overlap between Girk2 and calbindin staining. Nevertheless, the fact that the two DA neurons subtypes were not homogeneously distributed within the graft might indicate that there is an environmental effect of the periphery and the centre of the graft on either survival or differentiation of DA neuron subtypes.

Both DA neuron subtypes survive in VM grafts in the striatum and TH-ir neurons extend axonal projections to their normal targets depending on the phenotype, e.g. the A9 type DA neurons innervate the surrounding striatum, whereas the A10 type DA neurons project to the PFC (Thompson et al., 2005). This indicates that, depending on the afferent DA innervation, the host environment might favour the development and survival of either one or the other DA neuron subtype in the graft, an issue which has not yet been looked at experimentally.

4.1.1 Aims of the chapter

The current experiment investigated grafts derived from E12 and E14 rat VM tissue and implanted into different cerebral targets to determine if the site of transplantation affected the populations of DA cell phenotypes seen in the graft. The striatum receives the A9 type DA innervation from the SNpc and, as seen from previous studies, there are generally higher numbers of A9 type DA neurons than A10 type DA neurons in the graft (Chapter 2 and Bye et al., 2012). The N.Acc and the PFC, both receive the A10 type innervation from the VTA, which might influence the differentiation and survival of A10 type DA neurons in grafts transplanted into these regions. The hippocampus receives very sparse (<5%) DA innervation from the VTA and rich NA innervation from the LC and might serve as a control site (Lindvall and Bjorklund, 1974). In the present experiment, the striatum, N.Acc, PFC and the hippocampus were chosen as 4 implantation sites to determine if different cell populations and DA innervation targets in the host environment might affect the success of allogeneic DA neuron transplantation in terms of:

1. Motor function recovery
2. Neuron survival
3. DA cell survival
4. A9 and A10 DA neuron phenotype yield and distribution in grafts
5. A9 type and A10 type DA cell size

4.2 Experimental Procedure

To reduce the number of animals used in the experiment each animal received 2 grafts into 2 different transplantation sites on the same side of the brain. Striatum and N.Acc can be considered independent from the PFC and hippocampus because they are not adjacent cerebral regions. Therefore, each animal received the first transplant into either the striatum or N.Acc and the second transplant into either the PFC or hippocampus.

All of the methods used in this experiment are described in Chapter 2. Female SD rats (n = 36) were unilaterally lesioned with 6-OHDA (Chapter 2.3.1) and the lesions confirmed with drug-induced rotation tests (Chapter 2.4). Animals were balanced based on the number of amphetamine-induced net ipsilateral rotations and allocated into 8 groups so that the variance between the groups was minimal (Table 4.1; Group, $F_{(7,28)} = 0.01$, n.s.; one-way ANOVA).

Transplantation site / Donor age	Striatum PFC	N.Acc PFC	Striatum Hippocampus	N.Acc Hippocampus
E12	1242 ± 273 (n = 5)	1268 ± 260 (n = 4)	1307 ± 500 (n = 4)	1245 ± 264 (n = 5)
E14	1246 ± 195 (n = 5)	1270 ± 294 (n = 4)	1298 ± 428 (n = 4)	1245 ± 227 (n = 5)

Table 4.1 Group allocation for transplantation. Animals were distributed in 8 groups based on the number of amphetamine-induced net ipsilateral rotations following 6-OHDA lesion. One-way ANOVA, n.s. Data are presented as group means ± SEM.

Six weeks post-lesion, three E12 and two E14 litters were harvested and VM cell suspensions were prepared for grafting as described in Chapter 2.3.2 (**E12 1:** 63,500 cells/VM, viability data n/a; **E12 2:** 117,000 cells/VM, viability – 99.19%; **E12 3:** 134,000 cells/VM, viability 98.27%; **E14 1:** 500,000 cells/VM, viability – 95.24%; **E14 2:** 535,000 cells/VM, viability – 95.22%). The PFC is a much smaller cerebral target than the striatum, N.Acc or the hippocampus and, for safety reasons, cell numbers equivalent to ½ VM per graft were used in the current experiment. Every animal received 2 grafts into the designated sites, each graft containing cell numbers equivalent to ½ VM in 2 µl of the cell suspension. Overall, a total of 9 animals received grafts of each donor age transplanted into each cerebral target. Stereotaxic co-ordinates were as follows: **Striatum** AP: +0.6 mm, ML: -3.0 mm, DV: -5.0 mm; **N.Acc** AP: +1.6 mm,

ML: -1.5 mm, DV: -7.5 mm; **PFC** AP: +4.7 mm, ML: -2.0 mm, DV: -1.9 mm; **Hippocampus** AP: -5.2 mm, ML: -5.2 mm, DV: -5.4 mm (Paxinos and Watson, 2003). Efficacy of the grafts was confirmed with amphetamine-induced rotation tests at 4 and 6 weeks post-grafting. Following the final rotation test animals were sacrificed, transcardially perfused, the brains fixed, and coronal sections of brains collected for IHC (Chapter 2.5).

A one-in-twelve series of sections was stained using IHC for DAB NeuN. A second one-in-six series was stained for DAB TH; two series were double labelled for TH and Girk2, and TH and calbindin, respectively (Chapter 2.6.1). Fluorescent and DAB cell counts were obtained blind to the experimental condition abiding by the stereological principles (Chapter 2.8). Counts of double labelled cells in the centre and the periphery of the graft were obtained as described in Chapter 2.8.2.

Three measures of the number of TH-ir neurons in the grafts were obtained from three different stainings. The counts obtained from fluorescent Girk2/TH and calbindin/TH stainings were consistently higher than DAB TH-ir cell counts (Table 4.2; within-subject factor – Staining, $F_{(2,132)} = 181.99$, $p<0.001$; two-way ANOVA with repeated measures; TH < Girk2/TH = calbindin/TH, $p<0.001$; Bonferroni correction). Given that the actual number of TH-ir cells is the same across three series of sections, the threshold for counting a cell as immunoreactive is lower in fluorescent staining than DAB staining. Additionally, sections containing the graft in the PFC were missing from the DAB TH staining. Therefore, the total number of TH-ir neurons per graft was calculated as an average TH-ir cell count from Girk2/TH and calbindin/TH staining for statistical analysis.

	TH	Girk2/TH	calbindin/TH
E12	2349 ± 153	3849 ± 204	3791 ± 211
E14	1208 ± 158	2109 ± 211	2185 ± 217

Table 4.2 A summary of TH-ir cell numbers/graft across all sites in the E12 and E14 groups obtained from three different stainings. In both donor age groups: TH < Girk2/TH = calbindin/TH ($p<0.001$). Data are presented as group means ± SEM.

Statistical analyses were performed in SPSS as described in Chapter 2.9. A four–way ANOVA with repeated measures was used to analyse behavioural data from drug-induced rotation tests. This analysis was performed orthogonally, treating grafts in the striatum or N.Acc as the primary graft and grafts in the PFC or hippocampus as the secondary graft, to investigate whether PFC or Hippocampus subgroups differed in

either Striatum or N.Acc groups. Two-way ANOVAs were used to analyse NeuN-ir cell yield, TH-ir cell yield, graft volumes, and DA neuron density in the grafts. Three- and four-way ANOVAs with repeated measures were performed to analyse DA neuron subpopulations and their distribution within the graft, respectively. The A9 type and the A10 type DA cell diameters were analysed using a three-way ANOVA with repeated measures. Bonferroni correction for multiple comparisons was used to reveal significant differences between individual groups and results were considered to be significant if $p<0.05$ (*).

4.3 Results

4.3.1 Functionality of the grafts

Rotational asymmetry in response to the indirect dopamine agonist, amphetamine, was assessed at 6 weeks post-lesion and at 4 and 6 weeks post-grafting. Post-lesion, net rotation in both groups of animals was ipsilateral toward the lesioned side in response to the amphetamine. Pre- and post-grafting rotational behaviour was significantly different in most animals (within-subject factor – Transplantation, $F_{(2,56)} = 13.93$, $p<0.001$). Grafts in the striatum and N.Acc produced significantly different drug-induced rotational responses in animals (Primary graft, $F_{(1,28)} = 55.57$, $p<0.001$). Six weeks after grafting all animals which had received grafts into the striatum now rotated contralaterally to the lesioned side (Figure 4.1A; $p<0.001$). Animals which had received grafts into the N.Acc continued to rotate ipsilaterally to the lesioned side, most probably due to DA release in the N.Acc having an excitatory effect and increasing the phenotype of drug-induced ipsilateral rotational behaviour (Figure 4.1B; $p<0.05$). Grafts in either the PFC or hippocampus did not influence drug-induced rotational response in animals (Secondary graft, $F_{(1,28)} = 1.31$, n.s.; no associated significant interactions). Rotational behaviour in the E12 and E14 groups was generally very similar (Donor Age, $F_{(1,28)} = 1.38$, n.s.). Only post-grafting rotational behaviour induced by the grafts in the N.Acc was significantly different between the two donor age groups at both 4 and 6 week time points ($p<0.05$). In the E14 donor age group in the N.Acc, the asymmetry in post-lesion rotational behaviour was significantly lower than the asymmetry in rotational behaviour at both 4 and 6 weeks post-grafting ($p<0.05$). Grafts in the striatum induced a highly significant behavioural recovery in drug-induced rotations at 4 and 6 weeks post-grafting in both donor age groups ($p<0.001$).

Three animals that received transplants into the N.Acc (one from the E14 and two from the E12 donor age group) rotated contralaterally to the lesioned side. Examination of TH-stained brain sections revealed that the animal from the E14 group had a graft in the dorsomedial striatum instead of N.Acc and therefore was transferred to the Striatum group for further analysis. The two animals from the E12 group had grafts that were equally positioned in the striatum and N.Acc which suggests that DA activity in the striatum over-compensated the DA activity in the N.Acc in response to the drug leading to the restoration of lesion-induced rotational asymmetry during the test. Because the grafts were nevertheless positioned in the N.Acc these animals were not excluded from the analysis of the environmental effects of the N.Acc on DA neuron phenotypes within the grafts.

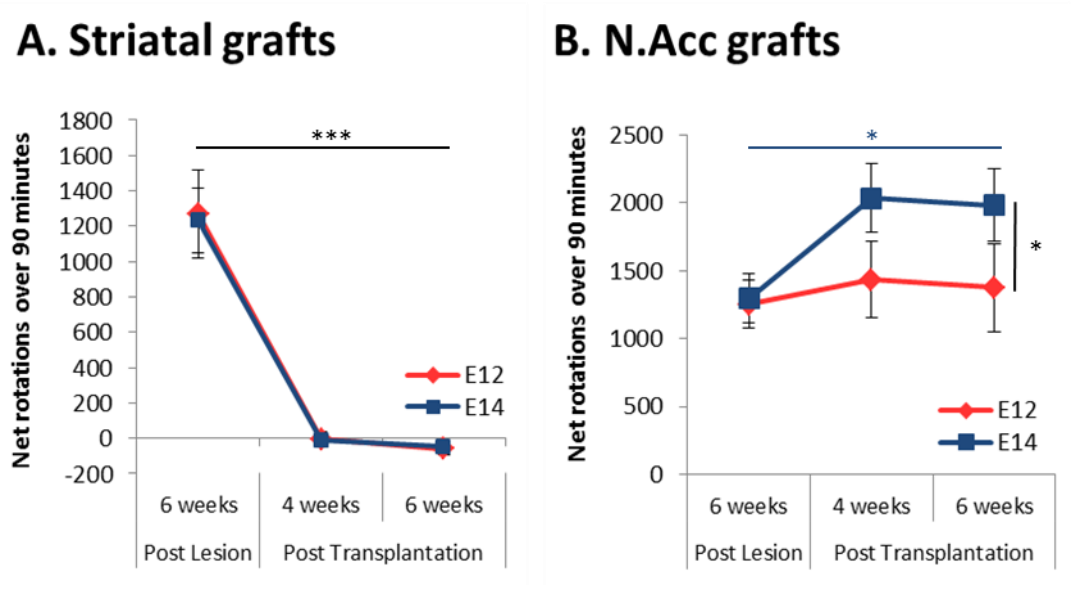

Figure 4.1 Drug-induced rotational response following an i.p. injection of 2.5mg/kg metamphetamine in lesioned and grafted rats in the E12 (red) and the E14 (blue) groups. Data are collapsed across the secondary graft factor. **(A)** Both donor age graft groups produced a recovery of the lesion-induced behavioural deficit in the striatal graft group. There was a change (***) from ipsilateral rotation observed post-lesion to a net contralateral rotation post-grafting, the classic over-compensatory response ($p<0.001$). **(B)** Animals in the N.Acc graft group exhibited enhanced (*) ipsilateral rotational behaviour post-grafting ($p<0.05$). Data are presented as a mean (ipsilateral minus contralateral) rotation score for each group over 90 minutes, error bars indicate ± SEM, significance levels: * $p<0.05$, *** $p<0.001$.

4.3.2 Surviving grafts in each transplantation site group

TH and NeuN stained sections revealed well positioned grafts in most animals. In the E14 donor age group, two animals were missing grafts in the PFC and one in the hippocampus because the transplantation site was missed during the surgery, and as a result cells were most likely injected into the subdural space or a sub-ventricular space

because no trace of cells was found. In the E12 donor age group, one graft was injected too anteriorly in the PFC and brain sections were too damaged to collect comparable cell counts for analysis (no sections containing this graft were present in the Girk2/TH and calbindin/TH stained sections) so the animal was excluded from the analysis. Additionally, NeuN staining of one brain in the E12 PFC group was too patchy to obtain a reliable NeuN-ir cell count. Two E12 and three E14 grafts in the PFC group penetrated into the subdural space but they, nevertheless, extended TH-ir fibres into the PFC so the animals were included in the analysis. Also, in some animals, the first collected PFC section contained a big portion of the graft in 4 E12 grafts and 4 E14 grafts suggesting that there was a portion of the graft anterior to the first collected PFC section and it was lost. The resulting numbers of grafts in each group used in further analysis were as follows: Striatum – 9 E12 and 10 E14 grafts, N.Acc – 9 E12 and 8 E14 grafts, PFC – 8 E12 (7 E12 grafts in the NeuN staining analysis) and 7 E14 grafts, Hippocampus – 9 E12 and 8 E14 grafts.

4.3.3 Neuron yield in the grafts

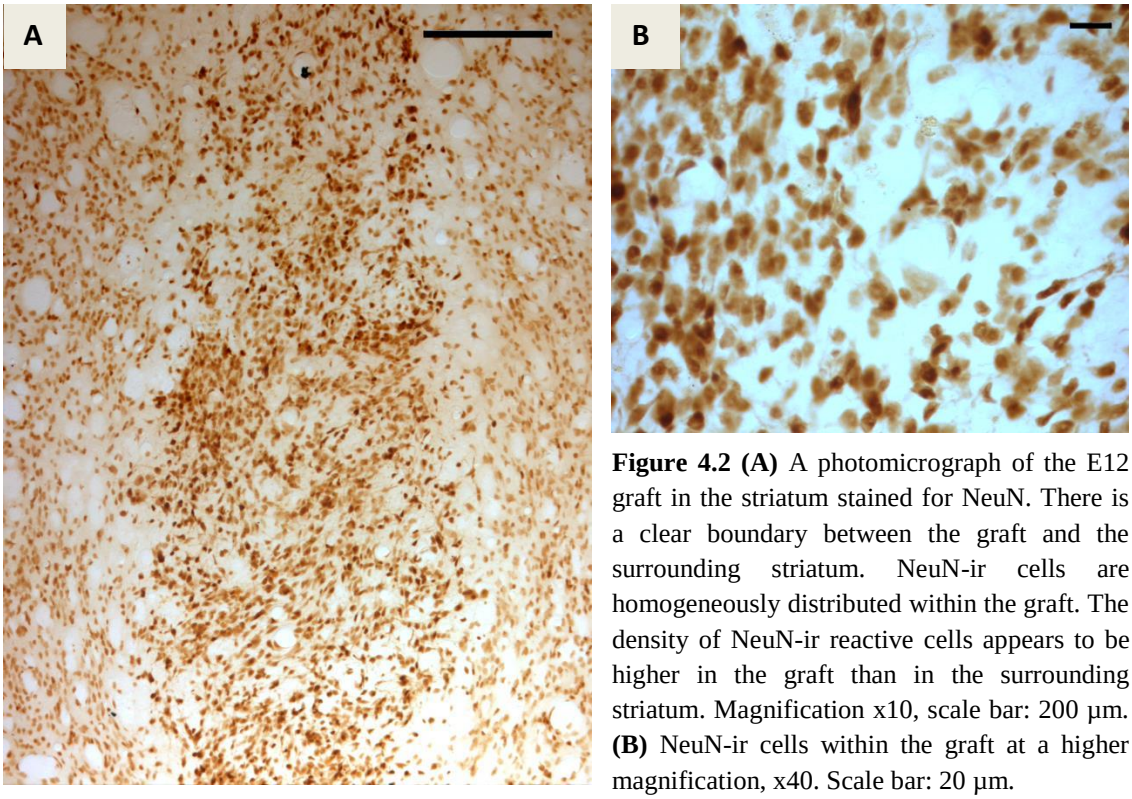

Figure 4.2 (A) A photomicrograph of the E12 graft in the striatum stained for NeuN. There is a clear boundary between the graft and the surrounding striatum. NeuN-ir cells are homogeneously distributed within the graft. The density of NeuN-ir reactive cells appears to be higher in the graft than in the surrounding striatum. Magnification x10, scale bar: 200 µm. **(B)** NeuN-ir cells within the graft at a higher magnification, x40. Scale bar: 20 µm.

Examination of NeuN-stained sections revealed surviving grafts in most animals with large numbers of NeuN-ir cells homogeneously distributed within the grafts as depicted in Figure 4.2A. Given that E14 VMs contained almost 5 times more cells than

E12 VMs at the time of transplantation, the yield of NeuN-ir neurons might have been expected to be different between the two donor age groups. However, as shown in Figure 4.3, the yield of grafted neurons was not affected by the donor age group ($F_{(1,59)}$ = 0.51, n.s.) or the transplantation site group ($F_{(3,59)}$ = 0.45, n.s.) and neither by an interaction between the two factors ($F_{(3,59)}$ = 0.13, n.s.). This might be due to either poorer survival of differentiated cells in the E14 VM tissue or proliferation of neural cell precursors in the E12 VM tissue, or both.

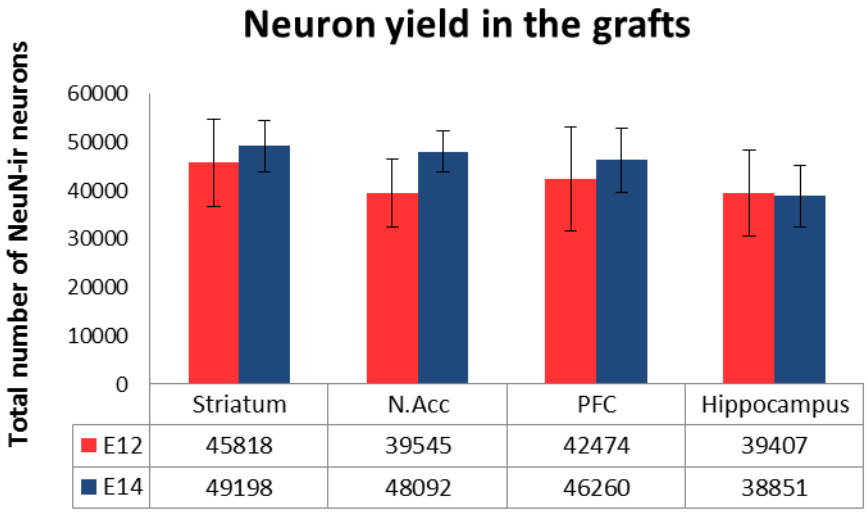

Figure 4.3 Total NeuN-ir cell numbers in E12 and E14 grafts at all transplantation sites at 6 weeks post grafting. No significant differences were found between the donor age groups and transplantation site groups (n.s.). Columns depict group means; error bars illustrate SEM.

4.3.4 DA neuron yield in the grafts

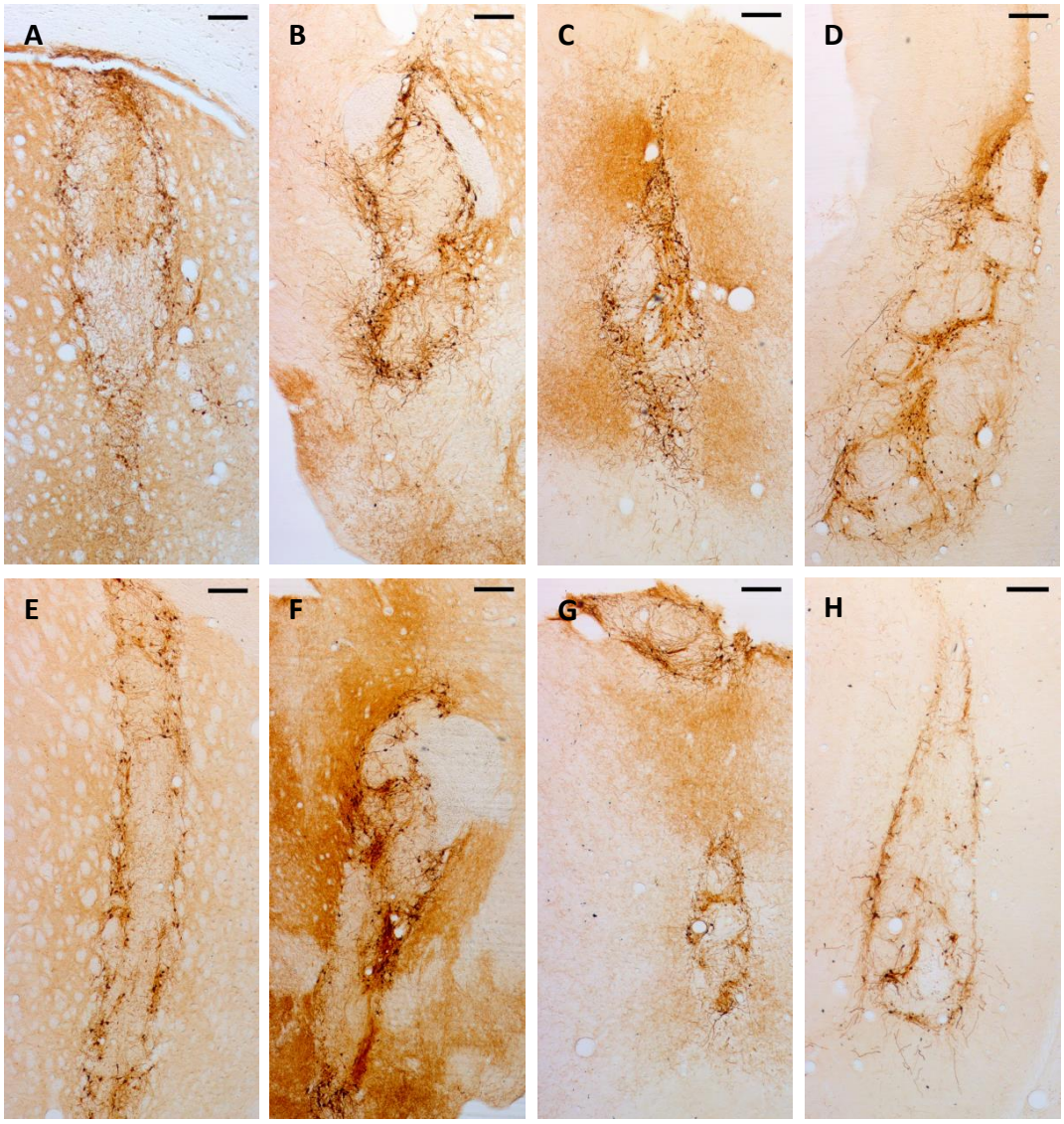

Figure 4.4 Photomicrographs (x10) of E12 grafts in the striatum **(A)**, N.Acc **(B)**, PFC **(C)**, and hippocampus **(D)**, and E14 grafts in the same cerebral targets (**E, F, G**, and **H**, respectively) at 6 weeks post transplantation. In most grafts, most DA cells were located at the periphery of the graft and extended axons to re-innervate the surrounding environment. However, E12 grafts in the hippocampus contained a significant population of TH-ir cells in the core. **(I)** A higher magnification photomicrograph (x40) of TH-ir neurons in the striatal graft clearly shows DA cells extending axons into the surrounding tissue. Scale bars: 200 μm (A – H) and 20 μm (I).

Examination of TH-stained sections showed large numbers of TH-ir cells in all surviving grafts with extensive innervation by the grafts of the surrounding striatum, N.Acc and to some extent PFC as expected (Figure 4.4). Surprisingly, extensive TH-ir fibre outgrowth was also observed in the grafts in hippocampus (Figure 4.4D, H). E14 grafts contained most TH-ir neurons in the periphery of the graft and only a few in the centre of the graft. E12 grafts displayed a more homogeneous distribution of cells and a high density of TH processes within the graft. The group means of TH-ir cell numbers (derived from implantation of ½ VM) are shown in the table below the graph in Figure 4.5A. A two-way ANOVA analysis confirmed a main effect of the donor age group ($F_{(1,60)} = 36.18$, $p<0.001$), a main effect of the transplantation site group ($F_{(3,60)} = 2.98$, $p<0.05$) and no interaction ($F_{(3,60)} = 2.12$, n.s.) on the total TH-ir cell numbers in the grafts. E12 grafts produced a significantly higher yield of TH-ir cells than E14 transplants in the striatum ($p<0.001$), N.Acc ($p<0.05$) and hippocampus ($p<0.01$). Interestingly, in the E12 donor age group grafts in the striatum were the most populous in TH-ir cells numbers than grafts in any other location whereas for the E14 donor age group the largest grafts were in the N.Acc. Also, grafts in the hippocampus contained unexpectedly high numbers of TH-ir cells, especially in the E12 donor age group. Analysis of simple effects confirmed a significant effect of transplantation site in the E12 donor age group ($F_{(3,60)} = 4.65$, $p<0.01$) but not the E14 donor age group ($F_{(3,60)} = 0.41$, n.s.). However, only grafts in the striatum yielded a significantly higher number of TH-ir neurons than grafts in the PFC in the E12 donor age group ($p<0.01$).

Given that the total number of surviving neurons was not significantly different between the groups, there should be a higher percentage of TH-ir/NeuN-ir cells in the E12 donor age group than E14 group to account for a significantly higher dopamine neuron yield in E12 grafts. As expected, a two-way ANOVA confirmed a main effect of the donor age group ($F_{(1,59)} = 24.02$, $p<0.001$; Figure 4.5B) but no effect of the transplantation site group ($F_{(3,59)} = 0.44$, n.s.) or an interaction between the two factors ($F_{(3,59)} = 0.67$, n.s.). Grafts derived from E12 rat embryos yielded a higher percentage of TH-ir/NeuN-ir neurons than E14 grafts in the striatum ($p<0.01$), N.Acc ($p<0.01$) and the hippocampus ($p<0.05$) but not the PFC.

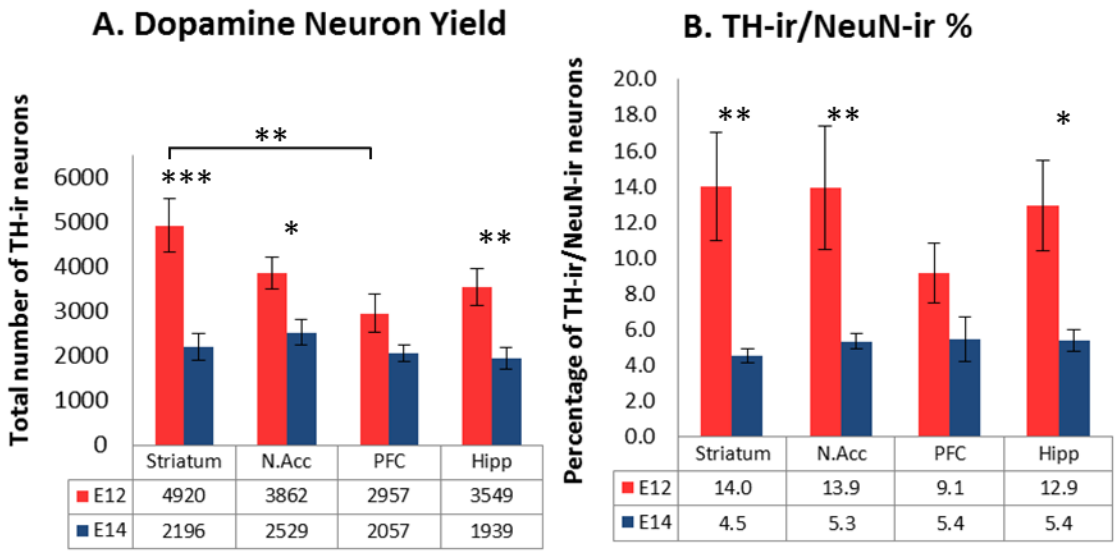

Figure 4.5 (**A)** Total TH-ir cell numbers in E12 and E14 grafts in all implantation sites at 6 weeks post grafting. There was a significant difference in total TH-ir neuron numbers between the two donor age groups ($F_{(1,60)} = 36.18$, $p<0.001$). Significant differences in DA neuron yield between E12 and E14 grafts at different transplantation sites are depicted on the graph. The transplantation site had a significant main effect on the DA neuron yield ($F_{(3,60)} = 2.98$, $p<0.05$). E12 grafts in the Striatum group produced significantly higher TH-ir cell numbers than E12 grafts in the PFC ($p<0.01$). **(B)** Effect of the donor age group and the transplantation site group on the percentage of TH-ir/NeuN-ir neurons. There was no significant effect of the transplantation site and no interaction, but there was a significant effect of the donor age group ($F_{(1,59)} = 24.02$, $p<0.001$). Significant differences between the two donor age groups at different levels of the transplantation site group are depicted on the graph. Columns depict group means; error bars illustrate SEM; significance levels: * $p<0.05$, ** $p<0.01$, *** $p<0.001$.

E12 grafts were slightly bigger in volume than E14 grafts in all transplantation sites ($F_{(1,60)} = 4.12$, $p<0.05$; Figure 4.6A), despite the smaller numbers of cells implanted. Despite the fact that brain tissue in each transplantation site is different in cell composition and density it did not affect the growth of grafts (Transplantation Site, $F_{(3,60)} = 0.06$, n.s.; Donor Age x Transplantation site, $F_{(3,60)} = 0.22$, n.s.). No significant differences in graft volume between individual groups were found. Analysis of DA cell densities in the grafts (Figure 4.6B) showed a main effect of the donor age group ($F_{(1,60)} = 14.30$, $p<0.001$) but again no main effect of the transplantation site group ($F_{(3,60)} = 0.76$, n.s.) and no interaction between the two ($F_{(3,60)} = 0.96$, n.s.). TH-ir cell density was significantly higher in E12 grafts than E14 grafts in the striatum ($p<0.01$) and N.Acc ($p<0.05$). Thus, the increase in the total number of TH-ir cells in grafts derived from younger donor tissues can be attributed to a denser distribution of DA neurons within the graft which is accompanied by a slight increase in the graft volume.

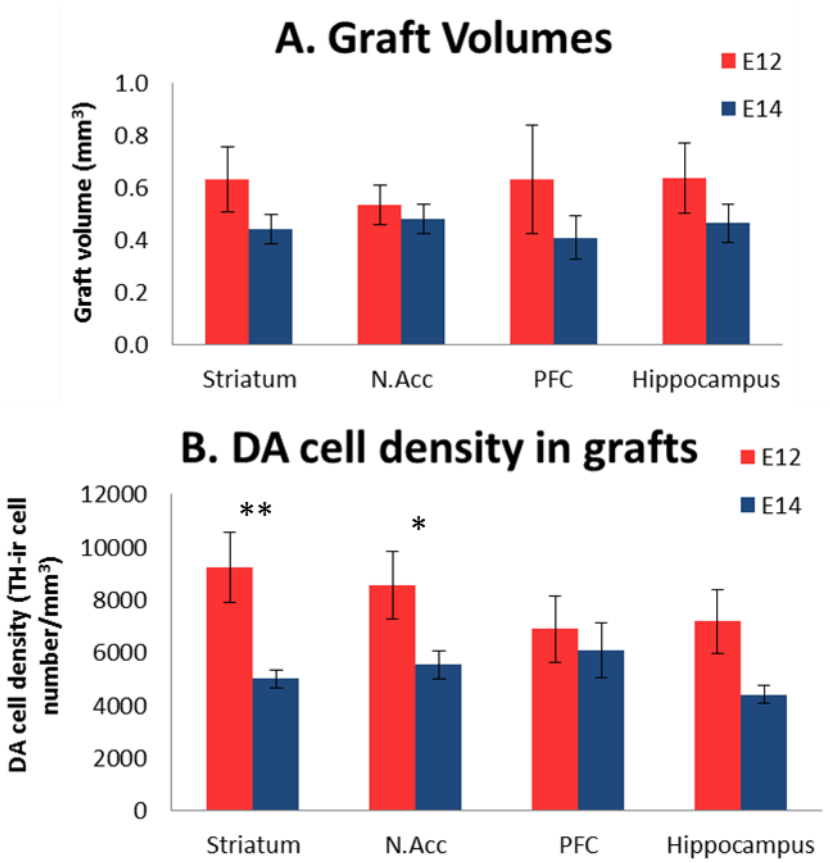

Figure 4.6 (A) A summary of graft volumes in each donor age and transplantation site group. E12 grafts were significantly bigger ($F_{(1,60)} = 4.12$, $p<0.05$). There was no effect of the transplantation site group or an interaction between the two factors. **(B)** TH-ir cell density in the grafts in each group. There was a main effect of the donor age group ($F_{(1,60)} = 14.30$, $p<0.001$), DA neuron density was significantly higher in E12 grafts than E14 grafts in the Striatum and N.Acc. Again there was no main effect of the transplantation site group and no interaction between the two factors. Columns depict group means; error bars illustrate SEM; significance levels: * $p<0.05$, ** $p<0.01$.

4.3.5 DA neuron subtypes in E12 and E14 grafts

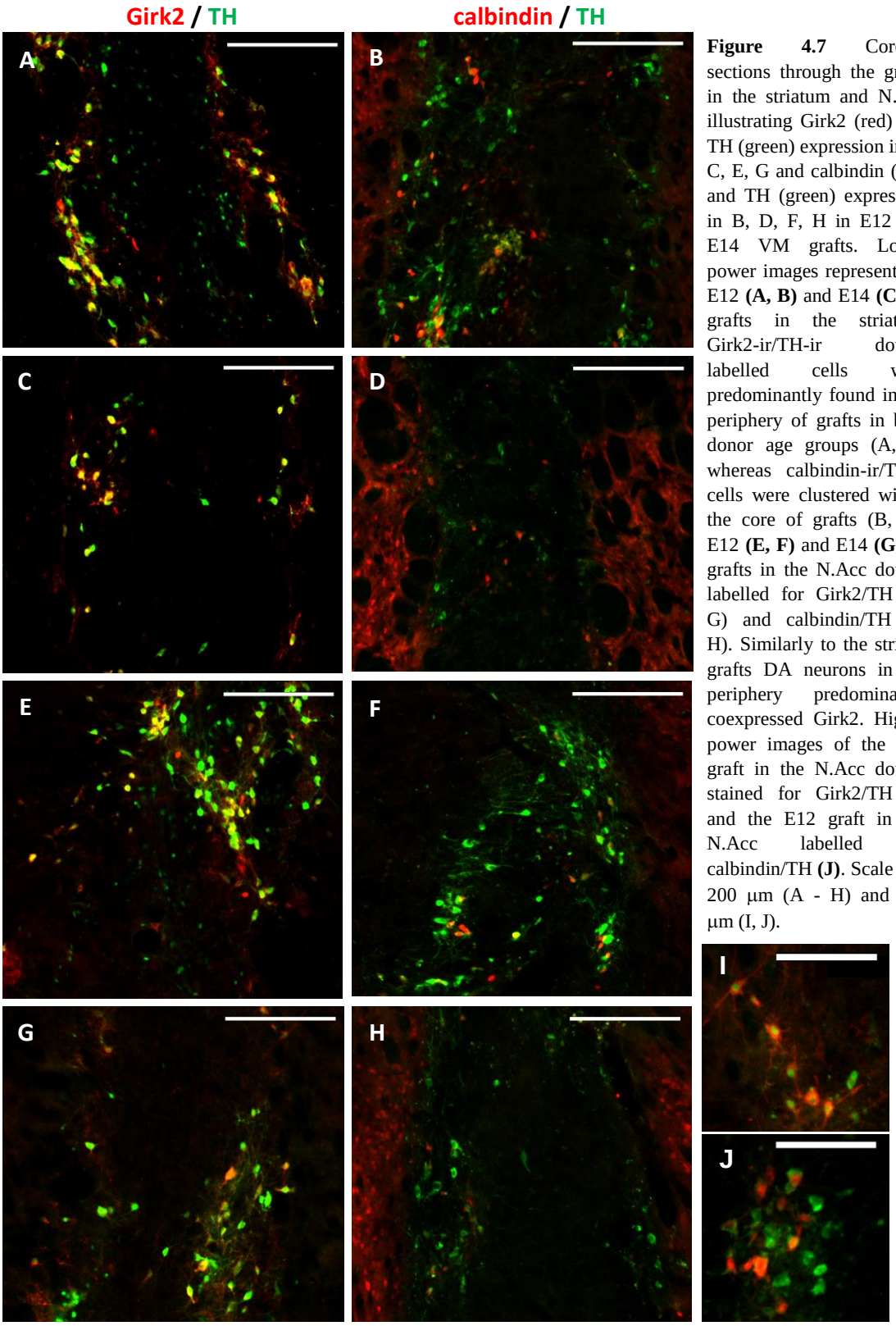

Figure 4.7 Coronal sections through the grafts in the striatum and N.Acc illustrating Girk2 (red) and TH (green) expression in A, C, E, G and calbindin (red) and TH (green) expression in B, D, F, H in E12 and E14 VM grafts. Lower power images represent the E12 **(A, B)** and E14 **(C, D)** grafts in the striatum. Girk2-ir/TH-ir double labelled cells were predominantly found in the periphery of grafts in both donor age groups (A, C) whereas calbindin-ir/TH-ir cells were clustered within the core of grafts (B, D). E12 **(E, F)** and E14 **(G, H)** grafts in the N.Acc double labelled for Girk2/TH (E, G) and calbindin/TH (F, H). Similarly to the striatal grafts DA neurons in the periphery predominantly coexpressed Girk2. Higher power images of the E14 graft in the N.Acc double stained for Girk2/TH **(I)** and the E12 graft in the N.Acc labelled for calbindin/TH **(J)**. Scale bar: 200 µm (A - H) and 100 µm (I, J).

Fluorescent double IHC for Girk2/TH and calbindin/TH revealed surviving A9 and A10 type DA neurons in all grafts (Figure 4.7). Girk2 and caldindin co-localised with TH in the cytoplasm of grafted neurons as demonstrated in Figure 4.7I and J, respectively. The yield of A9 type DA neurons was predicted to be higher in the striatum and A10 type DA neuron yield was expected to be higher in the N.Acc and PFC due to differential A9 and A10 type innervation of these brain regions. Indeed, there was a highly significant difference between A9 and A10 type DA neuron yields (within-subject factor – Staining, $F_{(1,60)} = 111.48$, $p<0.001$). There was a main effect of the donor age group ($F_{(1,60)} = 31.59$, $p<0.001$) and the transplantation site group ($F_{(3,60)} = 14.19$, $p<0.001$) as well as an interaction between the two factors ($F_{(3,60)} = 4.48$, $p<0.01$). The number of Girk2-ir/TH-ir cells was significantly higher than calbindin-ir/TH-ir cell counts in the striatum and surprisingly in the N.Acc in both donor age groups ($p<0.001$) and lower in the hippocampus in E12 grafts ($p<0.05$; Figure 4.8A). In comparison to E14 grafts, E12 grafts produced a higher yield of both Girk2-ir/TH-ir cells and calbdindin-ir/TH-ir cells in the striatum ($p<0.001$) and N.Acc ($p<0.05$) and a higher yield of calbindin-ir/TH-ir cells in the hippocampus ($p<0.05$). This effect of the donor age group was not unexpected since E12 grafts yielded a significantly higher number of TH-ir cells than E14 grafts in all transplantation sites apart from the PFC. Girk2-ir/TH-ir cells were abundant in grafts in the striatum and N.Acc in both donor age groups. There were noticeably fewer Girk2/TH double labelled cells in grafts in the PFC and hippocampus as depicted in Figure 4.8B. Differences in the number of calbindin-ir/TH-ir cells in grafts in different transplantation sites were less prominent (Figure 4.8C). There was no effect of the transplantation site on the number of calbindin-ir/TH-ir cells in E14 grafts ($F_{(3,60)} = 0.85$, n.s.) but there was an effect of the transplantation site in the E12 group ($F_{(3,60)} = 3.5$, $p<0.05$), grafts in the striatum yielded a significantly higher number of A10 type DA neurons than grafts in the PFC ($p<0.05$).

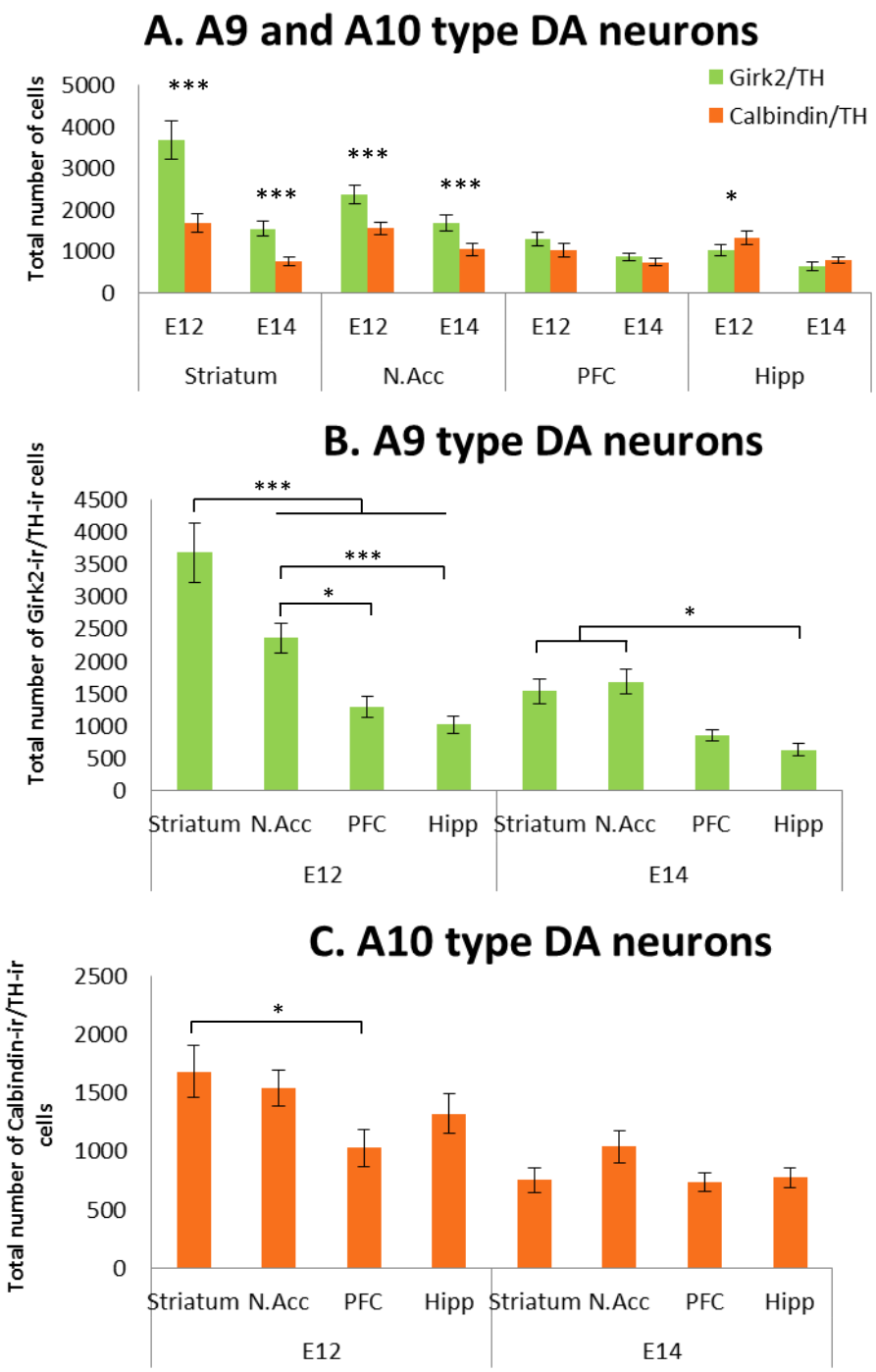

Figure 4.8 (**A)** A summary of Girk2-ir/TH-ir and calbindin-ir/TH-ir cell yields in grafts. Significant differences between the two populations of DA neurons were observed in E12 and E14 grafts in the striatum and N.Acc, and E12 grafts in the Hipp. **(B)** Survival of Girk2-ir/TH-ir neurons (data is extracted from Figure 4.8A for presentation clarity). Effect of the transplantation site on the number of A9 type DA neurons was more prominent in the E12 donor age group. Individual differences between the groups are depicted on the graph. **(C)** Survival of the A10 type DA neurons was less affected by the transplantation site (data is extracted from Figure 4.8A for presentation clarity). Only E12 grafts in the striatum differed significantly from E12 grafts in the PFC ($p<0.05$). Columns depict group means; error bars illustrate SEM; significance levels: * $p<0.05$, ** $p<0.01$, *** $p<0.001$.

In order to account for the difference in TH-ir cell numbers, the survival of TH-ir neurons that double-labelled with Girk2 and calbindin was calculated as a percentage of overall number of TH-ir neurons. The percentages of Girk2-ir/TH-ir and calbindin-ir/TH-ir cells in the striatum and N.Acc added up to 105%, suggesting at least a 5% overlap in Girk2 and calbindin stainings (Figure 4.9A). Interestingly, the sum of percentages of A9 and A10 type DA neurons was 78% and 69% in grafts in the PFC and hippocampus, respectively, indicating that almost a third of TH-ir neurons were neither of A9 nor A10 type. There was a highly significant difference between the percentages of A9 and A10 type DA neurons in the grafts (within-subject factor – Staining, $F_{(1,60)} = 268.87$, $p<0.001$). As expected, significant differences between the percentages of Girk2-ir/TH-ir and calbindin-ir/TH-ir neurons (Figure 4.9A) corresponded to significant differences between the A9 and A10 type DA neurons in different graft groups (Figure 4.8A). There was a main effect of the transplantation site group ($F_{(3,60)} = 91.81$, $p<0.001$) but no main effect of the donor age group ($F_{(1,60)} = 1.14$, n.s.) and no significant interaction ($F_{(3,60)} = 1.82$, n.s.). The gain in the Girk2-ir/TH-ir and calbindin-ir/TH-ir cell yields in the E12 donor age group did not outweigh the general increase in the number of TH-ir neurons between the two donor age groups. A significantly higher percentage of Girk2-ir/TH-ir cells was observed in grafts in the striatum than N.Acc and it continued to decrease in grafts in the PFC and hippocampus (Figure 4.9B). Thus, although the total number of TH-ir neurons was affected by the environment, the decrease in Girk2-ir/TH-ir cell numbers outweighed the general decrease. There was a small increase in the percentage of calbindin-ir/TH-ir cells in grafts in the N.Acc as compared to grafts in other transplantation sites in both donor age groups (Figure 4.9C). However, even though there was a main effect of the transplantation site on the percentage of calbindin-ir/TH-ir cells ($F_{(3,60)} = 4.68$, $p<0.01$) no significant differences between the groups were found.

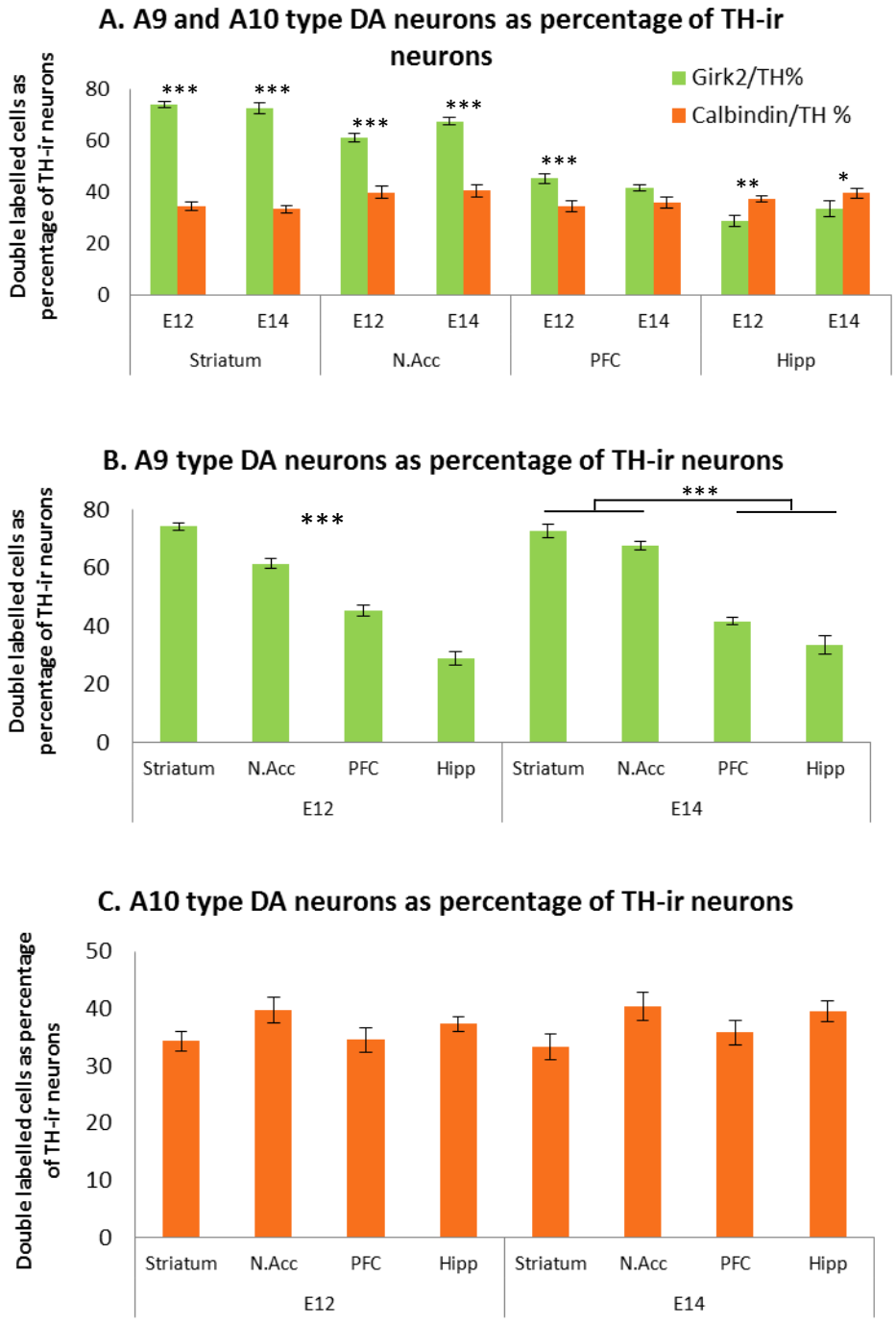

Figure 4.9 (A) A summary of the percentage of Girk2-ir/TH-ir and calbindin-ir/TH-ir cell yields in grafts. Significant differences between the proportions of the A9 and A10 type DA neurons were observed in all graft groups apart from the E14 PFC; E12 grafts were not significantly different from E14 grafts. **(B)** Percentage of Girk2-ir/TH-ir neurons (data is extracted from Figure 4.9A for presentation clarity). Effect of the transplantation site on the number of A9 type DA neurons was more prominent in the E12 donor age group. Individual differences between the groups are depicted on the graph. **(C)** Percentage of calbindin-ir/TH-ir neurons (data is extracted from Figure 4.9A for presentation clarity). No significant differences in the gain or loss of the A10 type DA neurons between the transplantation sites were found (n.s.). Columns depict group means; error bars illustrate SEM; significance levels: * $p<0.05$, ** $p<0.01$, *** $p<0.001$.

The composition of the periphery was generally very different from the composition of the core within the graft (within-subject factor – Location, $F_{(1,60)}$ = 47.29, $p<0.001$). The A9 type DA cells were affected more than the A10 type DA neurons by the environment within the graft (Location x Staining, $F_{(1,60)}$ = 55.04, $p<0.001$; A9 – $p<0.001$; A10 – n.s.). Girk2-ir/TH-ir neurons were found predominantly in the periphery of grafts rather than in the core while calbindin-ir/TH-ir neurons were distributed more homogeneously within the graft (Figure 4.10A, B). In N.Acc grafts, both A9 and A10 type DA neurons were found mostly in the periphery of grafts but in grafts in the Striatum group this was true for Girk2-ir/TH-ir and not calbindin-ir/TH-ir neurons. There was a significantly higher percentage of A10 type DA neurons in the periphery of grafts than in the centre in N.Acc grafts in both donor age groups ($p<0.05$). This suggests that environmental cues in the N.Acc might have influenced either the differentiation or survival, or both, of A10 type DA neural precursor cells. Interestingly, percentages of Girk2-ir/TH-ir and calbindin-ir/TH-ir cells in the periphery of grafts added up to 90-100% in all groups apart from the Hippocampus group. There were ≈50% of TH-ir cells in the centre of the graft in all groups that did not coexpress neither Girk2 nor calbindin suggesting that they most likely silenced their A9 and A10 phenotypes.

There was no main effect of the donor age group ($F_{(1,60)}$ = 2.67, n.s.) but there was a strong main effect of the transplantation site group ($F_{(3,60)}$ = 3.44, $p<0.05$) and a strong interaction between the donor age and transplantation site groups ($F_{(3,60)}$ = 2.96, $p<0.05$). Only the percentage of Girk2-ir/TH-ir cells in the periphery of grafts was affected by the transplantation site in both donor age groups ($F_{(3,60)}$ = 10.50, $p<0.001$). The percentage of A9 type DA neurons in the periphery of grafts was significantly less in grafts in the hippocampus than in the striatum and N.Acc ($p<0.01$) in the E12 donor age group. In E14 grafts, the percentage of Girk2-ir/TH-ir cells was significantly less in the periphery of grafts in the PFC ($p<0.05$) and hippocampus ($p<0.01$) than in the striatum. Without the necessary environmental cues DA precursors might have failed to survive or mature into functional A9 type DA neurons in the periphery of grafts in the PFC and hippocampus. There was a higher percentage of calbindin-ir/TH-ir neurons in the periphery of E12 grafts in the N.Acc than in other transplantation sites but the difference was not significant. Transplantation site did not affect the percentage of A10 type DA neurons neither in the periphery nor in the centre of grafts.

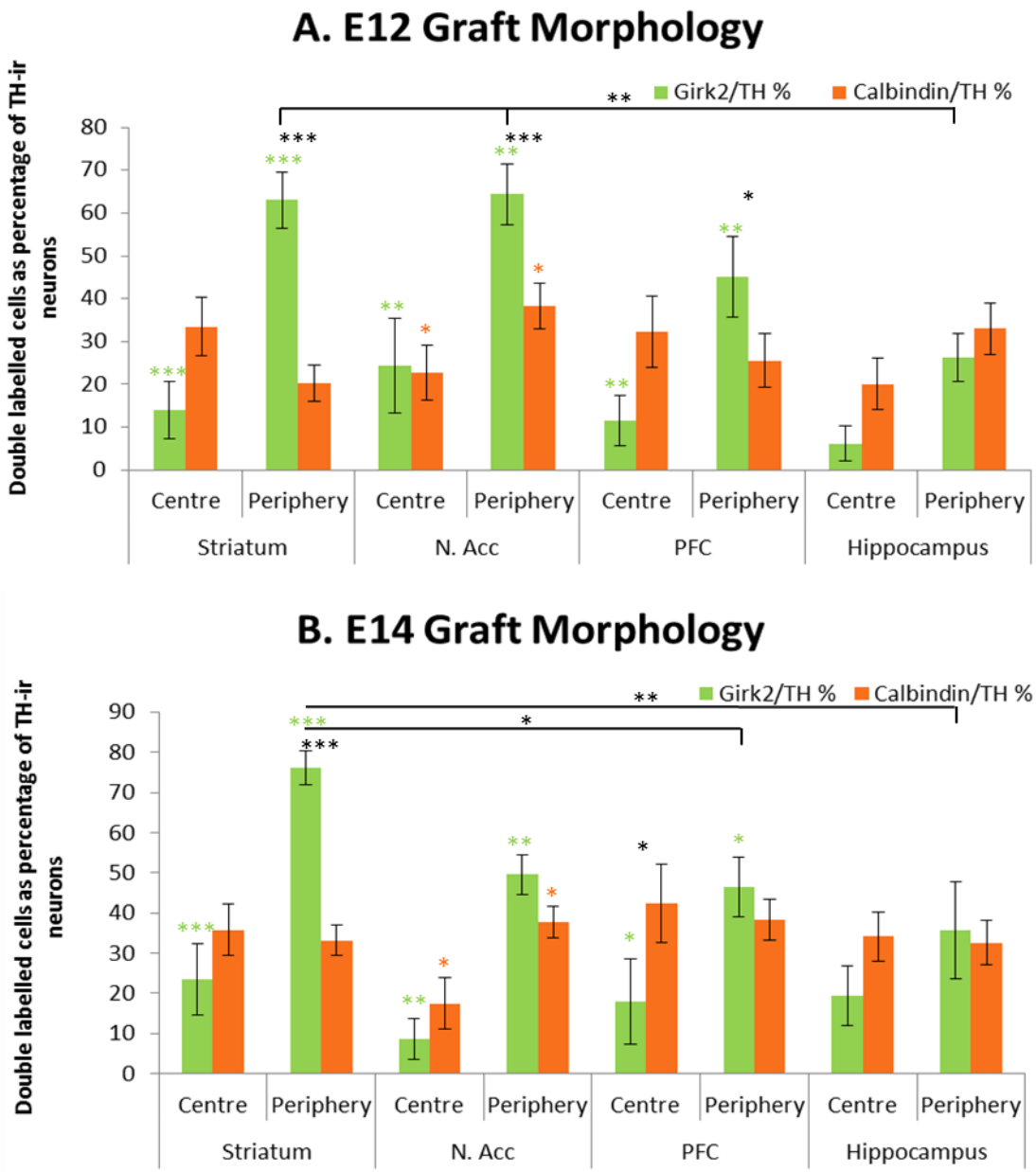

Figure 4.10 Percentages of Girk2-ir/TH-ir and calbindin-ir/TH-ir neurons in the periphery and in the centre of E12 (**A**) and E14 grafts (**B**) at 6 weeks post-transplantation. **(A)** Compared to the hippocampus, grafts in the striatum and N.Acc had a significantly higher percentage of Gitk-2-ir/TH-ir cells in the periphery of grafts. **(B)** E14 grafts in the striatum had a significantly higher percentage of Gitk-2-ir/TH-ir cells in the periphery of grafts than grafts in the PFC and hippocampus. **(A, B)** The A9 type DA neurons were residing predominantly in the periphery rather than the core of grafts while A10 type DA neurons were more homogeneously distributed within the graft. Significant differences between individual groups are depicted on the graph. Columns depict group means; error bars illustrate SEM; significance levels: * $p<0.05$, ** $p<0.01$, *** $p<0.001$.

The yields of DA neurons in the periphery and the centre of grafts were assessed from two TH-ir cell counts from Girk2/TH and calbindin/TH stainings (Figure 4.11). There were significantly more DA neurons in the periphery than in the centre of grafts (within-subject factor – Location, $F_{(1,60)} = 16.30$, $p<0.001$). However, this difference was significant only in grafts in the striatum and N.Acc in the E14 donor age group

(Figure 4.11B). As expected, TH-ir cell yields were higher in grafts in the E12 donor age group than E14 group (Donor Age, $F_{(1,60)} = 4.26$, $p<0.05$). The transplantation site had an effect on the yield of DA neurons in the periphery but not the centre of grafts (Location x Environment, $F_{(3,60)} = 4.56$, $p<0.01$), significant differences are summarised in Figure 4.11A, B.

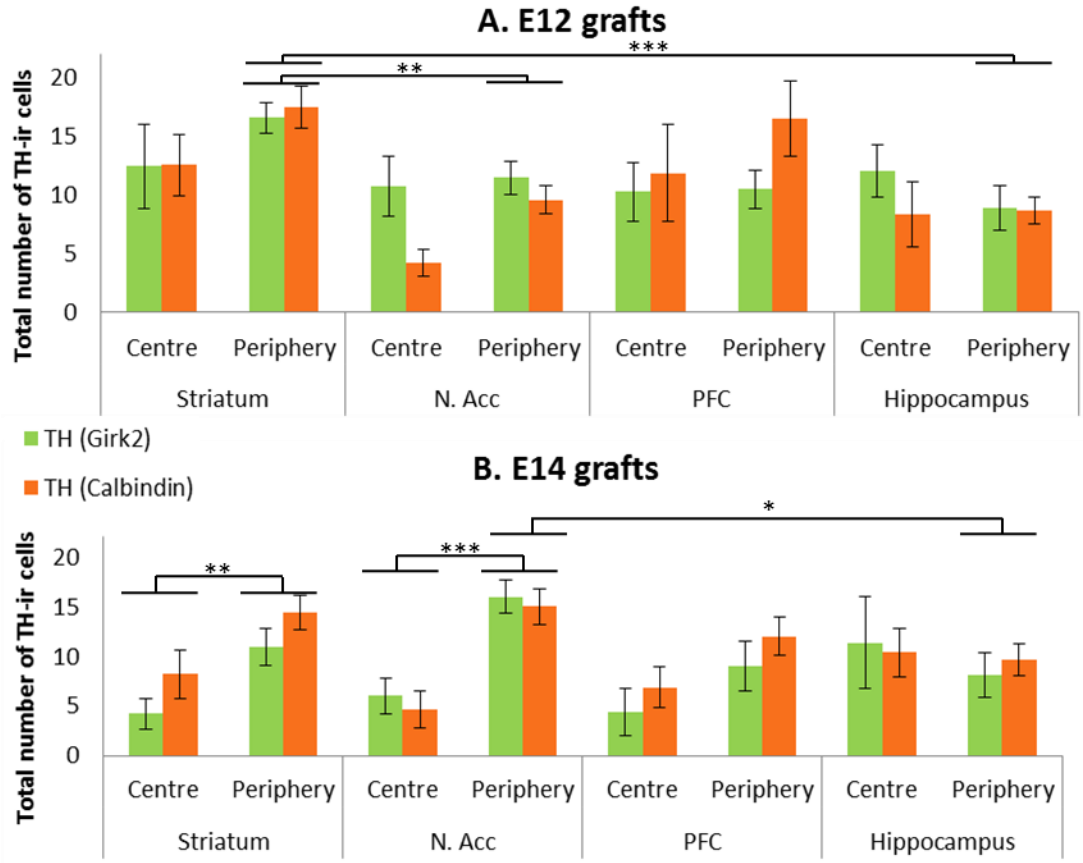

Figure 4.11 Total numbers of TH-ir cells from Girk2/TH and calbindin/TH stainings in the periphery and in the centre of E12 (**A**) and E14 grafts (**B**). **(A)** In the E12 donor age group, grafts in the striatum had significantly more surviving DA neurons in the periphery of grafts than grafts in the hippocampus and N.Acc. **(B)** In the E14 donor age group, there were significantly more surviving TH-ir cells in the periphery than the centre of grafts in the striatum and N.Acc. The yield of DA neurons was significantly lower in the periphery of grafts in the hippocampus than in the periphery of grafts in the N.Acc. The graph depicts significant differences between individual groups for pooled TH-ir cell yield data from two stainings to increase the power of the analysis. Columns depict group means; error bars illustrate SEM; significance levels: * $p<0.05$, ** $p<0.01$, *** $p<0.001$.

4.3.6 A9 and A10 type DA cell sizes

A9 and A10 type DA neuron diameters are shown in Figure 4.12. Girk2-ir/TH-ir cells were significantly bigger than calbindin-ir/TH-ir cells in all transplantation sites in both donor age groups ($F_{(1,32)}$ = 267.85, p<0.001). A9 type DA neurons in E14 grafts were bigger than in the E12 grafts ($F_{(1,32)}$ = 41.78, p<0.001). The transplantation site had a significant effect on the size of A9 type DA neurons ($F_{(3,32)}$ = 10.56, p<0.001). Girk2-ir/TH-ir cells in E14 grafts were significantly bigger than in E12 grafts in all transplantation sites. Also, Girk2-ir/TH-ir cells were significantly bigger in E12 grafts in the striatum than in the PFC and hippocampus. There were no significant differences in the A10 type DA cell diameters in the grafts between donor age groups and transplantation sites.

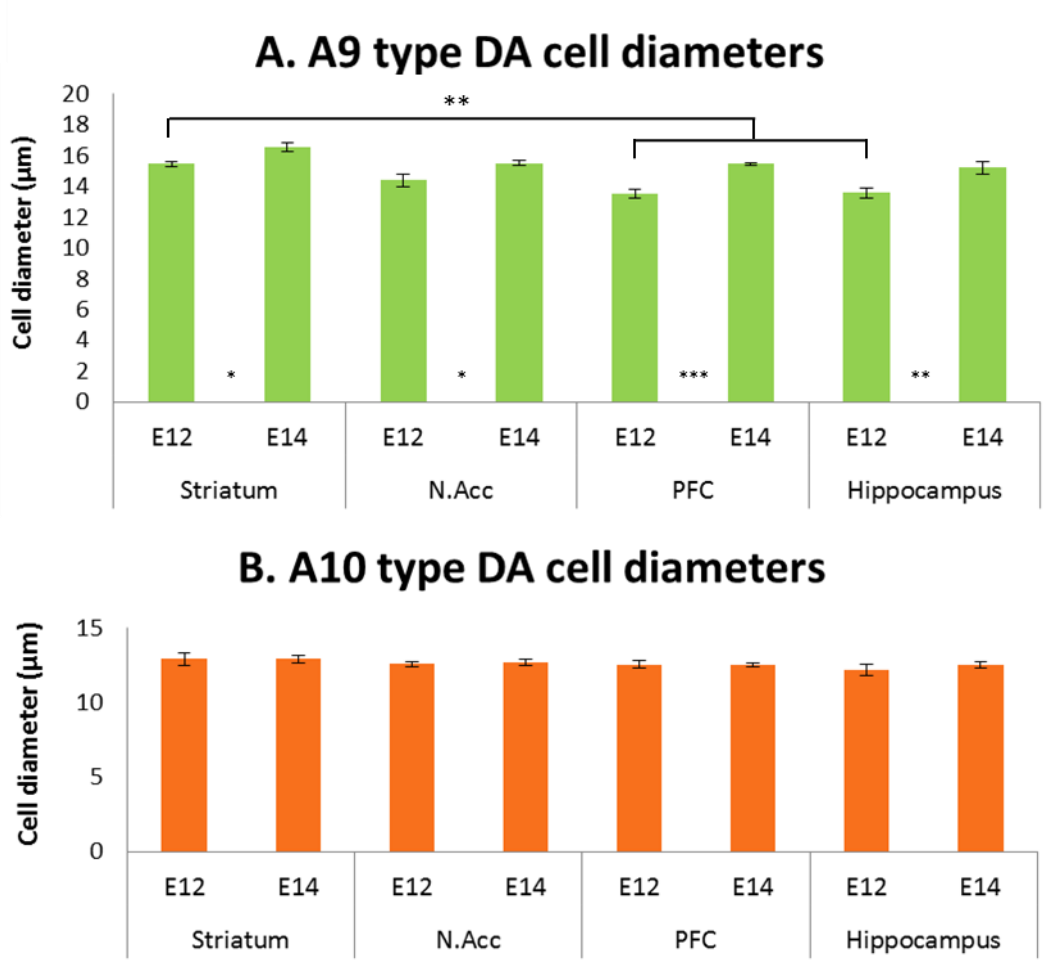

Figure 4.12 (**A)** Girk2-ir/TH-ir cell diameters. A9 type DA neurons were bigger in E14 grafts than E12 grafts. Also, Girk2-ir/TH-ir cells were bigger in the striatum than the PFC and hippocampus in the E12 donor age group. **(B)** Calbindin-ir/TH-ir cell diameters. The A9 type DA neurons were significantly bigger than the A10 type DA neurons in all groups. A10 type DA neurons were of similar size in all groups. Significant differences between individual groups are depicted on the graph. Columns depict group means; error bars illustrate SEM; significance levels: * p<0.05, ** p<0.01, *** p<0.001.

4.4 Discussion

In the developing peripheral and central nervous systems, neuronal innervation is guided by environmental cues such as trophic factors exerted by the target tissues during critical stages of development (Hendry, 1975, Landmesser, 1978). Removal of target organs prevents the survival of neurons innervating the target, and, conversely, experimentally induced increase in targets produces an increased survival of the innervating neurons. The degree of innervation, the patterning of the regenerating axons and the sprouting of appropriate transplanted neurons into the target have all been shown to be influenced by the environment in sympathetic ganglia (Olson and Malmfors, 1970), hippocampus (Bjorklund and Stenevi, 1981), and the striatum (Thompson et al., 2005). This neuron-target interaction has been studied by transplanting different types of neurons into the same target and tracking their afferent projections, which can form distinctly different patterns depending on the type of neurons grafted (Nilsson et al., 1988, Bjorklund et al., 1990, Clarke et al., 1990). For instance, DA neurons from the VM after transplantation to the hippocampus ramified extensively in the denervated perforant path zone but showed no tendency to grow into the normal terminal zones of the noradrenergic afferents (Bjorklund et al., 1976). Significant differences in the A9 and A10 type DA neuron populations within striatal grafts observed in our previous experiments as well as independent studies (Mendez et al., 2005, Thompson et al., 2005) suggest that the host striatum may influence the development and/or survival of DA neuron subtypes in the grafts.

In this experiment the environment was shown to have little influence on the total number of neurons in the grafts derived from E12 and E14 rat embryos and transplanted into the striatum, N.Acc, PFC and hippocampus. All grafts contained differentiated TH-ir neurons, with the TH-ir neuronal component representing 12.48% and 5.15% of the transplanted neurons in E12 and E14 grafts, respectively. A higher yield of TH-ir cell numbers in E12 grafts than equivalent E14 grafts in all four transplantation sites is comparable to previously observed properties of the rat E12 VM which yields a several-fold greater number of TH-ir neurons than equivalent E14-derived grafts (Chapter 3 and Torres et al., 2007). The transplantation site affected the TH-ir neuron yield only in E12 grafts, with the grafts in the PFC producing a lower number of TH-ir neurons than grafts in the striatum. As mentioned in Chapter 4.3.2, not all sections of the PFC containing the graft were collected for immunohistochemistry. Thus, this drop in the TH-ir cell yield in E12 grafts in the PFC could be an artefact of

missing anterior sections of the PFC that contained the graft. Moreover, functionality of the VM graft cannot be assessed based solely on the number of TH-ir cells because TH is not selective in labelling the two DA neuron subtypes. Therefore, when assessing the effect of the transplantation site on the development and survival of DA neurons, it is more important to look at the DA neuron subtypes.

All grafts contained both the A9 type and A10 type DA neurons. The yield of A9 type DA neurons followed an expected pattern with the highest number of Girk2-ir/TH-ir cells found in grafts in the striatum, which receives the A9 type DA innervation from the midbrain, followed by a progressive decrease in the number of A9 type DA neurons in E12 grafts in the N.Acc, PFC and hippocampus in the absence of the A9 type DA innervation. E14 grafts in the striatum and N.Acc yielded similar numbers of the A9 type DA neurons indicating that the survival of developmentally older DA cells was less affected by the presence of environmental cues. Nevertheless, in the absence of the A9 type targets for innervation, E14 grafts in the PFC and hippocampus produced lower numbers of the A9 type DA neurons than grafts in the striatum and N.Acc. The A10 type DA innervation of the N.Acc and PFC did not result in a significant increase in the number of A10 type DA neurons as compared to grafts in the striatum and hippocampus. There was a slight increase in the number of A10 type DA neurons in E14 grafts in the N.Acc but it did not reach statistical significance. Despite different types of DA innervation of the striatum, N.Acc and PFC, all grafts in these transplantation sites contained more A9 type than A10 type DA neurons, an effect which was seen in both donor age groups. Only in the grafts in the hippocampus, was there a big enough decrease in the number of A9 type DA neurons to bring their yield below the yield of the A10 type DA neurons in both donor age groups. Despite a significantly higher yield of TH-ir cells in the E12 grafts, the percentages of A9 type and A10 type DA neurons in grafts in each transplantation site were similar between the two donor age groups. Interestingly, the effect of the transplantation site on the percentages of Girk2-ir/TH-ir and caldindin-ir/TH-ir cells was identical to significant differences in the total number of A9 type and A10 type DA neurons in grafts in different transplantation sites. Thus, although the total number of TH-ir cells was affected by the environment, the differences in the number of A9 type DA neurons in grafts between different transplantation sites were not due to DA neuron death but rather due to silencing of the A9 phenotype of DA neurons in the absence of the A9 type target innervation in the host brain. Indeed, the sum of percentages of A9 and A10 type DA neurons in the striatum and N.Acc was ≈105% whereas in the PFC and

hippocampus it was 78% and 69%, respectively, indicating that almost a third of TH-ir neurons were neither of A9 nor of A10 type in grafts in the PFC and hippocampus. The absence of an effect of the transplantation site on the total number of A10 type DA neurons could be due to the fact that a unilateral 6-OHDA lesion of the median forebrain bundle causes only a partial loss of DA neurons in the VTA and subsequently achieves only a partial denervation of the N.Acc and PFC. Previous studies indicated that post lesion amphetamine-induced rotation rates comparable with those observed in the present experiment are associated with DA depletions of more than 99% in the striatum and 25% in the N.Acc caused by DA neuron losses of more than 99% in the SNpc and 50% in the VTA (Olds et al., 2006).

It is important to consider the number of a therapeutic cell type as a function of graft volume in transplantation-based therapies for brain repair. Grafts should produce a sufficient cell yield to achieve the desired functional effect, while the graft size should be small enough as not to cause any damage to the host brain at the site of transplantation. Based on the average cell densities and graft volumes, the density of the A9 type DA neurons at each graft site was in the order of $1.3 – 5.8 \times 10^3$ Girk2-ir/TH-ir neurons/mm^3 and the density of the A10 type DA neurons was $1.6 – 2.8 \times 10^3$ calbindin-ir/TH-ir neurons/mm^3. In this context, the present results, even for grafts in the hippocampus, compare favourably to findings from human VM transplantation into the putamen of patients with PD. Recent post-mortem studies in two patients showed that a therapeutic benefit up to 3 years after transplantation was achieved by grafts with the DA neuron density in the order of 0.2 to 2.4×10^3 DA cells/mm^3 (Mendez et al., 2005). Thus, despite a significant loss of the A9 phenotype of DA neurons in grafts in the N.Acc, PFC and hippocampus, the cell densities observed in all grafts remained within the known functional range.

The present findings revealed that the A9 type DA neurons clustered at the periphery of grafts in the striatum, N.Acc and PFC, but not in the hippocampus, whereas the distribution of the A10 type DA neurons was more homogeneous within the graft. The striatum was found to positively influence the yield of the A9 type DA neurons in the periphery of grafts as compared to transplants in PFC and hippocampus in both donor age groups, and additionally in E14 grafts in the N.Acc. Furthermore, E12 grafts in the N.Acc contained slightly more A10 type DA neurons in the periphery of grafts than grafts in the striatum but the difference was not significant. Not surprisingly, the effect of the environment on two DA neuron subtypes was more detectable in the periphery of grafts rather than in the centre because neurons in the periphery of grafts

are more exposed to the environmental cues and are more likely to be affected by them. However, it is important to note that the measured effect represents a combination of the effect of the transplantation site on the graft and the effect of the environment within the graft on two DA neuron populations. TH-ir neurons in the core of grafts are less likely to be affected by the host environment cues because they are not directly exposed to them but they will be affected by the local microenvironment within the graft. Indeed, the TH-ir cell yield was affected by the transplantation site in the periphery but not in the core of grafts, whereas local environment within the graft caused a decrease in the total number of TH-ir neurons within the core as compared to the periphery in E14 grafts in the striatum and N.Acc. Location within the graft might have a greater influence on the differentiation, survival and migration of the A9 type DA neurons than the A10 type DA neurons. The A9 type DA neurons are known to be more susceptible to oxidative stress (Lotharius and Brundin, 2002, Smits et al., 2006) and therefore their survival might be affected more within the core of the graft than in the periphery with a less well established blood and nutrient supply. This was reflected, at least in part, in the fact that the A9 type DA neurons were predominantly found in the periphery of grafts than in the centre in all transplantation sites. Even when there were no environmental cues in the cerebral environment to attract their migration to and/or survival in the periphery of grafts, the A9 type DA neurons still survived better in the periphery than in the core of grafts. The distribution of the A10 type DA neurons was more homogeneous within the graft regardless of the transplantation site indicating that these neurons were less dependent on cues or resources from the host environment for their survival.

The TH-ir reactive fibres extending from the developing VM do not reach the ganglionic eminence until day 19 of embryonic development in the rat (Gates et al., 2004). Thus, there is also a possibility that DA neuron precursors in the core of grafts do not die, but instead fail to differentiate into a certain DA neuron subtype in the absence of functional connections and as a result silence their Girk2/calbindin expression altogether and differentiate into a different type of CA neuron. Indeed, ≈50% of TH-ir neurons in the core of the grafts did not coexpress neither Girk2 nor calbindin. Also, a great portion of TH-ir cells in grafts in the hippocampus (41% in the E12 group, 33% in the E14 group) failed to co-express either Girk2 or calbindin. Developmental signals available within the graft might not have sufficed to drive DA precursors towards the correct developmental pathway. Both E12 and E14 rat VM, especially in E12 grafts, contain a mix of differentiated and undifferentiated DA precursors, and

current evidence suggests that not only their survival but also to a great extent their differentiation into either type of DA neurons are affected by both the location within the graft and the host environment of the transplantation target. Grafts derived from E10 mice donor tissue (equivalent to E11.5 in rats) are enriched with mitotic DA neuroblasts which contribute to a higher yield of the A9 type DA neurons within the grafts in the mouse striatum (Bye et al., 2012). This suggests that younger DA neurons have better responsiveness to guidance cues present within the grafts and the surrounding striatum. Studies have demonstrated that such responsiveness is downregulated in older neurons (Van den Heuvel and Pasterkamp, 2008). Indeed, in this experiment we observed that the transplantation site affected E12 grafts to a greater extent than E14 grafts.

The transplantation site also affected the DA neuron cell sizes. The A9 type DA neurons were once again generally bigger than the A10 type DA neurons as already seen in previous studies (Chapter 3 and Thompson et al., 2005). Interestingly, E14-derived A9 type DA neurons were bigger than E12-derived A9 type DA neurons in all transplantation sites. Most importantly, the A9 type DA neurons were smaller in E12 grafts in the PFC and hippocampus than in the striatum. Cell body size is dependent on the metabolic activity of the cell, and clearly in E12 grafts in the PFC and hippocampus, in the absence of target innervation, the A9 type DA neurons were less active and failed to reach the normal cell body size. *In vitro* studies have demonstrated that the presence of normal target tissues results in the increase in fibre elongation, cell body and nuclear size, and catecholamine and TH content in cultured sympathetic neurons (Chamley and Dowel, 1975, Coughlin et al., 1978).

4.5 Conclusion

This experiment has demonstrated a significant effect of the transplantation site on both DA neuron phenotypes in the grafts and the distribution of A9 and A10 type DA neurons across the periphery and the centre of the graft. Also, there was a significant effect of the environment on the percentage of A9 type but not A10 type DA neurons in the grafts. The evidence suggests that the environment affects differentiation of DA neurons more than their survival. It is unclear however, as to what extent post-graft proliferation and differentiation of DA precursor cells contribute to different A9 and A10 type DA neuron populations and their distribution within the graft. A future experiment will investigate proliferation of DA neural precursor cells post-grafting and

the contribution of cell birth in the host to the yield of A9 type and A10 type DA neurons in intrastriatal grafts.

Chapter 5. The A9 and A10 Type Dopamine Neuron Proliferation Post-grafting in Ventral Mesencephalon Transplants

Summary

The aims of this chapter were (i) to quantify the populations of the A9 type and A10 type DA neurons in grafts derived from E12 and E14 VM rat tissue, and (ii) to determine whether proliferation of A9 type DA precursor cells contributes to the enriched composition of younger donor tissue grafts. To that end, 6-OHDA unilaterally lesioned rats received E12 and E14 VM transplants and a sub-cohort of grafted animals in each group were injected i.p. 4 hours post-transplantation with 120mk/kg BrdU to label mitotic cells. The results revealed no toxic effect of the BrdU dose on the DA neuron yield in the grafts. Grafts derived from younger donor tissue contained bigger subpopulations of DA progenitors that continued dividing in the host striatum and subsequently matured into A9 type and A10 type DA neurons. The A9 type DA neuron birth post-grafting significantly enriched E12 grafts with the SNpc DA neurons with little effect on the VTA DA neurons as compared to grafts in the E14 group. Also, the majority of DA neurons born post-grafting were found at the periphery of the graft rather than in the centre of grafts suggesting that direct access to the functional targets in the striatum may be necessary for mitotic DA precursor cells to survive and differentiate into mature neurons.

5.1 Introduction

Clinical trials of cell transplantation therapy in PD have so far been based on the use of postmitotic DA neurons obtained from the developing human embryonic VM, aged 6-9 weeks post-conception (Freeman et al., 1995a, Hagell et al., 1999, Brundin et al., 2000b, Baker et al., 2000, Freed et al., 2001, Olanow et al., 2003). This critical time window corresponds to the peak ontogeny of DA neurons when their fate is already determined but the cells have no extensive outgrowth of neuritic processes yet, which may compromise DA neuron survival during graft tissue dissection and preparation for implantation (Freeman et al., 1995b). Historically, the time of maximal neurogenesis for midbrain DA neurons in the rat has been considered to occur at E14, at a CRL of 10.5-11.5mm (Bjorklund et al., 1980b, Altman and Bayer, 1981, Brundin et al., 1985b, Brundin et al., 1988, Dunnett and Bjorklund, 1992). At this stage, a high proportion of DA neurons are about to complete differentiation or already express TH but still have small, or no, axonal arbours. Other studies have suggested that only DA neurons that underwent their final division in utero before removal from the donor embryo were able to survive transplantation, develop into mature DA neurons and make functional connections with the host striatum (Sinclair et al., 1999). Thus, E14 rat embryos have been the predominant source of midbrain DA neurons in cell transplantation research in animal models of PD over the years (Barker et al., 1995, Barker et al., 1996, Agrawal et al., 2004, Dowd and Dunnett, 2004, Breysse et al., 2007, Kuan et al., 2007, Terpstra et al., 2007). Grafts derived from the rat E14 VM and the equivalent gestation human VM yielded DA neuron survival rates of 5 – 10% of the expected adult DA complement and restored behavioural deficits (Fawcett et al., 1995, Barker et al., 1996, Dowd and Dunnett, 2004, Sortwell et al., 2004). Embryonic VMs both younger and older than E14 produced even smaller yields of DA neurons and were dismissed as the donor tissue for transplantation until 7 years ago.

Most recent studies suggest that TH-ir neurons can be identified in the developing rat VM as early as E12 and that by E14 large numbers of DA neurons extend axonal projections (>1 mm) to the ventral forebrain (Gates et al., 2004). Re-examination of the ontogeny of SNpc DA neurons reveals that up to 80% of DA neurons in the SNpc might be born over a 24-hour period on E12 in SD rats (Gates et al., 2006). These younger DA precursor cells have been shown to provide an enhanced DA neuron yield in grafts and restore behavioural deficits in 6-OHDA lesioned rats

(Torres et al., 2007, Torres et al., 2008a). Transplanted E12 VM tissue contains a mixture of differentiated DA neurons that have already undergone final mitosis and developing DA neural progenitor cells that continue to proliferate in the host and mature into functional DA neurons after transplantation (Weyrauch, 2009). Levels of continued cell division in the A9 and A10 subpopulations of DA neurons in the graft remain unknown. In Chapter 4, we have already demonstrated that both E12 and E14 A9 type DA precursor cells might be less committed to their neuronal fate than the A10 type DA precursor cells at the time of transplantation and that, in the absence of correct functional targets, a substantial number of A9 type DA precursor cells either fail to follow the correct developmental pathway or silence their A9 phenotype. This suggests that it is predominantly the A9 type and not the A10 type DA precursor cells that contribute to DA neuron birth post-transplantation.

Dividing cells and their lineages can be traced using the thymidine analogue 5-bromo-2-deoxyuridine (BrdU), which is incorporated into the newly synthesized DNA instead of thymidine during the S-phase of the cell cycle and therefore is used to specifically label dividing cells (Kriss and Revesz, 1962, Yamada et al., 2005). The cell cycle of embryonic neural progenitor cells is 12-14 hours and the S-phase equates to one third or half of this period (Hayes and Nowakowski, 2000, Hayes and Nowakowski, 2002). Reliable long-term labelling of mitotic grafted cells in adult rodents with no BrdU-associated toxic effects has been demonstrated with BrdU doses of >100mg/kg (Weyrauch, 2009, Bye et al., 2012).

5.1.1. Aims of this chapter

The present study was undertaken to determine the origin of ongoing DA precursor cell division within grafts derived from rat E12 and E14 VM tissue. BrdU was used to label mitotic DA precursor cells that continued to proliferate after transplantation. The aims of this experiment were:

1. To quantify levels of continued cell birth in the A9 and A10 subpopulations of DA neurons in both E12 and E14 grafts
2. To determine whether the enrichment for A9 type DA neurons seen in VM grafts originates from increased cell birth of the A9 type DA neural progenitors post-transplantation

5.2 Experimental Procedure

This study initially was planned as a pilot experiment aimed to test BrdU labelling of dividing DA neurons in grafts after transplantation in a small cohort of animals (n = 6). However, based on the previous work done in our lab demonstrating successful labelling of dividing grafted neurons using the same dose of BrdU the decision was made to transplant a second cohort of animals to complete the data for a full experiment (n = 16). Thus, the grafts in each group were derived from multiple cell suspensions in each donor age group, which is essential for studies of this kind.

All of the methods used in this experiment are described in Chapter 2. In this study, 22 female SD rats received a unilateral lesion to the right MFB via the injection of 6-OHDA (Chapter 2.3.1) and were assessed for motor deficits using drug-induced rotation tests (Chapter 2.4). Due to the temporary unavailability of methamphetamine at the time, $_{D}$-Amphetamine (Sigma-Aldrich) was used to assess rotational behaviour after lesion and after grafting in the first cohort of animals. Methamphetamine was used for the drug-induced rotation test in the second cohort of animals. In agreement with previous studies (Romero et al., 2006), both drugs elicited a similar rotational behaviour in the two cohorts of animals (one-way ANOVA with repeated measures; Drug, $F_{(1,20)} = 1.89$, n.s.). The rats were allocated into 2 homogeneous groups based on their performances on the drug-induced rotation test post-lesion (**E12**: 1391.1 ± 84.3; **E14:** 1407 ± 155; mean ± SEM) and no statistical differences between the groups were confirmed with a one-way ANOVA (Group, $F_{(1,20)} = 0.01$, n.s.).

Six weeks post-lesion, the animals received an intrastriatal transplant containing cell numbers equivalent to 1 VM in 2 µl of the cell suspension as described in Chapter 2.3.2. Stereotaxic co-ordinates for the placement of grafts into the striatum were as follows: AP: +0.6 mm, ML: -3.0 mm, DV: -5.0 mm (Paxinos and Watson, 2003). In the E12 group, one animal in the first cohort did not recover after the transplantation surgery. An additional lesioned animal received an E12 transplant during a different surgery session to replace the lost animal and complete the group numbers. The second cohort of animals (n = 8) was grafted from a single E12 cell suspension. There were no significant differences between the three E12 cell suspensions used to graft 11 animals (**E12 1:** 101,000 cells/VM, viability –

94.33%; **E12 2:** 100,000 cells/VM, viability – 94.9%; **E12 3:** 109,000 cells/VM, viability – 91.93%). In the E14 group, one suspension per cohort was used to graft 3 animals in the first cohort and 8 animals in the second cohort (**E14 1:** 497,500 cells/VM, viability – 95.3%; **E14 2:** 503,000 cells/VM, viability – 92.31%). Again, no significant differences between the two E14 cell suspensions were identified. In both donor age groups, 3 grafted animals in the first cohort and 5 out of 8 grafted animals in the second cohort received i.p. injections of BrdU (120mg/kg) within 4 hours after transplantation (see Chapter 2.7.1 for details on BrdU preparation). Drug-induced rotation tests were performed 4 and 6 weeks post-transplantation to assess graft functionality. All animals were transcardially perfused 7 weeks after transplantation and coronal brain sections were collected for IHC processing (Chapter 2.5).

Brain tissue from both cohorts of animals was processed together for IHC analysis. A one-in-twelve series of sections was processed for BrdU-immunoreactivity using DAB and subsequently for nuclei staining using Mayer's haematoxylin. Two one-in-twelve series of sections were processed for BrdU, Girk2, TH and BrdU, calbindin, TH, respectively, using fluorescent triple labelling IHC (refer to Chapter 2.6 for more details and antibody concentrations). Cells were counted blind to the experimental condition abiding by the stereological principles (Chapter 2.8). The total number of TH-ir neurons per graft was calculated as an average TH-ir cell count obtained from BrdU/Girk2/TH and BrdU/calbindin/TH stainings. Due to very low numbers of triple labelled cells per graft, especially in the centre of the graft (in most cases only 1 triple labelled cell in the centre of the graft was found), a standard method of unbiased sampling of the periphery and the centre of the graft (see Chapter 2.8.2) was not applicable. Instead, analysis of the total number of counted triple labelled cells either in the periphery or the centre of the graft is presented here.

Statistical analyses were performed in SPSS as described in Chapter 2.9. Behavioural data was analysed using a three-way ANOVA with repeated measures. One- and two-way ANOVAs were used to analyse TH-ir cell yield and BrdU-ir cell yield. DA neuron subpopulations, their proliferation post-grafting and distribution within the graft were analysed using two- or three-way ANOVAs with repeated measures. Where applicable a Bonferroni correction for multiple comparisons was

used to reveal significant differences between individual groups and results were considered to be significant if $p<0.05$ (*).

5.3 Results

5.3.1 Functionality of the grafts

The functional ability of the graft to release dopamine and restore lesion-induced motor deficits was assessed by the drug-induced rotation test at 4 and 6 weeks after transplantation. There were no differences in amphetamine-induced rotational behaviour at either time point between BrdU-treated animals and controls in both donor age groups (BrdU, $F_{(1,18)} = 2.06$, n.s.; no significant interactions associated with BrdU). Therefore, subsequent analysis was performed on the combined data within each donor age group. Figure 5.1 shows the total number of net rotations performed over 90 minutes, ipsilateral minus contralateral to the lesioned side. Post-lesion, the animals rotated ipsilaterally to the lesioned side, a classic rotational behaviour induced by the 6-OHDA lesion to the nigrostriatal pathway in response to amphetamine. Fluorescent TH IHC revealed virtually no surviving TH-ir neurons in the lesioned SNpc but the extent of lesions was not quantified. In both donor age groups, grafts in the striatum significantly reduced the net number of rotations and ameliorated the lesion-induced rotational behaviour 4 and 6 weeks post-transplantation (within-subject factor – Transplantation, $F_{(2,40)} = 205.18$, $p<0.001$). There were no differences in rotational behaviour between the E12 and E14 groups (Donor Age, $F_{(1, 20)} = 0.16$, n.s; Donor Age x Transplantation, $F_{(2,40)} = 0.09$, n.s.). In both donor age groups, there was a significant decrease in the net number of ipsilateral rotations at 4 and 6 weeks post-grafting compared to post-lesion ($p<0.001$). At 6 weeks post-grafting, most animals rotated contralaterally to the lesioned side, a classic over compensatory response. However, this further reduction in the net number of rotations at 6 weeks as compared to 4 weeks post-transplantation was significant only in the E12 group ($p<0.05$).

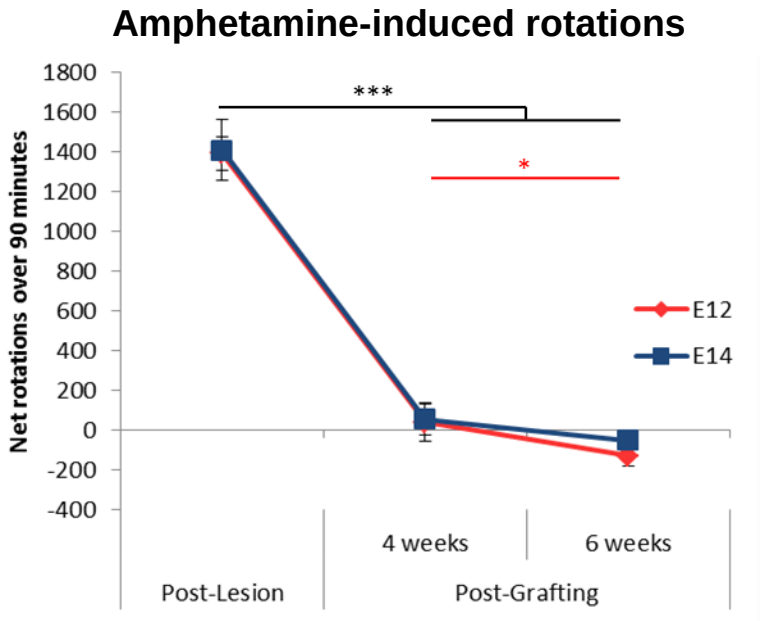

Figure 5.1 Amphetamine-induced net rotational behaviour post-lesion and post-grafting in the E12 (red) and E14 (blue) groups (data from BrdU-treated animals and controls is pooled together). Both E12 and E14 intrastriatal grafts produced a significant recovery of the lesion-induced behavioural deficits. There was a highly significant change (***) from ipsilateral rotation observed post-lesion to a net contralateral rotation post-grafting, the classic over-compensatory response ($F_{(1,20)}$ = 205.18, $p<0.001$). Data are presented as a mean number of net rotations (ipsilateral minus contralateral) over 90 minutes, error bars indicate SEM, significance levels: * $p<0.05$, *** $p<0.001$.

5.3.2 Dopamine neuron yield in the grafts

Examination of TH staining confirmed the presence of well positioned grafts in the dorsal striatum of most animals in both donor age groups. Grafts contained large numbers of surviving TH-ir neurons and extensively innervated the surrounding striatum. Larger TH-ir neurons with angular cell bodies resided in the periphery of the graft and smaller rounder TH-ir cells clustered in the centre of the graft. No surviving TH-ir neurons were found in the striatum of one animal in the E14 BrdU group. The staining was repeated on a one-in-six series in an attempt to detect surviving DA neurons in case the graft was very small. However, no sections containing the graft were present. Nevertheless, no toxic effect of the BrdU dose on the survival of TH-ir neurons was detected in either donor age group as depicted in Figure 5.2A (BrdU, $F_{(1,18)}$ = 0.01, n.s.; BrdU x Donor Age, $F_{(1,18)}$ = 0.35, n.s.). The animal that did not contain the graft was excluded from further analysis of DA neuron proliferation and maturation post-grafting. Grafts in the E12 group produced

a 2.28-fold higher yield of TH-ir neurons than grafts in the E14 group (Figure 5.2B). As previously, younger DA precursor cells yielded significantly higher numbers of DA neurons in the grafts (Donor Age, $F_{(1,19)} = 7.54$, $p<0.05$).

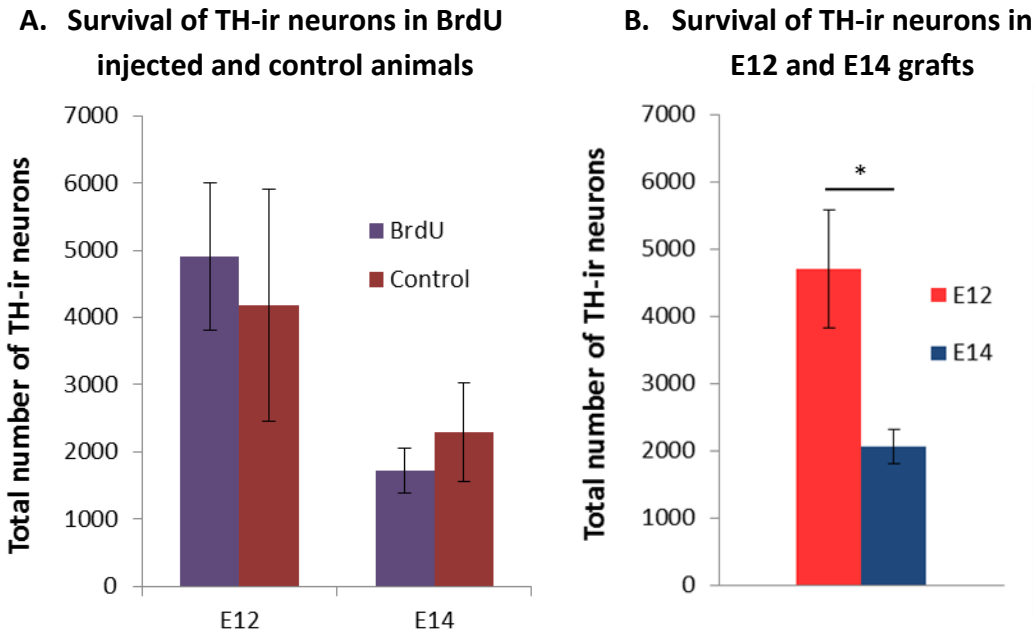

Figure 5.2 (A) TH-ir neuron yields in grafts in the E12 and E14 groups in animals that received a BrdU injection after transplantation and in control animals. No significant effect of the BrdU dose on the number of TH-ir neurons in the grafts was found. **(B)** Total TH-ir neuron numbers in the two groups 7 weeks post-transplantation. Grafts in the E12 group contained significantly more DA neurons than in the E14 group (data from BrdU-treated animals and controls is pooled together). Data are presented as group means, error bars correspond to SEM, significance level: * $p<0.05$.

5.3.3 Continued cell and DA neuron division in the grafts after transplantation

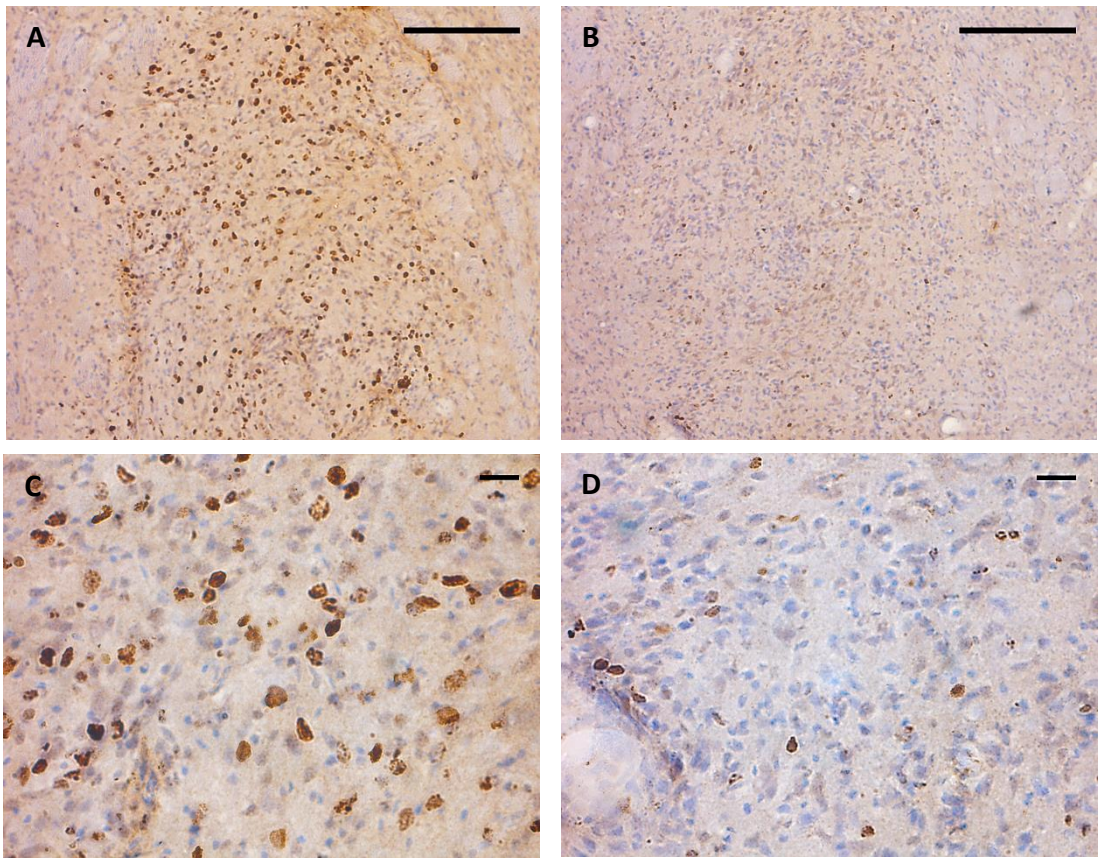

Figure 5.3 Photomicrographs of representative grafts derived from rat E12 **(A, C)** and E14 **(B, D)** VM showing surviving cells that continued to divide after transplantation (brown) counterstained with haematoxylin (blue) both at x10 **(A, B)** and x40 **(C, D)** magnification. There were very clearly discernible BrdU-ir cells in grafts in both donor age groups. Grafts in the E12 group contained a dense population of BrdU-ir cells that were homogeneously distributed within the graft. Fewer BrdU-ir cells could be identified in grafts in the E14 group. Scale bars: 200 µm (A, B); 20 µm (C, D).

All surviving grafts in both donor age groups exhibited similarly strong nuclear BrdU staining. Large populations of homogeneously distributed BrdU-ir cells were observed in grafts in the E12 group (Figure 5.3A, C). Grafts in the E14 group contained fewer BrdU-ir cells that were sparsely distributed within the graft (Figure 5.3B, D). When comparing the number of BrdU-ir cells per transplant, a significant difference between the two donor age groups was detected. As shown in Figure 5.4A, 11.74-fold more surviving cells incorporated BrdU shortly after transplantation in the E12 group than E14 group indicating that E12 VM contains a larger population of young precursor cells that continue to proliferate after transplantation and are able to survive and differentiate into mature functional cells (Donor Age, $F_{(1,13)} = 13.76$, $p<0.01$). However,

only a small number of BrdU-ir cells belonged to the DA neuron population in the grafts. In the E12 group, out of almost 6000 BrdU-ir cells in the grafts (5938.4 ± 1357.8; mean ± SEM) only 158 ± 37.26 cells co-labelled with TH. In the E14 group, the mean number of DA neurons that incorporated BrdU was 32.71 ± 6.77 while the total yield of BrdU-ir cells was 506.04 ± 145.46. There were significantly higher numbers of BrdU-ir/TH-ir neurons in the E12 group than E14 group (Figure 5.4B; Donor Age, $F_{(1,13)} = 9.64$, $p<0.01$). The increase in the number of BrdU-ir/TH-ir neurons in grafts in the E12 group outweighed the general increase in the number of TH-ir neurons between grafts in the two donor age groups. Post-grafting proliferation of DA precursor cells contributed to a higher yield of DA neurons in the E12 group as indicated by a significant difference in the percentage of BrdU-ir/TH-ir neurons (Figure 5.4C; Donor Age, $F_{(1,13)} = 5.6$, $p<0.05$).

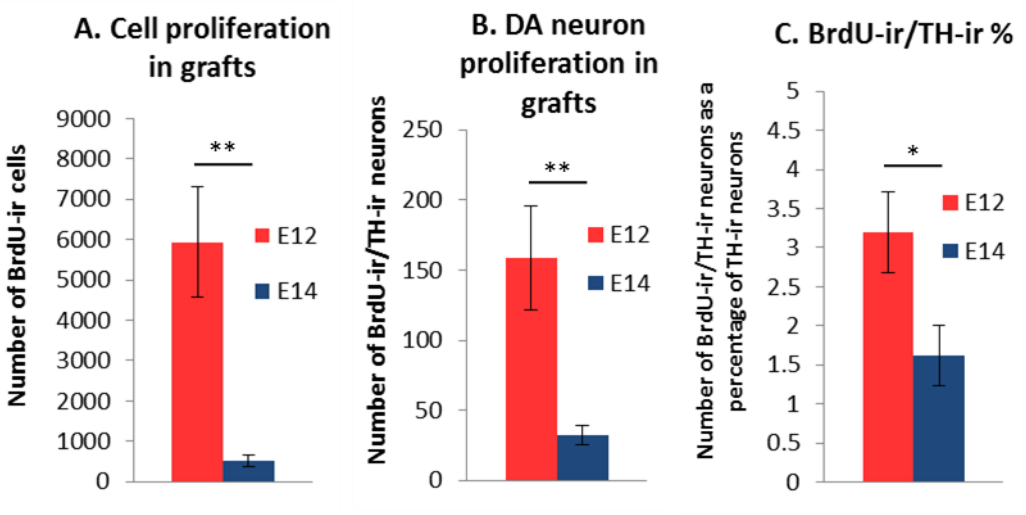

Figure 5.4 (A) Total numbers of BrdU-ir cells in the grafts. Grafts in the E12 group contained significantly more BrdU-ir cells than E14 group. **(B)** Comparison of the numbers of surviving DA neurons that were mitotic at the time of transplantation. There was a significantly higher level of DA precursor cell proliferation post-grafting in grafts in the E12 group than E14 group as indicated by the difference in the number of BrdU-ir/TH-ir neurons in the grafts. **(C)** Effect of the donor age on the percentage of BrdU-ir/TH-ir neurons in the grafts. Grafts in the E12 group contained a significantly higher percentage of TH-ir neurons that co-labelled with BrdU. Data are presented as group means ± SEM, significance levels: * $p<0.05$, ** $p<0.01$.

5.3.4 The A9 and A10 type DA precursors in the grafts

Fluorescent triple BrdU/Girk2/TH and BrdU/calbindin/TH labelling successfully identified subpopulations of the A9 and A10 type DA neurons, respectively, that continued to divide in the host striatum after transplantation in grafts in both donor age

groups. As depicted in Figure 5.5, strong nuclear BrdU staining co-localised with cytoplasmic Girk2/TH and calbindin/TH stainings of DA neurons. Fluorescent BrdU staining exhibited the same trend as DAB BrdU, grafts derived from E12 VM displayed abundant BrdU-ir cells and grafts in the E14 group contained fewer BrdU-ir cells.

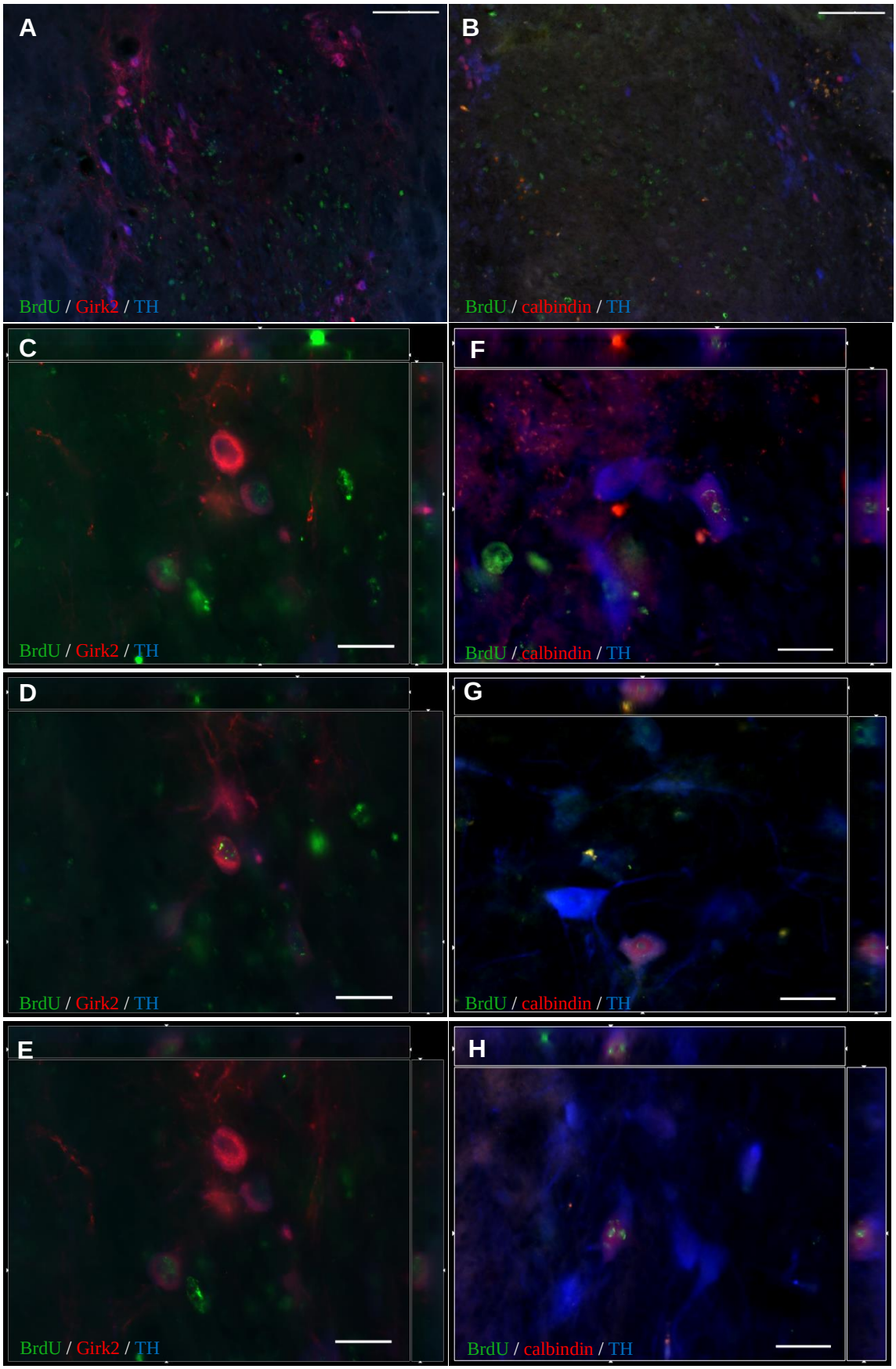

Figure 5.5 Coronal sections through the striatum showing positive staining for BrdU, Grik2, TH **(A)** and BrdU, calbindin, TH **(B)** within E12 VM donor grafts at 6 weeks post-transplantation. A small population of both A9 type and A10 type DA precursor cells were dividing and incorporated BrdU at 4 hours post-grafting and subsequently matured into functional DA neurons. A series of higher power panels illustrates the A9 type DA neurons **(C-E)** and the A10 type DA neurons **(F-H)** born in the graft. Scale bars: 100 µm (A, B); 20 µm (C-H).

As seen in previous experiments (Chapter 3, 4), grafts in the E12 group yielded higher numbers of both Girk2-ir/TH-ir and calbindin-ir/TH-ir neurons than grafts in the E14 group (Figure 5.6). A two-way ANOVA with repeated measures confirmed a highly significant difference between the numbers of A9 and A10 type DA neurons in the grafts (within-subject factor - Staining, $F_{(1,19)} = 41.05$, $p<0.001$), a main effect of the donor age group ($F_{(1,19)} = 8.23$, $p<0.05$) and a significant interaction ($F_{(1,19)} = 9.57$, $p<0.01$). There were significantly more Girk2-ir/TH-ir neurons than calbindin-ir/TH-ir neurons in grafts both in the E12 ($p<0.001$) and E14 donor age groups ($p<0.05$). Grafts in the E12 group, contained significantly more A9 type and A10 type DA neurons than grafts in the E14 group ($p<0.01$ and $p<0.05$, respectively). Grafts in the E12 group, contained not only an increased number of Girk2-ir/TH-ir neurons than grafts in the E14 group but also a higher proportion of TH-ir neurons that co-expressed Girk2 (80% and 73%, respectively) indicating an enriched composition ($p<0.001$). A similar proportion of TH-ir neurons co-labelled with calbindin (22-23%) in grafts in both donor age groups. These results are comparable to previous findings described in Chapter 3.

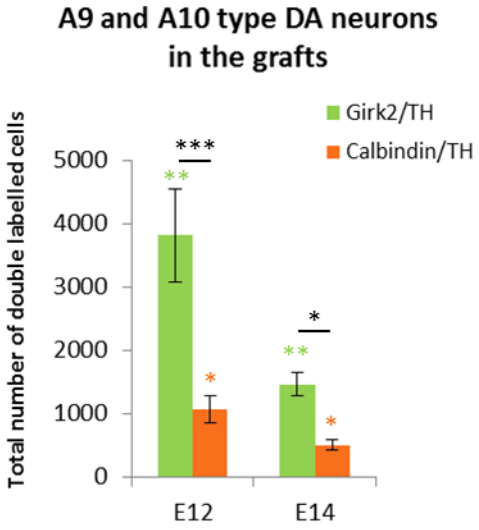

Figure 5.6 Total numbers of Girk2-ir/TH-ir (green) and calbindin-ir/TH-ir (orange) neurons in the grafts (data from BrdU-treated animals and controls is pooled together). Grafts in the E12 group produced higher numbers of both DA neuron subtypes than in the E14 group. Also, Girk2-ir/TH-ir neurons were more abundant than calbindin-ir/TH-ir neurons in grafts in both donor age groups. Data presented as group means ± SEM, significance levels: * $p<0.05$, ** $p<0.01$, *** $p<0.001$.

Cell counts of BrdU-ir/Girk2-ir/TH-ir and BrdU-ir/calbindin-ir/TH-ir cells were quite low in all grafts regardless of the donor age group (Figure 5.7). Nevertheless, grafts in the E12 and E14 groups showed distinctive differences between the two populations of DA neuron precursor cells that were still at the mitotic developmental

stage at the time of transplantation and subsequently were capable of surviving and maturing into functional DA neurons in the host (within-subject factor – Staining, $F_{(1,13)} = 8.9$, $p<0.05$). The numbers of both the A9 and A10 type DA neurons that co-labelled with BrdU were higher in grafts in the E12 group than E14 group (Donor Age, $F_{(1,13)} = 9.68$, $p<0.01$). More A9 type than A10 type DA neuron precursor cells continued to proliferate in the host after transplantation in grafts in the E12 group ($p<0.01$) while a similar number of BrdU-ir/TH-ir neurons coexpressed either Girk2 or calbindin in grafts in the E14 group (Staining x Donor Age, $F_{(1,13)} = 9.64$, $p<0.01$). Grafts in the E12 group contained significantly bigger populations of both BrdU-ir/Girk2-ir/TH-ir and BrdU-ir/calbindin-ir/TH-ir neurons than in the E14 group ($p<0.01$ and $p<0.05$).

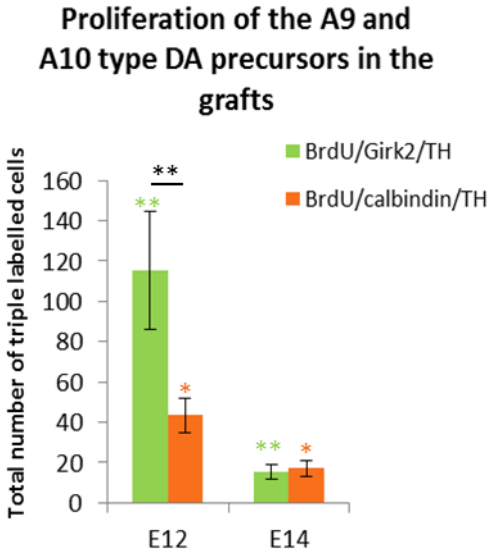

Figure 5.7 A summary of BrdU-ir/Girk2-ir/TH-ir and BrdU-ir/calbindin-ir/TH-ir cell yields in grafts in the E12 and E14 groups. Grafts in the E12 group contained significantly bigger A9 type and A10 type DA neuron populations than the E14 group that had incorporated BrdU 4 hours after transplantation. Also, significantly more Girk2-ir/TH-ir neurons than calbindin-ir/TH-ir neurons co-labelled with BrdU in grafts in the E12 group. Data are presented as group means; error bars indicate SEM; significance levels: * $p<0.05$, ** $p<0.01$.

Grafts in the E12 group yielded significantly higher numbers of DA neurons than grafts in the E14 group and the number of triple labelled cells was calculated as a percentage of TH-ir neurons to account for the difference in overall TH-ir cell numbers. Post-grafting proliferation of either subtype of DA precursor cells contributed little to the total DA neuron yield in grafts in both donor age groups (Figure 5.8A). The percentage of TH-ir cells that co-labelled with BrdU/Girk2 in the E12 group was 2.23±0.42% (mean ± SEM) while less than 1% of TH-ir neurons co-expressed

BrdU/Girk2 in the E14 group. In both donor age groups, less than 1% of DA neurons in the grafts were BrdU-ir/calbindin-ir. Nevertheless, there were significant differences between the percentages of triple labelled neurons in grafts in the E12 and E14 groups (within subject-factor – Staining, $F_{(1,13)} = 7.29$, $p<0.05$; Donor Age, $F_{(1,13)} = 5.62$, $p<0.05$; Staining x Donor Age, $F_{(1,13)} = 10.23$, $p<0.01$). In the E12 group, a significantly higher percentage of DA neurons co-labelled with BrdU/Girk2 than BrdU/calbindin ($p<0.01$). Also, the percentage of BrdU-ir/Girk2-ir/TH-ir neurons was greater in grafts in the E12 group than E14 group ($p<0.01$). Furthermore, two thirds of BrdU-ir/TH-ir neurons co-labelled with Girk2 and one third co-expressed calbindin in grafts in the E12 group ($p<0.01$). In the E14 group, the ratio of mitotic A9 type and A10 type DA neurons was 50/50 (Figure 5.7B).

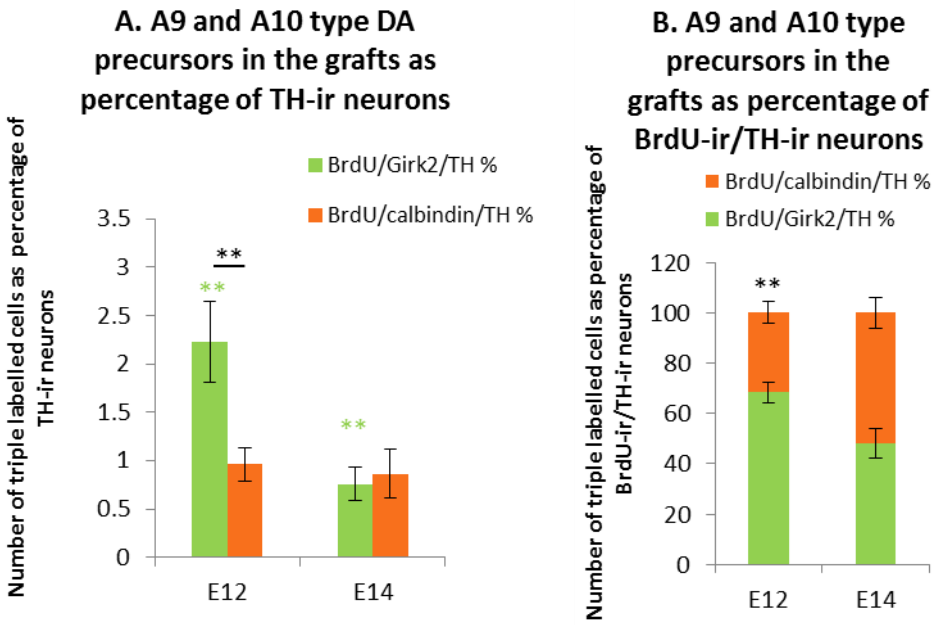

Figure 5.8 (A) Percentages of TH-ir cells that co-labelled with BrdU/Girk2 and BrdU/calbindin in both groups. Post-grafting proliferation of the A9 type DA precursor cells in grafts in the E12 group contributed the most to the total TH-ir cell yield as compared to all other groups. **(B)** Percentage of BrdU-ir/TH-ir that co-expressed either Girk2 or calbindin in both groups. In the E12 group, two thirds of mitotic DA precursor cells that matured into functional neurons became the A9 type DA neurons and one third became the A10 type DA neurons. In the E14 group, equal numbers of BrdU-ir/TH-ir cells differentiated into A9 and A10 DA neurons. Columns depict group means; error bars illustrate SEM; significance level: ** $p<0.01$.

In order to account for differences between the A9 and A10 type DA neuron yields in grafts in the two donor age groups, the number of triple labelled cells was calculated as a percentage of corresponding DA neuron subtype population. As shown in Figure 5.9A, there was a significantly higher percentage of Girk2-ir/TH-ir neurons that co-labelled with BrdU in grafts in the E12 group than E14 group ($F_{(1,13)} = 8.66$,

p<0.05). There was no difference between the percentages of calbindin-ir/TH-ir neurons in grafts in the E12 group and E14 group that incorporated BrdU after transplantation (Figure 5.9B; $F_{(1,13)} = 0.19$, n.s).

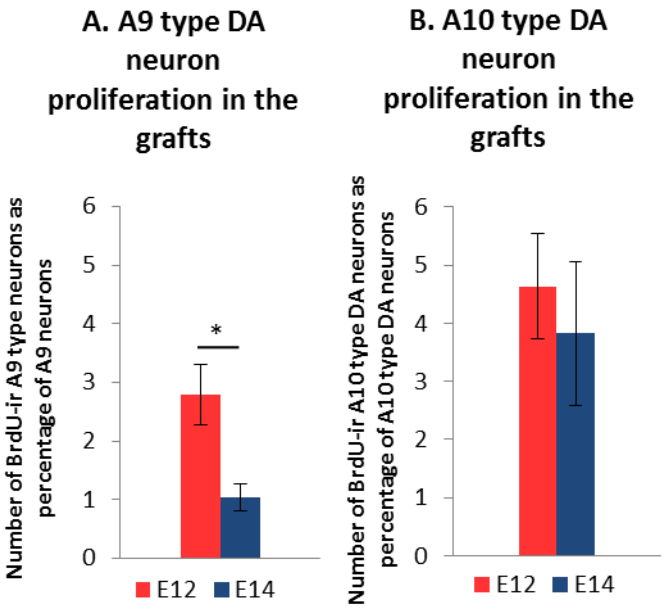

Figure 5.9 (A) Percentage of surviving A9 type DA neurons that continued to divide after transplantation. Grafts in the E12 group contained a significantly higher percentage of Girk2-ir/TH-ir neurons that co-labelled with BrdU than grafts in the E14 group. **(B)** Percentage of surviving A10 type DA neurons that continued to proliferate post-grafting. No significant difference was found between grafts in the E12 and E14 groups. Columns depict group means; error bars illustrate SEM; significance levels: * p<0.05.

The majority of both types of triple labelled cells were found in the periphery of grafts in both donor age groups. Only a few BrdU-ir/Girk2-ir/TH-ir and BrdU-ir/calbindin-ir/TH-ir cells resided in the centre of the graft. In both donor age groups, 9% of counted BrdU-ir A9 type DA neurons resided in the centre of grafts while 91% of triple labelled cells were found in the periphery of grafts. Similarly, 9% of BrdU-ir A10 type DA neurons resided in the centre of grafts and 91% in the periphery of grafts in the E12 group. In the E14 group, all BrdU-ir A10 type DA neurons were located in the periphery of grafts. However, in the E12 group, 50% of the grafts contained no BrdU-ir DA neurons of either phenotype in the core of the grafts. In the E14 group, only 1 BrdU-ir/Girk2-ir/TH-ir cell was found in the centre of a single graft and no BrdU-ir/calbindin-ir/TH-ir neurons resided in the centre of grafts. Figure 5.10 shows the numbers of triple labelled cells found either in the periphery or centre of the graft in both donor age groups. As expected more triple labelled cells of both types were found

in the periphery than centre of the graft (within-subject factor – Location, $F_{(1,13)} = 17.52$, $p<0.01$). Overall, significantly more A9 type than A10 type DA neurons co-labelled with BrdU (within-subject factor – Staining, $F_{(1,13)} = 8.94$, $p<0.05$). Also, grafts in the E12 group contained more BrdU-ir DA neurons of both subtypes than grafts in the E14 group both in the centre and periphery of the graft (Donor Age, $F_{(1,13)} = 9.67$, $p<0.01$). Both BrdU-ir/Girk2-ir/TH-ir and BrdU-ir/calbindin-ir/TH-ir neuron yields in the periphery of the graft were significantly higher in grafts in the E12 group than E14 group ($p<0.05$). The numbers of both A9 and A10 type DA neurons that were born in the host were higher in the periphery than centre of grafts in the E12 group ($p<0.01$ and $p<0.001$, respectively). In the E14 group, only the yield of BrdU-ir A10 type DA neurons in the periphery of the graft was significantly higher than in the centre of the graft ($p<0.05$). As shown before, there was a higher yield of BrdU-ir A9 type than A10 type DA neurons in grafts in the E12 group so, not surprisingly, the number of counted BrdU-ir/Girk2-ir/TH-ir neurons in the periphery of grafts was significantly higher than BrdU-ir/calbindin-ir/TH-ir neurons ($p<0.01$).

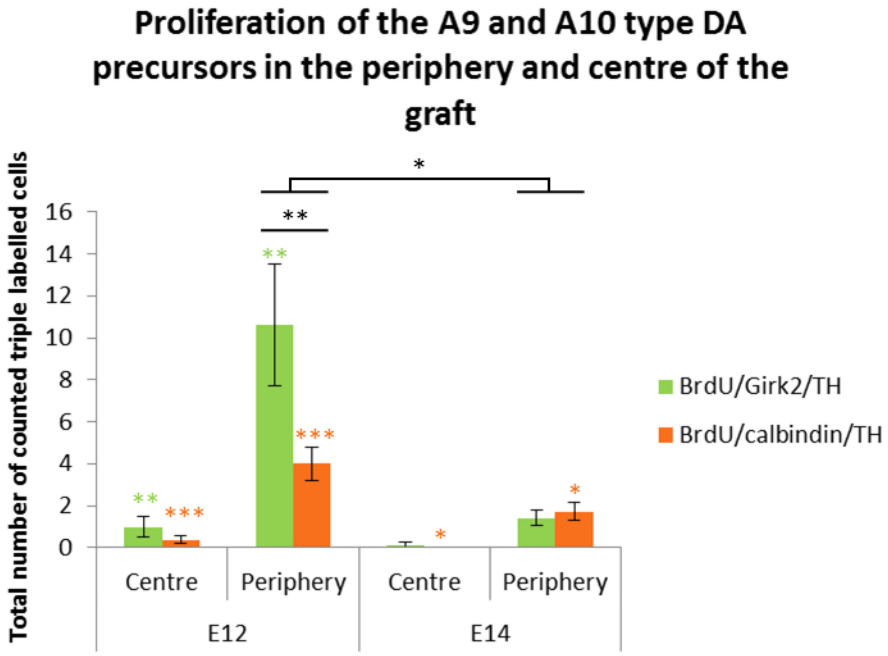

Figure 5.10 A summary of the numbers of BrdU-ir/Girk2-ir/TH-ir and BrdU-ir/calbindin-ir/TH-ir neurons and their location within the graft in both donor age groups. The majority of both phenotypes of DA neurons that continued to proliferate in the graft after transplantation were found in the periphery of all grafts. Significant differences between the groups are depicted on the graph. Data presented as group means ± SEM; significance levels: * $p<0.05$, ** $p<0.01$, *** $p<0.001$.

5.4. Discussion

This study examined the A9 type and A10 type DA precursor cell proliferation and subsequent differentiation into functional DA neurons within the environment of intrastriatal grafts derived from E12 and E14 rat VM. Both donor ages lie within the 2-3 day period of embryonic development when maximal neurogenesis of SNpc DA neurons occurs. However, there is some discrepancy in the evidence of the day of embryogenesis on which the generation of midbrain DA neurons is at its height.

The earliest ontological studies using catecholamine fluorescence revealed that DA neurons in the rat VM start to appear in E10-11, 7mm embryos, rapidly increase in numbers at E12-13 and continue to increase in numbers at E15-16 (Olson and Seiger, 1972, Seiger and Olson, 1973). Another study showed that TH-ir neurons with a few thin processes are detectable in the developing VM at E12.5, in 9 mm embryos, greatly increase in numbers by E13.5, in 11 mm embryos, exhibit an even more extensive distribution and project axons to the caudate-putamen by E14.5, in 15 mm embryos (Specht et al., 1981). Note that according to the most recent staging scale a CRL of 7 mm corresponds to E12.5 rat embryos, 9 mm – E13, 11mm – E14, 15 mm – E16 (Torres et al., 2008b). First examination of cell birth using tritiated thymidine (which incorporates into cell DNA during mitosis when injected into pregnant dams) provided evidence that neurons in the SNpc are born at E13-15 and neurons in the VTA are born slightly later, at E13-16 (Altman and Bayer, 1981, Marchand and Poirier, 1983). Another independent study mainly supported these results and showed that the generation of SNpc neurons occurs at E12-15 (Marchand and Poirier, 1983). Double labelling of BrdU-labelled neurons with TH produced similar results and showed that DA neurons in the SNpc develop between E12 and E16, rapidly increasing in numbers from E13 onwards to a maximum at E14 and E15 [with the day after overnight mating designated as E1 (Sinclair et al., 1999)]. Using a similar technique, a more recent study provided evidence that the peak neurogenesis of DA neurons occurs earlier than at E14, in fact, the majority of DA neurons in the SNpc make their final division at E12 (Gates et al., 2006). However, in this experiment, the mating session was conducted for 2 hours in the evening and the following day was designated as E0. Thus, E12 as designated in this study most likely corresponds to E12.5 if the nomenclature is adjusted according to our breeding protocol (Chapter 2.2). Clearly, laboratory practise significantly varies in the aforementioned studies. There are differences in the duration of mating sessions

(from 2 hours to overnight mating) and in the methods used to designate embryonic age (day of plugging varied from E0 to E1). Therefore, the days of embryonic neurogenesis reported in these studies as the peak of DA neuron birth in the VM might be off by 12-24 hours due to variability in the methods of reporting.

In the present study, the animals were mated for a maximum of 3 hours and the day of mating was designated as E0. Previous research in our lab shows that about 10% of TH-ir neurons in the SNpc incorporated BrdU when pregnant dams were injected with the compound at E12 while more than 16% co-labelled with BrdU at E14 (Weyrauch, 2009). This evidence suggests that the peak neurogenesis of DA neurons in the SNpc occurs after E12 and possibly closer to E14 in embryos produced by our standard breeding protocol and that E12 VM mostly contains undifferentiated DA precursor cells at the time of transplantation.

The BrdU dose of 120mg/kg injected i.p. produced reliable strong labelling of mitotic cells in grafts derived from E12 and E14 rat VMs. There were no differences in DA neuron yields or the functionality of the grafts between BrdU-treated animals and controls. These results corroborate previous findings of no toxic effects of BrdU doses >100mg/kg on foetal graft maturation and integration into the host striatum (Weyrauch, 2009, Bye et al., 2012).

Figure 5.3C shows both strong and pale BrdU-ir staining of cell nuclei in grafts in the E12 group. One possible explanation of different intensity of BrdU staining is that strongly stained cells most likely divided only once when they incorporated the compound. Paler staining, on the other hand, might be indicative of the second and third generation descendants of the originally marked precursors. BrdU signal intensity is reduced with each cell division and disappears after 4 days of continued cell proliferation (Dayer et al., 2003). Also, it could be that glial BrdU nucleic staining is stronger than neuronal nucleic staining due to a higher density of chromatin in the nuclei of glial cells. Both haematoxylin and Nissl stains mark glial cells with a higher intensity than neurons. Similarly in fluorescent IHC, BrdU signal in the majority of BrdU-ir/TH-ir neurons was weaker than in the surrounding single labelled BrdU-ir cells. Furthermore, depending on the stage of the S-phase at the time of BrdU injection, the staining in the cell nucleus was either diffused or punctate. Punctate staining represents the end of the S-phase when chromatin replication occurs (Cameron and McKay, 2001).

Labelling mitotic cells with BrdU has a number of limitations. Cameron and McKay (2001) have shown that only a high dose of BrdU (300 mg/kg) reliably labels all

cells in the S-phase in the adult rat dentate gyrus while lower doses label only a fraction of cells. Also, high doses of BrdU have been suggested for long-term labelling of dividing cells in adult animals (Dayer et al., 2003, McDonald and Wojtowicz, 2005, Wojtowicz and Kee, 2006). However, doses as low as 50mg/kg have been demonstrated to be toxic for embryos and cause developmental abnormalities when administered into pregnant dams (Kolb et al., 1999). Hence, high doses of BrdU while harmless to neurogenesis in the adult dendate gyrus might be toxic to the embryonic neurons in the grafts. Additionally, BrdU is quickly metabolised to half its concentration within an hour after administration which highlights the desirability of using a higher dose (Kriss and Revesz, 1962, Packard et al., 1973). This illustrates a classic challenge, which is a compromise between BrdU signal strength and toxicity when selecting the dose to be administered. As mentioned in Chapter 5.1, the S-phase equates to one third or half of the 12-14 hour cell cycle of progenitor cells (Hayes and Nowakowski, 2000, Hayes and Nowakowski, 2002). Hence, up to 4 injections of BrdU might be required in order to label all dividing cells within a 24 hour period. Thus, results presented here likely account for only a fraction of the cell populations in the grafts that were born within the 4-10 hour period after transplantation.

There was a high level of cell proliferation as early as 3-4 hours after transplantation in grafts derived from E12 VM and a great number of cell precursors subsequently differentiated into mature cells in the grafts as revealed by a high yield of BrdU-ir cells (Figure 5.4A). These results are comparable to the numbers of BrdU-ir cells found in E12 VM grafts when animals received BrdU injections either 1 or 2 days post-transplantation (Weyrauch, 2009). This provides evidence that E12 VM contains a large population of precursor cells that continue to proliferate in the host over a course of a few days post-grafting. As seen in Chapter 4, grafts derived from E12 and E14 VMs yield similar numbers of neurons despite the fact that E12 VM contains 5-fold fewer cells at the time of transplantation than E14 VM. Thus, post-grafting proliferation of precursor cells in the E12 group, at least in part, might account for that. The number of BrdU-ir cells in grafts derived from E14 VM was 2.6-fold lower than previously reported for E14 grafts at the same time point of BrdU injection post-transplantation (Sinclair et al., 1999). However, Sinclair *et al.* injected BrdU into the lateral ventricle adjacent to the grafted striatum while the compound was injected i.p. in the current study. Intracerebral delivery might give BrdU a better access to the grafted cells and explain a higher yield of BrdU-ir neurons in the grafts.

Grafts in both donor age groups were found to be functional as indicated by drug-induced rotations (Figure 5.1) and a correspondingly high yield of DA neurons (Figure 5.2B). Grafts in the E12 group yielded more DA neurons than grafts in the E14 group, this replicates previous findings (Chapters 3 and 4; Torres et al., 2007). More DA precursor cells were proliferating at the time of BrdU injection 4 hours after transplantation and subsequently were capable of differentiating into DA neurons in grafts in the E12 group than E14 group (Figure 5.4B). A higher percentage of TH-ir neurons that co-labelled with BrdU in grafts in the E12 group (3.2%) than E14 group (1.6%) suggests that post-grafting proliferation of DA precursor cells contribute to a higher yield of DA neurons in grafts derived from E12 VM (Figure 5.4C). These results complement previous findings in E12 grafts that revealed that a small percentage of DA neurons in mature grafts were proliferating DA precursor cells as late as 1 and 2 days after transplantation (Weyrauch, 2009). Also, a small percentage of E14 DA neurons was reported to incorporate BrdU 2 hours post-grafting while virtually no proliferating DA precursor cells were found 1 and 2 days after transplantation (Sinclair et al., 1999). Combined together, these results describe modest levels of DA neuron birth in the host over the course of a few days, in grafts derived from younger as compared to older donor tissue, congruent to normal development where SNpc DA neurogenesis occurs sometime between E12.5-E14.

The percentages of TH-ir neurons that co-labelled with BrdU in the grafts in both donor age groups were considerably lower than those found in a normally developed SNpc when pregnant dams were injected with BrdU at E12 and E14 (Sinclair et al., 1999, Gates et al., 2006, Weyrauch, 2009). Several factors have been identified to have an impact on E14 VM cell survival during cell suspension preparation (30% cell death) and within first week after surgery (Barker et al., 1995, Fawcett et al., 1995). It is possible that especially young precursor cells are vulnerable to mechanical and chemical dissociation of the tissue, hypoxia and hypoglycaemia associated with the transplantation process, however, this has not yet been addressed experimentally.

As shown in Figure 5.6, grafts derived from E12 VM yielded higher numbers of both the A9 type and A10 type DA neurons than grafts in the E14 group, a finding that corroborates our previous work (Chapters 3 and 4). In agreement with results described in Chapter 3, grafts in the E12 group were enriched with the A9 type DA neurons as compared to grafts in the E14 group. Small numbers of both A9 type and A10 type DA neurons born after transplantation were found in all grafts indicating that at least a subpopulation of mitotic DA precursor cells are committed to their fate and the graft in

combination with the host striatum provide the necessary environment for precursor cells to follow their correct developmental pathway (Figure 5.7A). Only proliferation of A9 type DA precursor cells in grafts in the E12 group contributed significantly more than others to the resulting TH-ir cell yield (Figure 5.8A). Figure 5.8B shows that mitotic population of TH-ir is enriched with A9 type DA precursor cells in grafts in the E12 group while the ratio is shifted towards the A10 type DA precursor cells in grafts in the E14 group. These results support previous research, which suggests that SNpc DA neuron birth precedes VTA DA neuron birth in the normal developing midbrain (Altman and Bayer, 1981). As shown in Figure 5.9A, the enriched yield of A9 type DA neurons in the E12 grafts is the result not only of phenotypic maturation of post-mitotic neurons but also to some extent of cell birth in the host. However, post-grafting proliferation of A10 type DA precursor cells does not contribute to a higher yield of these neurons in mature grafts derived from E12 VM as compared to grafts from older donor tissue. Previous research in a mouse model of PD demonstrated similar trends of increased levels of A9 type DA neuron cell birth in grafts derived from E10 mouse VM and, conversely, increased A10 type DA neuron birth in E12.5 grafts (Bye et al., 2012).

The yield of BrdU-ir A9 type and A10 type DA neurons in the centre of grafts was significantly lower than in the periphery of grafts in both donor age groups. As shown in Chapters 3 and 4, the numbers of DA neurons were lower in the centre than periphery of the graft in both donor age groups. Although not quantified, the distribution of BrdU-ir cells appeared to be homogeneous within the graft in both donor age groups. This suggests that either the survival of young mitotic DA precursor cells is promoted at the periphery of the grafts, or impaired in the centre of grafts, or that whilst still at an early stage of development, young DA precursors might be able to migrate to the periphery of grafts to make functional connections with the host striatum.

Conclusion

The aim of this chapter to determine levels of the A9 type and A10 type DA neuron birth in the grafts derived from E12 and E14 VMs has been achieved. Younger donor tissue contained bigger subpopulations of DA progenitors that continued to divide in the host striatum. Current evidence suggests that younger donor tissue grafts enrich with the A9 type DA neurons as compared to grafts in the E14 group due to, at least in part, a higher level of post-grafting proliferation of the A9 type DA precursor cells. Also, the majority of DA neurons born post-grafting were found in the periphery of

grafts suggesting that the proximity to the functional targets might be required for mitotic DA precursor cells to survive and differentiate into mature neurons. Although current findings sufficiently describe relative contributions of the A9 type and A10 type DA neuron birth in the grafts towards the DA neuron yields in both donor age groups, the results presented here might still account for only a fraction of actual populations of mitotic cells due to limitations of BrdU labelling. We have demonstrated here that E12 VM tissue is a better candidate for cell transplantation therapy in a rat model of PD.

Chapter 6. General Discussion

Summary

The work discussed in this thesis adds further knowledge regarding the survival of embryonic DA grafts in the rat model of PD in terms of the populations of cells involved, their distribution within the grafts and how these are affected by the donor age and the host environment in to which they are implanted.

The current data further underline the impact of the donor age on DA neuron yields in the grafts (Torres et al., 2007, Torres et al., 2008a, Bye et al., 2012), and reinforce the notion that harvesting embryonic VM tissue before the peak of DA neurogenesis yields more DA cells in the grafts and, more importantly, also more A9 type DA neurons, which are an important determinant for functional recovery (Chapters 3, 4, and 5).

A9 type DA neurons were found to be influenced both by the environment within the graft and by the host environment in the transplantation site to a higher extent than the A10 type DA neurons (Chapters 3 and 4). The present results suggest that differentiation of DA neural precursor cells rather than their survival might be affected by the afferent DA innervation of the transplantation site (Chapter 4).

DA neural progenitors cells procured from rat embryos at E12 were shown to have a greater potential to proliferate post-graft and differentiate into mature DA neurons as compared to embryos at E14 (Chapter 5). In vivo proliferation of younger precursor cells significantly contributed to the higher yields of the A9 type DA neurons in the grafts. With this improved yield of the A9 type DA neurons fewer human donors might suffice to produce functional grafts in PD patients.

Improvement of the functional efficacy of the cell replacement therapy for PD is still a major challenge that needs to be overcome before this treatment can be brought into the clinic. The aim of this PhD thesis was to identify some of the critical factors that influence the functionally important A9 type DA neuron component in VM grafts in the 6-OHDA lesion rat model. VM grafts derived from E12 rat embryos have previously been shown to significantly improve DA neuron yield but not to improve behavioural recovery of lesion-induced deficits over and above that achieved using standard E14 VM tissue. The first part of this thesis was intended to measure the impact of the donor age on the A9 type and A10 type DA neuron subpopulations in intrastriatal VM grafts (Chapter 3). The present results show that there is enrichment for the A9 type DA neurons in grafts derived from younger embryonic VM tissue, and that this might be the result of target-specific cues in the striatum which favour the survival of this DA neuron subpopulation and/or enhance differentiation of the SNpc phenotype in implanted DA neural precursor cells. The second study was designed to address the question of the commitment of DA neural precursor cells to the SNpc and VTA fate and to investigate whether distinct DA and NA innervation of the transplantation site influenced the DA neuronal composition of the grafts (Chapter 4). The last part of this thesis aimed to determine whether the enrichment of DA neurons of the SNpc phenotype observed in younger tissue grafts is due to increased proliferation or improved survival of the A9 type DA neural progenitor cells post-transplantation (Chapter 5). An unexpected pattern emerged from all three studies suggesting that the E12 graft enrichment for the A9 type DA neurons might be influenced by the amount of VM tissue implanted.

6.1 Benefits of using younger donor tissue for transplantation

The work presented here and previous studies in the literature (Torres et al., 2007, Torres et al., 2008a) indicate that VM tissue derived from rat embryos at E12 significantly improves DA neuron yield in the grafts compared to tissue obtained at E14. It may be that immature E12 DA neural precursor cells survive the transplantation procedure better than newly born (post-mitotic) DA neurons because they lack extensive neurites (Gates et al., 2004), however, the exact reasons still remain unknown. Factors influencing the survival of mesencephalic DA neurons, such as tissue dissociation, cool storage, in vitro culture prior to transplantation, have been studied in detail in the past, however none of these studies included VM tissue derived as early as

E12 (Bjorklund et al., 1980b, Brundin et al., 1985a, Brundin et al., 1985b, Nikkhah et al., 1995). A growing body of evidence indicates that undifferentiated DA neural precursor cells rely on intrinsic signals present within the transplanted VM to follow the correct developmental pathway. The peak contribution of Shh-expressing cells in the VM floor plate to DA neurons was shown to occur at E10.5 in mice (considered to be equivalent to E12 in rats), a time point of most extensive labelling of Shh-expressing cells in the Lmx1a-positive putative DA precursor domain (Blaess et al., 2011), suggesting that the signalling activity within the developing VM that directs DA neuron specification might be at its highest at this time point. Previous studies, which used rat E12 VM tissue, have shown that the presence of Shh and a transforming growth factor TGF-β were required for DA neuron differentiation *in vitro* (Farkas et al., 2003) and that adenoviral-vector-delivered Shh improved (3-fold) the yield of DA neurons in grafts (Torres et al., 2005). Another study demonstrated that purifying mouse DA neural precursor cells at E10.5 and transplanting them into the DA-depleted striatum results in poor graft survival and low DA neuron yields (Jonsson et al., 2009). This indicates that other neural progenitor cells and glia present in the VM floor plate might be crucial for final differentiation of DA neurons and, although the cytoarchitecture of the VM is lost during cell suspension preparation, these cells are still capable of inducing DA fate in neural precursor cells in the graft.

DA neuron subtypes in the grafts, particularly the nigral A9 type, have been the focus of DA cell transplantation research for the last few years. Current work demonstrates, for the first time, that grafts derived from rat E12 VM tissue improve yields of both the A9 type (Girk2-ir) and A10 type (calbindin-ir) DA neurons. Previous studies have demonstrated that VM donor tissue generated larger grafts, presumably due to increased survival (Freeman et al., 1995b, Sinclair et al., 1999, Hahn et al., 2009). However, recent studies have demonstrated that transplanted E12 VM tissue contains a mixture of both differentiated DA neurons, that have already undergone their final mitosis, and DA neural progenitor cells that continue to proliferate in the host and mature into DA neurons after transplantation (Weyrauch, 2009). Grafts derived from E10 mice donor tissue (equivalent to E11.5 in rats) have been shown to be enriched with mitotic DA neuroblasts, which contribute to a higher yield of the A9 type DA neurons in the grafts (Bye et al., 2012). Similarly, the work carried out in Chapter 5 demonstrated that a substantial increase in E12 VM-derived mitotic cells soon after transplantation significantly contributes to larger grafts, and that improved enrichment for the DA neurons of the SNpc phenotype in grafts derived from younger rat embryos

results in part due to a higher level of the A9 type DA neuron birth post-transplantation. Also, when VMs are dissociated into a single cell suspension and the equivalent of one VM is transplanted into the striatum (Chapters 3 and 5), a higher enrichment for the functionally important A9 type DA neurons is observed in grafts derived from E12 embryos than E14 embryos (note that, no such difference was observed when the equivalent of ½ VM was transplanted into the striatum as described in Chapter 4). Smaller populations of transplanted cells might be unable to provide sufficient levels of developmental signalling *in vivo* to direct DA neural precursor cells towards the correct pathway. At this stage, it is not clear whether this drop in the enrichment of the grafts for the A9 type DA neurons can be attributed to different experimental conditions and future studies where even smaller proportions of the VM, e.g. ⅓ and ¼, are transplanted into the striatum are required to address this question.

Similar findings have been reported for grafts derived from mouse VM, where younger donor tissue improved enrichment of grafts for DA neurons belonging to the SNpc phenotype (Bye et al., 2012). The same study also reported that grafts derived from E12 mouse VM (considered to be equivalent to E13.5 in rats) contained a higher proportion of the A10 type DA neurons than grafts from the E10 group. However, increased proportions of DA neurons belonging to the VTA phenotype in grafts in the E14 group were not observed in any of the studies described here. This is most likely due to a combined effect of the 0.5 day difference between time points when embryos were harvested, and between-species differences in embryonic developmental stages (such that ages E12 in mice and E13.5 in rats are not truly identical) and not due to Girk2 and calbindin antibodies being unreliable markers of two DA neuron phenotypes in rats, as they were reported to label separate DA neuron populations in the SNpc and the VTA in mice and rats in an identical manner (Thompson et al., 2005). However, recent studies have suggested that high levels of Girk2 protein can be detected also in DA neurons located in the dorsal tier of the SNpc and in a proportion of DA neurons in the VTA in mice and humans (Reyes et al., 2012). Nevertheless, coexpression of calbindin in TH-ir neurons was found to be more restricted to the VTA regions and these two proteins were rarely found to be expressed together in DA neurons. Therefore, Girk2 and calbindin are still considered to be largely confined to two different populations of DA neurons.

E12 and E14 VM tissue, especially E12, contains a mix of fully developed DA neurons and undifferentiated DA neural precursor cells (Gates et al., 2006) that use both intrinsic cues present within the transplanted graft and target-specific cues in host

environment to direct their differentiation towards the correct DA phenotype as demonstrated in Chapter 4. In both donor age groups, fate specification of the A9 type DA neurons was more influenced by the host environment than that of the A10 type neurons, despite the fact that previous studies have shown that, in normal development, DA neurons in the SNpc complete differentiation process before DA neurons in the VTA (Bye et al., 2012). A10 type DA neural precursor cells and neurons derived from either E12 or E14 VM tissue remained committed to the VTA phenotype even when transplanted into the hippocampus, a site rich in NA innervation. A9 type DA neural precursors, on the other hand, were less likely to follow the correct developmental pathway in the absence of functional connections as evidenced by a greater proportion of TH-ir neurons that were negative for Girk2. When grafted into the striatum, A9 type DA neurons had a direct access to functional targets; however, while the target striatum remained in close proximity to neurons transplanted into the adjacent N.Acc, the access to functional targets was greatly reduced for grafts in the PFC and unavailable for transplants in the hippocampus. Also, the striatum is not only the correct target area but it is lesioned, and while the N.Acc and the PFC are also partially depleted of DA, the hippocampus is not. Although previous studies have suggested that DA grafts survive equally well both in the intact and lesioned striatal environment (Schmidt et al., 1981, Dunnett et al., 1988), afferent connections to the grafts in adult recipients are reportedly poor unless the host systems are deprived of their normal synaptic targets. This suggest that, the level of DA depletion in either A9 (striatum) or A10 (N.Acc) input nuclei in the basal ganglia might influence the preferential yield of DA neuron phenotypes in the grafts, an issue which has not yet been investigated experimentally. These findings have important implications for cell therapies first because they further highlight how crucial it is to choose the correct transplantation target to achieve optimal cell populations in the graft, and second because they demonstrate that developing neurons in the transplant use cues in the surrounding environment to complete differentiation. Indeed, during normal nervous system development, target tissues secrete trophic factors that attract axonal growth and support survival of neurons innervating the target (Hendry, 1975, Landmesser, 1978). Several studies have investigated this neuron-target interaction in the past and have demonstrated that when transplanted in the vicinity of the DA-depleted striatum, e.g. into the adjacent cortex or ventricle, grafts derived from human foetal VM tissue exhibited a target specific TH-ir fibre outgrowth (Stromberg et al., 1992). Another study has shown that DA neurons transplanted into the parietal cortex, which normally receives no DA innervation, survived in abundance but exhibited very

sparse axonal growth to the immediate vicinity to the transplantation site (Schmidt et al., 1981). Similarly, present findings demonstrate that, when compared to grafts in to the striatum, in grafts in to the hippocampus, in the absence of rich midbrain-derived innervation, a great proportion of DA neurons were negative for either Girk2 or calbindin, indicating that, in the absence of functional connections, they may have silenced their A9 and A10 phenotypes (Chapter 4). Moreover, neuron responsiveness to guidance cues was shown to decrease with donor age (Van den Heuvel and Pasterkamp, 2008), a finding corroborated in the present study: a change from the A9 type to the A10 type afferent innervation to the transplantation site resulted in a significant decrease in the proportion of the A9 type DA neurons between grafts in the striatum and N.Acc in the E12 group but not E14 group. Thus, VM tissue derived from younger donor age embryos contains proliferating DA neural precursor cells that are able to use environmental cues in the striatum to differentiate into the A9 type DA neurons and produces larger grafts that might improve DA cell therapy for PD.

A lot of research has been directed towards purification of A9 type DA neurons for transplantation purposes, since this component of the grafts is an important determinant for behavioural recovery (Mendez et al., 2005, Thompson et al., 2005, Grealish et al., 2010). Such studies have shown that reinnervation of the DA-depleted striatum is derived almost exclusively from the A9 type DA neurons in the grafts and that almost a complete elimination of the nigral DA neuron population from the graft with sparing of the A10 type DA neuron component results in partial behavioural recovery of lesion-induced deficits (Grealish et al., 2010). However, purification of the A9 type DA neuron population has proven to be a challenging task. It is possible to isolate the floor plate domain that gives rise to both subtypes of midbrain DA neurons based on the expression or lack of expression of Ngn2 depending on the developmental stage and produce small grafts that still induce behavioural recovery but these grafts still contain a mixed population of the A9 and A10 type DA neurons (Thompson et al., 2006, Jonsson et al., 2009). The absence of Corin expression at E10.5 in mice was used to isolate the A9 type DA neural progenitors but *in vivo* survival of these grafts was poor and only a trend towards behavioural recovery was observed (Jonsson et al., 2009). Isolated A9 type neural progenitor cells failed to differentiate *in vivo* in the absence of other cell types normally present in the developing VM suggesting that isolated cell populations should be expanded prior to implantation to boost the A9 type DA neuron yield in the grafts. During normal development, DA neurons rely on both intrinsic and external signals for fate induction, final differentiation, as well as axonal outgrowth, and

since unsorted VM tissue produces good grafts that achieve functional recovery, cell sorting of primary tissue grafts might not be required for practical applications.

6.2 Implications for foetal cell transplantation therapy

Two studies have reported different results regarding improved behavioural recovery offered by younger donor grafts. The first study demonstrated that despite producing higher yields of DA neurons, grafts derived from E12 rat VM tissue did not confer behavioural recovery of beyond the levels that can be achieved by standard E14 VM-derived transplants (Torres et al., 2008a). Another study has reported that younger donor tissue grafts promoted restoration of function in apomorphine-induced rotation test and stepping test (Hahn et al., 2009). However, due to different transplantation conditions, the yield of DA neurons in grafts in the second study was much lower (E12: 1500; E14: 846 DA neurons) than in the study conducted by Torres and colleagues (E12: 26,000; E14: 4,500 DA neurons) suggesting that differences in behavioural recovery seen were not truly representative of the impact of the donor age, but rather due to low numbers of DA neurons in the grafts. The experiments described in this thesis suggest that the enrichment of E12 VM-derived intrastriatal grafts for the A9 type DA neurons is influenced by the transplantation conditions. However, in all three of the present studies, a significantly higher yield of DA neurons of the SNpc phenotype was observed in intrastriatal grafts derived from younger donor tissue. Also, all grafts were enriched for the A9 type DA neurons, with the yield of these neurons being at least 2-fold higher than the yield of the A10 type DA neurons regardless of the donor age group. Thus, despite facilitating higher total numbers of DA neurons (Torres et al., 2008a) and functionally important A9 type DA neurons (Chapters 3, 4, and 5) grafts derived from younger VM tissue fail to enhance amelioration of lesion-induced deficits. This suggests that, even when using the most clinically relevant multiple placements of intrastriatal grafts, there is a limit to the behavioural recovery that can be achieved by tonic DA supply and reinnervation of the striatum provided by the transplant. Recovery of finer motor skills will most likely require a more global restoration of the basal ganglia circuitry. Indeed, simultaneous grafts in the striatum, SNpc and the STN restored forelimb function significantly better than grafts in the striatum alone (Mukhida et al., 2001, Mukhida et al., 2008). More global amelioration of symptoms induced by the loss of DA neurotransmission in the nigrostriatal pathway may require restoration of DA supply to the striatum plus either restoration of dopaminergic control in the SNpc

and the STN (Mukhida et al., 2001) or inhibition of the pathological overactivity in the SNpc and the STN (Mukhida et al., 2008).

The other limiting factor to clinical application of the transplantation cell therapy for PD is major cell loss post-grafting, such that 90-95% of the DA cells implanted are lost post-implantation. As a result, 6 to 8 donor embryos per unilateral transplant are required. As younger donor tissue grafts in both rats and mice produce significantly higher DA neuron yields with the main component of DA neuron population being of the SNpc phenotype, it ought to be possible to achieve a similar improvement of the human foetal transplantation therapy by similar use of younger DA neural precursor cells. If the correct human embryonic age could be identified, then clinical improvement in PD patients might be effected with fewer donor embryos. Based on the Carnegie staging scale and ontogeny studies of the VM (Nelander et al., 2009) the human equivalent of rat donor age should occur somewhere around 5 weeks post-conception, before there is appreciable TH expression in the VM, similar to what is seen in rat E12 and mouse E10.5 VM. Previous clinical trials have all used older donor embryos, aged 6 – 9 weeks post-conception equivalent to E14-15 rat embryos. Recent *in vitro* studies of DA neuron yields in VM cultures derived from medical terminations of pregnancies (MTOP), a method that is increasingly replacing surgical terminations of pregnancies in the UK, demonstrated that donor embryos that produced the highest numbers of DA neurons had CRLs of 18 – 27 mm, corresponding to the age of approximately 7 – 8 weeks post-conception (Weyrauch, 2009). However, the range of donor ages investigated in this study did not include ages younger than 6 weeks. Even if the 'ideal' donor age could be identified, the very limited human foetal tissue supply would simply increase the logistic challenges involved in sourcing tissue for human use. Thus whilst it is academically interesting to determine at which stage human foetal DA neural precursor cells might be more efficient in producing better grafts than newly differentiated DA neurons, if this donor age is younger or borderline with those currently supplied by the clinic, from 6 to 12 weeks post-conception (Kelly et al., 2011), procurement may prove impractical for clinical applications. Nevertheless, if implanting VM tissue obtained before the peak of DA neurogenesis could yield sufficiently high DA neuron numbers and greater yields of A9 type DA neurons, then a single embryo might suffice to transplant one patient unilaterally, and despite the logistic challenges this could be an important advance.

6.3 Implications beyond foetal transplantation

The current findings also have implications beyond foetal transplantation. Numerous efforts have been made to generate large pools of VM DA neurons for cell transplantation therapy including the expansion of foetal tissue (Parish et al., 2008, Ribeiro et al., 2013) and the generation VM DA neurons from PSCs (Bjorklund et al., 2002, Kriks et al., 2011). While this has been successfully achieved in a number of instances *in vitro*, poor graft survival and a lack of functional input of these therapies are generally observed *in vivo*. In agreement with recent studies conducted in mice (Bye et al., 2012), the present findings demonstrate that higher yields of functionally important A9 type DA neurons are produced by intrastriatal grafts derived from younger VM tissue, which contains proliferating DA neural precursor cells in the floor plate. This suggests that a combination of VM-derived developmental signals and striatum-derived target specific cues is sufficient to guide mitotic DA progenitors down their correct phenotype. Also, the yield of A9 type DA neurons falls by two thirds following implantation into the hippocampus, indicating that VM-like environment in the graft is able to support the A9 phenotype in a great number of DA neurons even in the absence of normally present innervation targets. The generally low DA neuron yields observed in expanded foetal tissue-derived grafts or in PSCs-derived grafts might be due to incomplete specification of these cells as a result of *in vitro* isolation from the normal embryonic environment prior to transplantation. Indeed, induction of the floor plate phenotype in hESCs prior to their differentiation into Nurr1-expressing DA neurons effectively produces engraftable TH-ir/FoxA2-ir neurons that mature into the A9 type and A10 type DA neurons in the host (Kriks et al., 2011). Identification of the region in the developing midbrain that gives rise exclusively to the A9 type neurons is of particular interest so that this region can be expanded *in vitro* prior to transplantation. Although, some progress has been made in this area, expansion of isolated VM DA progenitors and subsequent grafting have not yet been tested (Jonsson et al., 2009). If applicable in an ESC setting, these sorting tools can be used to generate well-characterised stem cell-derived VM DA neural progenitors free of potentially tumorigenic cell types for transplantation therapy for PD.

6.4 Conclusion

The work presented in this thesis has demonstrated further the importance of deriving rat foetal VM tissue at a younger donor age (E12), which generates increased

yields of A9 type DA neurons when transplanted into the right functional target. However, it is still not clear whether there is an equivalent human embryonic donor age that could be used to reproduce the present findings, and improve the DA neuron survival and functional outcome of cell transplantation in PD patients. ESC-derived grafts, on the other hand, might need to be utilised at an earlier developmental stage to improve the therapy and bring it closer to the clinic. Global functional outcome is dependent on more than just restoration of DA supply to the putamen and caudate nucleus and additional grafts into the STN should be considered for the restoration of the sensorimotor function in patients. PD is a complex heterogeneous progressive disorder and no currently available or 'in-development' treatments are able to either cure it or single-handedly address all the symptoms. There may be no universal solution to the treatment of PD.

List of References

AARSLAND, D., BRONNICK, K., EHRT, U., DE DEYN, P. P., TEKIN, S., EMRE, M. & CUMMINGS, J. L. 2007. Neuropsychiatric symptoms in patients with Parkinson's disease and dementia: frequency, profile and associated care giver stress. *Journal of Neurology Neurosurgery and Psychiatry,* 78**,** 36-42.

ABERCROMBIE, M. 1946. Estimation of nuclear population from microtome sections. *Anatomical Record,* 94**,** 239-247.

AGRAWAL, A. K., CHATURVEDI, R. K., SHUKLA, S., SETH, K., CHAUHAN, S., AHMAD, A. & SETH, P. K. 2004. Restorative potential of dopaminergic grafts in presence of antioxidants in rat model of Parkinson's disease. *Journal of Chemical Neuroanatomy,* 28**,** 253-264.

AHLSKOG, J. E. & MUENTER, M. D. 2001. Frequency of levodopa-related dyskinesias and motor fluctuations as estimated from the cumulative literature. *Movement Disorders,* 16**,** 448-458.

AKAO, Y., MARUYAMA, W., YI, H., SHAMOTO-NAGAI, M., YOUDIM, M. B. H. & NAOI, M. 2002. An anti-Parkinson's disease drug, N-propargyl-1(R)-aminoindan (rasagiline), enhances expression of anti-apoptotic Bcl-2 in human dopaminergic SH-SY5Y cells. *Neuroscience Letters,* 326**,** 105-108.

ALAM, M., MAYERHOFER, A. & SCHMIDT, W. J. 2004. The neurobehavioral changes induced by bilateral rotenone lesion in medial forebrain bundle of rats are reversed by L-DOPA. *Behavioural Brain Research,* 151**,** 117-124.

ALBIN, R. L., YOUNG, A. B. & PENNEY, J. B. 1989. The functional anatomy of basal ganglia disorders. *Trends in Neurosciences,* 12**,** 366-375.

ALMQVIST, P. M., AKESSON, E., WAHLBERG, L. U., PSCHERA, H., SEIGER, A. & SUNDSTROM, E. 1996. First trimester development of the human nigrostriatal dopamine system. *Experimental Neurology,* 139**,** 227-237.

ALTMAN, J. & BAYER, S. A. 1981. Development of the brain-stem in the rat .5. Thymidine-radiographic study of the time of origin of neurons in the midbrain tegmentum. *Journal of Comparative Neurology,* 198**,** 677-716.

ANDERSON, L. & CALDWELL, M. A. 2007. Human neural progenitor cell transplants into the subthalamic nucleus lead to functional recovery in a rat model of Parkinson's disease. *Neurobiology of Disease,* 27**,** 133-140.

ANDERSSON, E., TRYGGVASON, U., DENG, Q. L., FRILING, S., ALEKSEENKO, Z., ROBERT, B., PERLMANN, T. & ERICSON, J. 2006. Identification of intrinsic determinants of midbrain dopamine neurons. *Cell,* 124**,** 393-405.

ANNETT, L. E., TORRES, E. M., CLARKE, D. J., ISHIDA, Y., BARKER, R. A., RIDLEY, R. M., BAKER, H. F. & DUNNETT, S. B. 1997. Survival of nigral grafts within the striatum of marmosets with 6-OHDA lesions depends critically on donor embryo age. *Cell Transplant,* 6**,** 557-69.

ANTONINI, A., ISAIAS, I. U., CANESI, M., ZIBETTI, M., MANCINI, F., MANFREDI, L., DAL FANTE, M., LOPIANO, L. & PEZZOLI, G. 2007. Duodenal levodopa infusion for advanced Parkinson's disease: 12-month treatment outcome. *Movement Disorders,* 22**,** 1145-1149.

ARIMA, K., UEDA, K., SUNOHARA, N., ARAKAWA, K., HIRAI, S., NAKAMURA, M., TONOZUKA-UEHARA, H. & KAWAI, M. 1998. NACP/alpha-synuclein immunoreactivity in fibrillary components of neuronal and oligodendroglial cytoplasmic inclusions in the pontine nuclei in multiple system atrophy. *Acta Neuropathologica,* 96**,** 439-444.

BABA, M., NAKAJO, S., TU, P. H., TOMITA, T., NAKAYA, K., LEE, V. M. Y., TROJANOWSKI, J. Q. & IWATSUBO, T. 1998. Aggregation of alpha-synuclein in Lewy bodies of sporadic Parkinson's disease and dementia with lewy bodies. *American Journal of Pathology,* 152**,** 879-884.

BACK, S., PERANEN, J., GALLI, E., PULKKILA, P., LONKA-NEVALAITA, L., TAMMINEN, T., VOUTILAINEN, M. H., RAASMAJA, A., SAARMA, M., MANNISTO, P. T. & TUOMINEN, R. K. 2013. Gene therapy with AAV2-CDNF provides functional benefits in a rat model of Parkinson's disease. *Brain and behavior,* 3**,** 75-88.

BACKLUND, E. O., GRANBERG, P. O., HAMBERGER, B., KNUTSSON, E., MARTENSSON, A., SEDVALL, G., SEIGER, A. & OLSON, L. 1985. Transplantation of adrenal-medullary tissue to striatum in parkinsonism - 1st clinical-trials. *Journal of Neurosurgery,* 62**,** 169-173.

BAGHERI, H., DAMASE-MICHEL, C., LAPEYRE-MESTRE, M., CISMONDO, S., O'CONNELL, D., SENARD, J. M., RASCOL, O. & MONTASTRUC, J. L. 1999. A study of salivary secretion in Parkinson's disease. *Clinical Neuropharmacology,* 22**,** 213-215.

BAI, C. B., AUERBACH, W., LEE, J. S., STEPHEN, D. & JOYNER, A. L. 2002. Gli2, but not Gli1, is required for initial Shh signaling and ectopic activation of the Shh pathway. *Development,* 129**,** 4753-4761.

BAKER, K. A., SADI, D., HONG, M. & MENDEZ, I. 2000. Simultaneous intrastriatal and intranigral dopaminergic grafts in the Parkinsonian rat model: Role of the intranigral graft. *Journal of Comparative Neurology,* 426**,** 106-116.

BARKER, R. A., DUNNETT, S. B., FAISSNER, A. & FAWCETT, J. W. 1996. The time course of loss of dopaminergic neurons and the gliotic reaction surrounding grafts of embryonic mesencephalon to the striatum. *Experimental Neurology,* 141**,** 79-93.

BARKER, R. A., FRICKER, R. A., ABROUS, D. N., FAWCETT, J. & DUNNETT, S. B. 1995. A comparative-study of preparation techniques for improving the viability of nigral grafts using vital stains, in-vitro cultures, and in-vivo grafts. *Cell Transplantation,* 4**,** 173-200.

BAYER, S. A., WILLS, K. V., TRIARHOU, L. C. & GHETTI, B. 1995. Time of neuron origin and gradients of neurogenesis in midbrain dopaminergic-neurons in the mouse. *Experimental Brain Research,* 105**,** 191-199.

BENABID, A. L., BENAZZOUZ, A., GAO, D. M., HOFFMANN, D., LIMOUSIN, P., KOUDSIE, A., KRACK, P. & POLLAK, P. 1999. Chronic electrical stimulation of the ventralis intermedius nucleus of the thalamus and of other nuclei as a treatment for Parkinson's disease. *Techniques in Neurosurgery,* 5**,** 5-30.

BENABID, A. L., POLLAK, P., LOUVEAU, A., HENRY, S. & DEROUGEMONT, J. 1987. Combined (thalamotomy and stimulation) stereotactic surgery of the VIM thalamic nucleus for bilateral Parkinson disease. *Applied Neurophysiology,* 50**,** 344-346.

BENNETT, D. A., BECKETT, L. A., MURRAY, A. M., SHANNON, K. M., GOETZ, C. G., PILGRIM, D. M. & EVANS, D. A. 1996. Prevalence of Parkinsonian signs and associated mortality in a community population of older people. *New England Journal of Medicine,* 334**,** 71-76.

BERARDELLI, A., ROTHWELL, J. C., THOMPSON, P. D. & HALLET, M. 2001. Pathophysiology of bradykinesia in Parkinson's disease. *Brain,* 124**,** 2131-2146.

BERGMAN, H., WICHMANN, T. & DELONG, M. R. 1990. Reversal of experimental parkinsonism by lesions of the subthalamic nucleus. *Science,* 249**,** 1436-1438.

BETARBET, R., SHERER, T. B., DI MONTE, D. A. & GREENAMYRE, J. T. 2002. Mechanistic approaches to Parkinson's disease pathogenesis. *Brain Pathology,* 12**,** 499-510.

BETARBET, R., SHERER, T. B., MACKENZIE, G., GARCIA-OSUNA, M., PANOV, A. V. & GREENAMYRE, J. T. 2000. Chronic systemic pesticide exposure reproduces features of Parkinson's disease. *Nature Neuroscience,* 3**,** 1301-1306.

BETARBET, R., TURNER, R., CHOCKKAN, V., DELONG, M. R., ALLERS, K. A., WALTERS, J., LEVEY, A. I. & GREENAMYRE, J. T. 1997. Dopaminergic neurons intrinsic to the primate striatum. *Journal of Neuroscience,* 17**,** 6761-6768.

BEZARD, E., IMBERT, C., DELOIRE, X., BIOULAC, B. & GROSS, C. E. 1997. A chronic MPTP model reproducing the slow evolution of Parkinson's disease: evolution of motor symptoms in the monkey. *Brain Research,* 766**,** 107-112.

BEZARD, E., IMBERT, C. & GROSS, C. E. 1998. Experimental models of Parkinson's disease: From the static to the dynamic. *Reviews in the Neurosciences,* 9**,** 71-90.

BIRKMAYER, W. & HORNYKIEWICZ, O. 1961. The L-3,4-dioxyphenylalanine (DOPA)-effect in Parkinson-akinesia. *Wiener klinische Wochenschrift,* 73**,** 787-8.

BJORKLUND, A., DUNNETT, S. B., STENEVI, U., LEWIS, M. E. & IVERSEN, S. D. 1980a. Re-innervation of the denervated striatum by substantia nigra transplants - functional consequences as revealed by pharmacological and sensorimotor testing. *Brain Research,* 199**,** 307-333.

BJORKLUND, A., NILSSON, O. G. & KALEN, P. 1990. Reafferentation of the subcortically denervated hippocampus as a model for transplant-induced functional recovery in the CNS. *Progress in Brain Research,* 83.

BJORKLUND, A., SCHMIDT, R. H. & STENEVI, U. 1980b. Functional re-innervation of the neostriatum in the adult-rat by use of intraparenchymal grafting of dissociated cell-suspensions from the substantia nigra. *Cell and Tissue Research,* 212**,** 39-45.

BJORKLUND, A. & STENEVI, U. 1979. Reconstruction of the nigrostriatal dopamine pathway by intra-cerebral nigral transplants. *Brain Research,* 177**,** 555-560.

BJORKLUND, A. & STENEVI, U. 1981. Invivo evidence for a hippocampal adrenergic neuronotrophic factor specifically released on septal deafferentation. *Brain Research,* 229.

BJORKLUND, A., STENEVI, U., SCHMIDT, R. H., DUNNETT, S. B. & GAGE, F. H. 1983a. Intracerebral grafting of neuronal cell suspensions. I. Introduction and general methods of preparation. *Acta physiologica Scandinavica. Supplementum,* 522**,** 1-7.

BJORKLUND, A., STENEVI, U., SCHMIDT, R. H., DUNNETT, S. B. & GAGE, F. H. 1983b. Intracerebral grafting of neuronal cell suspensions. II. Survival and growth of nigral cell suspensions implanted in different brain sites. *Acta physiologica Scandinavica. Supplementum,* 522**,** 9-18.

BJORKLUND, A., STENEVI, U. & SVENDGAARD, N. A. 1976. Growth of transplanted monoaminergic neurons into adult hippocampus along perforant path. *Nature,* 262.

BJORKLUND, L. M., SANCHEZ-PERNAUTE, R., CHUNG, S. M., ANDERSSON, T., CHEN, I. Y. C., MCNAUGHT, K. S., BROWNELL, A. L., JENKINS, B. G., WAHLESTEDT, C., KIM, K. S. & ISACSON, O. 2002. Embryonic stem cells develop into functional dopaminergic neurons after transplantation in a Parkinson rat model. *Proceedings of the National Academy of Sciences of the United States of America,* 99**,** 2344-2349.

BLAESS, S., BODEA, G. O., KABANOVA, A., CHANET, S., MUGNIERY, E., DEROUICHE, A., STEPHEN, D. & JOYNER, A. L. 2011. Temporal-spatial changes in Sonic Hedgehog expression and signaling reveal different potentials of ventral mesencephalic progenitors to populate distinct ventral midbrain nuclei. *Neural Development,* 6.

BLANDINI, F., ARMENTERO, M.-T. & MARTIGNONI, E. 2008. The 6-hydroxydopamine model: news from the past. *Parkinsonism & related disorders,* 14 Suppl 2**,** S124-9.

BLESA, J., JURI, C., COLLANTES, M., PENUELAS, I., PRIETO, E., IGLESIAS, E., MARTI-CLIMENT, J., ARBIZU, J., ZUBIETA, J. L., CRUZ RODRIGUEZ-OROZ, M., GARCIA-GARCIA, D., RICHTER, J. A., CAVADA, C. & OBESO, J. A. 2010. Progression of dopaminergic depletion in a model of MPTP-induced Parkinsonism in non-human primates. An F-18-DOPA and C-11-DTBZ PET study. *Neurobiology of Disease,* 38**,** 456-463.

BLESA, J., PHANI, S., JACKSON-LEWIS, V. & PRZEDBORSKI, S. 2012. Classic and New Animal Models of Parkinson's Disease. *Journal of Biomedicine and Biotechnology*.

BLOCH, A., PROBST, A., BISSIG, H., ADAMS, H. & TOLNAY, M. 2006. alpha-Synuclein pathology of the spinal and peripheral autonomic nervous system in neurologically unimpaired elderly subjects. *Neuropathology and Applied Neurobiology,* 32**,** 284-295.

BOER, G. J. 1994. Ethical guidelines for the use of human embryonic or fetal tissue for experimental and clinical neurotransplantation and research. *Journal of Neurology,* 242**,** 1-13.

BONIFATI, V., RIZZU, P., VAN BAREN, M. J., SCHAAP, O., BREEDVELD, G. J., KRIEGER, E., DEKKER, M. C. J., SQUITIERI, F., IBANEZ, P., JOOSSE, M., VAN DONGEN, J. W., VANACORE, N., VAN SWIETEN, J. C., BRICE, A., MECO, G., VAN DUIJN, C. M., OOSTRA, B. A. & HEUTINK, P. 2003. Mutations in the DJ-1 gene associated with autosomal recessive early-onset parkinsonism. *Science,* 299**,** 256-259.

BONILLA, S., HALL, A. C., PINTO, L., ATTARDO, A., GOTZ, M., HUTTNER, W. B. & ARENAS, E. 2008. Identification of midbrain floor plate radial glia-like cells as dopaminergic progenitors. *Glia,* 56**,** 809-820.

BONUCCELLI, U., DEL DOTTO, P. & RASCOL, O. 2009. Role of dopamine receptor agonists in the treatment of early Parkinson's disease. *Parkinsonism & related disorders,* 15 Suppl 4**,** S44-53.

BOREK, L. L., KOHN, R. & FRIEDMAN, J. H. 2007. Phenomenology of dreams in Parkinson's disease. *Movement Disorders,* 22**,** 198-202.

BOREL, J. F., FEURER, C., GUBLER, H. U. & STAHELIN, H. 1976. Biological effects of Cyclosporin-a - new antilymphocytic agent. *Agents and Actions,* 6**,** 468-475.

BOWER, J. H., MARAGANORE, D. M., MCDONNELL, S. K. & ROCCA, W. A. 1999. Incidence and distribution of parkinsonism in Olmsted County, Minnesota, 1976-1990. *Neurology,* 52**,** 1214-1220.

BRAAK, H., DEL TREDICI, K., RUB, U., DE VOS, R. A. I., STEUR, E. & BRAAK, E. 2003. Staging of brain pathology related to sporadic Parkinson's disease. *Neurobiology of Aging,* 24**,** 197-211.

BREESE, G. R. & TRAYLOR, T. D. 1971. Depletion of brain noradrenaline and dopamine by 6-hydroxydopamine. *British Journal of Pharmacology,* 42**,** 88-&.

BREYSSE, N., CARLSSON, T., WINKLER, C., BJORKLUND, A. & KIRIK, D. 2007. The functional impact of the intrastriatal dopamine neuron grafts in parkinsonian rats is reduced with advancing disease. *Journal of Neuroscience,* 27**,** 5849-5856.

BRODSKY, H., VUONG, K. D., THOMAS, M. & JANKOVIC, J. 2004. Glabellar and palmomental reflexes in parkinsonian disorders. *Neurology,* 63**,** 1096-1098.

BROOKS, A. I., CHADWICK, C. A., GELBARD, H. A., CORY-SLECHTA, D. A. & FEDEROFF, H. J. 1999. Paraquat elicited neurobehavioral syndrome caused by dopaminergic neuron loss. *Brain Research,* 823**,** 1-10.

BROTCHIE, J. M., MITCHELL, I. J., SAMBROOK, M. A. & CROSSMAN, A. R. 1991. Alleviation of parkinsonism by antagonism of excitatory amino-acid transmission in the medial segment of the globus-pallidus in rat and primate. *Movement Disorders,* 6**,** 133-138.

BRUNDIN, P., BARBIN, G., ISACSON, O., MALLAT, M., CHAMAK, B., PROCHIANTZ, A., GAGE, F. H. & BJORKLUND, A. 1985a. Survival of intracerebrally grafted rat dopamine neurons previously cultured invitro. *Neuroscience Letters,* 61**,** 79-84.

BRUNDIN, P., BARBIN, G., STRECKER, R. E., ISACSON, O., PROCHIANTZ, A. & BJORKLUND, A. 1988. Survival and function of dissociated rat dopamine neurons grafted at different developmental stages or after being cultured invitro. *Developmental Brain Research,* 39**,** 233-243.

BRUNDIN, P., ISACSON, O. & BJORKLUND, A. 1985b. Monitoring of cell viability in suspensions of embryonic CNS tissue and its use as a criterion for intracerebral graft-survival. *Brain Research,* 331**,** 251-259.

BRUNDIN, P., KARLSSON, J., EMGARD, M., SCHIERLE, G. S. K., HANSSON, O., PETERSEN, A. & CASTILHO, R. F. 2000a. Improving the survival of grafted dopaminergic neurons: A review over current approaches. *Cell Transplantation,* 9**,** 179-195.

BRUNDIN, P., POGARELL, O., HAGELL, P., PICCINI, P., WIDNER, H., SCHRAG, A., KUPSCH, A., CRABB, L., ODIN, P., GUSTAVII, B., BJORKLUND, A., BROOKS, D. J., MARSDEN, C. D., OERTEL, W. H., QUINN, N. P., REHNCRONA, S. & LINDVALL, O. 2000b. Bilateral caudate and putamen grafts of embryonic mesencephalic tissue treated with lazaroids in Parkinson's disease. *Brain,* 123**,** 1380-1390.

BURNS, R. S., CHIUEH, C. C., MARKEY, S. P., EBERT, M. H., JACOBOWITZ, D. M. & KOPIN, I. J. 1983. A primate model of parkinsonism - selective destruction of dopaminergic-neurons in the pars compacta of the substantia nigra by n-methyl-4-phenyl-1,2,3,6-tetrahydropyridine. *Proceedings of the National Academy of Sciences of the United States of America-Biological Sciences,* 80**,** 4546-4550.

BURNSTEIN, R. M., FOLTYNIE, T., HE, X. L., MENON, D. K., SVENDSEN, C. N. & CALDWELL, M. A. 2004. Differentiation and migration of long term expanded human neural progenitors in a partial lesion model of Parkinson's disease. *International Journal of Biochemistry & Cell Biology,* 36**,** 702-713.

BYE, C. R., THOMPSON, L. H. & PARISH, C. L. 2012. Birth dating of midbrain dopamine neurons identifies A9 enriched tissue for transplantation into Parkinsonian mice. *Experimental Neurology,* 236.

CALDWELL, M. A., HE, X., WILKIE, N., POLLACK, S., MARSHALL, G., WAFFORD, K. A. & SVENDSEN, C. N. 2001. Growth factors regulate the survival and fate of cells derived from human neurospheres. *Nat Biotechnol,* 19**,** 475-9.

CAMERON, H. A. & MCKAY, R. D. G. 2001. Adult neurogenesis produces a large pool of new granule cells in the dentate gyrus. *Journal of Comparative Neurology,* 435**,** 406-417.

CANNON, J. R., TAPIAS, V., NA, H. M., HONICK, A. S., DROLET, R. E. & GREENAMYRE, J. T. 2009. A highly reproducible rotenone model of Parkinson's disease. *Neurobiology of Disease,* 34**,** 279-290.

CAPARROS-LEFEBVRE, D., BLOND, S., FELTIN, M. P., POLLAK, P. & BENABID, A. L. 1999. Improvement of levodopa induced dyskinesias by thalamic deep brain stimulation is related to slight variation in electrode placement: possible involvement of the centre median and parafascicularis complex. *Journal of Neurology Neurosurgery and Psychiatry,* 67**,** 308-314.

CARLSSON, A., FALCK, B. & HILLARP, N. A. 1962. Cellular localization of brain monoamines. *Acta physiologica Scandinavica. Supplementum,* 56**,** 1-28.

CARLSSON, A., LINDQVIST, M. & MAGNUSSON, T. 1957. 3,4-dihydroxyphenylalanine and 5-hydroxytryptophan as reserpine antagonists. *Nature,* 180**,** 1200.

CARLSSON, M. & CARLSSON, A. 1989. The NMDA antagonist MK-801 causes marked locomotor stimulation in monoamine-depleted mice. *Journal of Neural Transmission,* 75**,** 221-226.

CARLSSON, T., CARTA, M., WINKLER, C., BJORKLUND, A. & KIRIK, D. 2007. Serotonin neuron transplants exacerbate L-DOPA-induced dyskinesias in a rat model of Parkinson's disease. *Journal of Neuroscience,* 27**,** 8011-8022.

CARPENTER, M. K., CUI, X., HU, Z. Y., JACKSON, J., SHERMAN, S., SEIGER, A. & WAHLBERG, L. U. 1999. In vitro expansion of a multipotent population of human neural progenitor cells. *Experimental Neurology,* 158**,** 265-278.

CARTA, M., CARLSSON, T., KIRIK, D. & BJORKLUND, A. 2007. Dopamine released from 5-HT terminals is the cause of L-DOPA-induced dyskinesia in Parkinsonian rats. *Brain,* 130**,** 1819-1833.

CASSARINO, D. S., FALL, C. P., SWERDLOW, R. H., SMITH, T. S., HALVORSEN, E. M., MILLER, S. W., PARKS, J. P., PARKER, W. D. & BENNETT, J. P. 1997. Elevated reactive oxygen species and antioxidant enzyme activities in animal and cellular models of Parkinson's disease. *Biochimica Et Biophysica Acta-Molecular Basis of Disease,* 1362**,** 77-86.

CAYUSO, J., ULLOA, F., COX, B., BRISCOE, J. & MARTI, E. 2006. The Sonic hedgehog pathway independently controls the patterning, proliferation and survival of neuroepithelial cells by regulating Gli activity. *Development,* 133**,** 517-528.

CHAMLEY, J. H. & DOWEL, J. J. 1975. Specificity of nerve-fiber attraction to autonomic effector organs in tissue-culture. *Experimental Cell Research,* 90.

CHANG, J. Y., SHI, L. H., LUO, F., ZHANG, W. M. & WOODWARD, D. J. 2007. Studies of the neural mechanisms of deep brain stimulation in rodent models of Parkinson's disease. *Neuroscience and Biobehavioral Reviews,* 31**,** 643-657.

CHARTIER-HARLIN, M.-C., DACHSEL, J. C., VILARINO-GUEELL, C., LINCOLN, S. J., LEPRETRE, F., HULIHAN, M. M., KACHERGUS, J., MILNERWOOD, A. J., TAPIA, L., SONG, M.-S., LE RHUN, E., MUTEZ, E., LARVOR, L., DUFLOT, A., VANBESIEN-MAILLIOT, C., KREISLER, A., ROSS, O. A., NISHIOKA, K., SOTO-ORTOLAZA, A. I., COBB, S. A., MELROSE, H. L., BEHROUZ, B., KEELING, B. H., BACON, J. A., HENTATI, E., WILLIAMS, L., YANAGIYA, A., SONENBERG, N., LOCKHART, P. J., ZUBAIR, A. C., UITTI, R. J., AASLY, J. O., KRYGOWSKA-WAJS, A., OPALA, G., WSZOLEK, Z. K., FRIGERIO, R., MARAGANORE, D. M., GOSAL, D., LYNCH, T., HUTCHINSON, M., BENTIVOGLIO, A. R., VALENTE, E. M., NICHOLSO, W. C., PANKRATZ, N., FOROUD, T., GIBSON, R. A., HENTATI, F., DICKSON, D. W., DESTEE,

A. & FARRER, M. J. 2011. Translation Initiator EIF4G1 Mutations in Familial Parkinson Disease. *American Journal of Human Genetics,* 89**,** 398-406.

CHATURVEDI, R. K., SHUKLA, S., SETH, K. & AGRAWAL, A. K. 2006. Nerve growth factor increases survival of dopaminergic graft, rescue nigral dopaminergic neurons and restores functional deficits in rat model of Parkinson's disease. *Neuroscience Letters,* 398**,** 44-49.

CHAUDHURI, K. R., ODIN, P., ANTONINI, A. & MARTINEZ-MARTIN, P. 2011. Parkinson's disease: The non-motor issues. *Parkinsonism & Related Disorders,* 17**,** 717-723.

CHAUDHURI, K. R. & SCHAPIRA, A. H. V. 2009. Non-motor symptoms of Parkinson's disease: dopaminergic pathophysiology and treatment. *Lancet Neurology,* 8**,** 464-474.

CHIUEH, C. C., MARKEY, S. P., BURNS, R. S., JOHANNESSEN, J. N., PERT, A. & KOPIN, I. J. 1984. Neurochemical and behavioral-effects of systemic and intranigral administration of n-methyl-4-phenyl-1,2,3,6-tetrahydropyridine in the rat. *European Journal of Pharmacology,* 100**,** 189-194.

CHO, M. S., LEE, Y.-E., KIM, J. Y., CHUNG, S., CHO, Y. H., KIM, D.-S., KANG, S.-M., LEE, H., KIM, M.-H., KIM, J.-H., LEEM, J. W., OH, S. K., CHOI, Y. M., HWANG, D.-Y., CHANG, A. W. & KIM, D.-W. 2008. Highly efficient and large-scale generation of functional dopamine neurons from human embryonic stem cells. *Proceedings of the National Academy of Sciences of the United States of America,* 105**,** 3392-3397.

CHU, Y. P., KOMPOLITI, K., COCHRAN, E. J., MUFSON, E. J. & KORDOWER, J. H. 2002. Age-related decreases in Nurr1 immunoreactivity in the human substantia nigra. *Journal of Comparative Neurology,* 450**,** 203-214.

CHUNG, C. Y., SEO, H., SONNTAG, K. C., BROOKS, A., LIN, L. & ISACSON, O. 2005. Cell type-specific gene expression of midbrain dopaminergic neurons reveals molecules involved in their vulnerability and protection. *Human Molecular Genetics,* 14**,** 1709-1725.

CLARKE, D. J., BRUNDIN, P., STRECKER, R. E., NILSSON, O. G., BJORKLUND, A. & LINDVALL, O. 1988. Human-fetal dopamine neurons grafted in a rat model of Parkinsons-disease - ultrastructural evidence for synapse formation using tyrosine-hydroxylase immunocytochemistry. *Experimental Brain Research,* 73**,** 115-126.

CLARKE, D. J., NILSSON, O. G., BRUNDIN, P. & BJORKLUND, A. 1990. Synaptic connections formed by grafts of different types of cholinergic neurons in the host hippocampus. *Experimental Neurology,* 107.

COLLIER, T. J., KANAAN, N. M. & KORDOWER, J. H. 2011. Ageing as a primary risk factor for Parkinson's disease: evidence from studies of non-human primates. *Nature Reviews Neuroscience,* 12**,** 359-366.

COLLIER, T. J. & SORTWELL, C. E. 1999. Therapeutic potential of nerve growth factors in Parkinson's disease. *Drugs & Aging,* 14**,** 261-287.

COLLIER, T. J., SORTWELL, C. E., ELSWORTH, J. D., TAYLOR, J. R., ROTH, R. H., SLADEK, J. R., JR. & REDMOND, D. E., JR. 2002. Embryonic ventral mesencephalic grafts to the substantia nigra of MPTP-treated monkeys: feasibility relevant to multiple-target grafting as a therapy for Parkinson's disease. *J Comp Neurol,* 442**,** 320-30.

COOPER, J. A., SAGAR, H. J., TIDSWELL, P. & JORDAN, N. 1994. Slowed central processing in simple and go no-go reaction-time tasks in Parkinsons-disease. *Brain,* 117**,** 517-529.

COTZIAS, G. C., PAPAVASI.PS & GELLENE, R. 1969. Modification of parkinsonism - chronic treatment with L-DOPA. *New England Journal of Medicine,* 280**,** 337-&.

COUGHLIN, M. D., DIBNER, M. D., BOYER, D. M. & BLACK, I. B. 1978. Factors regulating development of an embryonic mouse sympathetic-ganglion. *Developmental Biology,* 66.

DAHLSTROM, A. & FUXE, K. 1964. Localization of monoamines in lower brain stem. *Experientia,* 20**,** 398-399.

DAUER, W., KHOLODILOV, N., VILA, M., TRILLAT, A. C., GOODCHILD, R., LARSEN, K. E., STAAL, R., TIEU, K., SCHMITZ, Y., YUAN, C. A., ROCHA, M., JACKSON-LEWIS, V., HERSCH, S., SULZER, D., PRZEDBORSKI, S., BURKE, R. & HEN, R. 2002. Resistance of alpha-synuclein null mice to the parkinsonian neurotoxin MPTP. *Proceedings of the National Academy of Sciences of the United States of America,* 99**,** 14524-14529.

DAVIS, G. C., WILLIAMS, A. C., MARKEY, S. P., EBERT, M. H., CAINE, E. D., REICHERT, C. M. & KOPIN, I. J. 1979. Chronic parkinsonism secondary to intravenous-injection of meperidine analogs. *Psychiatry Research,* 1**,** 249-254.

DAWSON, T. M., KO, H. S. & DAWSON, V. L. 2010. Genetic Animal Models of Parkinson's Disease. *Neuron,* 66**,** 646-661.

DAY, M., WANG, Z. F., DING, J., AN, X. H., INGHAM, C. A., SHERING, A. F., WOKOSIN, D., ILIJIC, E., SUN, Z. X., SAMPSON, A. R., MUGNAINI, E., DEUTCH, A. Y., SESACK, S. R., ARBUTHNOTT, G. W. & SURMEIER, D. J. 2006. Selective elimination of glutamatergic synapses on striatopallidal neurons in Parkinson disease models. *Nature Neuroscience,* 9**,** 251-259.

DAYER, A. G., FORD, A. A., CLEAVER, K. M., YASSAEE, M. & CAMERON, H. A. 2003. Short-term and long-term survival of new neurons in the rat dentate gyrus. *Journal of Comparative Neurology,* 460**,** 563-572.

DEHAY, B., MARTINEZ-VICENTE, M., CALDWELL, G. A., CALDWELL, K. A., YUE, Z., COOKSON, M. R., KLEIN, C., VILA, M. & BEZARD, E. 2013. Lysosomal impairment in Parkinson's disease. *Movement Disorders,* 28**,** 725-732.

DENIAU, J. M. & CHEVALIER, G. 1985. Disinhibition as a basic process in the expression of striatal functions .2. The striato-nigral influence on thalamocortical cells of the ventromedial thalamic nucleus. *Brain Research,* 334**,** 227-233.

DERIJK, M. C., BRETELER, M. M. B., GRAVELAND, G. A., OTT, A., GROBBEE, D. E., VANDERMECHE, F. G. A. & HOFMAN, A. 1995. Prevalence of Parkinson's disease in the elderly: The Rotterdam study. *Neurology,* 45**,** 2143-2146.

DEXTER, D. T., CARTER, C. J., WELLS, F. R., JAVOYAGID, F., AGID, Y., LEES, A., JENNER, P. & MARSDEN, C. D. 1989. Basal lipid-peroxidation in substantia nigra is increased in Parkinsons-disease. *Journal of Neurochemistry,* 52**,** 381-389.

DI FONZO, A., ROHE, C. F., FERREIRA, R. J., CHIEN, H. F., VACCA, L., STOCCHI, F., GUEDES, L., FABRIZIO, E., MANFREDI, M., VANACORE, N., GOLDWURM, S., BREEDVELD, G., SAMPAIO, C., MECO, G., BARBOSA, E., OOSTRA, B. A., BONIFATI, V. & ITALIAN PARKINSON GENETICS, N. 2005. A frequent LRRK2 gene mutation associated with autosomal dominant Parkinson's disease. *Lancet,* 365**,** 412-415.

DI MONTE, D. A., MCCORMACK, A., PETZINGER, G., JANSON, A. M., QUIK, M. & LANGSTON, W. J. 2000. Relationship among nigrostriatal denervation,

parkinsonism, and dyskinesias in the MPTP primate model. *Movement Disorders,* 15**,** 459-466.

DOUCET, G., MURATA, Y., BRUNDIN, P., BOSLER, O., MONS, N., GEFFARD, M., OUIMET, C. C. & BJORKLUND, A. 1989. Host afferents into intrastriatal transplants of fetal ventral mesencephalon. *Experimental Neurology,* 106**,** 1-19.

DOUDET, D., GROSS, C., LEBRUNGRANDIE, P. & BIOULAC, B. 1985. MPTP primate model of Parkinsons-disease - a mechanographic and electromyographic study. *Brain Research,* 335**,** 194-198.

DOWD, E. & DUNNETT, S. B. 2004. Deficits in a lateralized associative learning task in dopamine-depleted rats with functional recovery by dopamine-rich transplants. *European Journal of Neuroscience,* 20**,** 1953-1959.

DOWD, E. & DUNNETT, S. B. 2005a. Comparison of 6-hydroxydopamine-induced medial forebrain bundle and nigrostriatal terminal lesions in a lateralised nose-poking task in rats. *Behavioural Brain Research,* 159**,** 153-161.

DOWD, E. & DUNNETT, S. B. 2005b. Comparison of 6-hydroxydopamine-induced medial forebrain bundle and nigrostriatal terminal lesions in rats using a lateralised nose-poking task with low stimulus-response compatibility. *Behavioural Brain Research,* 165**,** 181-186.

DUNN, E. H. 1917. Primary and secondary findings in a series of attempts to transplant cerebral cortex in the albino rat. *Journal of Comparative Neurology,* 27**,** 565-582.

DUNNETT, S. B. & BJORKLUND, A. 1992. Staging and dissection of rat embryos. *In:* DUNNETT, S. B. & BJORKLUND, A. (eds.) *Neural Transplantation: A Practical Approach.* Oxford: IRL.

DUNNETT, S. B. & BJORKLUND, A. 1997. *Basic neural transplantation techniques. I.Dissociated cell suspension grafts of embryonic ventral mesencephalon in the adult rat brain.,* Brain Res Protoc.

DUNNETT, S. B., BJORKLUND, A., SCHMIDT, R. H., STENEVI, U. & IVERSEN, S. D. 1983. Intracerebral grafting of neuronal cell suspensions. IV. Behavioural recovery in rats with unilateral 6-OHDA lesions following implantation of nigral cell suspensions in different forebrain sites. *Acta Physiol Scand Suppl,* 522**,** 29-37.

DUNNETT, S. B., HERNANDEZ, T. D., SUMMERFIELD, A., JONES, G. H. & ARBUTHNOTT, G. 1988. Graft-derived recovery from 6-OHDA lesions: specificity of ventral mesencephalic graft tissues. *Exp Brain Res,* 71**,** 411-24.

DUNNETT, S. B., ROGERS, D. C. & RICHARDS, S. J. 1989. Nigrostriatal reconstruction after 6-OHDA lesions in rats - combination of dopamine-rich nigral grafts and nigrostriatal bridge grafts. *Experimental Brain Research,* 75**,** 523-535.

ELAHI, B., PHIELIPP, N. & CHEN, R. 2012. N-Methyl-D-Aspartate Antagonists in Levodopa Induced Dyskinesia: A Meta-Analysis. *Canadian Journal of Neurological Sciences,* 39**,** 465-472.

ELBAZ, A. & MOISAN, F. 2008. Update in the epidemiology of Parkinson's disease. *Current Opinion in Neurology,* 21**,** 454-460.

EMBORG, M. E., MA, S. Y., MUFSON, E. J., LEVEY, A. I., TAYLOR, M. D., BROWN, W. D., HOLDEN, J. E. & KORDOWER, J. H. 1998. Age-related declines in nigral neuronal function correlate with motor impairments in rhesus monkeys. *Journal of Comparative Neurology,* 401**,** 253-265.

ENGLUND, U., BJORKLUND, A. & WICTORIN, K. 2002. Migration patterns and phenotypic differentiation of long-term expanded human neural progenitor cells after transplantation into the adult rat brain. *Developmental Brain Research,* 134**,** 123-141.

ERIKSSON, T., GRANERUS, A. K., LINDE, A. & CARLSSON, A. 1988. On-off phenomenon in Parkinsons-disease - relationship between DOPA and other large neutral amino-acids in plasma. *Neurology,* 38**,** 1245-1248.

EULITZ, D., PRUSS, H., DERST, C. & VEH, R. W. 2007. Heterogeneous distribution of Kir3 potassium channel proteins within dopaminergic neurons in the mesencephalon of the rat brain. *Cellular and Molecular Neurobiology,* 27**,** 285-302.

FAHN, S. 2009. Parkinson's disease and related disorders. *In:* HALTER, J., OUSLANDER, J., TINETTI, M., STUDENSKI, S., HIGH, K. & ASTHANA, S. (eds.) *Hazzard's geriatric medicine and gerontology. Part IV Organ systems and diseases.* 6 ed. USA: McGraw-Hill Medical.

FALCK, B., THIEME, G., HILLARP, N. A. & TORP, A. 1962. Fluorescence of catechol amines and related compounds condensed with formaldehyde. *Journal of Histochemistry & Cytochemistry,* 10**,** 348-354.

FALLON, J. H. & LOUGHLIN, S. E. 1982. Monoamine innervation of the forebrain - collateralization. *Brain Research Bulletin,* 9**,** 295-307.

FARKAS, L. M., DUNKER, N., ROUSSA, E., UNSICKER, K. & KRIEGLSTEIN, K. 2003. Transforming growth factor-beta s are essential for the development of midbrain dopaminergic neurons in vitro and in vivo. *Journal of Neuroscience,* 23**,** 5178-5186.

FAWCETT, J. W., BARKER, R. A. & DUNNETT, S. B. 1995. Dopaminergic neuronal survival and the effects of BFGF in explant, 3-dimensional and monolayer-cultures of embryonic rat ventral mesencephalon. *Experimental Brain Research,* 106**,** 275-282.

FEANY, M. B. & BENDER, W. W. 2000. A Drosophila model of Parkinson's disease. *Nature,* 404**,** 394-398.

FERNANDEZ, H. H. & LAPANE, K. L. 2002. Predictors of mortality among nursing home residents with a diagnosis of Parkinson's disease. *Medical science monitor : international medical journal of experimental and clinical research,* 8**,** CR241-6.

FERRANTE, R. J., SCHULZ, J. B., KOWALL, N. W. & BEAL, M. F. 1997. Systemic administration of rotenone produces selective damage in the striatum and globus pallidus, but not in the substantia nigra. *Brain Research,* 753**,** 157-162.

FOLEY, P., GERLACH, M., DOUBLE, K. L. & RIEDERER, P. 2004. Dopamine receptor agonists in the therapy of Parkinson's disease. *Journal of Neural Transmission,* 111**,** 1375-1446.

FORNO, L. S., DELANNEY, L. E., IRWIN, I. & LANGSTON, J. W. 1993. Similarities and differences between MPTP-induced parkinsonism and Parkinsons-disease - neuropathologic considerations. *Parkinsons Disease : from Basic Research to Treatment,* 60**,** 600-608.

FREED, C. R., BREEZE, R. E., ROSENBERG, N. L., SCHNECK, S. A., KRIEK, E., QI, J. X., LONE, T., ZHANG, Y. B., SNYDER, J. A., WELLS, T. H., RAMIG, L. O., THOMPSON, L., MAZZIOTTA, J. C., HUANG, S. C., GRAFTON, S. T., BROOKS, D., SAWLE, G., SCHROTER, G. & ANSARI, A. A. 1992. Survival of implanted fetal dopamine cells and neurologic improvement 12 to 46 months after transplantation for Parkinsons-disease. *New England Journal of Medicine,* 327**,** 1549-1555.

FREED, C. R., GREENE, P. E., BREEZE, R. E., TSAI, W. Y., DUMOUCHEL, W., KAO, R., DILLON, S., WINFIELD, H., CULVER, S., TROJANOWSKI, J. Q., EIDELBERG, D. & FAHN, S. 2001. Transplantation of embryonic dopamine neurons for severe Parkinson's disease. *New England Journal of Medicine,* 344**,** 710-719.

FREEMAN, T. B., OLANOW, C. W., HAUSER, R. A., NAUERT, G. M., SMITH, D. A., BORLONGAN, C. V., SANBERG, P. R., HOLT, D. A., KORDOWER, J. H., VINGERHOETS, J. G., SNOW, B. J., CALNE, D. & GAUGER, L. I. 1995a. Bilateral fetal nigral transplantation into the postcommissural putamen in Parkinsons-disease. *Annals of Neurology,* 38**,** 379-388.

FREEMAN, T. B., SANBERG, P. R., NAUERT, G. M., BOSS, B. D., SPECTOR, D., OLANOW, C. W. & KORDOWER, J. H. 1995b. The influence of donor age on the survival of solid and suspension intraparenchymal human embryonic nigral grafts. *Cell Transplantation,* 4**,** 141-154.

FREEMAN, T. B., SPENCE, M. S., BOSS, B. D., SPECTOR, D. H., STRECKER, R. E., OLANOW, C. W. & KORDOWER, J. H. 1991. Development of dopaminergic-neurons in the human substantia-nigra. *Experimental Neurology,* 113**,** 344-353.

FREUND, T. F., BOLAM, J. P., BJORKLUND, A., STENEVI, U., DUNNETT, S. B., POWELL, J. F. & SMITH, A. D. 1985. Efferent synaptic connections of grafted dopaminergic-neurons reinnervating the host neostriatum - a tyrosine-hydroxylase immunocytochemical study. *Journal of Neuroscience,* 5**,** 603-616.

FRICKER, R. A., CARPENTER, M. K., WINKLER, C., GRECO, C., GATES, M. A. & BJORKLUND, A. 1999. Site-specific migration and neuronal differentiation of human neural progenitor cells after transplantation in the adult rat brain. *J Neurosci,* 19**,** 5990-6005.

FUNAYAMA, M., HASEGAWA, K., KOWA, H., SAITO, M., TSUJI, S. & OBATA, F. 2002. A new locus for Parkinson's disease (PARK8) maps to chromosome 12p11.2-q13.1. *Annals of Neurology,* 51**,** 296-301.

GALVIN, J. E., POLLACK, J. & MORRIS, J. C. 2006. Clinical phenotype of Parkinson disease dementia. *Neurology,* 67**,** 1605-1611.

GASPAR, P., BERGER, B., ALVAREZ, C., VIGNY, A. & HENRY, J. P. 1985. Catecholaminergic innervation of the septal area in man - immunocytochemical study using TH and DBH antibodies. *Journal of Comparative Neurology,* 241**,** 12-33.

GASPAR, P., BERGER, B., FEBVRET, A., VIGNY, A., KRIEGER-POULET, M. & BORRI-VOLTATTORNI, C. 1987. Tyrosine hydroxylase-immunoreactive neurons in the human cerebral cortex: a novel catecholaminergic group? *Neuroscience Letters,* 80**,** 257-62.

GATES, M. A., COUPE, V. M., TORRES, E. M., FRICKER-GATES, R. A. & DUNNETT, S. B. 2004. Spatially and temporally restricted chemoattractive and chemorepulsive cues direct the formation of the nigro-striatal circuit. *European Journal of Neuroscience,* 19**,** 831-844.

GATES, M. A., TORRES, E. M., WHITE, A., FRICKER-GATES, R. A. & DUNNETT, S. B. 2006. Re-examining the ontogeny of substantia nigra dopamine neurons. *European Journal of Neuroscience,* 23**,** 1384-1390.

GELB, D. J., OLIVER, E. & GILMAN, S. 1999. Diagnostic criteria for Parkinson disease. *Archives of Neurology,* 56**,** 33-39.

GERFEN, C. R., ENGBER, T. M., MAHAN, L. C., SUSEL, Z., CHASE, T. N., MONSMA, F. J. & SIBLEY, D. R. 1990. D1 and D2 dopamine receptor regulated gene-expression of striatonigral and striatopallidal neurons. *Science,* 250**,** 1429-1432.

GERFEN, C. R., HERKENHAM, M. & THIBAULT, J. 1987. The neostriatal mosaic. II. patch-directed and matrix-directed mesostriatal dopaminergic and non-dopaminergic systems. *The Journal of Neuroscience,* 7**,** 3915-34.

GERLACH, M., DESSER, H., YOUDIM, M. B. J. & RIEDERER, P. 1996. New horizons in molecular mechanisms underlying Parkinson's disease and in our

understanding of the neuroprotective effects of selegiline. *Journal of Neural Transmission Supplement,* 48**,** 7-21.

GERLACH, M., RIEDERER, P., PRZUNTEK, H. & YOUDIM, M. B. H. 1991. MPTP mechanisms of neurotoxicity and their implications for Parkinsons-disease. *European Journal of Pharmacology-Molecular Pharmacology Section,* 208**,** 273-286.

GERMAN, D. C. & MANAYE, K. F. 1993. Midbrain dopaminergic-neurons (nuclei a8, a9, and a10) - 3-dimensional reconstruction in the rat. *Journal of Comparative Neurology,* 331**,** 297-309.

GERMAN, D. C., NELSON, E. L., LIANG, C. L., SPECIALE, S. G., SINTON, C. M. & SONSALLA, P. K. 1996. The neurotoxin MPTP causes degeneration of specific nucleus A8, A9 and A10 dopaminergic neurons in the mouse. *Neurodegeneration,* 5**,** 299-312.

GIASSON, B. I., DUDA, J. E., MURRAY, I. V. J., CHEN, Q. P., SOUZA, J. M., HURTIG, H. I., ISCHIROPOULOS, H., TROJANOWSKI, J. Q. & LEE, V. M. Y. 2000. Oxidative damage linked to neurodegeneration by selective alpha-synuclein nitration in synucleinopathy lesions. *Science,* 290**,** 985-989.

GIASSON, B. I., DUDA, J. E., QUINN, S. M., ZHANG, B., TROJANOWSKI, J. Q. & LEE, V. M. Y. 2002. Neuronal alpha-synucleinopathy with severe movement disorder in mice expressing A53T human alpha-synuclein. *Neuron,* 34**,** 521-533.

GIBB, W. R. G. & LEES, A. J. 1989. The significance of the Lewy Body in the diagnosis of idiopathic Parkinsons-disease. *Neuropathology and Applied Neurobiology,* 15**,** 27-44.

GIBB, W. R. G. & LEES, A. J. 1991. Anatomy, pigmentation, ventral and dorsal subpopulations of the substantia-nigra, and differential cell-death in Parkinsons-disease. *Journal of Neurology Neurosurgery and Psychiatry,* 54**,** 388-396.

GILADI, N., MCDERMOTT, M. P., FAHN, S., PRZEDBORSKI, S., JANKOVIC, J., STERN, M., TANNER, C. & PARKINSON STUDY, G. 2001. Freezing of gait in PD - Prospective assessment in the DATATOP cohort. *Neurology,* 56**,** 1712-1721.

GLINKA, Y., GASSEN, M. & YOUDIM, M. B. H. 1997. Mechanism of 6-hydroxydopamine neurotoxicity. *Journal of Neural Transmission-Supplement***,** 55-66.

GOETZ, C. G., NUTT, J. G. & STEBBINS, G. T. 2008. The Unified Dyskinesia Rating Scale: Presentation and Clinimetric Profile. *Movement Disorders,* 23**,** 2398-2403.

GOETZ, C. G., STEBBINS, G. T., KLAWANS, H. L., KOLLER, W. C., GROSSMAN, R. G., BAKAY, R. A. E. & PENN, R. D. 1991. United-Parkinson-Foundation neurotransplantation registry on adrenal-medullary transplants - presurgical, and 1-year and 2-year follow-up. *Neurology,* 41**,** 1719-1722.

GOOD, P. F., HSU, A., WERNER, P., PERL, D. P. & OLANOW, C. W. 1998. Protein nitration in Parkinson's disease. *Journal of Neuropathology and Experimental Neurology,* 57**,** 338-342.

GOSSEL, M., SCHMIDT, W. J., LOSCHER, W., ZAJACZKOWSKI, W. & DANYSZ, W. 1995. Effect of coadministration of glutamate-receptor antagonists and dopaminergic agonists on locomotion in monoamine-depleted rats. *Journal of Neural Transmission-Parkinsons Disease and Dementia Section,* 10**,** 27-39.

GRAFF-RADFORD, J., FOOTE, K. D., RODRIGUEZ, R. L., FERNANDEZ, H. H., HAUSER, R. A., SUDHYADHOM, A., ROSADO, C. A., SANCHEZ, J. C. & OKUN, M. S. 2006. Deep brain stimulation of the internal segment of the globus pallidus in delayed runaway dyskinesia. *Arch Neurol,* 63**,** 1181-4.

GRANT, R. J. & CLARKE, P. B. S. 2002. Susceptibility of ascending dopamine projections to 6-hydroxydopamine in rats: Effect of hypothermia. *Neuroscience,* 115**,** 1281-1294.

GREALISH, S., JONSSON, M. E., LI, M., KIRIK, D., BJORKLUND, A. & THOMPSON, L. H. 2010. The A9 dopamine neuron component in grafts of ventral mesencephalon is an important determinant for recovery of motor function in a rat model of Parkinson's disease. *Brain,* 133**,** 482-495.

GREENE, J. G., DINGLEDINE, R. & GREENAMYRE, J. T. 2005. Gene expression profiling of rat midbrain dopamine neurons: implications for selective vulnerability in parkinsonism. *Neurobiology of Disease,* 18**,** 19-31.

GREFFARD, S., VERNY, M., BONNET, A.-M., SEILHEAN, D., HAUW, J.-J. & DUYCKAERTS, C. 2010. A stable proportion of Lewy body bearing neurons in the substantia nigra suggests a model in which the Lewy body causes neuronal death. *Neurobiology of Aging,* 31**,** 99-103.

GRIMM, J., MUELLER, A., HEFTI, F. & ROSENTHAL, A. 2004. Molecular basis for catecholaminergic neuron diversity. *Proceedings of the National Academy of Sciences of the United States of America,* 101**,** 13891-13896.

HABER, S. N. 2003. The primate basal ganglia: parallel and integrative networks. *Journal of Chemical Neuroanatomy,* 26**,** 317-330.

HAGELL, P., PICCINI, P., BJORKLUND, A., BRUNDIN, P., REHNCRONA, S., WIDNER, H., CRABB, L., PAVESE, N., OERTEL, W. H., QUINN, N., BROOKS, D. J. & LINDVALL, O. 2002. Dyskinesias following neural transplantation in Parkinson's disease. *Nature Neuroscience,* 5**,** 627-628.

HAGELL, P., SCHRAG, A., PICCINI, P., JAHANSHAHI, M., BROWN, R., REHNCRONA, S., WIDNER, H., BRUNDIN, P., ROTHWELL, J. C., ODIN, P., WENNING, G. K., MORRISH, P., GUSTAVII, B., BJORKLUND, A., BROOKS, D. J., MARSDEN, C. D., QUINN, N. P. & LINDVALL, O. 1999. Sequential bilateral transplantation in Parkinson's disease - Effects of the second graft. *Brain,* 122**,** 1121-1132.

HAHN, M., TIMMER, M. & NIKKHAH, G. 2009. Survival and Early Functional Integration of Dopaminergic Progenitor Cells Following Transplantation in a Rat Model of Parkinson's Disease. *Journal of Neuroscience Research,* 87**,** 2006-2019.

HALLIDAY, G., TRINIDAD HERRERO, M., MURPHY, K., MCCANN, H., ROS-BERNAL, F., BARCIA, C., MORI, H., BLESA, F. J. & OBESO, J. A. 2009. No Lewy Pathology in Monkeys with Over 10 Years of Severe MPTP Parkinsonism. *Movement Disorders,* 24**,** 1519-1523.

HAMILTON, D. 2012. Clinical and academic transplantation in Paris. *A History of Organ Transplantation.* 1st edition ed.: University of Pittsburgh Pre.

HAYES, L., ZHANG, Z., ALBERT, P., ZERVAS, M. & AHN, S. 2011. Timing of Sonic Hedgehog and Gli1 Expression Segregates Midbrain Dopamine Neurons. *Journal of Comparative Neurology,* 519**,** 3001-3018.

HAYES, N. L. & NOWAKOWSKI, R. S. 2000. Exploiting the dynamics of S-phase tracers in developing brain: Interkinetic nuclear migration for cells entering versus leaving the S-phase. *Developmental Neuroscience,* 22**,** 44-55.

HAYES, N. L. & NOWAKOWSKI, R. S. 2002. High doses of bromodeoxyuridine increase number of labeled cells in adult mouse dentate gyrus by decreasing tracer loading time. *Society for Neuroscience Abstract Viewer and Itinerary Planner,* 2002**,** Abstract No. 126.3-Abstract No. 126.3.

HEIKKILA, R. E., SHAPIRO, B. S. & DUVOISIN, R. C. 1981. The relationship between loss of dopamine nerve-terminals, striatal H-3 spiroperidol binding and

rotational behavior in unilaterally 6-hydroxydopamine-lesioned rats. *Brain Research,* 211**,** 285-292.

HEIKKILA, R. E. & SONSALLA, P. K. 1992. The MPTP-treated mouse as a model of parkinsonism - how good is it. *Neurochemistry International,* 20**,** S299-S303.

HELY, M. A., MORRIS, J. G. L., REID, W. G. J. & TRAFFICANTE, R. 2005. Sydney multicenter study of Parkinson's disease: non-L-dopa-responsive problems dominate at 15 years. *Movement Disorders,* 20**,** 190-199.

HENDRY, I. A. 1975. Retrograde trans-synaptic control of development of cholinergic terminals in sympathetic-ganglia. *Brain Research,* 86**,** 483-487.

HERTZMAN, C., WIENS, M., BOWERING, D., SNOW, B. & CALNE, D. 1990. Parkinsons-disease - a case-control study of occupational and environmental risk-factors. *American Journal of Industrial Medicine,* 17**,** 349-355.

HERZOG, J., POGARELL, O., PINSKER, M. O., KUPSCH, A., OERTEL, W. H., LINDVALL, O., DEUSCHL, G. & VOLKMANN, J. 2008. Deep brain stimulation in Parkinson's disease following fetal nigral transplantation. *Mov Disord,* 23**,** 1293-6.

HEUER, A., LELOS, M. J., KELLY, C. M., TORRES, E. M. & DUNNETT, S. B. 2013a. Dopamine-rich grafts alleviate deficits in contralateral response space induced by extensive dopamine depletion in rats. *Experimental Neurology,* 247**,** 485-495.

HEUER, A., NGOC-NGA, V. & DUNNETT, S. B. 2013b. Behavioural recovery on simple and complex tasks by means of cell replacement therapy in unilateral 6-hydroxydopamine-lesioned mice. *European Journal of Neuroscience,* 37**,** 1691-1704.

HIRSCH, E. C., GRAYBIEL, A. M., DUYCKAERTS, C. & JAVOYAGID, F. 1987. Neuronal loss in the pedunculopontine tegmental nucleus in Parkinson disease and in progressive supranuclear palsy. *Proceedings of the National Academy of Sciences of the United States of America,* 84**,** 5976-5980.

HUGHES, A. J., DANIEL, S. E., BLANKSON, S. & LEES, A. J. 1993. A clinicopathological study of 100 cases of Parkinsons-disease. *Archives of Neurology,* 50**,** 140-148.

HUNG, H. C. & LEE, E. H. Y. 1998. MPTP produces differential oxidative stress and antioxidative responses in the nigrostriatal and mesolimbic dopaminergic pathways. *Free Radical Biology and Medicine,* 24**,** 76-84.

HURD, Y. L., PRISTUPA, Z. B., HERMAN, M. M., NIZNIK, H. B. & KLEINMAN, J. E. 1994. The dopamine transporter and dopamine-D-2 receptor messenger-RNAs are differentially expressed in limbic-related and motor-related subpopulations of human mesencephalic neurons. *Neuroscience,* 63**,** 357-362.

ILINSKY, I. A., KULTASILINSKY, K. & SMITH, K. R. 1982. Organization of basal ganglia inputs to the thalamus - a light and electron-microscopic study in the cat. *Applied Neurophysiology,* 45**,** 230-237.

INDEN, M., KITAMURA, Y., ABE, M., TAMAKI, A., TAKATA, K. & TANIGUCHI, T. 2011. Parkinsonian Rotenone Mouse Model: Reevaluation of Long-Term Administration of Rotenone in C57BL/6 Mice. *Biological & Pharmaceutical Bulletin,* 34**,** 92-96.

INDEN, M., KITAMURA, Y., TAKEUCHI, H., YANAGIDA, T., TAKATA, K., KOBAYASHI, Y., TANIGUCHI, T., YOSHIMOTO, K., KANEKO, M., OKUMA, Y., TAIRA, T., ARIGA, H. & SHIMOHAMA, S. 2007. Neurodegeneration of mouse nigrostriatal dopaminergic system induced by repeated oral administration of rotenone is prevented by 4-phenylbutyrate, a chemical chaperone. *Journal of Neurochemistry,* 101**,** 1491-1504.

IRAVANI, M. M., SYED, E., JACKSON, M. J., JOHNSTON, L. C., SMITH, L. A. & JENNER, P. 2005. A modified MPTP treatment regime produces reproducible partial nigrostriatal lesions in common marmosets. *European Journal of Neuroscience,* 21**,** 841-854.

JANKOVIC, J. 2008. Parkinson's disease: clinical features and diagnosis. *Journal of Neurology Neurosurgery and Psychiatry,* 79**,** 368-376.

JAVITCH, J. A., DAMATO, R. J., STRITTMATTER, S. M. & SNYDER, S. H. 1985. Parkinsonism-inducing neurotoxin, n-methyl-4-phenyl-1,2,3,6-tetrahydropyridine - uptake of the metabolite n-methyl-4-phenylpyridine by dopamine neurons explains selective toxicity. *Proceedings of the National Academy of Sciences of the United States of America,* 82**,** 2173-2177.

JIANG, H., JACKSONLEWIS, V., MUTHANE, U., DOLLISON, A., FERREIRA, M., ESPINOSA, A., PARSONS, B. & PRZEDBORSKI, S. 1993. Adenosine receptor antagonists potentiate dopamine receptor agonist-induced rotational behavior in 6-hydroxydopamine-lesioned rats. *Brain Research,* 613**,** 347-351.

JOKSIMOVIC, M., YUN, B. A., KITTAPPA, R., ANDEREGG, A. M., WCHANG, W., TAKETO, M. M., MCKAY, R. D. G. & AWATRAMANI, R. B. 2009. Wnt antagonism of Shh facilitates midbrain floor plate neurogenesis. *Nature Neuroscience,* 12**,** 125-131.

JONSSON, M. E., ONO, Y., BJORKLUND, A. & THOMPSON, L. H. 2009. Identification of transplantable dopamine neuron precursors at different stages of midbrain neurogenesis. *Experimental Neurology,* 219**,** 341-354.

KATZENSCHLAGER, R., HEAD, J., SCHRAG, A., BEN-SHLOMO, Y., EVANS, A., LEES, A. J. & PARKINSON'S DIS RES GRP UNITED, K. 2008. Fourteen-year final report of the randomized PDRG-UK trial comparing three initial treatments in PD. *Neurology,* 71**,** 474-480.

KAUFMAN, M. P., LONGHURST, J. C., RYBICKI, K. J., WALLACH, J. H. & MITCHELL, J. H. 1983. Effects of static muscular-contraction on impulse activity of group-iii and group-iv afferents in cats. *Journal of Applied Physiology,* 55**,** 105-112.

KAY, D. M., FACTOR, S. A., SAMII, A., HIGGINS, D. S., GRIFFITH, A., ROBERTS, J. W., LEIS, B. C., NUTT, J. G., MONTIMURRO, J. S., KEEFE, R. G., ATKINS, A. J., YEAROUT, D., ZABETIAN, C. P. & PAYAMI, H. 2008. Genetic Association Between alpha-Synuclein and Idiopathic Parkinson's Disease. *American Journal of Medical Genetics Part B-Neuropsychiatric Genetics,* 147B**,** 1222-1230.

KELE, J., SIMPLICIO, N., FERRI, A. L. M., MIRA, H., GUILLEMOT, F., ARENAS, E. & ANG, S. L. 2006. Neurogenin 2 is required for the development of ventral midbrain dopaminergic neurons. *Development,* 133**,** 495-505.

KELLY, C. M., PRECIOUS, S. V., TORRES, E. M., HARRISON, A. W., WILLIAMS, D., SCHERF, C., WEYRAUCH, U. M., LANE, E. L., ALLEN, N. D., PENKETH, R., AMSO, N. N., KEMP, P. J., DUNNETT, S. B. & ROSSER, A. E. 2011. Medical Terminations of Pregnancy: A Viable Source of Tissue for Cell Replacement Therapy for Neurodegenerative Disorders. *Cell Transplantation,* 20**,** 503-513.

KIM, H.-J., SUGIMORI, M., NAKAFUKU, M. & SVENDSEN, C. N. 2007. Control of neurogenesis and tyrosine hydroxylase expression in neural progenitor cells through bHLH proteins and Nurr1. *Experimental Neurology,* 203**,** 394-405.

KIRIK, D., GEORGIEVSKA, B., BURGER, C., WINKLER, C., MUZYCZKA, N., MANDEL, R. J. & BJORKLUND, A. 2002. Reversal of motor impairments in parkinsonian rats by continuous intrastriatal delivery of L-dopa using rAAV-

mediated gene transfer. *Proceedings of the National Academy of Sciences of the United States of America,* 99**,** 4708-4713.

KISH, S. J., SHANNAK, K. & HORNYKIEWICZ, O. 1988. Uneven pattern of dopamine loss in the striatum of patients with idiopathic Parkinsons-disease - pathophysiologic and clinical implications. *New England Journal of Medicine,* 318**,** 876-880.

KITADA, T., ASAKAWA, S., HATTORI, N., MATSUMINE, H., YAMAMURA, Y., MINOSHIMA, S., YOKOCHI, M., MIZUNO, Y. & SHIMIZU, N. 1998. Mutations in the parkin gene cause autosomal recessive juvenile parkinsonism. *Nature,* 392**,** 605-608.

KOHLER, C., EVERITT, B. J., PEARSON, J. & GOLDSTEIN, M. 1983. Immunohistochemical evidence for a new group of catecholamine-containing neurons in the basal forebrain of the monkey. *Neuroscience Letters,* 37**,** 161-166.

KOLB, B., PEDERSEN, B., BALLERMANN, M., GIBB, B. & WHISHAW, I. Q. 1999. Embryonic and postnatal injections of bromodeoxyuridine produce age-dependent morphological and behavioral abnormalities. *Journal of Neuroscience,* 19**,** 2337-2346.

KORDOWER, J. H., CHU, Y. P., HAUSER, R. A., FREEMAN, T. B. & OLANOW, C. W. 2008a. Lewy body-like pathology in long-term embryonic nigral transplants in Parkinson's disease. *Nature Medicine,* 14**,** 504-506.

KORDOWER, J. H., CHU, Y. P., HAUSER, R. A., OLANOW, C. W. & FREEMAN, T. B. 2008b. Transplanted Dopaminergic Neurons Develop PD Pathologic Changes: A Second Case Report. *Movement Disorders,* 23**,** 2303-2306.

KORDOWER, J. H., FREEMAN, T. B., CHEN, E. Y., MUFSON, E. J., SANBERG, P. R., HAUSER, R. A., SNOW, B. & OLANOW, C. W. 1998. Fetal nigral grafts survive and mediate clinical benefit in a patient with Parkinson's disease. *Movement Disorders,* 13**,** 383-393.

KORDOWER, J. H., GOETZ, C. G., FREEMAN, T. B. & OLANOW, C. W. 1997a. Dopaminergic transplants in patients with Parkinson's disease: Neuroanatomical correlates of clinical recovery. *Experimental Neurology,* 144**,** 41-46.

KORDOWER, J. H., KANAAN, N. M., CHU, Y., BABU, R. S., STANSELL, J., III, TERPSTRA, B. T., SORTWELL, C. E., STEECE-COLLIER, K. & COLLIER, T. J. 2006. Failure of proteasome inhibitor administration to provide a model of Parkinson's disease in rats and monkeys. *Annals of Neurology,* 60**,** 264-268.

KORDOWER, J. H., ROSENSTEIN, J. M., COLLIER, T. J., BURKE, M. A., CHEN, E. Y., LI, J. M., MARTEL, L., LEVEY, A. E., MUFSON, E. J., FREEMAN, T. B. & OLANOW, C. W. 1996. Functional fetal nigral grafts in a patient with Parkinson's disease: Chemoanatomic, ultrastructural, and metabolic studies. *Journal of Comparative Neurology,* 370**,** 203-230.

KORDOWER, J. H., STYREN, S., CLARKE, M., DEKOSKY, S. T., OLANOW, C. W. & FREEMAN, T. B. 1997b. Fetal grafting for Parkinson's disease: expression of immune markers in two patients with functional fetal nigral implants. *Cell Transplant,* 6**,** 213-9.

KOTKOVA, P. & WEISS, P. 2013. Psychiatric factors related to sexual functioning in patients with Parkinson's disease. *Clinical Neurology and Neurosurgery,* 115**,** 419-424.

KRACK, P., BENAZZOUZ, A., POLLAK, P., LIMOUSIN, P., PIALLAT, B., HOFFMANN, D., XIE, J. & BENABID, A. L. 1998. Treatment of tremor in Parkinson's disease by subthalamic nucleus stimulation. *Movement Disorders,* 13**,** 907-914.

KRAMER, M. L. & SCHULZ-SCHAEFFER, W. J. 2007. Presynaptic alpha-synuclein aggregates, not Lewy bodies, cause neurodegeneration in dementia with Lewy bodies. *Journal of Neuroscience,* 27**,** 1405-1410.

KRAYENBUHL, H. & YASARGIL, M. G. 1960. Bilateral thalamotomy in parkinsonism. *Journal of Nervous and Mental Disease,* 130**,** 538-541.

KRAYENBUHL, H., YASARGIL, M. G. & WYSS, O. A. M. 1961. Bilateral thalamotomy and pallidotomy as treatment for bilateral parkinsonism. *Journal of Neurosurgery,* 18**,** 429-&.

KRIKS, S., SHIM, J.-W., PIAO, J., GANAT, Y. M., WAKEMAN, D. R., XIE, Z., CARRILLO-REID, L., AUYEUNG, G., ANTONACCI, C., BUCH, A., YANG, L., BEAL, M. F., SURMEIER, D. J., KORDOWER, J. H., TABAR, V. & STUDER, L. 2011. Dopamine neurons derived from human ES cells efficiently engraft in animal models of Parkinson's disease. *Nature,* 480**,** 547-U177.

KRISS, J. P. & REVESZ, L. 1962. Distribution and fate of bromodeoxyuridine and bromodeoxycytidine in mouse and rat. *Cancer Research,* 22**,** 254-&.

KRUGER, R., KUHN, W., MULLER, T., WOITALLA, D., GRAEBER, M., KOSEL, S., PRZUNTEK, H., EPPLEN, J. T., SCHOLS, L. & RIESS, O. 1998. Ala30Pro mutation in the gene encoding alpha-synuclein in Parkinson's disease. *Nature Genetics,* 18**,** 106-108.

KUAN, W. L., LIN, R., TYERS, P. & BARKER, R. A. 2007. The importance of A9 dopaminergic neurons in mediating the functional benefits of fetal ventral mesencephalon transplants and levodopa-induced dyskinesias. *Neurobiology of Disease,* 25**,** 594-608.

KUUSISTO, E., PARKKINEN, L. & ALAFUZOFF, I. 2003. Morphogenesis of Lewy bodies: Dissimilar incorporation of alpha-synuclein, ubiquitin, and p62. *Journal of Neuropathology and Experimental Neurology,* 62**,** 1241-1253.

LACEY, M. G., MERCURI, N. B. & NORTH, R. A. 1987. Dopamine acts on D2 receptors to increase potassium conductance in neurons of the rat substantia-nigra zona compacta. *Journal of Physiology-London,* 392**,** 397-416.

LADER, M. 2008. Antiparkinsonian medication and pathological gambling. *Cns Drugs,* 22**,** 407-416.

LAMMEL, S., HETZEL, A., HAECKEL, O., JONES, I., LISS, B. & ROEPER, J. 2008. Unique properties of mesoprefrontal neurons within a dual mesocorticolimbic dopamine system. *Neuron,* 57**,** 760-773.

LANDMESSER, L. 1978. Interactions between neurons and their targets during invivo synaptogenesis. *Federation Proceedings,* 37.

LANG, A. E. & LOZANO, A. M. 1998. Parkinson's disease - Second of two parts. *New England Journal of Medicine,* 339**,** 1130-1143.

LANGSTON, J. W., BALLARD, P., TETRUD, J. W. & IRWIN, I. 1983. Chronic parkinsonism in humans due to a product of meperidine-analog synthesis. *Science,* 219**,** 979-980.

LANGSTON, J. W., FORNO, L. S., REBERT, C. S. & IRWIN, I. 1984. Selective nigral toxicity after systemic administration of 1-methyl-4-phenyl-1,2,5,6-tetrahydropyrine (MPTP) in the squirrel-monkey. *Brain Research,* 292**,** 390-394.

LASAK, J. M. & GORECKI, J. P. 2009. The History of Stereotactic Radiosurgery and Radiotherapy. *Otolaryngologic Clinics of North America,* 42**,** 593-599.

LEE, K. H., CHANG, S. Y., ROBERTS, D. W. & KIM, U. 2004. Neurotransmitter release from high-frequency stimulation of the subthalamic nucleus. *Journal of Neurosurgery,* 101**,** 511-517.

LEES, A. J., HARDY, J. & REVESZ, T. 2009. Parkinson's disease. *Lancet,* 373**,** 2055-2066.

LESAGE, S., DURR, A., TAZIR, M., LOHMANN, E., LEUTENEGGER, A. L., JANIN, S., POLLAK, P., BRICE, A. & FRENCH PARKINSON'S DIS GENETICS, S. 2006. LRRK2 G2019S as a cause of Parkinson's disease in North African Arabs. *New England Journal of Medicine,* 354**,** 422-423.

LEVIVIER, M., DETHY, S., RODESCH, F., PESCHANSKI, M., VANDESTEENE, A., DAVID, P., WIKLER, D., GOLDMAN, S., CLAES, T., BIVER, F., LIESNARD, C., GOLDMAN, M., HILDEBRAND, J. & BROTCHI, J. 1997. Intracerebral transplantation of fetal ventral mesencephalon for patients with advanced Parkinson's disease - Methodology and 6-month to 1-year follow-up in 3 patients. *Stereotactic and Functional Neurosurgery,* 69**,** 99-111.

LI, J.-Y., ESPAY, A. J., GUNRAJ, C. A., PAL, P. K., CUNIC, D. I., LANG, A. E. & CHEN, R. 2007. Interhemispheric and ipsilateral connections in Parkinson's disease: Relation to mirror movements. *Movement Disorders,* 22**,** 813-821.

LI, J. Y., ENGLUND, E., HOLTON, J. L., SOULET, D., HAGELL, P., LEES, A. J., LASHLEY, T., QUINN, N. P., REHNCRONA, S., BJORKLUND, A., WIDNER, H., REVESZ, T., LINDVALL, O. & BRUNDIN, P. 2008. Lewy bodies in grafted neurons in subjects with Parkinson's disease suggest host-to-graft disease propagation. *Nature Medicine,* 14**,** 501-503.

LI, Y., LIU, W., OO, T. F., WANG, L., TANG, Y., JACKSON-LEWIS, V., ZHOU, C., GEGHMAN, K., BOGDANOV, M., PRZEDBORSKI, S., BEAL, M. F., BURKE, R. E. & LI, C. 2009. Mutant LRRK2(R1441G) BAC transgenic mice recapitulate cardinal features of Parkinson's disease. *Nature Neuroscience,* 12**,** 826-828.

LIBOW, L. S., FRISINA, P. G., HAROUTUNIAN, V., PERL, D. P. & PUROHIT, D. P. 2009. Parkinson's disease dementia - A diminished role for the Lewy body. *Parkinsonism & Related Disorders,* 15**,** 572-575.

LIM, S.-Y., EVANS, A. H. & MIYASAKI, J. M. 2008. Impulse Control and Related Disorders in Parkinson's Disease Review. *Year in Neurology 2008,* 1142**,** 85-107.

LIMA, M. M. S., MARTINS, E. F., DELATTRE, A. M., PROENCA, M. B., MORI, M. A., CARABELLI, B. & FERRAZ, A. C. 2012. Motor and Non-Motor Features of Parkinson's Disease - A Review of Clinical and Experimental Studies. *Cns & Neurological Disorders-Drug Targets,* 11**,** 439-449.

LIMOUSIN, P., POLLAK, P., BENAZZOUZ, A., HOFFMANN, D., LEBAS, J. F., BROUSSOLLE, E., PERRET, J. E. & BENABID, A. L. 1995. Effect on parkinsonian signs and symptoms of bilateral subthalamic nucleus stimulation. *Lancet,* 345**,** 91-95.

LIMOUSIN, P., SPEELMAN, J. D., GIELEN, F. & JANSSENS, M. 1999. Multicentre European study of thalamic stimulation in parkinsonian and essential tremor. *Journal of Neurology Neurosurgery and Psychiatry,* 66**,** 289-296.

LINDVALL, O. & BJORKLUND, A. 1974. The organization of the ascending catecholamine neuron systems in the rat brain as revealed by the glyoxylic acid fluorescence method. *Acta physiologica Scandinavica. Supplementum,* 412**,** 1-48.

LINDVALL, O., BRUNDIN, P., WIDNER, H., REHNCRONA, S., GUSTAVII, B., FRACKOWIAK, R., LEENDERS, K. L., SAWLE, G., ROTHWELL, J. C., MARSDEN, C. D. & BJORKLUND, A. 1990. Grafts of fetal dopamine neurons survive and improve motor function in Parkinsons-disease. *Science,* 247**,** 574-577.

LINDVALL, O., REHNCRONA, S., BRUNDIN, P., GUSTAVII, B., ASTEDT, B., WIDNER, H., LINDHOLM, T., BJORKLUND, A., LEENDERS, K. L., ROTHWELL, J. C., FRACKOWIAK, R., MARSDEN, C. D., JOHNELS, B.,

STEG, G., FREEDMAN, R., HOFFER, B. J., SEIGER, A., BYGDEMAN, M., STROMBERG, I. & OLSON, L. 1989. Human-fetal dopamine neurons grafted into the striatum in 2 patients with severe Parkinsons-disease - a detailed account of methodology and a 6-month follow-up. *Archives of Neurology,* 46**,** 615-631.

LINDVALL, O., SAWLE, G., WIDNER, H., ROTHWELL, J. C., BJORKLUND, A., BROOKS, D., BRUNDIN, P., FRACKOWIAK, R., MARSDEN, C. D., ODIN, P. & REHNCRONA, S. 1994. Evidence for long-term survival and function of dopaminergic grafts in progressive Parkinsons-disease. *Annals of Neurology,* 35**,** 172-180.

LINDVALL, O., WIDNER, H., REHNCRONA, S., BRUNDIN, P., ODIN, P., GUSTAVII, B., FRACKOWIAK, R., LEENDERS, K. L., SAWLE, G., ROTHWELL, J. C., BJORKLUND, A. & MARSDEN, C. D. 1992. Transplantation of fetal dopamine neurons in Parkinsons-disease - one-year clinical and neurophysiological observations in 2 patients with putaminal implants. *Annals of Neurology,* 31**,** 155-165.

LOPEZ-LOZANO, J. J., BRAVO, G., BRERA, B., MILLAN, I., DARGALLO, J., SALMEAN, J., URIA, J. & INSAUSTI, J. 1997. Long-term improvement in patients with severe Parkinson's disease after implantation of fetal ventral mesencephalic tissue in a cavity of the caudate nucleus: 5-year follow up in 10 patients. Clinica Puerta de Hierro Neural Transplantation Group. *J Neurosurg,* 86**,** 931-42.

LOTHARIUS, J. & BRUNDIN, P. 2002. Pathogenesis of Parkinson's disease: Dopamine, vesicles and alpha-synuclein. *Nature Reviews Neuroscience,* 3**,** 932-942.

LOUGHLIN, S. E. & FALLON, J. H. 1984. Substantia nigra and ventral tegmental area projections to cortex - topography and collateralization. *Neuroscience,* 11**,** 425-435.

LOWE, J., BLANCHARD, A., MORRELL, K., LENNOX, G., REYNOLDS, L., BILLETT, M., LANDON, M. & MAYER, R. J. 1988. Ubiquitin is a common factor in intermediate filament inclusion-bodies of diverse type in man, including those of Parkinsons-disease, Picks disease, and Alzheimers-disease, as well as rosenthal fibers in cerebellar astrocytomas, cytoplasmic bodies in muscle, and mallory bodies in alcoholic liver-disease. *Journal of Pathology,* 155**,** 9-15.

LUNDBLAD, M., DECRESSAC, M., MATTSSON, B. & BJORKLUND, A. 2012. Impaired neurotransmission caused by overexpression of alpha-synuclein in nigral dopamine neurons. *Proceedings of the National Academy of Sciences of the United States of America,* 109**,** 3213-3219.

LYNDBALTA, E. & HABER, S. N. 1994. The organization of midbrain projections to the striatum in the primate - sensorimotor-related striatum versus ventral striatum. *Neuroscience,* 59**,** 625-640.

MACHT, M., KAUSSNER, Y., MOELLER, J. C., STIASNY-KOLSTER, K., EGGERT, K. M., KRUEGER, H.-P. & ELLGRING, H. 2007. Predictors of freezing in Parkinson's disease: A survey of 6,620 patients. *Movement Disorders,* 22**,** 953-956.

MADRAZO, I., DRUCKERCOLIN, R., DIAZ, V., MARTINEZMATA, J., TORRES, C. & BECERRIL, J. J. 1987. Open microsurgical autograft of adrenal-medulla to the right caudate-nucleus in 2 patients with intractable Parkinsons-disease. *New England Journal of Medicine,* 316**,** 831-834.

MANCA, D., COSSU, G., MURGIA, D., MOLARI, A., FERRIGNO, P., MARCIA, E. & MELIS, M. 2009. Reversible Encephalopathy and Axonal Neuropathy in

Parkinson's Disease During Duodopa Therapy. *Movement Disorders,* 24**,** 2293-2294.

MANN, D. M. A. & YATES, P. O. 1983. Pathological basis for neurotransmitter changes in Parkinsons-disease. *Neuropathology and Applied Neurobiology,* 9**,** 3-19.

MAO, L. M., LAU, Y. S., PETROSKE, E. & WANG, J. Q. 2001. Profound astrogenesis in the striatum of adult mice following nigrostriatal dopaminergic lesion by repeated MPTP administration. *Developmental Brain Research,* 131**,** 57-65.

MARCHAND, R. & POIRIER, L. J. 1983. Isthmic origin of neurons of the rat substantia-nigra. *Neuroscience,* 9**,** 373-381.

MARIES, E., KORDOWER, J. H., CHU, Y., COLLIER, T. J., SORTWELL, C. E., OLARU, E., SHANNON, K. & STEECE-COLLIER, K. 2006. Focal not widespread grafts induce novel dyskinetic behavior in parkinsonian rats. *Neurobiol Dis,* 21**,** 165-80.

MARSDEN, C. D. 1994. Problems with long-term levodopa therapy for Parkinsons-disease. *Clinical Neuropharmacology,* 17**,** S32-S44.

MARTINAT, C., SHENDELMAN, S., JONASON, A., LEETE, T., BEAL, M. F., YANG, L. C., FLOSS, T. & ABELIOVICH, A. 2004. Sensitivity to oxidative stress in DJ-1-deficient dopamine neurons: An ES-derived cell model of primary Parkinsonism. *Plos Biology,* 2**,** 1754-1763.

MARUYAMA, W., TAKAHASHI, T., YOUDIM, M. & NAOI, M. 2002. The anti-parkinson drug, rasagiline, prevents apoptotic DNA damage induced by peroxynitrite in human dopaminergic neuroblastoma SH-SY5Y cells. *Journal of Neural Transmission,* 109**,** 467-481.

MASLIAH, E., ROCKENSTEIN, E., VEINBERGS, I., MALLORY, M., HASHIMOTO, M., TAKEDA, A., SAGARA, Y., SISK, A. & MUCKE, L. 2000. Dopaminergic loss and inclusion body formation in alpha-synuclein mice: Implications for neurodegenerative disorders. *Science,* 287**,** 1265-1269.

MASLIAH, E., ROCKENSTEIN, E., VEINBERGS, I., SAGARA, Y., MALLORY, M., HASHIMOTO, M. & MUCKE, L. 2001. beta-Amyloid peptides enhance alpha-synuclein accumulation and neuronal deficits in a transgenic mouse model linking Alzheimer's disease and Parkinson's disease. *Proceedings of the National Academy of Sciences of the United States of America,* 98**,** 12245-12250.

MCCORMACK, A. L., ATIENZA, J. G., LANGSTON, J. W. & DI MONTE, D. A. 2006. Decreased susceptibility to oxidative stress underlies the resistance of specific dopaminergic cell populations to paraquat-induced degeneration. *Neuroscience,* 141**,** 929-937.

MCCORMACK, A. L., THIRUCHELVAM, M., MANNING-BOG, A. B., THIFFAULT, C., LANGSTON, J. W., CORY-SLECHTA, D. A. & DI MONTE, D. A. 2002. Environmental risk factors and Parkinson's disease: Selective degeneration of nigral dopaminergic neurons caused by the herbicide paraquat. *Neurobiology of Disease,* 10**,** 119-127.

MCDONALD, H. Y. & WOJTOWICZ, J. M. 2005. Dynamics of neurogenesis in the dentate gyrus of adult rats. *Neuroscience Letters,* 385**,** 70-75.

MCDONNELL, S. K., SCHAID, D. J., ELBAZ, A., STRAIN, K. J., BOWER, J. H., A-HLSKOG, J. E., MARAGANORE, D. M. & ROCCA, W. A. 2006. Complex segregation analysis of Parkinson's disease: The Mayo Clinic family study. *Annals of Neurology,* 59**,** 788-795.

MENDEZ, I., DAGHER, A., HONG, M., GAUDET, P., WEERASINGHE, S., MCALISTER, V., KING, D., DESROSIERS, J., DARVESH, S., ACORN, T. & ROBERTSON, H. 2002. Simultaneous intrastriatal and intranigral fetal

dopaminergic grafts in patients with Parkinson disease: a pilot study. Report of three cases. *J Neurosurg,* 96**,** 589-96.

MENDEZ, I., ELISEVICH, K. & FLUMERFELT, B. 1991. Dopaminergic innervation of substance p-containing striatal neurons by fetal nigral grafts - an ultrastructural double-labeling immunocytochemical study. *Journal of Comparative Neurology,* 308**,** 66-78.

MENDEZ, I., SADI, D. & HONG, M. 1996. Reconstruction of the nigrostriatal pathway by simultaneous intrastriatal and intranigral dopaminergic transplants. *J Neurosci,* 16**,** 7216-27.

MENDEZ, I., SANCHEZ-PERNAUTE, R., COOPER, O., VINUELA, A., FERRARI, D., BJORKLUND, L., DAGHER, A. & ISACSON, O. 2005. Cell type analysis of functional fetal dopamine cell suspension transplants in the striatum and substantia nigra of patients with Parkinson's disease. *Brain,* 128**,** 1498-1510.

MENDEZ, I., VINUELA, A., ASTRADSSON, A., MUKHIDA, K., HALLETT, P., ROBERTSON, H., TIERNEY, T., HOLNESS, R., DAGHER, A., TROJANOWSKI, J. Q. & ISACSON, O. 2008. Dopamine neurons implanted into people with Parkinson's disease survive without pathology for 14 years. *Nature Medicine,* 14**,** 507-509.

MENTZEL, C. L., TENBACK, D. E., TIJSSEN, M. A. J., VISSER-VANDEWALLE, V. E. R. M. & VAN HARTEN, P. N. 2012. Efficacy and Safety of Deep Brain Stimulation in Patients With Medication-Induced Tardive Dyskinesia and/or Dystonia: A Systematic Review. *Journal of Clinical Psychiatry,* 73**,** 1434-1438.

MEYERS, R. 1942. Surgical interruption of pallidofugal fibres: Its effect on the syndrome paralysis agitans and technical considerations in its application. *New York State Journal of Medicine,* 42**,** 317-325.

MEYERS, R. 1951. Surgical experiments in the therapy of certain 'extrapyramidal' diseases: a current evaluation. *Acta psychiatrica et neurologica. Supplementum,* 67**,** 1-42.

MICALLEF, J., REY, M., EUSEBIO, A., AUDEBERT, C., ROUBY, F., JOUVE, E., TARDIEU, S. & BLIN, O. 2009. Antiparkinsonian drug-induced sleepiness: a double-blind placebo-controlled study of L-dopa, bromocriptine and pramipexole in healthy subjects. *British Journal of Clinical Pharmacology,* 67**,** 333-340.

MICHELL, A. W., BARKER, R. A., RAHA-CHOWDHURY, R. & RAHA, S. K. 2005. A case of late onset sporadic Parkinson's disease with an A53T mutation in alpha-synuclein. *Journal of Neurology Neurosurgery and Psychiatry,* 76**,** 596-597.

MIHM, M. J., SCHANBACHER, B. L., WALLACE, B. L., WALLACE, L. J., URETSKY, N. J. & BAUER, J. A. 2001. Free 3-nitrotyrosine causes striatal neurodegeneration in vivo. *Journal of Neuroscience,* 21**,** art. no.-RC149.

MINGUEZ-MINGUEZ, S., DEL POZO, J. S. G. & JORDAN, J. 2013. Rasagiline in Parkinson's disease: A review based on meta-analysis of clinical data. *Pharmacological Research,* 74**,** 78-86.

MOLINA, H., QUINONES-MOLINA, R., MUNOZ, J., ALVAREZ, L., ALAMINOS, A., ORTEGA, I., OHYE, C., MACIAS, R., PIEDRA, J., GONZALEZ, C. & ET AL. 1994. Neurotransplantation in Parkinson's disease: from open microsurgery to bilateral stereotactic approach: first clinical trial using microelectrode recording technique. *Stereotact Funct Neurosurg,* 62**,** 204-8.

MOORE, D. J. & DAWSON, T. M. 2008. Value of genetic models in understanding the cause and mechanisms of Parkinson's disease. *Current Neurology and Neuroscience Reports,* 8**,** 288-296.

MORENS, D. M., DAVIS, J. W., GRANDINETTI, A., ROSS, G. W., POPPER, J. S. & WHITE, L. R. 1996. Epidemiologic observations on Parkinson's disease: Incidence and mortality in a prospective study of middle-aged men. *Neurology,* 46**,** 1044-1050.

MUKHIDA, K., BAKER, K. A., SADI, D. & MENDEZ, I. 2001. Enhancement of sensorimotor behavioral recovery in hemiparkinsonian rats with intrastriatal, intranigral, and intrasubthalamic nucleus dopaminergic transplants. *J Neurosci,* 21**,** 3521-30.

MUKHIDA, K., HONG, M., MILES, G. B., PHILLIPS, T., BAGHBADERANI, B. A., MCLEOD, M., KOBAYASHI, N., SEN, A., BEHIE, L. A., BROWNSTONE, R. M. & MENDEZ, I. 2008. A multitarget basal ganglia dopaminergic and GABAergic transplantation strategy enhances behavioural recovery in parkinsonian rats. *Brain,* 131**,** 2106-26.

MULLER, T., VAN LAAR, T., CORNBLATH, D. R., ODIN, P., KLOSTERMANN, F., GRANDAS, F. J., EBERSBACH, G., URBAN, P. P., VALLDEORIOLA, F. & ANTONINI, A. 2013. Peripheral neuropathy in Parkinson's disease: Levodopa exposure and implications for duodenal delivery Universally Available. *Parkinsonism & Related Disorders,* 19**,** 501-507.

MUNOZ, A., LI, Q., GARDONI, F., MARCELLO, E., QIN, C., CARLSSON, T., KIRIK, D., DI LUCA, M., BJORKLUND, A., BEZARD, E. & CARTA, M. 2008. Combined 5-HTIA and 5-HTIB receptor agonists for the treatment of L-DOPA-induced dyskinesia. *Brain,* 131**,** 3380-3394.

MURATA, M. & KANAZAWA, I. 1993. Repeated L-DOPA administration reduces the ability of dopamine storage and abolishes the supersensitivity of dopamine-receptors in the striatum of intact rat. *Neuroscience Research,* 16**,** 15-23.

NAIR-ROBERTS, R. G., CHATELAIN-BADIE, S. D., BENSON, E., WHITE-COOPER, H., BOLAM, J. P. & UNGLESS, M. A. 2008. Stereological estimates of dopaminergic, gabaergic and glutamatergic neurons in the ventral tegmental area, substantia nigra and retrorubral field in the rat. *Neuroscience,* 152**,** 1024-1031.

NARENDRA, D., TANAKA, A., SUEN, D.-F. & YOULE, R. J. 2008. Parkin is recruited selectively to impaired mitochondria and promotes their autophagy. *Journal of Cell Biology,* 183**,** 795-803.

NARENDRA, D. P., JIN, S. M., TANAKA, A., SUEN, D. F., GAUTIER, C. A., SHEN, J., COOKSON, M. R. & YOULE, R. J. 2010. PINK1 Is Selectively Stabilized on Impaired Mitochondria to Activate Parkin. *Plos Biology,* 8.

NAYLOR, J. L., WIDDOWSON, P. S., SIMPSON, M. G., FARNWORTH, M., ELLIS, M. K. & LOCK, E. A. 1995. Further evidence that the blood-brain-barrier impedes Paraquat entry into the brain. *Human & Experimental Toxicology,* 14**,** 587-594.

NELANDER, J., HEBSGAARD, J. B. & PARMAR, M. 2009. Organization of the human embryonic ventral mesencephalon. *Gene Expression Patterns,* 9**,** 555-561.

NIKKHAH, G., EBERHARD, J., OLSSON, M. & BJORKLUND, A. 1995. Preservation of fetal ventral mesencephalic cells by cool storage - in-vitro viability and TH-positive neuron survival after microtransplantation to the striatum. *Brain Research,* 687**,** 22-34.

NILSSON, O. G., CLARKE, D. J., BRUNDIN, P. & BJORKLUND, A. 1988. Comparison of growth and reinnervation properties of cholinergic neurons from different brain-regions grafted to the hippocampus. *Journal of Comparative Neurology,* 268.

NUTT, J. G., WOODWARD, W. R., HAMMERSTAD, J. P., CARTER, J. H. & ANDERSON, J. L. 1984. The on off phenomenon in Parkinsons-disease - relation to levodopa absorption and transport. *New England Journal of Medicine,* 310**,** 483-488.

O'KEEFFE, F. E., SCOTT, S. A., TYERS, P., O'KEEFFE, G. W., DALLEY, J. W., ZUFFEREY, R. & CALDWELL, M. A. 2008. Induction of A9 dopaminergic neurons from neural stem cells improves motor function in an animal model of Parkinsons disease. *Brain,* 131**,** 630-641.

OBESO, J. & LANG, A. 2006. Evolution of Parkinson's Disease and Treatment Requirements: What New Treatments are needed and the Role of Striatal Grafting. *In:* BRUNDIN, P. & OLANOW, C. (eds.) *Restorative Therapies in Parkinson's Disease.* New York, USA: Springer.

OLANOW, C. W., GOETZ, C. G., KORDOWER, J. H., STOESSL, A. J., SOSSI, V., BRIN, M. F., SHANNON, K. M., NAUERT, G. M., PERL, D. P., GODBOLD, J. & FREEMAN, T. B. 2003. A double-blind controlled trial of bilateral fetal nigral transplantation in Parkinson's disease. *Annals of Neurology,* 54**,** 403-414.

OLDS, M. E., JACQUES, D. B. & KOPYOV, O. 2006. Relation between rotation in the 6-OHDA, lesioned rat and dopamine loss in striatal and substantia nigra subregions. *Synapse,* 59**,** 532-544.

OLSON, L. & MALMFORS, T. 1970. Growth characteristics of adrenergic nerves in the adult rat. Fluorescence histochemical and 3H-noradrenaline uptake studies using tissue transplantations to the anterior chamber of the eye. *Acta physiologica Scandinavica. Supplementum,* 348.

OLSON, L. & SEIGER, A. 1972. Early prenatal ontogeny of central monoamine neurons in rat - fluorescence histochemical observations. *Zeitschrift Fur Anatomie Und Entwicklungsgeschichte,* 137**,** 301-&.

OUREDNIK, V. & OUREDNIK, J. 2004. Multifaceted dialogue between graft and host in neurotransplantation. *J Neurosci Res,* 76**,** 193-204.

PACKARD, D. S., JR., MENZIES, R. A. & SKALKO, R. G. 1973. Incorportaiton of thymidine and its analogue, bromodeoxyuridine, into embryos and maternal tissues of the mouse. *Differentiation; research in biological diversity,* 1**,** 397-404.

PAGONABARRAGA, J. & CRUZ RODRIGUEZ-OROZ, M. 2013. Rasagiline in monotherapy in patients with early stages of Parkinson's disease and in combined and adjunct therapy to levodopa with moderate and advanced stages. *Revista De Neurologia,* 56**,** 25-34.

PALFI, S., LEVENTHAL, L., CHU, Y. P., MA, S. Y., EMBORG, M., BAKAY, R., DEGLON, N., HANTRAYE, P., AEBISCHER, P. & KORDOWER, J. H. 2002. Lentivirally delivered glial cell line-derived neurotrophic factor increases the number of striatal dopaminergic neurons in primate models of nigrostriatal degeneration. *Journal of Neuroscience,* 22**,** 4942-4954.

PARISH, C. L., CASTELO-BRANCO, G., RAWAL, N., TONNESEN, J., SORENSEN, A. T., SALTO, C., KOKAIA, M., LINDVALL, O. & ARENAS, E. 2008. Wnt5a-treated midbrain neural stem cells improve dopamine cell replacement therapy in parkinsonian mice. *Journal of Clinical Investigation,* 118**,** 149-160.

PARKINSON, J. 2002. An essay on the shaking palsy (Reprinted). *Journal of Neuropsychiatry and Clinical Neurosciences,* 14**,** 223-236.

PARKKINEN, L., SOININEN, H., LAAKSO, M. & ALAFUZOFF, I. 2001. alpha-Synuclein pathology is highly dependent on the case selection. *Neuropathology and Applied Neurobiology,* 27**,** 314-325.

PAXINOS, G. & WATSON, C. 2003. *The rat brain in stereotaxic coordinates.*, London, Academic Press.

PEARCE, R. K. B., HEIKKILA, M., LINDEN, I. B. & JENNER, P. 2001. L-dopa induces dyskinesia in normal monkeys: behavioural and pharmacokinetic observations. *Psychopharmacology,* 156**,** 402-409.

PERACHON, S., SCHWARTZ, J. C. & SOKOLOFF, P. 1999. Functional potencies of new antiparkinsonian drugs at recombinant human dopamine D-1, D-2 and D-3 receptors. *European Journal of Pharmacology,* 366**,** 293-300.

PERLOW, M. J., FREED, W. J., HOFFER, B. J., SEIGER, A., OLSON, L. & WYATT, R. J. 1979. Brain grafts reduce motor abnormalities produced by destruction of nigrostriatal dopamine system. *Science,* 204**,** 643-7.

PERRIER, A. L., TABAR, V., BARBERI, T., RUBIO, M. E., BRUSES, J., TOPF, N., HARRISON, N. L. & STUDER, L. 2004. Derivation of midbrain dopamine neurons from human embryonic stem cells. *Proceedings of the National Academy of Sciences of the United States of America,* 101**,** 12543-12548.

PESCHANSKI, M., DEFER, G., N'GUYEN, J. P., RICOLFI, F., MONFORT, J. C., REMY, P., GENY, C., SAMSON, Y., HANTRAYE, P., JENY, R. & ET AL. 1994. Bilateral motor improvement and alteration of L-dopa effect in two patients with Parkinson's disease following intrastriatal transplantation of foetal ventral mesencephalon. *Brain,* 117 (Pt 3)**,** 487-99.

PICCINI, P., BROOKS, D. J., BJORKLUND, A., GUNN, R. N., GRASBY, P. M., RIMOLDI, O., BRUNDIN, P., HAGELL, P., REHNCRONA, S., WIDNER, H. & LINDVALL, O. 1999. Dopamine release from nigral transplants visualized in vivo in a Parkinson's patient. *Nat Neurosci,* 2**,** 1137-40.

PICCINI, P., LINDVALL, O., BJORKLUND, A., BRUNDIN, P., HAGELL, P., CERAVOLO, R., OERTEL, W., QUINN, N., SAMUEL, M., REHNCRONA, S., WIDNER, H. & BROOKS, D. J. 2000. Delayed recovery of movement-related cortical function in Parkinson's disease after striatal dopaminergic grafts. *Ann Neurol,* 48**,** 689-95.

PINCUS, J. H. & BARRY, K. M. 1987. Plasma-levels of amino-acids correlate with motor fluctuations in parkinsonism. *Archives of Neurology,* 44**,** 1006-1009.

PLUCHINO, S., ZANOTTI, L., ROSSI, B., BRAMBILLA, E., OTTOBONI, L., SALANI, G., MARTINELLO, M., CATTALINI, A., BERGAMI, A., FURLAN, R., COMI, G., CONSTANTIN, G. & MARTINO, G. 2005. Neurosphere-derived multipotent precursors promote neuroprotection by an immunomodulatory mechanism. *Nature,* 436**,** 266-71.

POLYMEROPOULOS, M. H., LAVEDAN, C., LEROY, E., IDE, S. E., DEHEJIA, A., DUTRA, A., PIKE, B., ROOT, H., RUBENSTEIN, J., BOYER, R., STENROOS, E. S., CHANDRASEKHARAPPA, S., ATHANASSIADOU, A., PAPAPETROPOULOS, T., JOHNSON, W. G., LAZZARINI, A. M., DUVOISIN, R. C., DIIORIO, G., GOLBE, L. I. & NUSSBAUM, R. L. 1997. Mutation in the alpha-synuclein gene identified in families with Parkinson's disease. *Science,* 276**,** 2045-2047.

PONSEN, M. M., STOFFERS, D., BOOIJ, J., VAN ECK-SMIT, B. L. F., WOLTERS, E. C. & BERENDSE, H. W. 2004. Idiopathic hyposmia as a preclinical sign of Parkinson's disease. *Annals of Neurology,* 56**,** 173-181.

PORRITT, M. J., BATCHELOR, P. E., HUGHES, A. J., KALNINS, R., DONNAN, G. A. & HOWELLS, D. W. 2000. New dopaminergic neurons in Parkinson's disease striatum. *Lancet,* 356**,** 44-45.

PORRITT, M. J., KINGSBURY, A. E., HUGHES, A. J. & HOWELLS, D. W. 2006. Striatal dopaminergic neurons are lost with Parkinson's disease progression. *Movement Disorders,* 21**,** 2208-2211.

POULOPOULOS, M., LEVY, O. A. & ALCALAY, R. N. 2012. The neuropathology of genetic Parkinson's disease. *Movement Disorders,* 27**,** 831-842.

PRAMSTALLER, P. P., SCHLOSSMACHER, M. G., JACQUES, T. S., SCARAVILLI, F., ESKELSON, C., PEPIVANI, I., HEDRICH, K., ADEL, S., GONZALES-MCNEAL, M., HILKER, R., KRAMER, P. L. & KLEIN, C. 2005. Lewy body Parkinson's disease in a large pedigree with 77 Parkin mutation carriers. *Annals of Neurology,* 58**,** 411-422.

PRENSA, L. & PARENT, A. 2001. The nigrostriatal pathway in the rat: A single-axon study of the relationship between dorsal and ventral tier nigral neurons and the striosome/matrix striatal compartments. *Journal of Neuroscience,* 21**,** 7247-7260.

PURSIAINEN, V., HAAPANIEMI, T. H., KORPELAINEN, J. T., SOTANIEMI, K. A. & MYLLYLA, V. V. 2007. Sweating in parkinsonian patients with wearing-off. *Movement Disorders,* 22**,** 828-832.

PUSCHMANN, A., ENGLUND, E., ROSS, O. A., VILARINO-GUELL, C., LINCOLN, S. J., KACHERGUS, J. M., COBB, S. A., TORNQVIST, A.-L., REHNCRONA, S., WIDNER, H., WSZOLEK, Z. K., FARRER, M. J. & NILSSON, C. 2012. First neuropathological description of a patient with Parkinson's disease and LRRK2 p.N1437H mutation. *Parkinsonism & Related Disorders,* 18**,** 332-338.

QUINN, N. P. 1990. The clinical-application of cell grafting techniques in patients with Parkinsons-disease. *Neural Transplantation : from Molecular Basis to Clinical Applications,* 82**,** 619-625.

QUINN, N. P. 1998. Classification of fluctuations in patients with Parkinson's disease. *Neurology,* 51**,** S25-S29.

RAJPUT, A. H., FENTON, M. E., BIRDI, S., MACAULAY, R., GEORGE, D., ROZDILSKY, B., ANG, L. C., SENTHILSELVAN, A. & HORNYKIEWICZ, O. 2002. Clinical-pathological study of levodopa complications. *Movement Disorders,* 17**,** 289-296.

RAJPUT, A. H., ROZDILSKY, B. & RAJPUT, A. 1991. Accuracy of clinical-diagnosis in parkinsonism - a prospective-study. *Canadian Journal of Neurological Sciences,* 18**,** 275-278.

RAO, G., FISCH, L., SRINIVASAN, S., D'AMICO, F., OKADA, T., EATON, C. & ROBBINS, C. 2003. Does this patient have Parkinson disease? *Jama-Journal of the American Medical Association,* 289**,** 347-353.

REDMOND, D. E., VINUELA, A., KORDOWER, J. H. & ISACSON, O. 2008. Influence of cell preparation and target location on the behavioral recovery after striatal transplantation of fetal dopaminergic neurons in a primate model of Parkinson's disease. *Neurobiology of Disease,* 29**,** 103-116.

REINER, A., ALBIN, R. L., ANDERSON, K. D., DAMATO, C. J., PENNEY, J. B. & YOUNG, A. B. 1988. Differential loss of striatal projection neurons in Huntington disease. *Proceedings of the National Academy of Sciences of the United States of America,* 85**,** 5733-5737.

REYES, S., FU, Y., DOUBLE, K., THOMPSON, L., KIRIK, D., PAXINOS, G. & HALLIDAY, G. M. 2012. GIRK2 Expression in Dopamine Neurons of the Substantia Nigra and Ventral Tegmental Area. *Journal of Comparative Neurology,* 520**,** 2591-2607.

RIBEIRO, D., GOYA, R. L., RAVINDRAN, G., VUONO, R., PARISH, C. L., FOLDI, C., PIROTH, T., YANG, S. Z., PARMAR, M., NIKKHAH, G., HJERLING-LEFFLER, J., LINDVALL, O., BARKER, R. A. & ARENAS, E. 2013. Efficient expansion and dopaminergic differentiation of human fetal ventral

midbrain neural stem cells by midbrain morphogens. *Neurobiology of Disease,* 49**,** 118-127.

RILEY, D., LANG, A. E., BLAIR, R. D. G., BIRNBAUM, A. & REID, B. 1989. Frozen shoulder and other shoulder disturbances in Parkinsons-disease. *Journal of Neurology Neurosurgery and Psychiatry,* 52**,** 63-66.

ROMERO, C. A., BUSTAMANTE, D. A., ZAPATA-TORRES, G., GOINY, M., CASSELS, B. & HERRERA-MARSCHITZ, M. 2006. Neurochemical and behavioural characterisation of alkoxyamphetamine derivatives in rats. *Neurotoxicity Research,* 10**,** 11-22.

ROY, N. S., CLEREN, C., SINGH, S. K., YANG, L., BEAL, M. F. & GOLDMAN, S. A. 2006. Functional engraftment of human ES cell-derived dopaminergic neurons enriched by coculture with telomerase-immortalized midbrain astrocytes. *Nature Medicine,* 12**,** 1259-1268.

SAMARANCH, L., LORENZO-BETANCOR, O., ARBELO, J. M., FERRER, I., LORENZO, E., IRIGOYEN, J., PASTOR, M. A., MARRERO, C., ISLA, C., HERRERA-HENRIQUEZ, J. & PASTOR, P. 2010. PINK1-linked parkinsonism is associated with Lewy body pathology. *Brain,* 133**,** 1128-1142.

SAMII, A., NUTT, J. G. & RANSOM, B. R. 2004. Parkinson's disease. *Lancet,* 363**,** 1783-1793.

SCHAPIRA, A. H. V. 2011. Monoamine Oxidase B Inhibitors for the Treatment of Parkinson's Disease A Review of Symptomatic and Potential Disease-Modifying Effects. *Cns Drugs,* 25**,** 1061-1071.

SCHEIN, J. C., HUNTER, D. D. & ROFFLER-TARLOV, S. 1998. Girk2 expression in the ventral midbrain, cerebellum, and olfactory bulb and its relationship to the murine mutation weaver. *Developmental Biology,* 204**,** 432-450.

SCHENCK, C. H., BOEVE, B. F. & MAHOWALD, M. W. 2013. Delayed emergence of a parkinsonian disorder or dementia in 81% of older men initially diagnosed with idiopathic rapid eye movement sleep behavior disorder: a 16-year update on a previously reported series. *Sleep Medicine,* 14**,** 744-748.

SCHMIDT, R. H., BJORKLUND, A. & STENEVI, U. 1981. Intra-cerebral grafting of dissociated CNS tissue suspensions: a new approach for neuronal transplantation to deep brain sites. *Brain Research,* 218**,** 347-356.

SCHMIDT, R. H., INGVAR, M., LINDVALL, O., STENEVI, U. & BJORKLUND, A. 1982. Functional-activity of substantia nigra grafts reinnervating the striatum - neurotransmitter metabolism and c-14 2-deoxy-d-glucose autoradiography. *Journal of Neurochemistry,* 38**,** 737-748.

SCHNEIDER, J. S., YUWILER, A. & MARKHAM, C. H. 1987. Selective loss of subpopulations of ventral mesencephalic dopaminergic-neurons in the monkey following exposure to MPTP. *Brain Research,* 411**,** 144-150.

SCHNELL, L. & SCHWAB, M. E. 1990. Axonal regeneration in the rat spinal-cord produced by an antibody against myelin-associated neurite growth-inhibitors. *Nature,* 343**,** 269-272.

SCHULTZ, W. 2007. Multiple dopamine functions at different time courses. *Annual Review of Neuroscience,* 30**,** 259-288.

SCHWAB, M. E. 1990. Myelin-associated inhibitors of neurite growth and regeneration in the CNS. *Trends in Neurosciences,* 13**,** 452-456.

SEIGER, A. & OLSON, L. 1973. Late prenatal ontogeny of central monoamine neurons in rat - fluorescence histochemical observations. *Zeitschrift Fur Anatomie Und Entwicklungsgeschichte,* 140**,** 281-318.

SHERER, T. B., KIM, J. H., BETARBET, R. & GREENAMYRE, J. T. 2003. Subcutaneous rotenone exposure causes highly selective dopaminergic

degeneration and alpha-synuclein aggregation. *Experimental Neurology,* 179**,** 9-16.

SHIN, J.-H., KO, H. S., KANG, H., LEE, Y., LEE, Y.-I., PLETINKOVA, O., TROCONSO, J. C., DAWSON, V. L. & DAWSON, T. M. 2011. PARIS (ZNF746) Repression of PGC-1 alpha Contributes to Neurodegeneration in Parkinson's Disease. *Cell,* 144**,** 689-702.

SHULTS, C. W., HASHIMOTO, R., BRADY, R. M. & GAGE, F. H. 1990. Dopaminergic cells align along radial glia in the developing mesencephalon of the rat. *Neuroscience,* 38**,** 427-436.

SIEGFRIED, J. & LIPPITZ, B. 1994. Bilateral chronic electrostimulation of ventroposterolateral pallidum - a new therapeutic approach for alleviating all parkinsonian symptoms. *Neurosurgery,* 35**,** 1126-1129.

SIMONDS, G. R. & FREED, W. J. 1990. Effects of intraventricular substantia-nigra allografts as a function of donor age. *Brain Research,* 530**,** 12-19.

SINCLAIR, S. R., FAWCETT, J. W. & DUNNETT, S. B. 1999. Dopamine cells in nigral grafts differentiate prior to implantation. *European Journal of Neuroscience,* 11**,** 4341-4348.

SMITH, G. P. & YOUNG, R. C. 1974. A new experimental model of hypokinesia. *Advances in neurology,* 5**,** 427-32.

SMITS, S. M., BURBACH, J. P. H. & SMIDT, M. P. 2006. Developmental origin and fate of meso-diencephalic dopamine neurons. *Progress in Neurobiology,* 78**,** 1-16.

SOMME, J. H., GOMEZ-ESTEBAN, J. C., MOLANO, A., TIJERO, B., LEZCANO, E. & ZARRANZ, J. J. 2011. Initial neuropsychological impairments in patients with the E46K mutation of the alpha-synuclein gene (PARK 1). *Journal of the Neurological Sciences,* 310**,** 86-89.

SORTWELL, C. E., COLLIER, T. J., CAMARGO, M. D. & PITZER, M. R. 2004. An in vitro interval before transplantation of mesencephalic reaggregates does not compromise survival or functionality. *Experimental Neurology,* 187**,** 58-64.

SOTELO, C. & ALVARADOMALLART, R. M. 1987. Reconstruction of the defective cerebellar circuitry in adult Purkinje cell degeneration mutant mice by Purkinje cell replacement through transplantation of solid embryonic implants. *Neuroscience,* 20**,** 1-22.

SPECHT, L. A., PICKEL, V. M., JOH, T. H. & REIS, D. J. 1981. Light-microscopic immuno-cytochemical localization of tyrosine-hydroxylase in prenatal rat-brain .1. Early ontogeny. *Journal of Comparative Neurology,* 199**,** 233-253.

SPENCER, D. D., ROBBINS, R. J., NAFTOLIN, F., MAREK, K. L., VOLLMER, T., LERANTH, C., ROTH, R. H., PRICE, L. H., GJEDDE, A., BUNNEY, B. S. & ET AL. 1992. Unilateral transplantation of human fetal mesencephalic tissue into the caudate nucleus of patients with Parkinson's disease. *N Engl J Med,* 327**,** 1541-8.

SPILLANTINI, M. G., SCHMIDT, M. L., LEE, V. M. Y., TROJANOWSKI, J. Q., JAKES, R. & GOEDERT, M. 1997. alpha-synuclein in Lewy bodies. *Nature,* 388**,** 839-840.

STEECE-COLLIER, K., COLLIER, T. J., DANIELSON, P. D., KURLAN, R., YUREK, D. M. & SLADEK, J. R., JR. 2003. Embryonic mesencephalic grafts increase levodopa-induced forelimb hyperkinesia in parkinsonian rats. *Mov Disord,* 18**,** 1442-54.

STEECE-COLLIER, K., SODERSTROM, K. E., COLLIER, T. J., SORTWELL, C. E. & MARIES-LAD, E. 2009. Effect of levodopa priming on dopamine neuron transplant efficacy and induction of abnormal involuntary movements in parkinsonian rats. *J Comp Neurol,* 515**,** 15-30.

STERN, G. 1989. Did parkinsonism occur before 1817. *Journal of Neurology Neurosurgery and Psychiatry***,** 11-12.

STROMBERG, I., BYGDEMAN, M. & ALMQVIST, P. 1992. Target-specific outgrowth from human mesencephalic tissue grafted to cortex or ventricle of immunosuppressed rats. *Journal of Comparative Neurology,* 315**,** 445-456.

SVENDSEN, C. N., CALDWELL, M. A., SHEN, J., TERBORG, M. G., ROSSER, A. E., TYERS, P., KARMIOL, S. & DUNNETT, S. B. 1997. Long-term survival of human central nervous system progenitor cells transplanted into a rat model of Parkinson's disease. *Experimental Neurology,* 148**,** 135-146.

SVENDSEN, C. N., TER BORG, M. G., ARMSTRONG, R. J. E., ROSSER, A. E., CHANDRAN, S., OSTENFELD, T. & CALDWELL, M. A. 1998. A new method for the rapid and long term growth of human neural precursor cells. *Journal of Neuroscience Methods,* 85**,** 141-152.

SVENNILSON, E., TORVIK, A., LOWE, R. & LEKSELL, L. 1960. Treatment of parkinsonism by stereotactic thermolesions in the pallidal region - a clinical-evaluation of 81 cases. *Acta Psychiatrica Et Neurologica,* 35**,** 358-377.

TANDE, D., HOGLINGER, G., DEBEIR, T., FREUNDLIEB, N., HIRSCH, E. & FRANCOIS, C. 2006. New striatal dopamine neurons in MPTP-treated macaques result from a phenotypic shift and not neurogenesis. *Brain,* 129**,** 1194-1200.

TERPSTRA, B. T., COLLIER, T. J., MARCHIONINI, D. M., LEVINE, N. D., PAUMIER, K. L. & SORTWELL, C. E. 2007. Increased cell suspension concentration augments the survival rate of grafted tyrosine hydroxylase immunoreactive neurons. *Journal of Neuroscience Methods,* 166**,** 13-19.

TERZIOGLU, M. & GALTER, D. 2008. Parkinson's disease: genetic versus toxin-induced rodent models. *Febs Journal,* 275**,** 1384-1391.

THANVI, B., LO, N. & ROBINSON, T. 2007. Levodopa-induced dyskinesia in Parkinson's disease: clinical features, pathogenesis, prevention and treatment. *Postgraduate Medical Journal,* 83**,** 384-388.

THIFFAULT, C., LANGSTON, J. W. & DI MONTE, D. A. 2000. Increased striatal dopamine turnover following acute administration of rotenone to mice. *Brain Research,* 885**,** 283-288.

THIRUCHELVAM, M., BROCKEL, B. J., RICHFIELD, E. K., BAGGS, R. B. & CORY-SLECHTA, D. A. 2000. Potentiated and preferential effects of combined paraquat and maneb on nigrostriatal dopamine systems: environmental risk factors for Parkinson's disease? *Brain Research,* 873**,** 225-234.

THOMAS, B., MANDIR, A. S., WEST, N., LIU, Y., ANDRABI, S. A., STIRLING, W., DAWSON, V. L., DAWSON, T. M. & LEE, M. K. 2011. Resistance to MPTP-Neurotoxicity in alpha-Synuclein Knockout Mice Is Complemented by Human alpha-Synuclein and Associated with Increased beta-Synuclein and Akt Activation. *Plos One,* 6.

THOMPSON, L., BARRAUD, P., ANDERSSON, E., KIRIK, D. & BJORKLUND, A. 2005. Identification of dopaminergic neurons of nigral and ventral tegmental area subtypes in grafts of fetal ventral mesencephalon based on cell morphology, protein expression, and efferent projections. *Journal of Neuroscience,* 25**,** 6467-6477.

THOMPSON, L. H., ANDERSSON, E., JENSEN, J. B., BARRAUD, P., GUILLEMOT, F., PARMAR, M. & BJORKLUND, A. 2006. Neurogenin2 identifies a transplantable dopamine neuron precursor in the developing ventral mesencephalon. *Experimental Neurology,* 198**,** 183-198.

TORRES, E. M., DOWD, E. & DUNNETT, S. B. 2008a. Recovery of functional deficits following early donor age ventral mesencephalic grafts in a rat model of Parkinson's disease. *Neuroscience,* 154**,** 631-640.

TORRES, E. M., LANE, E. L., HEUER, A., SMITH, G. A., MURPHY, E. & DUNNETT, S. B. 2011. Increased efficacy of the 6-hydroxydopamine lesion of the median forebrain bundle in small rats, by modification of the stereotaxic coordinates. *Journal of Neuroscience Methods,* 200**,** 29-35.

TORRES, E. M., MONVILLE, C., GATES, M. A., BAGGA, V. & DUNNETT, S. B. 2007. Improved survival of young donor age dopamine grafts in a rat model of Parkinson's disease. *Neuroscience,* 146**,** 1606-1617.

TORRES, E. M., MONVILLE, C., LOWENSTEIN, P. R., CASTRO, M. G. & DUNNETT, S. B. 2005. Delivery of sonic hedgehog or glial derived neurotrophic factor to dopamine-rich grafts in a rat model of Parkinson's disease using adenoviral vectors - Increased yield of dopamine cells is dependent on embryonic donor age. *Brain Research Bulletin,* 68**,** 31-41.

TORRES, E. M., WEYRAUCH, U. M., SUTCLIFFE, R. & DUNNETT, S. B. 2008b. A rat embryo staging scale for the generation of donor tissue for neural transplantation. *Cell Transplantation,* 17**,** 535-542.

TWELVES, D., PERKINS, K. S. M. & COUNSELL, C. 2003. Systematic review of incidence studies of Parkinson's disease. *Movement Disorders,* 18**,** 19-31.

UNGERSTEDT, U. 1968. 6-hydroxy-dopamine induced degeneration of central monoamine neurons. *European Journal of Pharmacology,* 5**,** 107-110.

UNGERSTEDT, U. 1971a. Adipsia and aphagia after 6-hydroxydopamine induced degeneration of the nigro-striatal dopamine system. *Acta physiologica Scandinavica. Supplementum,* 367**,** 95-122.

UNGERSTEDT, U. 1971b. Postsynaptic supersensitivity after 6-hydroxy-dopamine induced degeneration of the nigro-striatal dopamine system. *Acta physiologica Scandinavica. Supplementum,* 367**,** 69-93.

UNGERSTEDT, U. 1971c. Striatal dopamine release after amphetamine or nerve degeneration revealed by rotational behaviour. *Acta physiologica Scandinavica. Supplementum,* 367**,** 49-68.

UNGERSTEDT, U. & ARBUTHNOTT, G. W. 1970. Quantitative recording of rotational behavior in rats after 6 hydroxy dopamine lesions of the nigrostriatal dopamine system. *Brain Research,* 24**,** 485-493.

UNGERSTEDT, U., AVEMO, A., AVEMO, E., LJUNGBERG, T. & RANJE, C. 1973. Animal models of parkinsonism. *Calne, D.B. (Ed.). Advances in Neurology, Vol. 3. Progress in the Treatment of Parkinsonism. Proceedings of a Symposium. London, England, January 5-6, 1973. Xiv+326p. Illus. Raven Press Publishers: New York, N.Y., U.S.A***,** 257-271.

VALENTE, E. M., ABOU-SLEIMAN, P. M., CAPUTO, V., MUQIT, M. M. K., HARVEY, K., GISPERT, S., ALI, Z., DEL TURCO, D., BENTIVOGLIO, A. R., HEALY, D. G., ALBANESE, A., NUSSBAUM, R., GONZALEZ-MALDONALDO, R., DELLER, T., SALVI, S., CORTELLI, P., GILKS, W. P., LATCHMAN, D. S., HARVEY, R. J., DALLAPICCOLA, B., AUBURGER, G. & WOOD, N. W. 2004. Hereditary early-onset Parkinson's disease caused by mutations in PINK1. *Science,* 304**,** 1158-1160.

VAN DEN HEUVEL, D. M. A. & PASTERKAMP, R. J. 2008. Getting connected in the dopamine system. *Progress in Neurobiology,* 85**,** 75-93.

VERNEY, C., ZECEVIC, N. & PUELLES, L. 2001. Structure of longitudinal brain zones that provide the origin for the substantia nigra and ventral tegmental area in human embryos, as revealed by cytoarchitecture and tyrosine hydroxylase,

calretinin, calbindin, and GABA immunoreactions. *Journal of Comparative Neurology,* 429**,** 22-44.

VEZOLI, J., FIFEL, K., LEVIEL, V., DEHAY, C., KENNEDY, H., COOPER, H. M., GRONFIER, C. & PROCYK, E. 2011. Early Presymptomatic and Long-Term Changes of Rest Activity Cycles and Cognitive Behavior in a MPTP-Monkey Model of Parkinson's Disease. *Plos One,* 6.

VILA, M., JACKSON-LEWIS, V., VUKOSAVIC, S., DJALDETTI, R., LIBERATORE, G., OFFEN, D., KORSMEYER, S. J. & PRZEDBORSKI, S. 2001. Bax ablation prevents dopaminergic neurodegeneration in the 1-methyl-4-phenyl-1,2,3,6-tetrahydropyridine mouse model of Parkinson's disease. *Proceedings of the National Academy of Sciences of the United States of America,* 98**,** 2837-2842.

VILARINO-GUEELL, C., WIDER, C., ROSS, O. A., DACHSEL, J. C., KACHERGUS, J. M., LINCOLN, S. J., SOTO-ORTOLAZA, A. I., COBB, S. A., WILHOITE, G. J., BACON, J. A., BEHROUZ, B., MELROSE, H. L., HENTATI, E., PUSCHMANN, A., EVANS, D. M., CONIBEAR, E., WASSERMAN, W. W., AASLY, J. O., BURKHARD, P. R., DJALDETTI, R., GHIKA, J., HENTATI, F., KRYGOWSKA-WAJS, A., LYNCH, T., MELAMED, E., RAJPUT, A., RAJPUT, A. H., SOLIDA, A., WU, R.-M., UITTI, R. J., WSZOLEK, Z. K., VINGERHOETS, F. & FARRER, M. J. 2011. VPS35 Mutations in Parkinson Disease. *American Journal of Human Genetics,* 89**,** 162-167.

WADE, L. A. & KATZMAN, R. 1975. Synthetic amino-acids and nature of L-DOPA transport at blood-brain-barrier. *Journal of Neurochemistry,* 25**,** 837-842.

WATERS, C. M., PECK, R., ROSSOR, M., REYNOLDS, G. P. & HUNT, S. P. 1988. Immunocytochemical studies on the basal ganglia and substantia nigra in Parkinsons-disease and Huntingtons-chorea. *Neuroscience,* 25**,** 419-438.

WENNING, G. K., ODIN, P., MORRISH, P., REHNCRONA, S., WIDNER, H., BRUNDIN, P., ROTHWELL, J. C., BROWN, R., GUSTAVII, B., HAGELL, P., JAHANSHAHI, M., SAWLE, G., BJORKLUND, A., BROOKS, D. J., MARSDEN, C. D., QUINN, N. P. & LINDVALL, O. 1997. Short- and long-term survival and function of unilateral intrastriatal dopaminergic grafts in Parkinson's disease. *Annals of Neurology,* 42**,** 95-107.

WENNING, G. K., SHEPHARD, B., HAWKES, C., PETRUCKEVITCH, A., LEES, A. & QUINN, N. 1995. Olfactory function in atypical parkinsonian syndromes. *Acta Neurologica Scandinavica,* 91**,** 247-250.

WEYRAUCH, U. M. 2009. *Cell transplantation in an animal model of Parkinson's disease: the influence of donor age on graft survival.* PhD, Cardiff University.

WEYRAUCH, U. M., TORRES, E. M., BAIRD, A. L. & DUNNETT, S. B. 2009. A Simple Breeding Protocol for the Procurement of Accurately Staged Rat Donor Embryos for Neural Transplantation. *Cell Transplantation,* 18**,** 471-476.

WILLIAMS, D. R. & LEES, A. J. 2005. Visual hallucinations in the diagnosis of idiopathic Parkinson's disease: a retrospective autopsy study. *Lancet Neurology,* 4**,** 605-610.

WILLIAMS, D. R., WATT, H. C. & LEES, A. J. 2006. Predictors of falls and fractures in bradykinetic rigid syndromes: a retrospective study. *Journal of Neurology Neurosurgery and Psychiatry,* 77**,** 468-473.

WILLIAMS, S. M. & GOLDMAN-RAKIC, P. S. 1998. Widespread origin of the primate mesofrontal dopamine system. *Cerebral Cortex,* 8**,** 321-345.

WINDLE, W. F. & CAMMERMEYER, J. 1958. Functional and structural observations on chronically reserpinized monkeys. *Science,* 127**,** 1503-1503.

WINKLER, C., BENTLAGE, C., NIKKHAH, G., SAMII, M. & BJORKLUND, A. 1999. Intranigral transplants of GABA-rich striatal tissue induce behavioral recovery in the rat Parkinson model and promote the effects obtained by intrastriatal dopaminergic transplants. *Exp Neurol,* 155**,** 165-86.

WOJTOWICZ, J. M. & KEE, N. 2006. BrdU assay for neurogenesis in rodents. *Nature Protocols,* 1**,** 1399-1405.

WOOTEN, G. F., CURRIE, L. J., BOVBJERG, V. E., LEE, J. K. & PATRIE, J. 2004. Are men at greater risk for Parkinson's disease than women? *Journal of Neurology Neurosurgery and Psychiatry,* 75**,** 637-639.

WORTH, P. F. 2013. How to treat Parkinson's disease in 2013. *Clinical Medicine,* 13**,** 93-96.

WU, Y. N. & JOHNSON, S. W. 2011. Dopamine oxidation facilitates rotenone-dependent potentiation of n-methyl-d-aspartate currents in rat substantia nigra dopamine neurons. *Neuroscience,* 195**,** 138-144.

WUERTHELE, S. M., FREED, W. J., OLSON, L., MORIHISA, J., SPOOR, L., WYATT, R. J. & HOFFER, B. J. 1981. Effect of dopamine agonists and antagonists on the electrical-activity of substantia nigra neurons transplanted into the lateral ventricle of the rat. *Experimental Brain Research,* 44**,** 1-10.

YAMADA, K., SEMBA, R., DING, X. H., MA, N. & NAGAHAMA, M. 2005. Discrimination of cell nuclei in early S-phase, mid-to-late S-phase, and G(2)/M-phase by sequential administration of 5-bromo-2'-deoxyuridine and 5-chloro-2'-deoxyuridine. *Journal of Histochemistry & Cytochemistry,* 53**,** 1365-1370.

YAZDANI, U., GERMAN, D. C., LIANG, C. L., MANZINO, L., SONSALLA, P. K. & ZEEVALK, G. D. 2006. Rat model of Parkinson's disease: Chronic central delivery of 1-methyl-4-phenylpyridinium (MPP+). *Experimental Neurology,* 200**,** 172-183.

YORITAKA, A., HATTORI, N., UCHIDA, K., TANAKA, M., STADTMAN, E. R. & MIZUNO, Y. 1996. Immunohistochemical detection of 4-hydroxynonenal protein adducts in Parkinson disease. *Proceedings of the National Academy of Sciences of the United States of America,* 93**,** 2696-2701.

YU, Z. W., XU, X. H., XIANG, Z. H., ZHOU, J. F., ZHANG, Z. H., HU, C. & HE, C. 2010. Nitrated alpha-Synuclein Induces the Loss of Dopaminergic Neurons in the Substantia Nigra of Rats. *Plos One,* 5**,** 17.

ZARRANZ, J. J., ALEGRE, J., GOMEZ-ESTEBAN, J. C., LEZCANO, E., ROS, R., AMPUERO, I., VIDAL, L., HOENICKA, J., RODRIGUEZ, O., ATARES, B., LLORENS, V., TORTOSA, E. G., DEL SER, T., MUNOZ, D. G. & DE YEBENES, J. G. 2004. The new mutation, E46K, of alpha-synuclein causes Parkinson and Lewy body dementia. *Annals of Neurology,* 55**,** 164-173.

ZIJLMANS, J. C. M., DANIEL, S. E., HUGHES, A. J., REVESZ, T. & LEES, A. J. 2004. Clinicopathological including investigation of vascular parkinsonism, including clinical criteria for diagnosis. *Movement Disorders,* 19**,** 630-640.

ZIMPRICH, A., BENET-PAGES, A., STRUHAL, W., GRAF, E., ECK, S. H., OFFMAN, M. N., HAUBENBERGER, D., SPIELBERGER, S., SCHULTE, E. C., LICHTNER, P., ROSSLE, S. C., KLOPP, N., WOLF, E., SEPPI, K., PIRKER, W., PRESSLAUER, S., MOLLENHAUER, B., KATZENSCHLAGER, R., FOKI, T., HOTZY, C., REINTHALER, E., HARUTYUNYAN, A., KRALOVICS, R., PETERS, A., ZIMPRICH, F., BRUECKE, T., POEWE, W., AUFF, E., TRENKWALDER, C., ROST, B., RANSMAYR, G., WINKELMANN, J., MEITINGER, T. & STROM, T. M. 2011. A Mutation in VPS35, Encoding a Subunit of the Retromer Complex, Causes Late-Onset Parkinson Disease. *American Journal of Human Genetics,* 89**,** 168-175.

ZIMPRICH, A., BISKUP, S., LEITNER, P., LICHTNER, P., FARRER, M., LINCOLN, S., KACHERGUS, J., HULIHAN, M., UITTI, R. J., CALNE, D. B., STOESSL, A. J., PFEIFFER, R. F., PATENGE, N., CARBAJAL, I. C., VIEREGGE, P., ASMUS, F., MULLER-MYHSOK, B., DICKSON, D. W., MEITINGER, T., STROM, T. M., WSZOLEK, Z. K. & GASSER, T. 2004. Mutations in LRRK2 cause autosomal-dominant Parkinsonism with pleomorphic pathology. *Neuron,* 44**,** 601-607.